

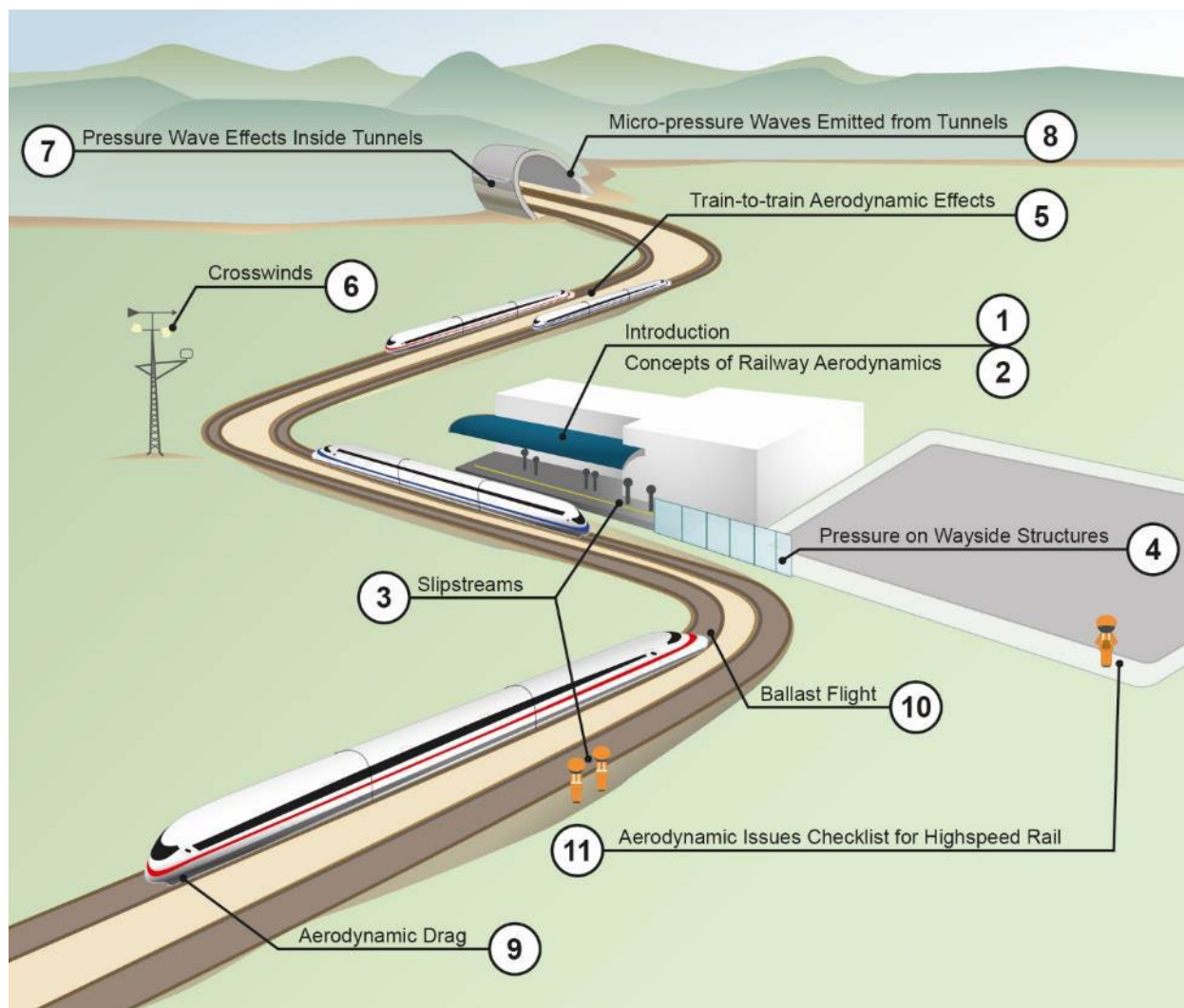


U.S. Department
of Transportation

Federal Railroad
Administration

Aerodynamic Assessment and Mitigation – Design Considerations for High-Speed Rail

Office of Research,
Development,
and Technology
Washington, DC 20590



NOTICE

This document is disseminated under the sponsorship of the Department of Transportation in the interest of information exchange. The U.S. Government assumes no liability for its contents or use thereof. Any opinions, findings and conclusions, or recommendations expressed in this material do not necessarily reflect the views or policies of the U.S. Government, nor does mention of trade names, commercial products, or organizations imply endorsement by the U.S. Government. The U.S. Government assumes no liability for the content or use of the material contained in this document.

NOTICE

The U.S. Government does not endorse products or manufacturers. Trade or manufacturers' names appear herein solely because they are considered essential to the objective of this report.

REPORT DOCUMENTATION PAGE			<i>Form Approved</i> OMB No. 0704-0188	
Public reporting burden for this collection of information is estimated to average 1 hour per response, including the time for reviewing instructions, searching existing data sources, gathering and maintaining the data needed, and completing and reviewing the collection of information. Send comments regarding this burden estimate or any other aspect of this collection of information, including suggestions for reducing this burden, to Washington Headquarters Services, Directorate for Information Operations and Reports, 1215 Jefferson Davis Highway, Suite 1204, Arlington, VA 22202-4302, and to the Office of Management and Budget, Paperwork Reduction Project (0704-0188), Washington, DC 20503.				
1. AGENCY USE ONLY (Leave blank)		2. REPORT DATE July 2022		3. REPORT TYPE AND DATES COVERED Technical Report, June 2017– October 2019
4. TITLE AND SUBTITLE Aerodynamic Assessment and Mitigation – Design Considerations for High-Speed Rail			5. FUNDING NUMBERS DFTR53-17-C-00011	
6. AUTHOR(S) Richard Sturt (Arup), Dr. Paul Lynch (Arup), Ryan Burns (Arup), Steve Clark (Arup), Dr. Bryan Horton (Arup), Paul Derkowski (Arup), Alexander Keylin (TTCI), Nicholas Wilson (TTCI)				
7. PERFORMING ORGANIZATION NAME(S) AND ADDRESS(ES) Arup Group Limited (primary contractor) 10370 Richmond Avenue, Suite 475 Houston, TX 77042 Transportation Technology Center, Inc. <i>A subsidiary of Association of American Railroads</i> 55500 DOT Road Pueblo, CO 81001			8. PERFORMING ORGANIZATION REPORT NUMBER	
9. SPONSORING/MONITORING AGENCY NAME(S) AND ADDRESS(ES) U.S. Department of Transportation Federal Railroad Administration Office of Railroad Policy and Development Washington, DC 20590			10. SPONSORING/MONITORING AGENCY REPORT NUMBER DOT/FRA/ORD-22/28	
11. SUPPLEMENTARY NOTES COR: Jeffrey Gordon				
12a. DISTRIBUTION/AVAILABILITY STATEMENT This document is available to the public through the FRA eLibrary .			12b. DISTRIBUTION CODE	
13. ABSTRACT (Maximum 200 words) This report presents the means to identify and assess impacts and mitigation methods for aerodynamic effects of high-speed trains on high-speed rail corridors for designers, operators, and other affected parties. It provides descriptions of basic concepts, criteria, standards, and examples of calculations and analysis of aerodynamic effects from the passage of high-speed trains and their effect on high-speed rail systems and passengers.				
14. SUBJECT TERMS High-speed rail, train aerodynamics, train slipstream, pressure pulse, tunnels, passenger safety, passenger comfort, ballast flight, aerodynamic drag, crosswinds, aerodynamic testing, aerodynamics, aerodynamic assessment.			15. NUMBER OF PAGES 331	
			16. PRICE CODE	
17. SECURITY CLASSIFICATION OF REPORT Unclassified	18. SECURITY CLASSIFICATION OF THIS PAGE Unclassified	19. SECURITY CLASSIFICATION OF ABSTRACT Unclassified	20. LIMITATION OF ABSTRACT	

NSN 7540-01-280-5500

Standard Form 298 (Rev. 2-89)
Prescribed by ANSI Std. Z39-18
298-102

METRIC/ENGLISH CONVERSION FACTORS

ENGLISH TO METRIC

LENGTH (APPROXIMATE)

1 inch (in)	=	2.5 centimeters (cm)
1 foot (ft)	=	30 centimeters (cm)
1 yard (yd)	=	0.9 meter (m)
1 mile (mi)	=	1.6 kilometers (km)

AREA (APPROXIMATE)

1 square inch (sq in, in ²)	=	6.5 square centimeters (cm ²)
1 square foot (sq ft, ft ²)	=	0.09 square meter (m ²)
1 square yard (sq yd, yd ²)	=	0.8 square meter (m ²)
1 square mile (sq mi, mi ²)	=	2.6 square kilometers (km ²)
1 acre = 0.4 hectare (he)	=	4,000 square meters (m ²)

MASS - WEIGHT (APPROXIMATE)

1 ounce (oz)	=	28 grams (gm)
1 pound (lb)	=	0.45 kilogram (kg)
1 short ton = 2,000 pounds (lb)	=	0.9 tonne (t)

VOLUME (APPROXIMATE)

1 teaspoon (tsp)	=	5 milliliters (ml)
1 tablespoon (tbsp)	=	15 milliliters (ml)
1 fluid ounce (fl oz)	=	30 milliliters (ml)
1 cup (c)	=	0.24 liter (l)
1 pint (pt)	=	0.47 liter (l)
1 quart (qt)	=	0.96 liter (l)
1 gallon (gal)	=	3.8 liters (l)
1 cubic foot (cu ft, ft ³)	=	0.03 cubic meter (m ³)
1 cubic yard (cu yd, yd ³)	=	0.76 cubic meter (m ³)

TEMPERATURE (EXACT)

$$[(x-32)(5/9)]^{\circ}\text{F} = y^{\circ}\text{C}$$

METRIC TO ENGLISH

LENGTH (APPROXIMATE)

1 millimeter (mm)	=	0.04 inch (in)
1 centimeter (cm)	=	0.4 inch (in)
1 meter (m)	=	3.3 feet (ft)
1 meter (m)	=	1.1 yards (yd)
1 kilometer (km)	=	0.6 mile (mi)

AREA (APPROXIMATE)

1 square centimeter (cm ²)	=	0.16 square inch (sq in, in ²)
1 square meter (m ²)	=	1.2 square yards (sq yd, yd ²)
1 square kilometer (km ²)	=	0.4 square mile (sq mi, mi ²)
10,000 square meters (m ²)	=	1 hectare (ha) = 2.5 acres

MASS - WEIGHT (APPROXIMATE)

1 gram (gm)	=	0.036 ounce (oz)
1 kilogram (kg)	=	2.2 pounds (lb)
1 tonne (t)	=	1,000 kilograms (kg)
	=	1.1 short tons

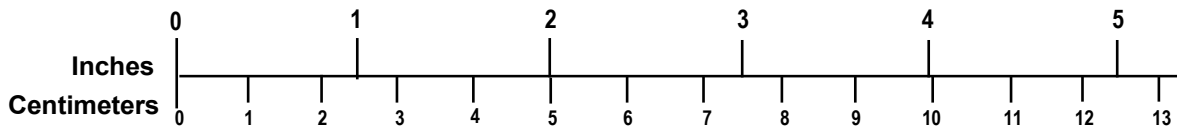
VOLUME (APPROXIMATE)

1 milliliter (ml)	=	0.03 fluid ounce (fl oz)
1 liter (l)	=	2.1 pints (pt)
1 liter (l)	=	1.06 quarts (qt)
1 liter (l)	=	0.26 gallon (gal)
1 cubic meter (m ³)	=	36 cubic feet (cu ft, ft ³)
1 cubic meter (m ³)	=	1.3 cubic yards (cu yd, yd ³)

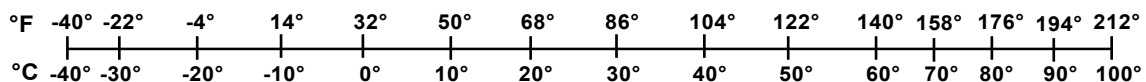
TEMPERATURE (EXACT)

$$[(9/5)y + 32]^{\circ}\text{C} = x^{\circ}\text{F}$$

QUICK INCH - CENTIMETER LENGTH CONVERSION



QUICK FAHRENHEIT - CELSIUS TEMPERATURE CONVERSION



For more exact and or other conversion factors, see NIST Miscellaneous Publication 286, Units of Weights and Measures. Price \$2.50 SD Catalog No. C13 10286

Updated 6/17/98

Acknowledgements

The authors wish to express special acknowledgement to Prof. Tanghong Liu (Central South University), Prof. Alan Vardy (Dundee Tunnel Research), and Prof. Chris Baker (University of Birmingham) for their contributions and review of this report, and for their research advancing high-speed train aerodynamics. The authors wish to thank Melissa Burton (Arup) and Emily Walport (Arup) for their contributions to the Crosswinds Section. The authors also thank Mylan Nguyen (Arup) for the illustrations provided in the report. The authors extend special thanks to Michael Trosino (Amtrak) for his industry review of portions of the document.

Contents

Executive Summary	1
1 Introduction	3
1.1 Background	3
1.2 Motivation	4
2 Concepts of Railway Aerodynamics	10
2.2.3 Crosswinds	11
2.2.4 Pressure Waves in Tunnels	12
2.2.5 Drag	12
2.2.6 Ballast Flight	12
2.3 High-Speed Train Dimensions and Aerodynamic Properties	13
2.3.1 International HST Cross-Section Dimensions	13
2.3.2 Baseline Train Dimensions and Aerodynamics Properties	14
2.4 Testing and Numerical Simulation Methods	17
2.6.1 Tunnel-Entry Pressure Gradient Test (Future Addition)	31
2.7 Unit Systems for Equations	31
3 Slipstreams	34
3.1 Introduction	34
3.2 Aerodynamic Principles and Phenomena	34
3.3 Influencing Factors	36
3.3.1 Train Speed	36
3.3.2 Processing of Air Speed Measurements	36
3.3.3 Distance from the Track	38
3.3.4 Elevation above Top of Rail	39
3.3.5 Platform Height	39
3.3.6 Train Type and Design	40
3.3.7 Confinement by Surroundings	40
3.3.8 Crosswinds	40
3.4 Impacts	40
3.4.1 Impacts on People on Platforms	40
3.4.2 Impacts on People Near Open Track	41
3.4.3 Impacts on Structures and Objects	41
3.4.4 Impacts on Trains on Adjacent Tracks	41
3.5 Mitigation Methods	42
3.5.1 Passengers at Platforms	42
3.5.2 Track-side Workers on Open Track	45
3.5.3 Members of the Public near Open Track	46
3.5.4 Loading of Objects and Structures Near the Track	46
3.6 Assessment	47
3.6.1 International Assessment Criteria	47
3.6.2 Estimation of Slipstream Air Speed for Baseline Trains	48
3.6.3 Assessment for Passengers at Platforms	50
3.6.4 Assessment for Trackside Workers	51
3.6.5 Assessment for Public near Open Track	53
3.6.6 Assessment Using Test Data	54

3.7	Examples	55
3.7.1	Select Required Safe Standing Distance Based on Speed.....	55
3.7.2	Determine Maximum Passing Speed for Platform	56
4	Pressures on Wayside Structures.....	57
4.1	Introduction	57
4.2	Aerodynamic Principles and Phenomena	57
4.3	Influencing Factors	59
4.3.1	Train Speed	59
4.3.2	Train Dimensions and Aerodynamic Performance.....	59
4.3.3	Confinement by Surroundings	59
4.3.4	Length along Track	59
4.3.5	Distance from the Track.....	59
4.4	Impacts	60
4.4.1	Impacts on Structures.....	60
4.4.2	Impacts on Trains	61
4.4.3	Impacts on People	61
4.5	Mitigation Methods.....	61
4.6	Assessment	61
4.6.1	Assessment Objective	61
4.6.2	Assessment Methods: Formulae for Design	61
4.6.3	Dynamic Analysis of Flexible Structures	69
4.6.4	Assessment Methods for Pressure Pulse Far from the Track.....	70
4.7	Example Calculations	71
4.7.1	Example 1	71
4.7.2	Example 2.....	73
5	Train-to-Train Aerodynamic Effects	75
5.1	Introduction	75
5.2	Aerodynamic Principles and Phenomena	76
5.3	Influencing Factors	76
5.3.1	Train Speed	76
5.3.2	Train Dimensions and Aerodynamic Performance.....	78
5.3.3	Confinement by Surroundings	78
5.3.4	Track Spacing.....	78
5.4	Impacts	80
5.4.1	Impacts on HSTs	80
5.4.2	Impacts on Conventional Passenger and Freight Trains	80
5.5	Mitigation Methods.....	81
5.5.1	Mitigation for Dedicated HSR ROW: Recommended Minimum Track Spacing.....	81
5.5.2	Mitigation for Shared ROW and Shared Corridors.....	84
5.5.3	Design of Rolling Stock.....	84
5.6	Assessment	84
5.6.1	Assessment Objectives.....	84
5.6.2	Assessment Principles.....	84
5.6.3	Calculation of Pressure Pulse Magnitude	85
5.6.4	Assessment by Comparing New and Existing Operations	86

5.6.5	Assessment by Full-Scale Testing	87
5.7	Examples	88
5.7.1	Select Required Track Spacing Based on Speed	88
5.7.2	Estimating Required Track Spacing Based on Existing Reference Operation	88
6	Crosswinds	90
6.1	Introduction	90
6.2	Aerodynamic Principles	90
6.2.1	Relevant Wind Speed Measurements	91
6.2.2	Definitions of Critical Wind Speed and Critical Gusts	91
6.2.3	The Need for a Probabilistic Approach to Assessment	92
6.2.4	Probabilistic Description of Wind Gust Speeds	92
6.2.5	Wind Angles and Interaction with Train Speed	92
6.2.6	Unbalanced Lateral Acceleration in Curves	95
6.2.7	Track Geometry Perturbations	96
6.2.8	Characteristic Wind Curves	97
6.2.9	Force and Moment Coefficients	98
6.2.10	U.S. Wind Climate	98
6.3	Influencing Factors	100
6.3.1	Wind Gust Speed	100
6.3.2	Wind Direction	100
6.3.3	Train Speed	101
6.3.4	Aerodynamic and Other Characteristics of Vehicles	101
6.3.5	Unbalanced Lateral Acceleration	101
6.3.6	Surface Roughness and Effect of Height	101
6.3.7	Wind Effects from Infrastructure Features	102
6.3.8	Wind Effects from Topography	103
6.4	Impacts	104
6.4.1	Derailment and Overturning	104
6.4.2	Impacts on Freight	104
6.4.3	Overhead Catenary System Damage	105
6.4.4	Accidents Caused Indirectly by Crosswinds	105
6.4.5	Previous Wind-Induced Accidents in the U.S.	105
6.5	Mitigation Methods	105
6.5.1	Rolling Stock Design	105
6.5.2	Wind Barriers	106
6.5.3	Speed Restrictions Applied Permanently at Crosswind “Hot-Spots”	106
6.5.4	Mitigation for Overhead Catenary System Blow-Off	106
6.5.5	Speed Restrictions Applied Temporarily	107
6.6	Crosswind Risk Assessment	108
6.6.1	Rail Vehicle Assessment	109
6.6.2	Route Assessment Methods – Overview	112
6.6.3	Probabilistic Route Assessment	113
6.6.4	Wind Speed Threshold Assessment (Operational Mitigation Measures Conditional on Wind Speed)	133
6.7	Route Assessment Examples	138

6.7.1	Calculation of Route Segment Risk (Probabilistic Method).....	138
6.7.2	Calculation of Operational Wind Gust Speed Thresholds	142
6.8	Operational Recommendations	143
7	Pressure Wave Effects Inside Tunnels	144
7.1	Introduction	144
7.2	Aerodynamic Principles and Phenomena	144
7.2.1	Conditions in the Vicinity of the Train.....	148
7.2.2	Wave Coincidence Effects	149
7.2.3	Single-track versus Double-track Tunnels	149
7.3	Influencing Factors	151
7.3.1	Blockage Ratio.....	151
7.3.2	Train Speed	152
7.3.3	Tunnel Length	152
7.3.4	Train Length.....	152
7.3.5	Air Shafts	153
7.3.6	Train Aerodynamic Design.....	153
7.3.7	Train Sealing.....	154
7.3.8	Carbody Shell Compressibility	156
7.3.9	Atmospheric Conditions in the Tunnel	157
7.4	Impacts	157
7.4.1	Impacts on Passengers and Crew	157
7.4.2	Impact on HST Railcar Design and Specification	158
7.4.3	Impact on Structures and Fixed Equipment Inside the Tunnel.....	158
7.4.4	Impact on Tunnel Design and Construction Cost.....	159
7.4.5	Impacts Where HSR Tunnels Are Shared with Conventional Traffic	159
7.4.6	Impact on Workers Inside Tunnels	159
7.4.7	Aerodynamic Impacts at Underground Stations.....	160
7.4.8	Micro-pressure Waves (“Sonic Booms”)	160
7.4.9	Other Aerodynamic Impacts in Tunnels	160
7.5	Mitigation Methods.....	161
7.5.1	Mitigation by Increasing Tunnel Size	161
7.5.2	Mitigation by Choice of Single-Track or Double-Track Tunnel Design...	162
7.5.3	Mitigation Using Air Shafts.....	162
7.5.4	Mitigation Using Cross-Passages	163
7.5.5	Mitigation of Aural Discomfort by Railcar Sealing	164
7.5.6	Mitigation by Aerodynamic Design of Trains.....	164
7.5.7	Mitigation by Reducing Speed	164
7.5.8	Mitigation for Conventional Traffic in Tunnels Shared with HSTs	164
7.5.9	Mitigation When Line Speed Is to Be Increased in Existing Tunnels	165
7.6	Assessment	165
7.6.1	Assessment Objectives.....	165
7.6.2	Assessment of New Tunnels: Rolling Stock Considerations.....	165
7.6.3	Assessment Methods.....	165
7.6.4	Nominal Tunnel Sizes for Initial Concept Design	166
7.6.5	Analysis Using Specialized Software	183
7.6.6	Wave Diagrams	193

7.6.7	Assessment by 3D CFD Analysis	194
7.6.8	Assessment by Reduced-Scale Testing	195
7.6.9	Assessment by Full-Scale Testing	196
7.6.10	Assessment Considerations for Cross-Passages Linking the Tubes of Single-Track Tunnels	196
7.6.11	Considerations for Assessing Fatigue Loading on Trains	196
7.6.12	Considerations for Assessing Tunnels Shared by HSTs and Conventional Traffic	198
7.6.13	Considerations for Assessing Aerodynamic Loading on Fixed Equipment in the Tunnel	198
7.6.14	Assessment Methods for Underground Stations	204
7.6.15	Assessment Criteria for Passengers and Crew	204
7.6.16	Assessment Criteria for Fatigue Loading on HSTs	212
7.6.17	Criteria for Aerodynamic Performance of Trains in Tunnels	213
7.6.18	Assessment Criteria for Fixed Equipment in the Tunnels	215
7.6.19	Assessment Criteria for Underground Stations	215
7.6.20	Examples	217
7.7	Inter-Related Considerations	219
7.7.1	Drag	219
7.7.2	Emergency Evacuation	219
7.7.3	Ventilation and Smoke Removal	219
8	Micro-Pressure Waves Emitted from Tunnels	221
8.1	Introduction	221
8.2	Aerodynamic Principles and Phenomena	221
8.2.1	Overview of the MPW Phenomenon	221
8.2.2	The Physics of MPWs	222
8.2.3	Relationship between Properties of MPW and Noise	225
8.2.4	Secondary Sources of MPWs	226
8.3	Influencing Factors	227
8.3.1	Train Speed	227
8.3.2	Pressure Gradient	228
8.3.3	Tunnel Length	229
8.3.4	Track Bed Type (Slab or Ballasted)	229
8.3.5	Blockage Ratio	229
8.3.6	Train Aerodynamic Design	230
8.3.7	Topography Near Tunnel Exit	230
8.3.8	Locations of Receivers	230
8.4	Impacts	230
8.4.1	Noise Impacts	230
8.4.2	Vibration Impacts	230
8.4.3	Impacts on Buildings	231
8.4.4	Impacts on People inside Trains	231
8.5	Mitigation Methods	231
8.5.1	Tunnel Entrance Hoods	231
8.5.2	Tunnel Portal Shape	233
8.5.3	Train Nose Design	234

8.5.4	Acoustic Absorbers	234
8.5.5	Ballast and Ballast Effect Mitigation Measures	235
8.5.6	Speed Restrictions	235
8.5.7	Other Beneficial Factors	236
8.6	Assessment	237
8.6.1	Assessment Objectives and Scope	237
8.6.2	Assessment Methods.....	239
8.6.3	Assessment Criteria.....	257
8.6.4	Example Calculations	262
9	Aerodynamic Drag Effect.....	269
9.1	Introduction	269
9.2	Aerodynamic Principles and Phenomena	269
9.2.1	The Davis Equation	270
9.2.2	Drag Coefficient.....	271
9.3	Influencing Factors	272
9.3.1	Speed	272
9.3.2	Aerodynamic Properties of Rolling Stock.....	272
9.3.3	Headwind.....	273
9.3.4	Crosswind	273
9.3.5	Tunnels	273
9.4	Impacts	274
9.4.1	Impacts on Operation and Planning.....	274
9.4.2	Impacts on Infrastructure Design	275
9.5	Mitigation Methods.....	275
9.5.1	Reducing Train Speeds	275
9.5.2	Procurement of Trains with Low Drag.....	275
9.5.3	Tunnels	276
9.6	Assessment	276
9.6.1	Assessment Objectives.....	276
9.6.2	Assessment Methods.....	276
9.6.3	Acceptability Criteria	285
9.6.4	Examples	286
10	Ballast Flight	288
10.1	Introduction	288
10.2	Ballast Flight Principles and Phenomenon.....	288
10.2.1	Recorded Incidents of Ballast Flight	290
10.3	Influencing Factors	292
10.3.1	Train Speed	292
10.3.2	Aerodynamic Design of the Train.....	292
10.3.3	Considerations for Ballast.....	292
10.3.4	Dynamics of Track	293
10.3.5	Environmental Factors	293
10.3.6	Secondary Factors.....	293
10.4	Impacts	294
10.4.1	Damage to Trains and Rails	294
10.4.2	Damage to Trackside Signs and Equipment.....	294

10.4.3	Impacts on People	294
10.4.4	Impacts on Operations and Selection of Track Type	294
10.5	Mitigation Methods	295
10.5.1	Reduction of Speed	295
10.5.2	Rolling Stock Design	295
10.5.3	Track Type	295
10.5.4	Ballast Design and Maintenance	295
10.5.5	Additional Measures	296
10.6	Assessment	297
11	Conclusion	298
12	References	301
	Abbreviations and Acronyms	313

Illustrations

Figure 1-1.	Designated High-Speed Rail Corridors and the Northeast Corridor.....	3
Figure 2-1.	Slipstreams and pressure pulses generated by a high-speed train. Red represents zones of high pressure, blue represents zones of low pressure.	11
Figure 2-2.	Crosswind	11
Figure 2-3.	Pressure wave created by a high-speed train in a tunnel	12
Figure 2-4.	Comparison of rolling stock static envelopes. Heights are measured from top of rail (TOR)	14
Figure 2-5.	Principle used in setting Baseline Train properties	17
Figure 2-6.	The “TRAIN rig” reduced-scale moving model testing facility in Derby, England, set up to measure pressure on a short overhead canopy; photo courtesy of Birmingham Centre for Railway Research and Education.....	21
Figure 2-7.	Measurement positions for European Rolling Stock TSI aerodynamic acceptance tests in the open environment.....	31
Figure 3-1.	Illustration of the airflow around a train, with the regions of the slipstream identified	35
Figure 3-2.	Recorded (unfiltered) slipstream air speed data for three nominally identical tests	35
Figure 3-3.	Example showing the influence of averaging time on maximum velocity coefficient.....	37
Figure 3-4.	Example of determining the upper 95 percent confidence interval for the maximum slipstream air speed	38
Figure 3-5.	Variation of peak slipstream velocity coefficient with distance from the track center: data from reduced-scale tests by Baker, Johnson & Holding and the author’s own tests, and full-scale tests by Deeg	39
Figure 3-6.	Illustration of slipstream loading of structures facing along the track	41
Figure 3-7.	Examples of platform edge safety markings (left image)	42
Figure 3-8.	Examples of platform screen doors and barriers. Top: full-height doors in China. Bottom-left: part-height solid barriers in Japan; Bottom-right: barrier fences in Germany	44
Figure 3-9.	Passage tracks	45
Figure 3-10.	Summary of international regulations on safe distances for track-side workers, measured from the nearest rail (from)	46
Figure 3-11.	Approximate variation of velocity coefficient with distance from track center on open track for Baseline Trains, overlaid on full-scale data from Baker and Deeg, (marked FS, with solid markers) and scale-model data from Baker, Johnson & Holding and the authors’ own tests (marked SM, with outline markers).....	49
Figure 3-12.	Aerodynamic minimum distances from nearest rail for track workers, with international regulations (from)	52
Figure 4-1.	Pressure near the nose and tail of a train (In the lower image, red represents zones of high pressure, and blue represents zones of low pressure.).....	58

Figure 4-2.	Magnitude of area-averaged pressure pulse on vertical surface as function of distance from track center for a streamlined HST	60
Figure 4-3.	Comparison of the pressure distribution on wayside structures inferred from the formulae in EN 14067-4, R1804.5501, and this report	62
Figure 4-4.	Idealization of pressure pulse on a vertical wayside structure	63
Figure 4-5.	Idealization of pressure pulse on a horizontal structure above the track ..	65
Figure 4-6.	Idealization of pressure pulse on a horizontal structure above and to the side of the track	66
Figure 4-7.	Idealization of pressure pulse on mixed vertical and inclined or horizontal structure at track-side	67
Figure 4-8.	Idealization of pressure pulse on a structure enclosing the track.....	68
Figure 4-9.	Typical form of pressure pulse from two trains coupled together, based on data from.....	70
Figure 5-1.	Key dimensions for train-to-train aerodynamic effects	76
Figure 5-2.	Variation of pressure pulse magnitude with train speed for track spacing of 13 ft (4.0 m) and train width 10 ft (3.0 m)	77
Figure 5-3.	Pressure pulses exerted by an acting train on an observing train.....	78
Figure 5-4.	Illustration of pressure pulse magnitude reduction with increased track spacing	79
Figure 5-5.	Variation of pressure pulse magnitude with track spacing for a HST of width $w=10$ ft.....	80
Figure 5-6.	Proposed aerodynamic minimum center-to-center track spacing for HST-to-HST and existing European and Chinese regulations	82
Figure 5-7.	Map of legal minimum track spacing for US states	83
Figure 5-8.	Relevant dimensions in pressure pulse calculation for trains meeting.....	85
Figure 6-1.	Crosswinds generate forces and moments that can cause derailment or overturning	91
Figure 6-2.	Natural wind, V_w , and apparent wind, U , relative to a moving train	93
Figure 6-3.	Influence of train speed on apparent wind	94
Figure 6-4.	Two combinations of train speed and natural wind speed resulting in a critical wheel unloading condition	94
Figure 6-5.	In curves, the tipping effect from unbalanced lateral acceleration can add to the tipping effect from wind	95
Figure 6-6.	CWCs for 90-degree natural wind angle and zero unbalanced lateral acceleration: Reference CWC from data for European trains TGV and ICE3 from.....	97
Figure 6-7.	Map showing occurrence of tornados and hurricanes, and "Special Wind Regions," associated with Downslope Winds; image from	100
Figure 6-8.	Trains exposed to stronger winds on viaducts due to greater distance from the ground.....	102
Figure 6-9.	Effects on wind of embankments (top left), cuttings (bottom left), and solid or porous barriers (top right and bottom right, respectively).....	103
Figure 6-10.	Wind can be strengthened by funneling through steep-sided valleys	104
Figure 6-11.	Main wind protection structures along the Lanxin Railway II. (a) Subgrade wind barriers; (b) bridge wind barriers; (c) wind-proof tunnels	106

Figure 6-12.	Wind tunnel test setup for measuring aerodynamic coefficients relevant to crosswind stability	110
Figure 6-13.	Example of the standard wind gust idealization as seen by a railcar passing through the gust.....	112
Figure 6-14.	Probabilistic route risk assessment overview.....	115
Figure 6-15.	Reference CWCs for U.S. compared to European CWCs from EN 14067-6:2018. ULA means unbalanced lateral acceleration.....	118
Figure 6-16.	Screenshot of ASCE 7 Hazard Tool – entering location, risk category, and hazard type (with permission from ASCE)	120
Figure 6-17.	ASCE 7 Hazard Tool – obtaining gust wind speeds from the "Details" button (with permission from ASCE)	120
Figure 6-18.	ASCE 7 Hazard Tool – "Overlay" function (with permission from ASCE)	121
Figure 6-19.	Sectors for assessment of terrain type.....	123
Figure 6-20.	Qualifying dimensions for applying the barrier factor (height measured from TOR).....	126
Figure 6-21.	Approximate method to determine for cases where is less than	129
Figure 6-22.	Assessment of wind gust speed thresholds for operational restrictions.	134
Figure 7-1.	Propagation and reflection of pressure waves inside a tunnel	145
Figure 7-2.	Sample pressure time-histories at a point on the tunnel wall and at a point on the train.....	147
Figure 7-3.	Conditions in the vicinity of the train	148
Figure 7-4.	Examples of single-track and double-track tunnels, as these terms are used in this report	150
Figure 7-5.	Cross-sectional area of train (left) and tunnel (right).....	151
Figure 7-6.	Schematic sketch of an air shaft (excludes typical emergency egress and ventilation infrastructure).....	153
Figure 7-7.	Pressure inside a sealed railcar in response to a step change of external pressure, showing influence of time constant τ	155
Figure 7-8.	Example of pressure changes inside sealed and unsealed railcars during passage through a tunnel	156
Figure 7-9.	Idealization of a railcar as a leaky, compressible box	156
Figure 7-10.	Single-track Nominal Tunnel Sizes for U.S./Euro Baseline Trains compared with internationally mandated tunnel sizes.....	169
Figure 7-11.	Double-track Nominal Tunnel Sizes for U.S./Euro Baseline Trains, compared with internationally mandated sizes	169
Figure 7-12.	Influence of tunnel size on aural comfort performance, 18-second dynamic sealing time constant, single-track tunnel, U.S./Euro Baseline Train. For U.S./Asian Baseline Trains, scale the tunnel area (x-axis) by 12/11. Approximate guideline only.....	177
Figure 7-13.	Influence of tunnel size on aural comfort, 10-second dynamic sealing time constant, single-track tunnel, U.S./Euro Baseline Train. For U.S./Asian Baseline Trains, scale the tunnel area (x-axis) by 12/11. Approximate guideline only	178
Figure 7-14.	Influence of tunnel size on pressure changes compared to Medical Safety Limit, single-track tunnel, U.S./Euro Baseline Train. For U.S./Asian	

	Baseline Trains, scale the tunnel area (x-axis) by 12/11. Approximate guideline only	179
Figure 7-15.	Influence of tunnel size on maximum pressure in tunnel, single-track tunnel, U.S./Euro Baseline Train. For U.S./Asian Baseline Trains, scale the tunnel area (x-axis) by 12/11. Approximate guideline only.....	180
Figure 7-16.	Influence of tunnel area on maximum net pressure on the train, single-track tunnel, U.S./Euro Baseline Train. For U.S./Asian Baseline Trains, scale the tunnel area (x-axis) by 12/11. Approximate guideline only	181
Figure 7-17.	Snapshot of an analysis using specialized software. The train has entered the tunnel from the left. Colors indicate pressure in the tunnel. Vertical dimensions are exaggerated in the image	183
Figure 7-18.	Diagrammatic representation of train model used in specialized one-dimensional analysis software	189
Figure 7-19.	Example analysis results for a two-train scenario. Maximum pressure in the tunnel for multiple analyses at different relative entry times.....	192
Figure 7-20.	An example of a pressure wave diagram (below) used to understand a pressure time-history from one-dimensional software (above)	194
Figure 7-21.	Net pressure on a railcar is the difference between external and internal pressure	197
Figure 7-22.	Pressure loading from pressure waves (loading shown by black arrows)	199
Figure 7-23.	Examples of net pressure across doors at a snapshot in time	200
Figure 7-24.	Example of maximum pressure load cycle amplitude from multiple train-passing scenarios: Net pressure on a door between bores of a tunnel. Maximum peak-to-peak pressure cycle amplitude is 1.81 psi in this example	201
Figure 7-25.	The nose and tail pressure pulses apply net pressure to doors and equipment that is sealed and contains air	202
Figure 7-26.	Airflow along the tunnel causes pressure loading on surfaces facing into the flow	202
Figure 7-27.	Medical Safety Limit assessment from pressure time-histories on the outside of the train	205
Figure 7-28.	Identification of maximum pressure changes for comparison against aural comfort criteria. Example shows pressure at rear of train	208
Figure 7-29.	Proposed aural comfort criteria for U.S. compared with international criteria and experimental results	210
Figure 7-30.	Measurement position for tunnel entry wave rolling stock acceptance tests	214
Figure 7-31.	Tunnel entry wave “signature”	215
Figure 8-1.	Micro-pressure wave generation, propagation, and emission	222
Figure 8-2.	Pressure gradient increasing during propagation, typical of slab track tunnels	224
Figure 8-3.	Pressure gradient decreasing during propagation, typical of ballasted track tunnels	224
Figure 8-4.	Pressure wave reflection and micro-pressure wave emission	225
Figure 8-5.	Example showing influence of train speed on MPW amplitude.....	228

Figure 8-6.	Influence of initial pressure gradient on inertial wave steepening.	229
Figure 8-7.	Japanese tunnel entrance hood (steel) – retro-fitted to Ohirayama tunnel, from Maeda et al; reproduced by kind permission of the authors	232
Figure 8-8.	Katzenberg tunnel entrance hood, from Hieke et al; photo reproduced with permission of DB Projektbau; schematic drawing with permission of DB SystemTechnik GmbH	233
Figure 8-9.	Scarfed portal shape.....	234
Figure 8-10.	Nose of Shinkansen E5	234
Figure 8-11.	Acoustic absorbers fitted in Euerwang Tunnel, from, photographer Peter Deeg, DB Systemtechnik GmbH.....	235
Figure 8-12.	Schematic sketch showing closed side passages	236
Figure 8-13.	MPW assessment and mitigation summary	239
Figure 8-14.	Nose-entry wave, actual and idealized	241
Figure 8-15.	Spherical influence of solid angle for vertical cliff face and flat topography	246
Figure 8-16.	Scale model test with tunnel hood	252
Figure 8-17.	CFD model for predicting pressure gradient in a tunnel with a hood, used with permission from.....	254
Figure 8-18.	Pressure and pressure gradient waveforms with optimal and non-optimal hoods – general form of graphs – after Rety and Gregoire.....	256
Figure 8-19.	C-weighting function (as used in German MPW criteria) compared with the A-weighting function more commonly used in noise assessments	260
Figure 9-1.	Tunnel drag effects (train moving from right to left)	274
Figure 9-2.	Car-to-car gap covering	276
Figure 9-3.	Drag force in open air, Baseline Trains with Davis Equation coefficients from Equations 9-6–9-8	282
Figure 9-4.	Power required to overcome drag in open air, Baseline Trains with Davis Equation coefficients from Equations 9-6–9-8	282
Figure 9-5.	Example aerodynamic drag force time-histories from one-dimensional analysis software	284
Figure 10-1.	Ballast flight chain reaction	289
Figure 10-2.	Left: Typical track ballast conditions. Right: lowered profile ballast less susceptible to aerodynamic effects from trains	293
Figure 10-3.	Example special aerodynamic tie (Aerotraviesa sleeper, a SENER project (©ADIF), used with permission).....	296
Figure 10-4.	Japanese ballast bags	297

Tables

Table 2-1.	Rolling stock dimensions	14
Table 2-2.	Properties of U.S./European and U.S./Asian Baseline Trains referenced in this report.....	16
Table 2-3.	HST Aerodynamic Acceptance Criteria from European TSI	29
Table 2-4.	Consistent unit systems	33
Table 3-1.	HST speed limits at platforms and corresponding safety marking distances in various countries	43
Table 3-2.	Aerodynamic minimum distances for track workers	53
Table 3-3.	Distance to track center for people near open track to achieve slipstream safety equivalent to that at a platform	54
Table 5-1.	Aerodynamic minimum center-to-center track spacing for HSTs	82
Table 6-1.	Examples of operational mitigation for crosswind risk	107
Table 6-2.	Input data required for crosswind route assessment	116
Table 6-3.	Example input data collection for crosswind route safety assessment ..	117
Table 6-4.	Height and terrain factor	122
Table 6-5.	Selection of terrain type	123
Table 6-6.	Infrastructure factor. Choose one of the options below.	124
Table 6-7.	Barrier factor	126
Table 6-8.	Selection of MRIs	127
Table 7-1.	Nominal Tunnel Sizes for initial concept design: single-track tunnels, area per tube.....	166
Table 7-2.	Nominal Tunnel Sizes for initial concept design: double-track tunnels ..	167
Table 7-3.	Approximate aerodynamic performance with Nominal Tunnel Sizes and Baseline Trains, train speed 125 mph	172
Table 7-4.	Approximate aerodynamic performance with Nominal Tunnel Sizes and Baseline Trains, train speed 150 mph	173
Table 7-5.	Approximate aerodynamic performance with Nominal Tunnel Sizes and Baseline Trains, train speeds 175 mph and above	174
Table 7-6.	Approximate aerodynamic performance for single-track tunnels smaller than the Nominal Tunnel Sizes for speeds 175 mph and above.....	176
Table 7-7.	Typical input data required by specialized software that predicts pressure wave effects in HSR tunnels – Tunnel data	186
Table 7-8.	Typical input data required by specialized software that predicts pressure wave effects in HSR tunnels – Train data	187
Table 7-9.	Typical input data required by specialized software that predicts pressure wave effects in HSR tunnels – Output data	188
Table 7-10.	Typical input data required by specialized software that predicts pressure wave effects in HSR tunnels – Atmospheric data	188
Table 7-11.	Typical input data required by specialized software that predicts pressure wave effects in HSR tunnels – Solution scheme variables	188
Table 7-12.	Standard atmospheric conditions for aerodynamic assessments	189
Table 7-13.	Proposed aural comfort criteria for U.S. (sealed trains)	207
Table 7-14.	Pressure changes compared to aural comfort criteria	208
Table 8-1.	Assessment methods for MPW.....	240

Table 8-2.	Summary of simplified assessment method.....	248
Table 8-3.	Parameters and wave-steepening calculation methods used in assessments of example tunnels	249
Table 8-4.	Example of MPW assessment results: short, double-track tunnel	250
Table 8-5.	Example of MPW assessment results: long, single-track tunnel.....	251
Table 9-1.	Approximate influence of speed on aerodynamic drag force and instantaneous power required to overcome aerodynamic drag	272
Table 10-1.	Reported ballast flight incidents (2001–2007).....	291
Table 10-2.	Ballast flight risk profiles	292

Executive Summary

This report provides methods for the assessment of potential aerodynamic impacts resulting from high-speed trains (HSTs) traveling at up to 250 mph for proposed high-speed rail (HSR) projects in the U.S. It includes recommendations for mitigation methods for the benefit of passengers, railroad employees, rail operators, and the general public. The report is intended for planners and operators of HSR systems, including the design of the infrastructure. It is not primarily intended for rolling stock designers but includes information that may assist with establishing certain aerodynamic performance criteria for rail vehicles in initial project planning.

The need for such design and mitigation guidance is well recognized as potential HSR network and system planning expands in the U.S. Aerodynamic issues become more significant as speeds increase, and the Federal Railroad Administration (FRA) anticipates future evolution of vehicles and infrastructure to allow for speeds up to 250 mph, which exceeds most foreign HSR standards and guidelines. This manual provides assessment methods and mitigations to the identified aerodynamic phenomena, which brings together guidance from Europe and Asia based on decades of operational experience on thousands of miles of HSR track. The report considers operations up to 250 mph while allowing maximum flexibility in the type of vehicles, operations, and right-of-way considerations for HSR operators in the American market.

Aerodynamics is a system issue involving both infrastructure and rolling stock. The design of infrastructure and operations to mitigate aerodynamic effects requires some knowledge of the properties of the trains. The report introduces the concept of Baseline Trains – dimensions and aerodynamic properties which can be used in assessments and mitigation design when actual vehicle properties may not be known. The properties have been chosen at the conservative end of the range for internationally available HSTs such that infrastructure designed for Baseline Trains can accommodate a wide range of actual trains. A U.S./European Baseline Train and a U.S./Asian Baseline Train are provided, reflecting the different dimensions of typical high-speed trains used in Europe and Asia, either of which might be adopted in the U.S. The report includes charts and tables that can be used directly in design, assuming Baseline Train dimensions and aerodynamic performance.

This research builds on the compilation and assessment of existing international guidelines and mitigation methods relating to aerodynamic issues provided in the [High-Speed Rail Aerodynamic Assessment and Mitigation Report](#) published by FRA in December 2015.

This report provides the basic concepts, mitigation methods, criteria, standards, assessment methods, design guidance, and example calculations for the identified aerodynamic phenomena of HSTs in open-air and tunnel environments, including slipstreams, pressures on wayside structures, train-to-train aerodynamic effects, crosswinds, pressure waves inside tunnels, micro-pressure waves emitted from tunnels, aerodynamic drag effects, and ballast flight.

For slipstreams, the authors recommend U.S. operators follow international practices, limiting train speeds at platforms to 125 mph and placing safety markings 5 feet from

the edge of platform. Recommended minimum distances away from track are provided for wayside workers to mitigate risks from train slipstreams.

For pressures on wayside structures, assessment methods are provided to calculate loading on structures near the track.

For train-to-train aerodynamic effects, recommended minimum center-to-center track spacing distances are provided, dependent upon design speed and train type.

For crosswinds, the authors provide assessment methods to determine and mitigate overturning risks for a given route or operation.

For pressure wave effects inside tunnels, nominal aerodynamic single-track and double-track tunnel sizes for the Baseline Trains are provided, together with advice on the more detailed aerodynamic analysis that is often necessary when designing tunnels. The report provides criteria for the aural comfort and safety of passengers and crew as well as considerations for the design of equipment inside tunnels to resist aerodynamic loading.

For micro-pressure waves emitted from tunnels (sometimes called sonic boom), the report provides assessment methods to determine if mitigation measures are required. Mitigation typically takes the form of an entrance hood. The report provides techniques for estimating the required length of hood for a particular tunnel.

For aerodynamic drag effects, the authors provide methods to calculate the impacts on energy consumption and the power requirement associated with high-speed operation.

For ballast flight, the report describes the risks and mitigation methods.

A summarized checklist of relevant aerodynamic issues and items for assessment or review is included in the Conclusion section. The authors encourage planners, engineers, operators, systems specialists, and administrators to utilize the assessment and mitigation guidance provided to ensure that the impacts on the rail infrastructure and surrounding public remain within tolerable limits.

1 Introduction

In this report, high-speed rail (HSR) encompasses the elements of a rail system and the surrounding environment impacted by aerodynamic effects related to the passage of high-speed trains (HSTs) with speeds up to 250 mph (400 km/h). These aerodynamic effects include air flows and pressure changes in open air and in tunnels that result in structural, safety-related, and operational impacts on people, structures, trains, and other equipment.

1.1 Background

The Acela Express currently operates as an HSR system in the Northeast Corridor (NEC). The California High-Speed Rail system and the Texas High-Speed Rail system are designed for higher speeds than Acela while other systems are being contemplated. [Figure 1-1](#) below depicts major high-speed corridors in operation, being planned, or under construction in the U.S. at the end of 2009. The Federal Railroad Administration (FRA) anticipates further evolution of vehicles and rail systems that will allow for increasing speeds up to 250 mph [\[50\]](#).

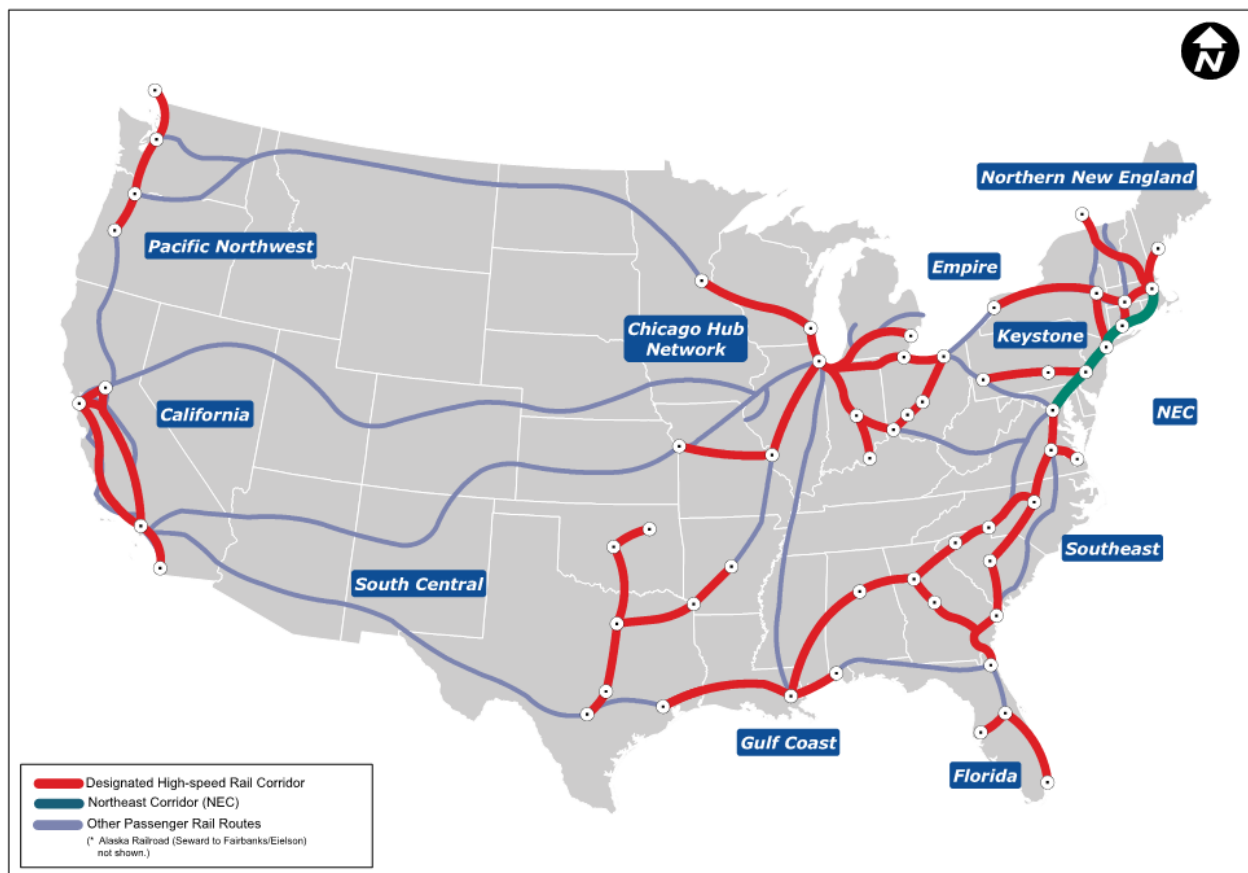


Figure 1-1. Designated High-Speed Rail Corridors and the Northeast Corridor
[\[52\]](#)

1.2 Motivation

Aerodynamic impacts become more significant as speeds increase. Phenomena that are insignificant at lower speeds can become governing considerations at higher speeds. Therefore, it is appropriate to offer guidance on aerodynamics specific to HSR, even though the same phenomena also occur on conventional railroads. There is, however, a lack of guidance for American operators and railway designers on how to identify, assess and mitigate aerodynamic impacts. The need for guidance has become more pressing as the potential HSR network and systems planned in the U.S. expand.

In the past two decades, FRA has sponsored many studies relating to aerodynamic performance of HSR operating in the NEC [90][91][92]. Other HSR projects currently under construction, such as the California High-Speed Rail, have included recommendations related to aerodynamics. However, these studies had a limited scope and were specific to their operating conditions.

Countries such as Germany, France, Japan, and China have a longer history of operating HSR lines and have accumulated a large volume of train aerodynamics knowledge and published literature. For some aerodynamic issues, national and international standards and regulations exist. However, few of these offer design guidance as such, and the limited information that can be used in design is scattered among different documents and is difficult for a non-specialist to assemble into a useable form.

In 2013, FRA commissioned a compilation and assessment of information in existing domestic and international published literature and standards pertinent to identifying, assessing, and addressing aerodynamic issues. That effort resulted in the publication by the FRA of the [High-Speed Rail Aerodynamic Assessment and Mitigation Report](#) in December 2015 [49]. The 2015 report forms the basis of the current study, which develops the information that can be used in the design and planning of HSR operations.

In summary, this report is needed for the following reasons:

- Aerodynamic issues are of particular concern for HSR because the impacts increase with speed.
- There is no existing single source of design guidance on HSR aerodynamic issues.
- There are currently no American established codes, standards, or best practices specifically related to HSR aerodynamics. Existing international information is fragmented, incomplete, and often stated in a form that is not directly useable in design.
- Much of the existing information can be interpreted only by aerodynamics specialists, and the implications for design are not clear to non-specialists.
- Train aerodynamics is a constantly developing field and some of the existing standards need to be updated.

- Most international standards pre-suppose certain train types and dimensions, whereas the American public, lawmakers, and rail industry desire standards that are more flexible in that respect.
- TFRA is interested in the development of guidelines for speeds up to 250 mph (400 km/h) which exceeds most foreign standards and guidelines for HSR [49] but will capture the upper limit of foreseeable planned projects.

1.3 Objectives

This report is designed to provide planners, engineers, operators, system specialists, and administrators with an understanding of the basic concepts, impacts and assessment methods related to HSR aerodynamics. Furthermore, it presents methods to mitigate the impacts for the benefit of passengers, railroad employees, rail operators, and the general public.

The report is intended for people who are not aerodynamics specialists and are involved in the planning and operation of HSR systems, including the design of the infrastructure. It is not primarily intended for rolling stock designers but includes information that may assist with establishing certain aerodynamic performance criteria for rail vehicles in initial project planning.

The authors recognize that any standard, regulation, or guideline is typically a compromise between multiple goals. These goals include maximization of safety and ease of use, maximization of flexibility, minimization of risks, and minimization of expenses in the construction and operation of HSR. This report is intended to assist in identifying and assessing impacts and developing mitigation methods while balancing the needs of the designer, operator, and other affected parties.

1.4 Overall Approach

Aerodynamics is a system issue involving both infrastructure and rolling stock. Impacts may be caused by air movements or pressures generated initially by the moving train; but mitigation is frequently achieved by appropriate design of the infrastructure near the track. For this reason, the design of infrastructure and operations to mitigate aerodynamic effects requires some knowledge of the properties of the trains. However, the trains may not have been selected at the time when the infrastructure is designed, and therefore the aerodynamic properties of the trains may be unknown; operators may not wish to design infrastructure that is specific to one particular train design (thereby limiting their choices of initial and future rolling stock). On the other hand, it is not economic to provide infrastructure that can accommodate any possible train, and as design guidance becomes more complex the more flexibility is required with regard to rolling stock.

In response to these issues, this study uses the concept of **Baseline Trains** – dimensions and aerodynamic properties which can be used in assessments and mitigation design when the actual vehicle properties may not be known. The properties have been chosen at the conservative end of the range for internationally available HSTs such that infrastructure designed for Baseline Trains can accommodate a wide range of actual trains. A U.S./European Baseline Train and a U.S./Asian Baseline Train

are provided, reflecting the different dimensions of typical HSTs used in Europe and Asia, either of which might be adopted in the U.S.

The assumption that aerodynamic performance of the trains will be no worse than the Baseline Trains has enabled simple-to-use tools to be provided in this report, such as charts and tables stating minimum track separation and tunnel sizes. However, the report also addresses how to perform more complex assessments that allow for trains that do not conform to the properties of the Baseline Trains, thus offering maximum flexibility in the type of vehicles that can be considered.

As well as the aerodynamic properties of trains, this study also relies on criteria defining what level of aerodynamic performance or impact should be considered acceptable. Where possible, the report adopts criteria already in use internationally, or, where these do not exist, uses international practice as a benchmark from which criteria are derived. For example, guidance on track separation and tunnel sizes for 250 mph (400 km/h) does not exist internationally, but the values provided in this report have been derived using the principle that aerodynamic impacts should be no worse than at the speeds for which guidance does exist internationally. Thus, the intent is to replicate aerodynamic conditions that exist in HSR systems with a history of successful operation without unacceptable aerodynamic impacts.

Where choices of criteria are available or where engineering judgment has been used to inform it, the report is intended to be on the conservative side. However, be mindful that there are many uncertainties in HSR aerodynamics, especially regarding how the measurable (or calculable) quantities, such as pressures and airflow speeds, relate to acceptable or unacceptable impacts. Therefore, the authors cannot offer any guarantees that unacceptable impacts will not occur, even if the methods in the report are followed. Prior to construction of a new HSR track or the introduction of HST service to existing infrastructure, all designs should be properly and comprehensively analyzed and approved by qualified technical specialists.

The approach used in this study differs somewhat from the treatment of noise and vibration described in the 2005 FRA [High-Speed Ground Transportation Noise and Vibration Impact Assessment](#) [44] report. Noise and vibration impact the wider public in the environment around a railway and therefore an assessment of the degree of impact on people plays a key role. In contrast, aerodynamic impacts are in general confined to the immediate vicinity of the track and therefore the assessments given in this report are mostly calculations or look-ups that quantify certain design parameters of the nearby infrastructure and may also influence the selection of rolling stock.

1.5 Scope

This manual covers HSR operations at speeds of 125 to 250 mph (200 to 400 km/h) only.

Aerodynamic phenomena arising from the pressures and airflows generated by trains in the open-air environment and in tunnels are included in the scope, as is the impact of wind on the safety of HSR operations. However, aerodynamic noise (i.e., noise generated by aerodynamic effects of passing trains) is not included. That subject is covered in the aforementioned 2005 FRA report [44].

TFRA classifies passenger equipment on U.S. railroads into three tiers [51]:

- Tier I equipment has a maximum operational speed below 125 mph (200 km/h). It can be intermixed with other passenger and freight operations.
- Tier II equipment has a maximum operational speed above 125 mph (200 km/h) but below 160 mph (260 km/h). It can be intermixed with other passenger and freight operations on shared right-of-way (ROW).
- Tier III equipment currently has a maximum operational speed above 125 mph (200 km/h) up to 220 mph (350 km/h) on exclusive ROW. It can only intermix with freight and other tiers of passenger equipment on shared ROW when operating at speeds below 125 mph (200 km/h)[51]. This report considers operations beyond the current Tier III limit of 220 mph in anticipation of the possible future evolution of vehicles and rule-making to allow for speeds up to 250 mph.

Because this report only covers speeds from 125 mph upwards, Tier I and freight are excluded, and no discussion is provided for route segments used by Tier II and Tier III equipment where the operating speed is less than 125 mph. At these speeds, HSTs can be comingled with any other types of trains. HSTs are better streamlined than other train types and are not expected to pose any particular aerodynamic risks over and above those from non-HSTs traveling at the same speeds on the same route segments. However, it cannot be stated for certain that no aerodynamic impacts will occur.

As used in this report, **Shared ROW** refers to locations where track centers are separated by less than 25 feet, and **Shared Corridor** refers to locations where the HSR and non-HSR track centers are separated by at least 25 ft. The term shared ROW includes shared tracks as well as separate HSR tracks within 25 ft of non-HSR tracks.

The situation where HSTs can operate at speeds above 125 mph on shared ROW exists only with Tier II, which is unique to the NEC. Operational experience over many years has not revealed any problematic aerodynamic issues under current NEC operating conditions, and no further Tier II operations in other parts of the U.S. are currently planned. For this reason, aerodynamic interactions between HSTs and Tier I or freight trains on adjacent tracks in shared ROW have been given little attention in this report. Given the unique characteristics of operations in the NEC, any further speed increase there should be subject to a route-specific risk assessment.

Tier III-exclusive ROW may be located in a shared corridor with Tier I and freight ROW. The 25 ft minimum track separation is considered to be far enough that aerodynamic interactions would be minimal; it is unlikely that any aerodynamic impacts from HSTs on freight or conventional passenger trains could be worse than the existing impacts between conventional trains on conventional tracks. Furthermore, considerations of ROW protection in the event of derailment or other reasons may lead operators to provide track separation between Tier III and Tier I tracks greater than 25 ft, which, as a by-product, would reduce aerodynamic impacts still further. Therefore, no specific details are provided for this situation.

1.6 Organization of the Report

Section 1 Introduction provides general information about the background, objectives, overall approach, scope, and organization of the report.

Section 2 Concepts of Railway Aerodynamics introduces the aerodynamic topics covered in later sections and includes material relevant to several or all of those topics, such as testing and analysis methods and codes and standards.

Section 3 through Section 10 present the main aerodynamic topics:

- **Section 3 Slipstreams** covers the airflows caused by trains (including turbulence) which can impact the safety of passengers at platforms and track workers.
- **Section 4 Pressures on Wayside Structures** describes the localized pressure loading on objects near the track caused by passing HSTs, which can potentially cause fatigue or other forms of structural failure.
- **Section 5 Train-to-train Aerodynamic Effects** covers the aerodynamic interactions that occur when two trains meet or pass each other, such as the buffeting induced by pressure pulses.
- **Section 6 Crosswinds** covers natural wind gusts which can create risks of train overturning and derailment for HSTs.
- **Section 7 Pressure Wave Effects inside Tunnels** describes pressure transients inside a railroad tunnel when an HST passes through it, the impacts on people in the trains, and the impacts on trains, structures, and equipment in the tunnel.
- **Section 8 Micro-Pressure Waves Emitted from Tunnels** covers the pulses of air pressure emitted from railroad tunnel entrances and exits that can manifest as audible noise or vibration, sometimes called sonic booms.
- **Section 9 Aerodynamic Drag Effect** covers the aerodynamic resistance to the motion of the train and its operational impacts.
- **Section 10 Ballast Flight** describes the phenomenon whereby ballast particles can be picked up and thrown violently against the HST or objects on or near the track.

Section 11 The Conclusion summarizes the main elements of the guidance in checklist form.

All the aerodynamic topics are organized in the following fashion:

- A short introduction is provided, including a brief summary of the section content.
- The general nature of the aerodynamic issue is presented, providing a basic understanding of the underlying physics and influencing factors.
- Impacts, mitigation measures, and assessment methodology are presented.
- Where appropriate, examples of assessment calculations are provided.

Section 12 provides a list of references.

An Abbreviations and Acronyms list for those terms used in the report is provided at the end of this manual.

2 Concepts of Railway Aerodynamics

2.1 Introduction

This section contains an introduction to the aerodynamic phenomena that will be described in detail in later sections and covers subjects relevant to several or all of those topics, including:

- The dimensions and properties of HSTs relevant to aerodynamics (Section 2.3), including the Baseline Trains used to characterize actual train properties and enable simple guidance in the later sections.
- Methods of physical testing and computer simulation (Section 2.4)
- International codes and standards (Section 2.5) and relevant criteria contained in them (Section 2.6)
- Notes on the units to be used in calculations (Section 2.7).

2.2 Aerodynamic Phenomena

2.2.1 Slipstreams

The air motion caused by the passage of a train is known as the slipstream and consists of a general airflow in the direction of the train's motion both alongside and behind the train (see Figure 2-1). Slipstreams are strongly turbulent, leading to the effect of a wind containing strong random gusts being experienced by any people, structures, objects, or other trains close to the passing train. Potential impacts include injuries to people from falling, wheelchairs and strollers on platforms being set into motion and colliding with the train, or people being struck by objects blown by the slipstream airflow. Mitigation generally consists of defining safe distances from the track beyond which people should remain while trains are passing.

Specific information on slipstreams is given in Section 3.

2.2.2 Pressure Pulses

The nose pressure pulse is a zone of high-pressure air that moves with the train just in front of the train nose, with a zone of low-pressure air immediately behind the nose. These zones are caused by the train pushing air out of its way. For the tail pressure pulse, the situation is reversed: there is a zone of low-pressure air just ahead of the tail of the train, and a zone of high-pressure air immediately behind the tail; see Figure 2-1. Similar pressure pulses arise from nose-to-nose couplings and inter-car gaps.

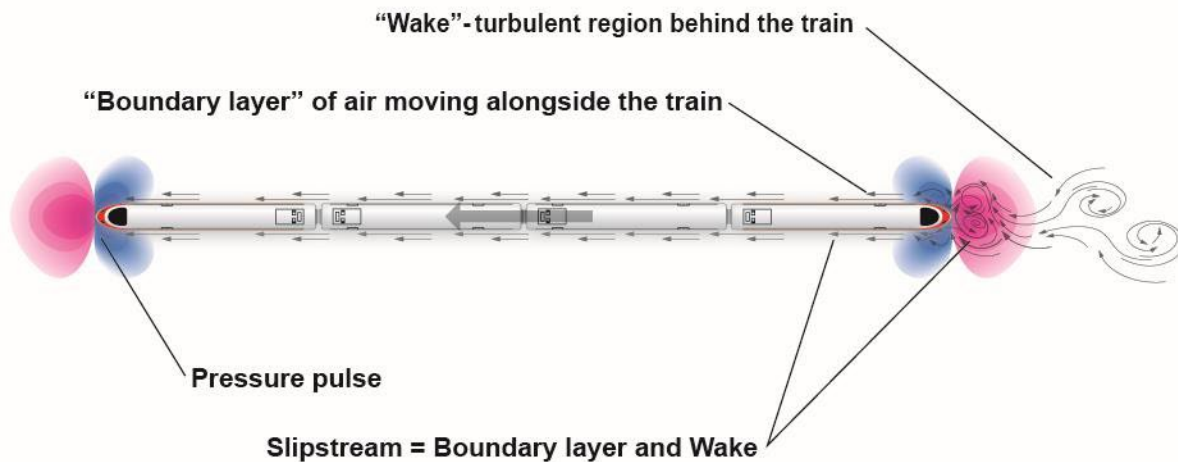


Figure 2-1. Slipstreams and pressure pulses generated by a high-speed train. Red represents zones of high pressure, blue represents zones of low pressure.

Any structures, objects, people, or other trains close to the passing train experience rapid pulses of positive and negative pressure as these zones pass over them. Potential impacts include damage to structures and equipment close to the track, such as fatigue damage to noise barriers, which should be designed to resist the aerodynamic loading. Guidance on this topic is given in Section 4.

The pressure pulses are also responsible for buffeting effects when trains meet, necessitating greater separation between tracks for higher speed operations as described in Section 5.

2.2.3 Crosswinds

A crosswind is any naturally-occurring wind (i.e., a wind not caused by trains), the direction of which is not aligned parallel to the track (see Figure 2-2).

Crosswinds have the potential to derail or overturn trains. Safety in crosswinds is an important consideration when planning new routes or introducing new rolling stock for both high-speed and conventional rail. A probabilistic approach to risk is appropriate when deciding on mitigation measures, which may include wind fences in particular locations, or operating procedures that address current or expected wind conditions.

Specific information on crosswinds is provided in Section 6.

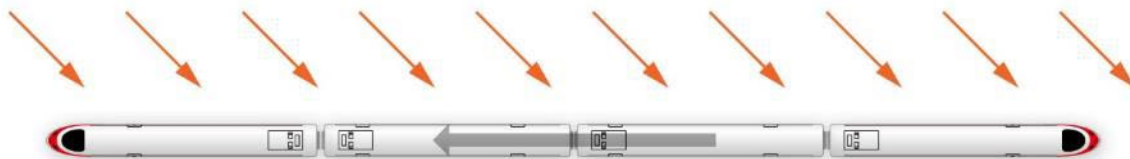


Figure 2-2. Crosswind

2.2.4 Pressure Waves in Tunnels

When a train enters a tunnel at high speed, it generates pressure waves in the air in the tunnel (piston effect); see [Figure 2-3](#). The waves propagate along the tunnel at the speed of sound and reflect when they reach the ends of the tunnel.

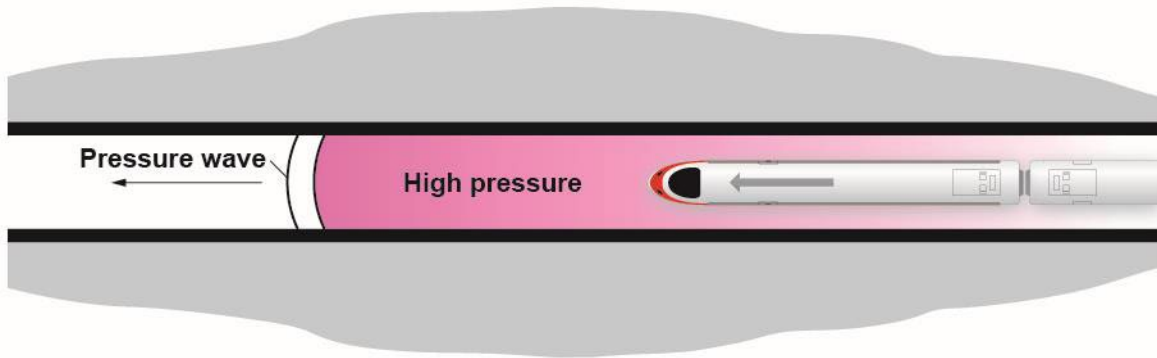


Figure 2-3. Pressure wave created by a high-speed train in a tunnel

Large, rapid changes in air pressures occur inside the tunnel each time a wave passes, leading to potential discomfort in the ears of people inside trains, and significant pressure loading on trains, fixed equipment, and structures in the tunnel. Addressing pressure wave effects is frequently the governing factor for establishing the size of HSR tunnels and hence may significantly impact construction costs. Further details are given in [Section 7](#).

Pressure waves inside the tunnel also lead to micro-pressure waves being emitted into the surrounding environment, potentially in the form of audible “sonic booms” which can cause annoyance for nearby residents – see [Section 8](#) for more information on this subject.

2.2.5 Drag

Aerodynamic drag is the resistance to the motion of a train caused by the air surrounding the train. Drag is an important subject for HSR because it contributes very significantly to energy costs and may even be a factor in deciding the operating speed of some HSR services. HST manufacturers pay considerable attention to providing design features that reduce drag. A specific description is given in [Section 9](#).

2.2.6 Ballast Flight

Ballast flight is the movement of ballast particles at high speed. It may be initiated by aerodynamic effects from passing trains. The particles may strike the underside of the train or land on the rails leading to the pitting of rails and wheels. If the train speed is high enough, ballast flight can develop into chain reactions involving large numbers of particles that can cause unacceptable levels of damage to HSTs. Mitigation is currently based around ballast placement and maintenance practices. This is effective at current operating speeds up to around 200 mph (320 km/h) but ballast flight is a potential limiting factor on the use of ballasted track for speeds as high as 250 mph (400 km/h). [Section 10](#) describes this topic.

2.3 High-Speed Train Dimensions and Aerodynamic Properties

2.3.1 International HST Cross-Section Dimensions

The train cross-sectional dimensions are a key input to assessments for most of the aerodynamic phenomena described in this report. For example, a wider train generates a wider slipstream, and a train with a larger cross-sectional area generates stronger pressure waves when entering a tunnel. Commercially available HSTs vary somewhat in their cross-sectional dimensions but broadly fall into two categories:

- European HSTs usually have a 2+2 seating arrangement in standard class, with cross-sections up to about 118 in (3.0 m) wide. They typically fit within the European “GB” reference profile for interoperable trains (described below).
- East Asian HSTs (China, Japan, and some other countries) usually have a 3+2 seating arrangement in standard class, which are up to 134 in (3.40 m) wide. The California HSR Authority has adopted similar dimensions for its design specifications.

The cross-sectional dimensions of trains may be described by the **static envelope** (the shape into which the train’s cross-section must fit, defining the maximum cross-sectional dimensions), by the **kinematic envelope** (which includes additional clearances for curving and movement of the car body on the suspension), or by the **structure gauge** (which defines the zone into which structures must not intrude). Additionally, Europe has the concept of **reference profiles** (defined in EN 15273 [36]), which are somewhere between static envelopes and structure gauges. They include an allowance for increased spacing in curves and are wider than static envelopes.

Two of the European reference profiles are called GB and GC. These have the same width, but GC is taller. Almost all European, commercially available HSTs fit within the GB profile, which is therefore considered in this report as representing the typical European HST. European HSTs exceeding the height of the GB profile (but fitting within the GC profile) do exist, but are rare.

Static envelopes for European and Asian HSTs [119][19] are presented in Figure 2-4 together with the envelope adopted for California HSR [15]. The European envelopes are taken from the GB and GC reference profiles defined in [36] but with the width reduced to the maximum width of the trains. Both European and Asian HSTs have widths close to the envelope widths in Figure 2-4, but may be significantly shorter than the static envelopes.

The European Infrastructure TSI [39] states the reference aerodynamic cross-sectional area for each envelope: 11 m² (118 ft²) for GB and 12 m² (129 ft²) for GC. Note that these numbers are smaller than the geometric cross-sectional areas of the envelopes presented, because the trains do not occupy the entire static envelope. Rolling stock dimensions in English and metric units are shown in Table 2-1.

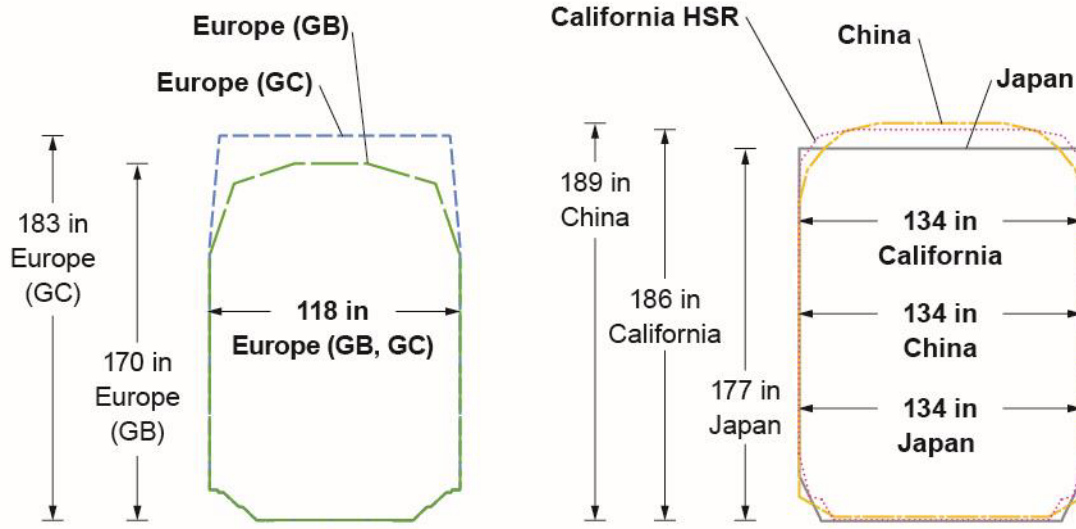


Figure 2-4. Comparison of rolling stock static envelopes. Heights are measured from top of rail (TOR) [15][19][119]

Table 2-1. Rolling stock dimensions

Rolling Stock Profile	Maximum Width ¹	Maximum Height ^{1,2}
Europe (classed as GB)	118 in (3.0 m) ³	170 in (4.32 m)
Europe (classed as GC)	118 in (3.0 m) ³	183 in (4.65 m)
California HSR [15]	134 in (3.4 m)	186 in (4.72 m)
China [19]	134 in (3.4 m)	189 in (4.8 m)
Japan [119]	134 in (3.4 m)	177 in (4.5 m)

Notes:

1. Rolling stock dimensions provided do not account for rooftop equipment or signs and lights mounted to either side of vehicles.
2. Height dimensions taken from top of rail (TOR).
3. This is the maximum width of the rolling stock. The width of the GB/GC reference profiles is 124 in (3.15 m).

2.3.2 Baseline Train Dimensions and Aerodynamics Properties

To design the infrastructure for HSR, designers need to know the aerodynamic properties (including relevant cross-sectional dimensions) of the trains that will cause the aerodynamic loading.

In this report, the term **Baseline Train** means a set of dimensions and aerodynamic properties which are intended to be used as follows:

- As values for use in calculations during design, when the properties of the actual trains are not available or are still to be assessed.
- Where the designer wishes to allow for a range of possible trains.
- To enable use of simpler methods, e.g., a look-up table instead of a complex calculation, when the properties of the actual trains are known and accord with the limiting values given for Baseline Trains.

Much of the technical detail in this manual is derived from international practice and is intended to replicate the aerodynamic conditions occurring in those operations; therefore, Baseline Train properties are based on typical HSTs available commercially rather than the maximum values permitted in regulations. Thus, when extrapolating for trains that have properties different from the baseline values, the “pivot point” represents successful operation experience. Furthermore, because the Baseline Train properties have been selected to lie toward the conservative end of the range of actual train properties, infrastructure designed using these properties should enable a wide choice of commercially available HSTs to be used. However, the authors cannot guarantee that all commercially available HSTs will conform to the Baseline Train properties. It is the responsibility of railway designers to work with equipment suppliers to confirm compatibility of the infrastructure design with the train aerodynamic properties.

Because U.S./U.S. HSR operators might choose to source trains of European or Asian sizes, two sets of Baseline Train data are given and referred to in this manual as **U.S./Euro Baseline Train** and **U.S./Asian Baseline Train**. [Table 2-2](#) sets out the dimensions and aerodynamic properties of the Baseline Trains. Guidance in this manual stated as applicable to Baseline Trains may be applied to operations where the trains accord with the values given in [Table 2-2](#). If the actual trains exceed the limits stated for U.S./Euro baseline but are within the limits stated for U.S./Asian baseline (for example, if the trains were 126 in (3.2 m) wide), guidance for U.S./Asian baseline may be followed.

There is no implication that trains larger than these, or whose properties do not conform to those detailed in [Table 2-2](#), should be avoided. Operators can allow for larger or less aerodynamic trains by following the approaches described in this report. Conversely, if the trains to be used are smaller or have better aerodynamic performance than the Baseline Trains given below, this can be considered in the assessments to design more economic infrastructure. For example, if the trains have a cross-sectional area 10 percent smaller than the 118 ft² (11 m²) reference area of the U.S./Euro Baseline Train, then the tunnels can be designed approximately 10 percent smaller than would be required for the U.S./Euro Baseline Trains; see [Section 7.6](#).

Table 2-2. Properties of U.S./European and U.S./Asian Baseline Trains referenced in this report

		U.S./Euro Baseline	U.S./Asian Baseline
Maximum width (static envelope)		121 in (3.07 m) ¹	134 in (3.4 m)
Maximum height from TOR		170 in (4.32 m)	189 in (4.8 m)
Maximum aerodynamic cross-sectional area		118 ft ² (11.0 m ²)	129 ft ² (12.0 m ²)
Maximum length		1,312 ft (400 m)	1,410 ft (430 m)
Maximum peak-to-peak pressure pulse, under TSI test conditions, defined in Table 2-3 ²		0.087 psi (600 Pa) ³	0.109 psi (750 Pa) ⁴
Maximum slipstream air velocity relevant to safety of track-side workers under TSI test conditions, defined in Table 2-3 ²		43 mph (19 m/s) ⁵	50 mph (22 m/s) ⁴
Maximum slipstream air velocity relevant to passengers on platforms under TSI test conditions, defined in Table 2-3 ²		29 mph (13 m/s) ⁶	33 mph (15 m/s) ⁴
Characteristic Wind Curves better than the Reference Curves given in Section 6.6.3.2		Yes	Yes
Passes TSI tunnel-entry pressure wave test, described in Section 7.6.17		Yes	See note below ⁷
Minimum dynamic sealing time constant for aural comfort in tunnels (see Section 7.3.7)	Lower comfort	10 s	10 s
	Higher comfort	18 s	18 s

Notes:

1. European HSTs are up to 118 in (3.0 m) wide. The maximum width given here accommodates trains that may be procured in the U.S. in the future which are slightly wider than European ones. The increase of width compared to the European trains is considered small enough that European-based aerodynamics guidance can still be followed.
2. Tests described in Section [2.6](#), conditions defined in [Table 2-3](#) including the train speeds and measurement positions at which the quoted limits apply.
3. Upper bound of existing European HSTs. TSI limit is 800 Pa (0.116 psi).
4. Extrapolated from upper bound of European HSTs, allowing for increased width.
5. Upper bound of existing European HSTs. TSI limit is 22 m/s (50 mph).
6. Upper bound of existing European HSTs. TSI limit is 15.5 m/s (35 mph).
7. To allow for their larger cross-sectional area, the test for the U.S./Asian Baseline Train may be performed with a 740 ft² (68.7 m²) tunnel.

The Baseline Train values in [Table 2-2](#) for pressure pulse and slipstream velocity are lower (i.e., better aerodynamically) than the maximum values permitted by international regulations. This is because the baseline properties encompass values from currently available trains, whereas the regulations were set so as to include the trains available at the time the regulations were established, and aerodynamic design has improved in the intervening years. This principle is illustrated in [Figure 2-5](#).

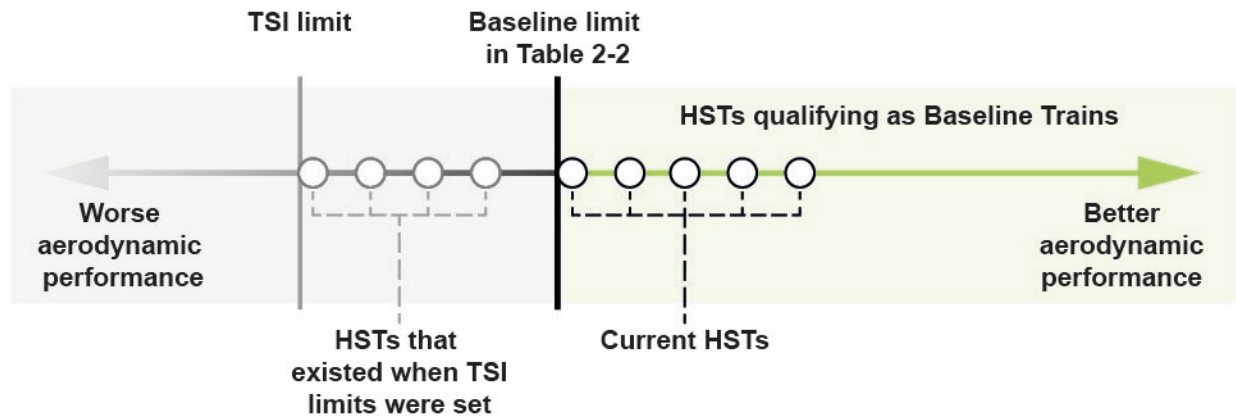


Figure 2-5. Principle used in setting Baseline Train properties

2.4 Testing and Numerical Simulation Methods

Aerodynamic testing and numerical simulation methods include:

- Full-scale testing: Measuring instruments are set up alongside an existing railway to record data from the regular operation or from specially arranged train passages at a pre-planned speed.
- Reduced-scale moving model testing, carried out in a specialist laboratory in which scale model trains are fired along a track at high speeds. Features such as wayside structures or tunnels are created at the same geometric scale as the trains.
- Wind tunnel testing, in which wind is blown across a stationary, reduced-scale model, used mainly to evaluate aerodynamic properties of railcars.
- Computational Fluid Dynamics (CFD)
- One-dimensional Pressure Wave Simulation for tunnels

2.4.1 Full-Scale Testing Methods

Full-scale testing is used to obtain aerodynamic coefficients for a train or for a train/structure combination. These may be used in developing train design, assessing wayside structure designs, confirming that the investigated train design or operation meets the required specification for conformance purposes, or providing data against which numerical models may be calibrated.

Full-scale testing is the benchmark against which other techniques are judged, but it has some disadvantages, such as:

- Logistical issues around access to trains and track
- Availability and set-up of measuring equipment
- Scheduling and extent of staffing to conduct the tests
- Expense
- Tests may have to be cancelled or rescheduled due to unfavorable weather.
- Even if the tests go ahead, measurements may be affected by environmental disturbances such as naturally occurring wind.

The variables most commonly measured are air velocity (for example, to characterize the slipstream) and air pressure (for example, to characterize the nose and tail pressure pulse). Measurements may be made either in the open environment or inside tunnels. The airflow around trains is very turbulent, which causes high test-to-test variability in air velocity measurements. Tests should incorporate a large number of runs in order to obtain a statistically reliable result.

Internationally adopted testing procedures include the following points:

- For open track, the required measurement positions are defined in terms of horizontal distance from the track centerline and vertical distance from top-of-rail (TOR). Tripods, frames, or similar methods are used to support the instruments at the correct position relative to the track.
- In tunnels, instruments would normally be fixed to the tunnel wall.
- For open-track measurements (where the track is not adjacent to platforms and other linear structures) the test site is to be straight, level, representative of track type and ballast height, and should not contain atypical features that concentrate the airflow or shelter the instruments such as buildings, hills, trees, etc.
- Even though certain regulatory acceptance tests are described as being relevant to passengers on platforms, the tests are performed on open track without a platform. This is because the worst case for passengers is a low platform, but these have limited influence on test results and suitable test sites with a low platform are hard to find.
- Measurements above a platform may be useful for research purposes. In that case, the site should have a representative platform design and height and be free of features that might affect the airflow or shelter the measurement probes from the effects of the train differently from the platforms being researched.
- The ambient temperature, pressure, and wind speed, along with actual speed of the train should be recorded.
- Train speed should be within 5 percent of the investigated train speed for at least 50 percent of the runs. Any runs with train speed not within 10 percent of the investigated speed should be discarded.

- Results should be scaled from the actual train speed to the investigated train speed, assuming that air velocity is proportional to train speed and pressure is proportional to train speed squared.
- Pressures are measured with pitot-static probes.
- Air velocity is measured with sensors capable of measuring flow in both longitudinal and lateral directions.
- Air velocity time-histories are filtered with a 1-second rolling average.
- Recording of measurements should begin at least 1 second before arrival of the train and continue at least one second (for pressure measurements) or 10 seconds (for air velocity measurements) after the tail of the train has passed.
- For pressure pulse measurements, a minimum of 10 runs is recommended, although in practice a smaller number may be used because test-to-test variability is usually small in the absence of crosswinds.
- For measurements of slipstream air velocity, test-to-test variability is much greater (due to the very turbulent and unsteady nature of the airflow around the train), and therefore a minimum of 20 runs is required.
- It is common practice to use multiple sets of instruments repeated along the track direction. This practice offers backup in case of instrument failure and can provide a greater number of independent measurements for the same number of actual train passages, thus increasing the statistical reliability of the results. The spacing along the track between the sets of instruments should be at least 67 ft (20 m) to ensure that the measurements are aerodynamically independent of each other.
- Results are often quoted as the upper 95 percent confidence limit (also called the **characteristic value**), defined as the mean of the measured values plus two standard deviations.
- It may be necessary to test different train configurations, including multiple trainsets.

Further details are given in EN 14067-4 [33], which includes information about testing in the open environment. For example, the standard gives the acceptable range of atmospheric conditions during testing and how to modify the results for conditions that vary from the assumed standard conditions. EN 14067-5 [34] includes information about testing in tunnels, and EN 14067-6 [35] includes information about testing related to safety in crosswinds.

Full-scale testing may also be used to assess drag, as described in Section 9.6.2.1.

2.4.2 Reduced-Scale Moving Model Testing

Scale model trains are propelled along a model track at high speed. Scale models of platforms, ballast shoulders, tunnels, walls, or other structures may be placed next to or over the track as required. Typical objectives of testing include:

- Estimating the pressure pulses or slipstream air velocities for a particular train
- Verifying the relationships of air pressure or air velocity with distance from the track
- Measuring the air pressures acting on different types of wayside structures
- Assessing the air pressure exerted by one train on another train on an adjacent track
- Studying tunnel aerodynamics issues such as the design of tunnel entrances to mitigate micro-pressure waves

Scale model testing provides a relatively quick and inexpensive tool for research and design purposes, but it should not be used to prove conformance to acceptance test requirements (only full-scale tests are considered acceptable for this purpose).

Reduced-scale moving model test facilities include those developed in Japan (Railway Technical Research Institute [RTRI]), Korea, China (Southwest Jiaotong University, Central South University, and Chinese Academy of Sciences), Germany (Deutsches Zentrum für Luft- und Raumfahrt e.V. [DLR]), and the UK. An example is shown in [Figure 2-6](#). This is the TRansient Aerodynamic INvestigation (TRAIN) testing rig in Derby, England, operated by the Birmingham Centre for Railway Research and Education, Birmingham University, England.¹ Twenty-fifth scale model trains are propelled down a 500 ft (150 m) long track by a catapult system [\[7\]](#).

¹ Further information may be found at <https://www.birmingham.ac.uk/research/railway/research/train-rig.aspx>



Figure 2-6. The “TRAIN rig” reduced-scale moving model testing facility in Derby, England, set up to measure pressure on a short overhead canopy; photo courtesy of Birmingham Centre for Railway Research and Education

Train models should accurately represent the shapes of the nose and tail and have a good representation of the trucks, inter-car gaps, and train exterior surface features. Typically, a moving model consists of the leading and trailing vehicle with two or three intermediate cars (**shortened train**). Most testing facilities cannot accommodate models of a full-length train. The effect of using shortened trains on pressure pulses is small. The effect is assumed to be small for air velocities also. The shortened train is likely to have a narrower boundary layer than a full-length train, but the influence of train length on the wake (where the highest air velocities occur) has not been fully resolved. When interpreting results, no adjustment is made for the fact that the scale model train is shorter than the real-life train.

The same geometric scale should be applied to the train, any models of structures, the distances between structures and track, and measurement positions relative to the track and ground. Where the measurements are intended to represent airflow above platforms, the platform should be modeled with the correct scaled height and overhang at the platform edge. Likewise, where the measurements are intended to quantify airflow on open track and where the real-life track is on ballast, the shape and height of the ballast shoulder should be included in the scale model.

While the geometric scale of the trains and structures is reduced, the geometric scaling factor is *not* applied to the speed at which the model trains are propelled. Speeds of the model trains should be of the same order of magnitude as the real-life operating speeds. For measuring pressures or air velocities in the open environment, results measured at one train speed can be scaled to predict the results at a different train

speed (see Section 2.4.3), so it is not important for the model to match the real-life train speed exactly. Typically, the model speed for open-environment tests is within a factor of about 2–3 of the real-life speed. For tunnels, however, the speed of the model should be the same as the real-life speed. This is because results depend on the train speed relative to the speed of sound in air, which is the same in the scale model as in real life.

In practice, the capability of the testing facility may limit the speed. The maximum speed of the TRAIN rig in Derby, England is 140 to 180 mph (225–290 km/h), depending on the weight of the train model, while the maximum speed of the facility operated by the Chinese Academy of Sciences is 310 mph (500 km/h).

Instruments for measuring velocity and pressure are the same as for full-scale testing and wind tunnels, but high data capture rates are required (typically of the order of 10,000 samples per second). To allow for test-to-test variability, several nominally identical runs (similar to the requirements for full-scale testing) should be performed, typically 5–10 for pressure measurements or at least 20 for air velocity measurements.

When interpreting reduced-scale model results to estimate full-scale results, the following scaling laws apply. These are to remove the effect of geometric scaling and are additional to the scaling required for train speed described in Section 2.4.3.

- After correcting for train speed, pressures and air velocities are expected to be the same at full-scale as at reduced-scale.
- The time axis on graphs should be multiplied by the geometric scale. For example, time measured in a 1/25 scale model should be multiplied by 25.
- Results are first converted to full-scale before applying any required filtering.
- Results are then processed in the same way as full-scale measurements, for example a rolling 1-second average is applied to air velocity time-histories.

A reasonably close agreement is obtainable between full-scale and reduced-scale moving model tests on this basis – for example, 5 to 10 percent for pressure coefficients, and within the standard uncertainty of the experiments for slipstream velocity coefficients [8].

2.4.3 Guidelines for Adjusting Test Results to Different Train Speeds

When estimating responses at different train speeds for the open environment, the following rules can be applied (for instance, when results are available from tests carried out with a slower train speed than the intended operating speed). This applies to full-scale and reduced-scale measurements.

- Air pressure scales with the train speed squared. For example, the pressure on a certain structure at a train speed of 250 mph is four times the pressure on the same structure at a train speed of 125 mph.
- Air velocity scales linearly with train speed. For example, the air velocity experienced by a track worker for a train speed of 250 mph is twice the air

velocity experienced by the same track worker at the same distance for a train with a speed of 125 mph.

- The time axis of graphs of response versus time scales linearly with the inverse of the train speed. For example, the time gap between the nose pressure pulse and the tail pressure pulse is half as great at 250 mph compared with 125 mph because the train passes twice as quickly.

As an approximate guideline, these rules may be taken to apply at all speeds. For higher train speeds (above about 185 mph, or 300 km/h) a “Mach number correction” may be applied for greater accuracy. However, the increase of accuracy is usually small compared with the uncertainties and variability of the source data, and furthermore the correction factor is valid only for 2-dimensional situations. Therefore, this study does not recommend Mach number corrections. Further information may be found in the FRA [High-Speed Rail Aerodynamic Assessment and Mitigation Report \[49\]](#), Section 3.5.2. Uncertainties in this regard can be avoided by conducting tests only at the speed for which results are required, thereby eliminating the need to scale results, if the required speed is greater than 185 mph (300 km/h).

The above rules apply to open-environment phenomena. In tunnels, the same rules apply to the amplitude of pressure waves generated when a train first enters a tunnel but for most other aerodynamic phenomena the situation is more complex. Results depend on the speed of propagation of pressure waves (the speed of sound) as well as on the speed of the train, and therefore results cannot simply be scaled to different train speeds. Testing related to tunnels should be carried out at the actual train speed. If this is not possible, numerical simulations may be validated against tests carried out at a lower speed, and further simulations used to predict results at the actual train speed.

2.4.4 Wind Tunnel Testing

Rail vehicle designers mostly use wind tunnel testing to measure the aerodynamic properties of proposed new railcar designs; for example, the properties relevant to overturning in crosswinds or drag. Since this manual is not primarily intended for rail vehicle designers, description of wind tunnel testing is limited to points that may be relevant when selecting or specifying rolling stock or using wind tunnel-derived data in crosswind safety assessments.

Wind tunnel testing may be used as a complementary technique with computational fluid dynamics (CFD) during design development. For example, wind tunnel test cases can be used to check the accuracy of CFD models before using CFD to develop the final design; and/or, a design developed using CFD could be validated by wind tunnel testing.

Challenges for wind-tunnel testing include:

- Wind tunnel testing is best suited to measuring characteristics of single vehicles, or trains consisting of a small number of vehicles only. The facilities are usually not long enough to include a whole train. The influence of using shortened trains on the accuracy of measurements of pressure pulses and slipstreams has been described in Section [2.4.2](#).

- For applications such as slipstreams and drag, results may be dependent on small details of the full-scale design that are difficult to incorporate in the models being tested.
- Results may be influenced by the fact that the train remains fixed relative to the ground. The air flow pattern is different when the train moves relative to the ground, as in the real-life situation. This becomes more problematic with longer train models, as the boundary layer becomes wider with increasing train length, and when the train does not move relative to the ground, a similar thick boundary layer develops on the ground (which is not realistic). Some facilities incorporate a moving belt either side of the train to counteract this, but it does not fully solve the problem.

2.4.5 Computational Fluid Dynamics

CFD can be used for many of the same purposes as reduced-scale moving model testing and wind tunnel testing. Compared with testing, CFD can offer greater insights into the airflow around trains, and hence, understanding of the reasons behind the results. However, the techniques necessary to obtain accurate simulations may in some cases involve long simulation times and heavy computational demand as well as requiring a high level of expertise. In general, CFD is of greatest use in assessing railcar designs. With regard to aerodynamic assessments of infrastructure, CFD has some specific uses where regular guidelines or methods do not exist or do not apply.

It is not the purpose of this report to provide detailed instructions on CFD simulations, which would likely be carried out by specialists. These notes are intended primarily for readers considering commissioning CFD analysis, rather than for the specialists who would carry it out.

Among the applications of CFD to HSR aerodynamics:

- Optimization of railcar designs and predicting their aerodynamic properties
- Understanding aerodynamic loads on wayside structures in cases not covered by standard guidelines in [Section 4](#)
- Predicting airflows in enclosed or underground stations
- Analyzing certain aerodynamic issues in tunnels where 3D effects are important (examples given in [Section 7.6.7](#)), but not pressure wave effects in general, which can be treated more efficiently with specialized one-dimensional analysis techniques
- Predicting pressure wave characteristics relevant to micro-pressure waves ([Section 8](#)), including entry of trains into tunnels of different shapes and sizes, the design of tunnel entrance hoods (described in [Section 8.6.2.5](#)), and pressure waves generated when trains pass geometric discontinuities inside the tunnel such as air shafts

CFD techniques vary according to the goal of the simulations:

- For predicting pressure pulses or steady-state aerodynamic pressure coefficients, the choice of turbulence model is often not critical to results and a Reynolds Averaged Navier-Stokes (RANS) [93] method can be used, or even the Euler solution method, which does not model turbulence at all.
- Where slipstream air velocities or the dynamic variation of pressure loads are of interest, capturing the unsteady nature of the airflow becomes much more demanding computationally: unsteady flow methods such as Large Eddy Simulation (LES) [67] or Detached Eddy Simulation (DES) [103] are required, typically with millions or tens of millions of nodes.
- For pressure wave simulations (which mostly relate to tunnels), the technique used must model unsteady compressible flow. The choice of turbulence model is usually not critical.
- In any application in which a fixed structure (such as a tunnel) is modeled along with the train, a method of having the train move through the air mesh is needed. For example, a tube of moving mesh located around the train with a “sliding interface” to the fixed mesh around the structure [68].
- Care should be taken that the extent of the domain is large enough that the artificial model boundaries do not influence results. In other words, if the model were extended to a greater distance from the region of interest, the results should not be affected significantly.
- The mesh (grid) size should be small enough to capture results with sufficient accuracy.
- When simulating pressure waves, the timestep is another important consideration. Depending on the solution method, it may be necessary to reduce the timestep to a value less than the **Courant timestep** (the time taken for a pressure wave traveling at the speed of sound to cross the smallest element).

2.4.6 One-dimensional Pressure Wave Simulation

Pressure wave effects in tunnels are typically assessed using specialized software that performs one-dimensional simulation of unsteady compressible flow. Here, “one-dimensional” means that conditions such as pressure and air velocity vary only along the longitudinal axis of the tunnel and not across the tunnel cross-section, and where flow is assumed to occur in the longitudinal axis direction only. This simplification enables simulations to be completed orders of magnitude faster than by a full 3D CFD calculation, while the software also includes features to represent the trains and typical features of HSR tunnels with minimal effort from the user. Further details are given in Section 7.6.5.

2.5 Codes, Standards, and Best Practices

There are currently no U.S.-established codes, standards, or best practices specifically related to HSR aerodynamics. Some relevant international standards and advisory documents available in English are summarized below. These are principally pan-European documents containing material on which consensus has been reached

among the contributing countries. However, several other aerodynamic issues are regulated by separate national standards which differ from country to country. The countries with greatest experience of HSR, such as Japan, China, France, Spain, and Germany do not publish their national standards in English (with some exceptions).

Standards that are applicable only to specific aerodynamic topics are described in the relevant section of this manual, for example those related only to crosswind safety are covered in Section 6.

2.5.1 EN 14067

The European standard EN 14067 applies to rail aerodynamics, and consists of six parts, of which one has now been withdrawn. The standard includes some acceptability criteria and much useful information regarding test methods and results processing.

- EN 14067 Part 1 [30] defines symbols and units.
- EN 14067 Part 2 [31] has now been withdrawn, and its contents absorbed into Part 4.
- EN 14067 Part 3 [32] gives a general introduction to HSR aerodynamic phenomena for the tunnel environment.
- EN 14067 Part 4 [33] is applicable to open-environment operations. This section contains detailed descriptions of requirements for full-scale testing and reduced-scale testing, the methods by which key test results (such as slipstream velocities, pressure pulse amplitudes, etc.) should be calculated, acceptability criteria, formulae for pressure loading on trackside structures, and some guidance on CFD analysis. A description of test procedures for rolling stock relevant to ballast flight is included; this is labelled “informative” (non-mandatory).
- EN 14067 Part 5 [34] is about tunnel aerodynamics. Testing as described in this standard is used to confirm compliance with the nose-entry pressure wave requirements of the Rolling Stock TSI described in Section 7.6.17. This part of the standard also contains guidance on topics such as pressure loading on trains in tunnels and assessing scenarios in which trains pass or meet within the tunnel. It provides formulae from which pressure wave amplitudes and drag in tunnels may be estimated. At the time of writing, a new revision of this standard is in preparation [112]. Descriptions regarding these issues may be found in Section 7.
- EN 14067 Part 6 [35] is concerned with crosswind assessment and the associated aerodynamic tests. The standard gives extensive guidance on the crosswind stability assessment of railcars, but methods of route risk assessment are lacking due to absence of agreement between the countries involved. The standard therefore provides only a partial methodology. Further description is given in Section 6.

Future revisions of this standard may include a separate document on ballast flight, which is in preparation at the time of writing.

2.5.2 *European Technical Specifications for Interoperability (TSIs)*

The European Technical Specifications for Interoperability (TSIs) consist of Europe-wide legal requirements for HSR. The scope of the TSIs covers operating speeds up to 350 km/h (220 mph).

The TSIs cover mostly non-aerodynamic requirements together with a few aerodynamic ones. The overall objective of the TSIs is to enable interoperability across the countries of Europe; for example, infrastructure designers in one country can assume certain aerodynamic performance of the HSTs that will operate on the infrastructure, even if those HSTs originate in a different country. There are 11 TSIs at the time of writing, of which 2 contain requirements directly related to aerodynamics: the **Rolling Stock TSI** [39] and the **Infrastructure TSI** [38].

The TSIs include the following points relevant to aerodynamics, many of which mirror and refer to information given in EN 14067:

- Maximum cross-sectional dimensions and profiles of railcars (see Section 2.3.1 above)
- Aerodynamic cross-sectional area for each profile
- Aerodynamic acceptance criteria for HSTs (given in Section 2.6 below)
- Methods by which the above should be measured
- Requirement for peak-to-peak pressure variation in tunnels not to exceed 10 kPa (1.45 psi), the so-called Medical Safety Limit, described in Section 7.6.15.1. See Infrastructure TSI [38] Section 4.2.10.1. The criterion applies to the pressure outside the train and is intended to protect passengers from permanent injury in the event of a sealing system failure or broken window.

Also relevant is the TSI for Safety in Tunnels [40]. Like National Fire Protection Association standard NFPA 130 [105], this TSI does not directly mention aerodynamics but its requirements strongly influence the design of tunnels and therefore impact on aerodynamics.

2.5.3 *Union Internationale de Chemins de Fer (UIC) Leaflets*

UIC Leaflet 779-1 [77] provides the same formulae as EN 14067-4 for assessing pressures on wayside structures, together with additional information relevant to the design of structures that may be subject to fatigue failure from aerodynamic loading, such as noise barriers or wind barriers.

UIC Leaflet 779-11 [77] contains information on pressure waves in tunnels, such as guidance and charts for selecting cross-sectional area for tunnels, background information on the Medical Safety Limit, and notes on pressure tightness of trains.

UIC Leaflet 660 [78] sets out further pressure comfort criteria for sealed trains and describes pressure tightness tests for trains.

2.5.4 Chinese Standards and Regulations

The People's Republic of China has several standards, regulations, and operational procedures related to HSR. These are contained in documents issued by the Ministry of Railways, China State Railway Group (China Railway), and other agencies. Most of these documents are not available in English (with the exception of the Code for Design of High-Speed Railway [99]).

Chinese aerodynamic acceptance criteria (such as slipstream speeds) and prescribed mitigation measures (minimum track spacing, platform safety distances, etc.) sometimes differ from their European equivalents. Nevertheless, European standards and TSIs are often used in China as references for details of test procedures (locations of pressure probes, number of test runs, etc.), since Chinese documents often do not specify such details.

China is currently developing a set of standards which will be similar in scope to EN 14067.

Normative documents currently used in China include the following information:

- Pressure comfort criteria for pressure changes inside the trains passing tunnels [21][100], given in Section 7.6.15.3
- Operational procedures related to crosswind safety [20][21], described in Section 6.5.5
- Acceptance criteria for micro-pressure waves [99], given in Section 8.6.3.1
- Criteria for aerodynamic drag performance [21][101], referenced in Section 9.6.3
- Criteria for maximum amplitude of a pressure wave generated when two trains meet at their maximum operating speeds in open air or in a tunnel [21][100][101], of which the upper limit is given in Section 7.6.16
- Minimum tunnel cross-sections [99], given in Section 7.6.4.1
- Criteria for safety of passengers on platforms, based on slipstream speed and wind force load on human body [20][100], given in Section 3.6.1
- Criteria for minimum safe distances for wayside workers and passengers [20][99], given in Sections 3.5.1 and 3.5.2

2.5.5 Japanese Standards

Despite being at the forefront of HSR aerodynamics internationally, Japan does not publish formal standards on this subject. Japanese practices have been referred to where appropriate elsewhere in this manual.

2.5.6 American Standards Having an Impact on Aerodynamic Design

National Fire Protection Association standard NFPA 130 [105] is related to fire safety and is not directly concerned with aerodynamics; but, its requirements do have an impact on aerodynamic design of tunnels. This is described further in Section 7.7.2.

2.6 European HST Aerodynamic Acceptance Criteria

In Europe, aerodynamic acceptance criteria for HSTs are mandated by the Rolling Stock TSI [39]. They are not mandatory in the U.S., but operators may wish to adopt them voluntarily or use them for reference when specifying new rolling stock. The purpose of the acceptance tests is to enable aerodynamics guidelines for infrastructure and operations that are independent of particular train designs. The acceptance tests effectively define a minimum standard of aerodynamic performance of the rolling stock that can be assumed when designing infrastructure or setting operating procedures to mitigate aerodynamic risks. The guidelines given in this report for baseline trains assume aerodynamic performance that at least meets these acceptance tests, or, in several cases, performance that is more demanding than the test criteria. This is explained in Section 2.3.2.

Table 2-3 below sets out the European HST aerodynamic acceptance criteria. The criteria must be met with the longest intended train formation, including multiple trainsets coupled together, if applicable. For HSTs not capable of operating at the stated speeds below, different rules apply – these may be found in the TSIs and in EN 14067 [30].

Table 2-3. HST Aerodynamic Acceptance Criteria from European TSI

Test condition and purpose	Measurement point	Train speed during test	Acceptance limit and TSI clauses	Further details
Pressure pulse, measured on open track	2.5 m (8.2 ft) horizontally from track center, 1.5 to 3.0 m (5 to 10 ft) above TOR	250 km/h (155 mph)	800 Pa (0.12 psi) peak-to-peak Rolling Stock TSI 4.2.6.2.2 and 6.2.3.14	See 2.4.1 and Figure 2-7.
Slipstream air velocity relevant to safety of track-side workers, measured on open track	3.0 m (10 ft) horizontally from track center, 0.2 m (8 in) above TOR	300 km/h (186 mph)	22 m/s (50 mph) (1 second rolling average, upper 95% confidence limit) Rolling Stock TSI 4.2.6.2.1 and 6.2.3.13	See 2.4.1 and Figure 2-7.
Slipstream air velocity relevant to passengers on platforms, measured on open track	3.0 m (10 ft) horizontally from track center, 1.4 m (4.6 ft) above TOR	200 km/h (124 mph)	15.5 m/s (35 mph) (1 second rolling average, upper 95% confidence limit) Rolling Stock TSI 4.2.6.2.1 and 6.2.3.13	See 2.4.1 and Figure 2-7.
Tunnel entry pressure wave	63 m ² (678 ft ²) tunnel	250 km/h (156 mph)	Pressure change limits as described in Section 7.6.17. Rolling Stock TSI 4.2.6.2.3 and 6.2.3.15	See Section 7.6.17.

Test condition and purpose	Measurement point	Train speed during test	Acceptance limit and TSI clauses	Further details
Crosswind Characteristic Wind Curve (CWC)	Most vulnerable railcar, 90% wheel unloading		See Figure 6-6 . Rolling Stock TSI 4.2.6.2.4, referencing EN 14067-6 [35]	See Section 6.6.3.2 .

Further information about these criteria:

- The **pressure pulse** acceptance criterion is relevant to pressure loading on wayside structures (Section [4](#)) and train-to-train aerodynamic interactions (Section [5](#)).
- The **slipstream air velocity** acceptance criterion relevant to safety of track-side workers is measured at 0.2 m above rail height because workers may be standing beside a ballast shoulder on ground that is lower than the track.
- The **slipstream air velocity** acceptance criterion relevant to the safety of people standing on platforms is measured 1.4 m above rail height. The testing is now carried out on open track without a platform being present. The requirement for testing with a platform was dropped some years ago due to the difficulty of finding suitable test sites.
- The **tunnel entry pressure wave** criteria are relevant to pressure wave effects in tunnels and enable tunnel sizing charts or tables such as those given in Section [7.6.4](#). Further information about the testing is given in Section [7.6.17](#).
- The **crosswind Characteristic Wind Curves** provide a level of resistance to overturning and derailment in strong wind gusts and enable crosswind risk assessments of new routes.

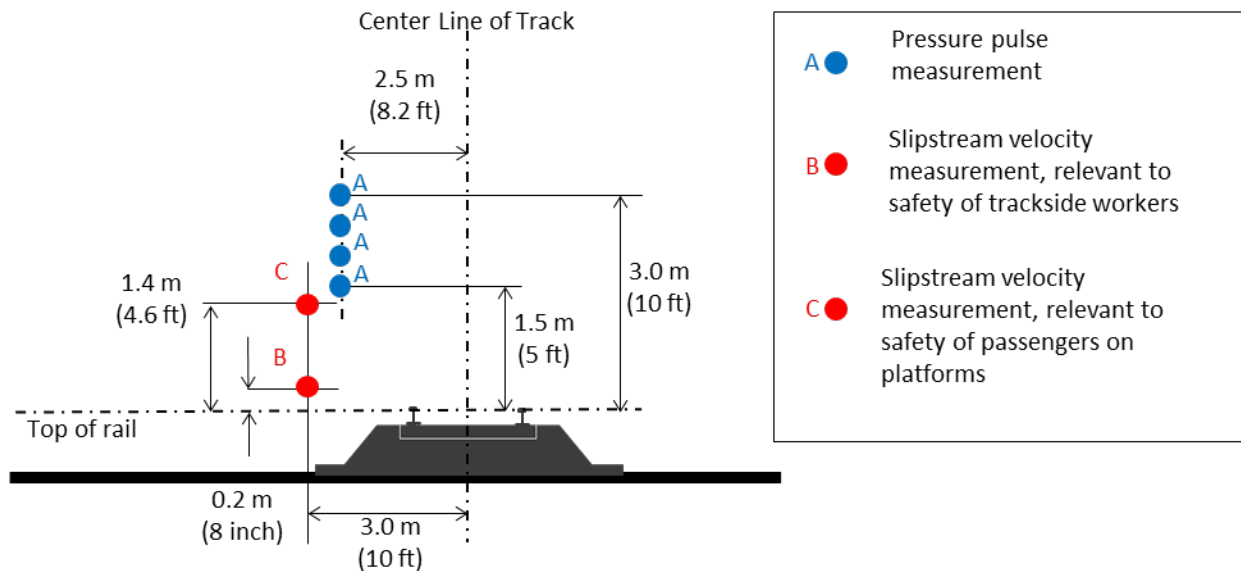


Figure 2-7. Measurement positions for European Rolling Stock TSI aerodynamic acceptance tests in the open environment

2.6.1 Tunnel-Entry Pressure Gradient Test (Future Addition)

The new revision of the European standard on tunnel aerodynamics [112] has added an acceptance criterion for rolling stock which specifies the maximum *gradient* of the nose-entry pressure wave in the tunnel-entry test. This relates to micro-pressure waves (described in Section 8) and is intended to ensure that new HSTs are no more prone to generate problematic micro-pressure waves than other typical HSTs. The new criterion is not yet mandatory at the time of writing but may become so in future revisions of the Rolling Stock TSI. Further details are given in Section 8.6.3.3.

2.7 Unit Systems for Equations

Where possible, equations in this report are provided in a format allowing flexibility regarding the units of the input terms. Any particular units required or assumed are noted below each equation.

Many of the more complex equations and formulae are described in the report as requiring **consistent units**. This means a system of units in which the basic equations of physics can be applied correctly without the use of conversion factors. For example, take Newton's second law:

$$Force = mass \times acceleration$$

SI units (Newtons, kilograms, meters, seconds) are consistent because equations like Newton's second law can be applied without conversion factors:

$$1\text{ N} = 1\text{ kg} \times 1\text{ m/s}^2$$

In a consistent unit system, derived units must follow from the principal units. For example, in the SI system speed must be in m/s, density must be in kg/m³ and pressures must be in N/m² (also called Pascals, abbreviated to Pa). For equations

requiring consistent units, all the terms in the equation must be in the same consistent unit system.

Consistent unit systems based on English units exist and can be used with the equations in this report if desired – for example, the foot-slug-second-pound force system is consistent – but SI units may result in fewer mistakes and are therefore recommended. The SI and foot-slug-second-pound units systems, together with example data, are given in [Table 2-4](#). Conversion factors between different unit systems may be found readily using internet search engines.

Table 2-4. Consistent unit systems

	SI (recommended)	ft-slug-s-lbf (for information)
Length unit	m	ft
Time unit	s	s
Mass unit	kg	slug
Force unit	N	lbf
Density unit	kg/m ³	slug/(cu ft)
Standard density of air	1.225	0.0023769
Pressure unit	N/m ² (same as Pa)	psf
Standard atmospheric pressure	101325	2116
Speed unit	m/s	ft/s
Speed of sound in air	340	1115.5
Acceleration unit	m/s ²	ft/s ²
Acceleration due to gravity	9.81	32.2

3 Slipstreams

3.1 Introduction

The term **slipstream** refers to the airflow generated alongside and behind a train as it moves. The slipstream is characterized by highly turbulent airflow with random fluctuations of air speed.

Impacts arise from the forces exerted by the slipstream on people and objects close to the track. It is typically the peak “gust” caused by the train, rather than the average air speed that has the potential to cause a safety concern (a notable exception is when strollers/wheelchairs begin rolling after being affected by elevated air speeds over a longer period). In this manual, the speed of this peak gust is referred to as the **maximum slipstream air speed**. Due to the random nature of these gusts, the maximum slipstream air speed varies widely from one train pass to another and cannot be predicted precisely. To address this issue, measured data are treated probabilistically to enable conservative assessments.

Guidelines for mitigating slipstream impacts consist of defining safe distances from the track. These are typically based on operational experience, rather than calculations. It is not possible to make an exact calculation of whether an impact will occur.

This section includes:

- Aerodynamic principles related to slipstreams
- The main influencing factors
- Impacts and mitigation measures for people on platforms
- Impacts and mitigation measures for people near open track
- Impacts on structures and objects
- Impacts on trains on adjacent tracks
- Methods for assessing slipstream air speeds
- Example calculations

3.2 Aerodynamic Principles and Phenomena

A moving train induces an airflow in the general direction of the train motion, consisting of several regions [5], as illustrated in [Figure 3-1](#).

- The nose region, characterized by an area of high pressure and a sudden increase in air speed close to the front of the train. This is not always considered as part of the slipstream as it does not exhibit the highly turbulent flow that characterizes the other parts of the slipstream.
- The boundary layer, containing highly turbulent air alongside the train. The thickness of the boundary layer is typically 2 to 4 ft for HSTs and increases toward the back of the train.

- The near wake, dominated by large-scale unsteady vortices (turbulent, swirling structures in the airflow) spreading laterally behind the train.
- The far wake, in which the air speed gradually decreases.

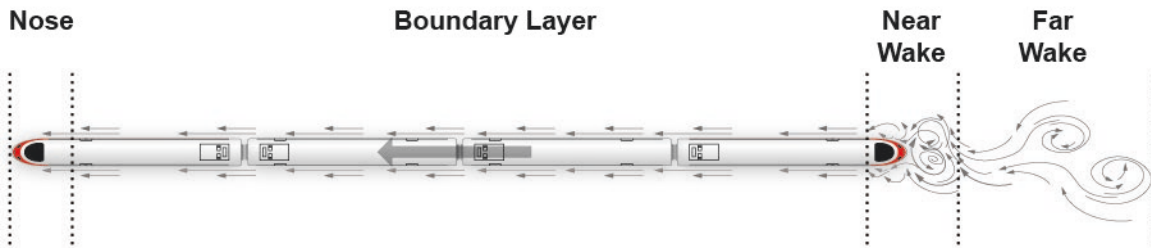


Figure 3-1. Illustration of the airflow around a train, with the regions of the slipstream identified

Collectively, these flow regions are known as the **slipstream**. When measuring slipstream air speed from well-streamlined HSTs at positions to the side of the track, the highest air speeds are usually found in the near wake shortly after the train has passed. Examples of measured air speeds are given in [Figure 3-2](#). The three time histories are from the same train passing the same measurement point at the same speed in three separate runs. Note the large differences from run to run – the maximum slipstream air speed measured is three times greater in Test 1 than in Test 2. This variability is characteristic of turbulent flows.

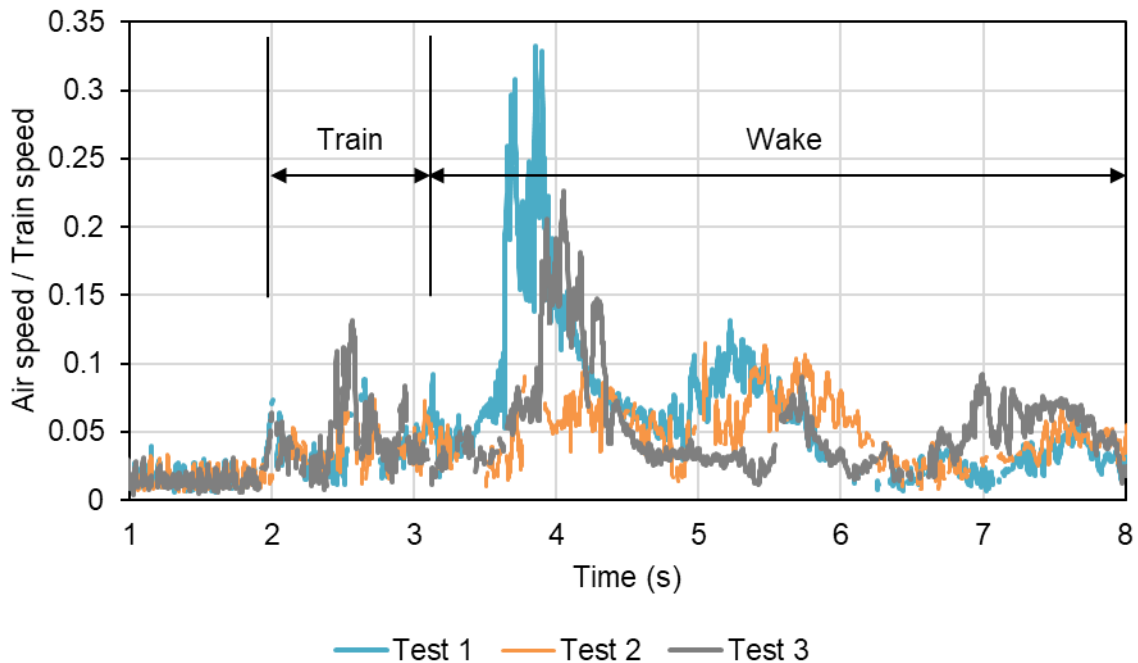


Figure 3-2. Recorded (unfiltered) slipstream air speed data for three nominally identical tests

Test data are typically presented as a **velocity coefficient** c_v , defined as the ratio between the horizontal component of the maximum slipstream air speed and the train speed:

$$c_v = \frac{V_{SS}}{V_T} \quad \text{Equation 3-1}$$

Where:

V_{SS} = Horizontal component of the maximum slipstream air speed; and,

V_T = Train speed.

The velocity coefficient is specific to a given measurement point defined by its horizontal distance from the track center and vertical distance from TOR. The maximum slipstream air speed at the measurement point can be calculated by multiplying the velocity coefficient by the proposed train speed.

The velocity coefficient is also specific to a particular train shape. Lower values indicate a shape that is less likely to generate high slipstream air speeds.

3.3 Influencing Factors

3.3.1 Train Speed

Slipstream air speeds increase proportionally with train speed. This applies to both the average air speed alongside the train and the magnitude of the gusts. Therefore, testing may be carried out at lower speeds and extrapolated to predict induced air speed at the full line speed.

3.3.2 Processing of Air Speed Measurements

Due to the noisy and random nature of slipstream air speed measurements (as shown in [Figure 3-2](#)), the maximum slipstream air speed measured in a single test is not useful. Furthermore, with respect to the impacts of slipstreams on people, these maxima usually do not last long enough to knock over a person. It is therefore necessary to filter the air speed measurements to remove the very short-duration peaks and to take enough measurements to be sure of a representative sample. The results may then be presented simply as a mean value, or else a statistical treatment may be applied to calculate a reasonable upper limit on the likely air speed allowing for random variation. The methods by which these steps are carried out have a large influence on the resulting velocity coefficient, and therefore when comparing velocity coefficients from different tests, it is essential to understand how the test data have been processed to arrive at the stated velocity coefficient and to avoid making direct comparisons of velocity coefficients derived by different methods.

The two most commonly used methods for filtering slipstream air speeds are the 1-second moving average and the 3-second moving average. The effects of applying these moving average methods to the raw measured data are shown in [Figure 3-3](#). This illustrates that differing choices of averaging time result in significantly different

results. There is no reliable means to convert between maximum velocity coefficients obtained from data processed with different averaging times.

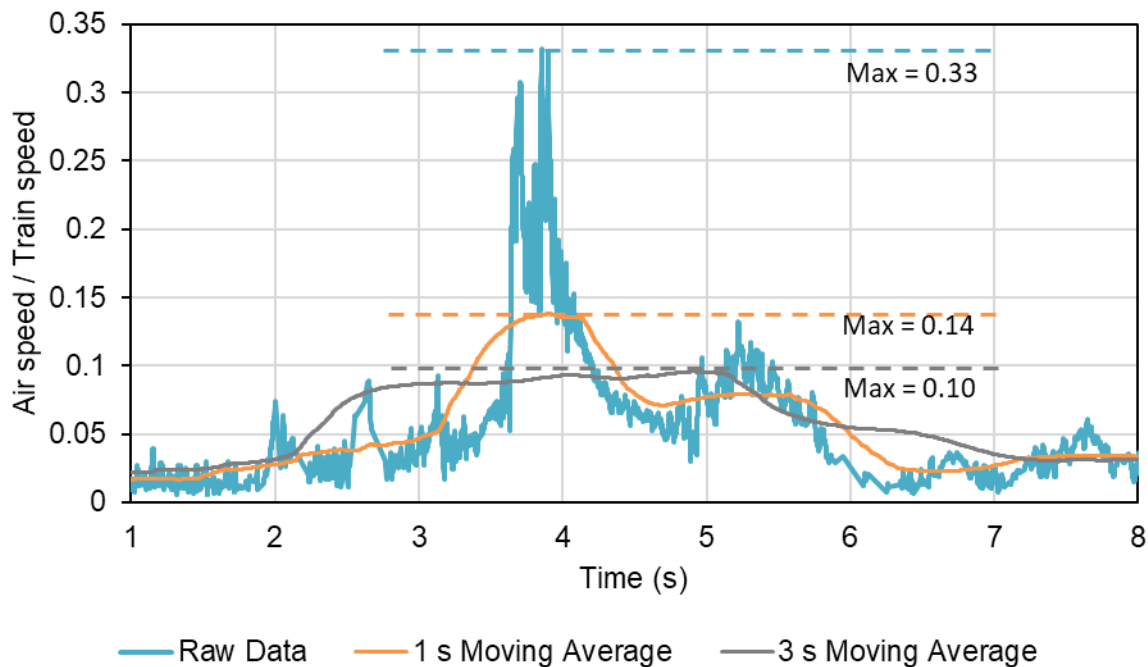


Figure 3-3. Example showing the influence of averaging time on maximum velocity coefficient

For compatibility with the majority of available measurements on HSTs internationally, operators in the U.S. should follow the method specified in the European Rolling Stock TSI [39] (referred to in this document as the **TSI method**) for calculating the velocity coefficient from full-scale tests (see Section 2.4.1). The same method should be used for data from reduced-scale model tests after scaling to the full-scale condition (see Section 2.4.2).

The TSI method requires that the air speed from each train passage be filtered using a 1-second moving average. This is preferred over the 3-second moving average because people can be knocked over by gusts of 1-second duration or less, so the 3-second moving average may smooth over a potentially dangerous gust.

To account for the variability between runs, slipstream air speeds from at least 20 train passes should be measured and the maximum 1-second moving average air speed identified for each train pass. The mean plus two standard deviations of the maxima (equivalent to the upper 95 percent confidence interval) is used as the stated velocity coefficient, as shown in Figure 3-4.

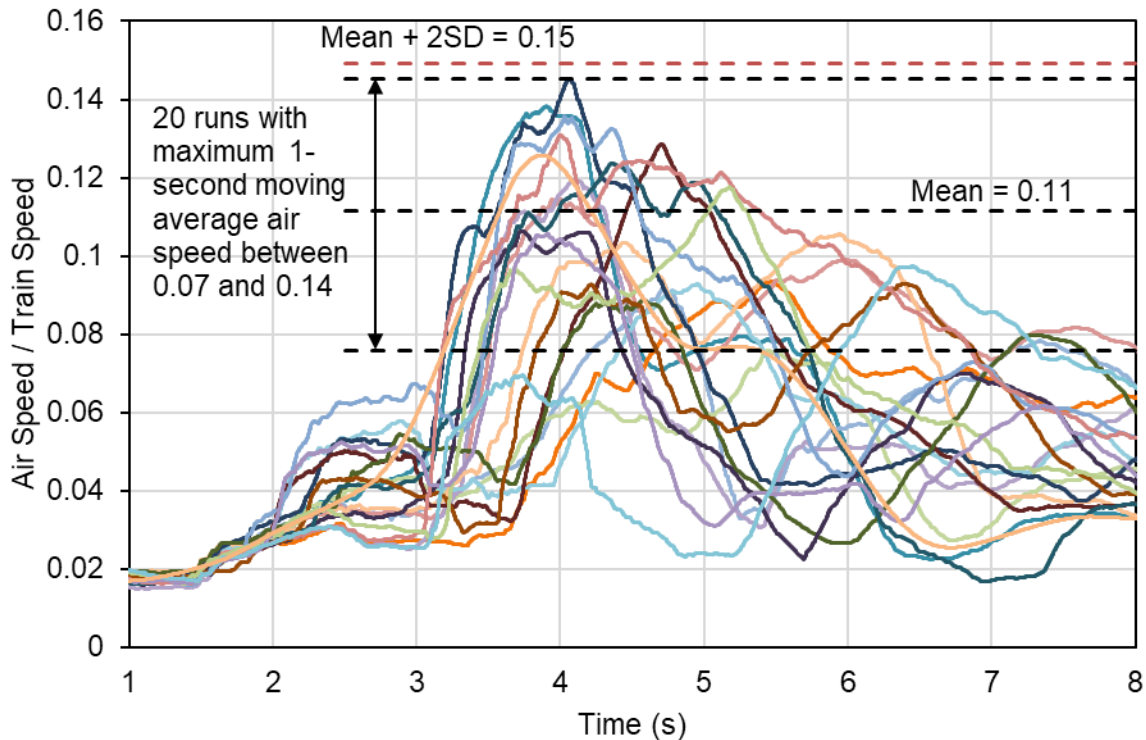


Figure 3-4. Example of determining the upper 95 percent confidence interval for the maximum slipstream air speed

3.3.3 Distance from the Track

The measured air speed in the slipstream reduces with distance from the track. The amount of reduction is dependent on the specific aerodynamic characteristics of the train and cannot be predicted with precision due to the highly turbulent nature of the slipstream.

Figure 3-5 shows a selection of scale model and full-scale test data from various high-speed trains, illustrating how the slipstream air speed decays with distance from the track. Each dataset in the figure shows a reduction of velocity coefficient with increasing distance from the track, but the shape of the decay curve varies from dataset to dataset due to the influence of train shape and the inherent randomness of slipstreams. The magnitude of the velocity coefficients in the different datasets shown in the figure should not be compared or used directly in assessments, because some are for trains that are less well-streamlined than current HSTs, the measurement locations are not the same across the different datasets, and some of the tests were performed with platforms and some without.

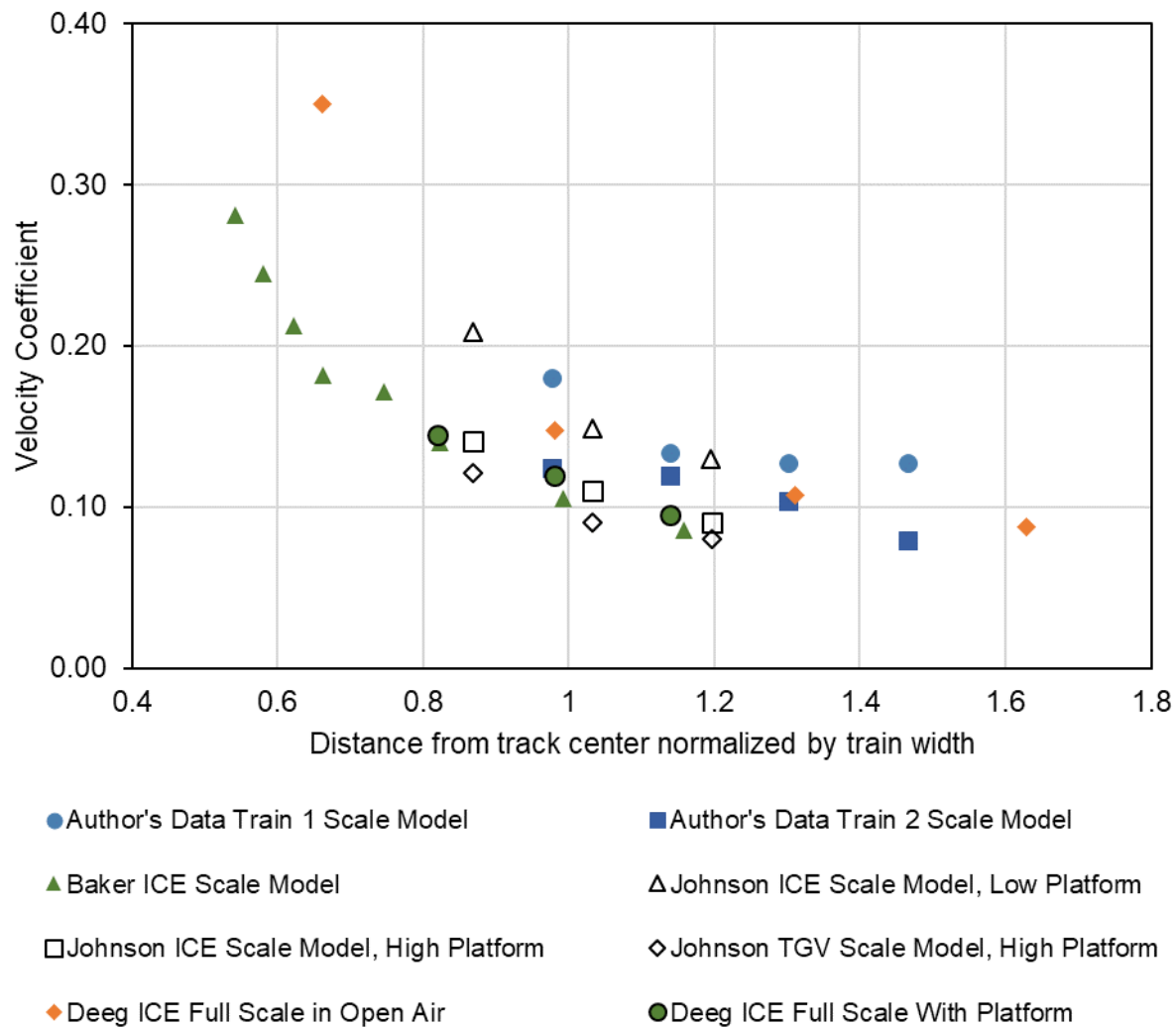


Figure 3-5. Variation of peak slipstream velocity coefficient with distance from the track center: data from reduced-scale tests by Baker [7], Johnson & Holding [82] and the author's own tests, and full-scale tests by Deeg [23]

3.3.4 Elevation above Top of Rail

The slipstream air speed is dependent on the height of the measurement point relative to the train. The greatest air speed is experienced level at the wheels and trucks of the train, with reduced air speeds higher up. This is one of the reasons why track workers may be exposed to higher air speeds than passengers on high platforms even at the same train speed.

3.3.5 Platform Height

Higher platforms reduce the slipstream air speed. The vertical face of a high platform blocks the slipstream generated by the wheels and trucks where air speeds are typically highest. Scale model tests [82] have indicated that slipstream air speeds on high

platforms (about 3 ft above TOR) are approximately one-third less than on low platforms (a few inches above TOR).

3.3.6 Train Type and Design

The speed, width, and turbulence profile of the slipstream is influenced by how streamlined the train design is. Compared to less streamlined conventional trains, well-designed HSTs have a narrower slipstream, and the velocity coefficient at a given measurement point is lower. Therefore, HSTs can compensate for their higher speed by their more streamlined designs.

Conventional passenger trains, and particularly freight trains, can generate significantly wider boundary layers than HSTs. With these trains, people on platforms can be subjected to slipstreams from the boundary layer as well as from the wake, even if they stand behind the safety markings, resulting in exposure to strong airflow for a relatively long period of time as the train passes. Thus, risks to passengers from slipstreams are not confined to HSTs and may be greater for conventional trains.

3.3.7 Confinement by Surroundings

The slipstream air speed is also dependent on the train's surroundings. Walls and building facades close to the platform edge can cause a funneling effect, magnifying the effect of the slipstream due to the enclosed space. This effect is believed to have contributed to incidents in Europe of wheelchairs and strollers being moved by passing trains, described in Section [3.4.1](#).

3.3.8 Crosswinds

Crosswinds can increase the slipstream air speed experienced on platforms and alongside the track because the highest-speed part of the wake, which is normally aligned with the track, is displaced by the crosswind to the side of the track.

3.4 Impacts

Potential impacts relate mainly to safety of people near the track, especially track workers and passengers on platforms.

3.4.1 Impacts on People on Platforms

Due to the potential for high-speed slipstream gusts, people standing on platforms might be knocked off-balance or injured by objects picked up by the slipstream. Infirm or elderly passengers are likely to be more vulnerable to injury.

Slipstreams present an important safety risk to children in strollers and people in wheelchairs. Fatal accidents and near-misses have occurred when strollers or wheelchairs were set rolling along a platform by the slipstream from a passing train. One incident ended with the stroller falling off the platform against the side of the train [\[144\]](#). Another resulted in a wheelchair colliding with the side of a train [\[115\]](#). These accidents involved freight trains passing platforms at relatively low speeds – 40 mph, in one case, where the space was confined by walls behind the platform. It is likely that these events were exacerbated by the effect mentioned in Section [3.3.6](#), where the

wide boundary layer generated by freight trains acts for long enough for the stroller or wheelchair to build up speed.

3.4.2 Impacts on People Near Open Track

As with people on platforms, if track workers are present while HSTs are operating, they could be at risk of slipstream gusts causing them to fall. There are also records of track workers being injured when tools were blown against them by strong gusts from slipstreams [116]. Track workers are expected to be aware of the safety issues related to working alongside tracks and are generally fit and able-bodied. Therefore, they may be expected to be less vulnerable than some groups of passengers. However, they are typically working level with the wheel height, where slipstream air speeds are higher.

The public could potentially be at risk from slipstreams if they are able to approach close enough to the track. In practice, fences or other barriers are normally provided alongside high-speed railroads to prevent public access and the distance of these from the track is usually more than sufficient to prevent impacts from slipstreams.

3.4.3 Impacts on Structures and Objects

The slipstream applies forces to any object close to the track. Since the direction of the airflow is principally along the track, loading may be assumed to be applied to surfaces facing back along the track (see Figure 3-6). Potentially, such loading could contribute to collapse or fatigue failure of signs or other objects, or structures close to the track if they were not designed to resist wind loading. This issue may require particular consideration in tunnels (see Section 7), where the slipstream is concentrated within the confined space of the tunnel.

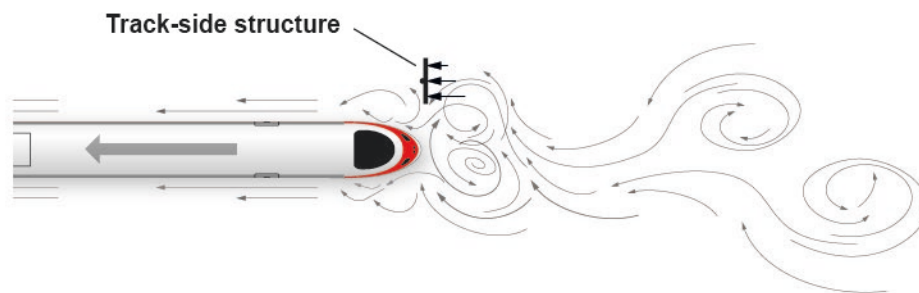


Figure 3-6. Illustration of slipstream loading of structures facing along the track

3.4.4 Impacts on Trains on Adjacent Tracks

Within current rail practices, slipstreams from HSTs are not considered to negatively impact other HSTs because those other trains are exposed to higher air speeds from their own motion and from the wind. The aerodynamic interaction between HSTs is dominated by the pressure pulses around the nose and tail of the trains, as described in Section 5.

In shared ROWs, there is potential for the slipstream from HSTs to dislodge loose items from freight vehicles, potentially creating a risk of damage from flying particles impacting on trains, other freight cargo, or on the rails. There is no existing guidance on this, and any potential risk should be considered on a case-by-case basis, based on any existing equivalent operations or full-scale testing. In the U.S., operational experience in the NEC has not indicated such problems at current operating speeds. Future Tier III operations will not share ROWs with freight vehicles except at speeds below 125 mph where aerodynamic impacts will be no worse than from conventional vehicles travelling at the same speeds, and in shared corridors the high-speed tracks will likely be sufficiently separated from tracks used by freight that no significant aerodynamic impacts should occur.

3.5 Mitigation Methods

3.5.1 *Passengers at Platforms*

At platforms, mitigation is achieved by encouraging a safe separation distance between people and the tracks, typically identified by a line along the platform, as shown in [Figure 3-7](#). These should be marked with clearly visible safe lines along with tactile strips of truncated cones per Americans with Disabilities Act (ADA) requirements. On platforms, trash cans, covers of drains, or inspection pits and any other loose equipment should be secured to prevent them being dislodged and/or blown around by the slipstream.



Figure 3-7. Examples of platform edge safety markings (left image [\[84\]](#))

The safe distance becomes larger as the operation speed increases. For tracks alongside platforms, speed limits are typically enforced. Practices in a number of countries is summarized in [Table 3-1](#). These are based on international experience of safe operation, not on calculations or assessments.

Table 3-1. HST speed limits at platforms and corresponding safety marking distances in various countries

Country	Speed limit at platforms	Distance of safety marking from platform edge	Reference
China - Conventional rail Platform height ≤ 0.5 m (1.6 ft)	125 mph (200 km/h)	6.6 ft (2.0 m)	[20]
China – HSR Platform height = 1.25 m (4.1 ft)	125 mph (200 km/h)	5 ft (1.5 m)	[20]
China (with platform screen doors)	155 mph (250 km/h)	–	[20]
Germany	125 mph (200 km/h)	5 ft (1.5 m)	[91]
Germany (with additional platform fences)	140 mph (230 km/h)	7.2 ft (2.2 m)	[91]
Japan	155 mph (250 km/h)	8.2 ft (2.5 m)	[91]
United Kingdom	125 mph (200 km/h)	5 ft (1.5 m)	[91]
U.S. (NEC)	150 mph (240 km/h) (de-facto)	2 ft (0.6 m) (ADA markings)	[147]
U.S. (California HSR, proposed)	125 mph (200 km/h)	5 ft (1.5 m)	[15]

As shown in the above table, international HSR practice typically sets the speed limit at platforms at 125 mph, with safety markings positioned 5 ft from the platform edge. A distance of 5 ft is sufficient to prevent passengers being affected by the boundary layer as an HST passes, although passengers will still experience gusts from the wake. Note that the height of the platform helps protect passengers from slipstreams and should be considered as part of the mitigation. In these countries, the platform height is at least 1.8 ft (0.55 m) above TOR, as specified by the European Infrastructure TSI and is around 3 to 4 ft (0.9 to 1.2 m) in many cases. Higher speeds are allowed in Japan, compensated by greater distance to the safety markings.

In countries such as China and Germany, speeds higher than 125 mph at platforms are allowed if platform screens or barriers are provided to protect passengers from passing trains (see examples in [Figure 3-8](#)). Full-height platform screens provide the maximum protection from slipstream air speeds. These are more commonly used in underground stations than in open air environments. Part-height screens and barrier fences protect passengers primarily by maintaining a safe distance from the platform edge, although solid screens also provide some protection from slipstream air speeds.

In addition to standard warning signs urging passengers to stay back, supervisory control communications or passenger information systems, such as electronic message boards, flashing lights, and automated audio announcements may also help reduce the risk to passengers, by alerting passengers to the arrival of passing trains and thereby reducing the element of surprise [90].



Figure 3-8. Examples of platform screen doors and barriers. Top: full-height doors in China [11]. Bottom-left: part-height solid barriers in Japan [29]; Bottom-right: barrier fences in Germany [13]

Systems for assessing and managing the overall risk from slipstreams to people on platforms have been developed, for example in the UK [62][111].

In some HSR systems, separate passage tracks enable HSTs to pass stations at full speed without delays caused by other trains stopping at the station (as illustrated in Figure 3-9). While intended for operational efficiency, the use of passage tracks also mitigates slipstream effects from the non-stopping trains by increasing the distance between trains and passengers.

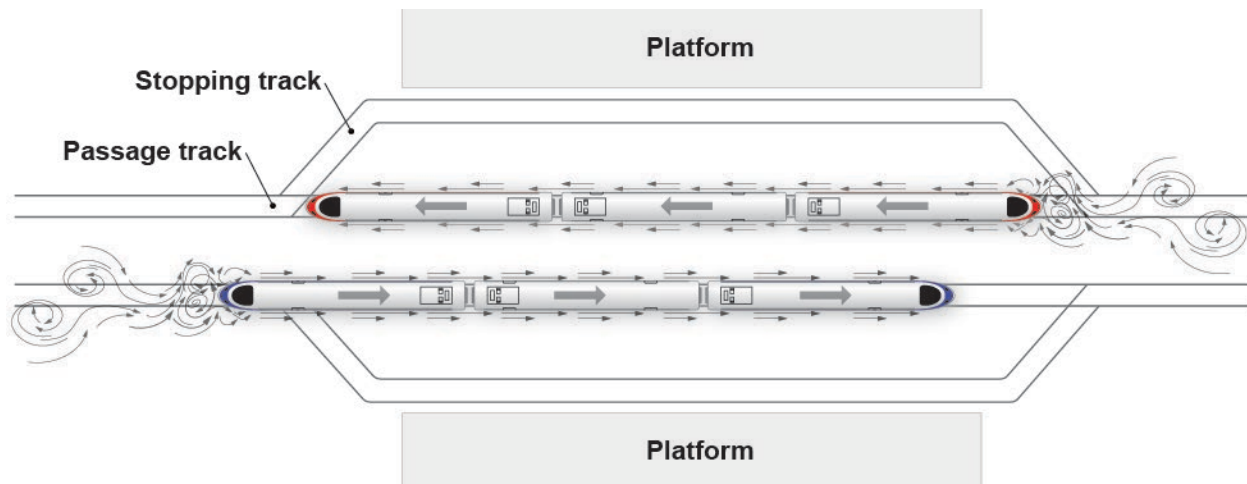


Figure 3-9. Passage tracks

As noted in [Table 3-1](#), current practice in some parts of the NEC is not in line with international practice and the recommendations within this manual. While no aerodynamic incidents are thought to have occurred as a result of this, safety concerns have been raised [130].

3.5.2 Track-side Workers on Open Track

Near open track, the aerodynamic risk to trackside workers may be mitigated by specifying minimum safe distances from the track at which workers should stand when trains pass, with the distance increasing with increased line speed.

In the U.S., the safety of track workers is regulated by 49 CFR 214 Subpart C (Roadway Worker Protection) [121]. The current version of the Code states that upon notification of an approaching train, workers must cease work and move from the track occupied by the approaching train to a predetermined place of safety. Furthermore, under certain conditions, workers working on a track adjacent to the track occupied by the approaching train must also move to a predetermined place of safety. However, the regulations do not make any particular provisions for HSR aerodynamics and do not specify the minimum distance between the tracks and the place of safety.

Internationally, it is not common to permit track workers to be present while HSTs are running at full speed to minimize the risk to their safety. However, rules do exist regarding minimum safe distances for workers, and these are shown in Figure 3-10 below.

As well as specifying a safe distance for workers on railroads with speeds up to 100 mph, Chinese rules [100] impose an additional requirement on the maximum slipstream air speed experienced by people including track workers; see Section 3.6.1. The rules do not quantify the distance from the track at which this slipstream air speed occurs.

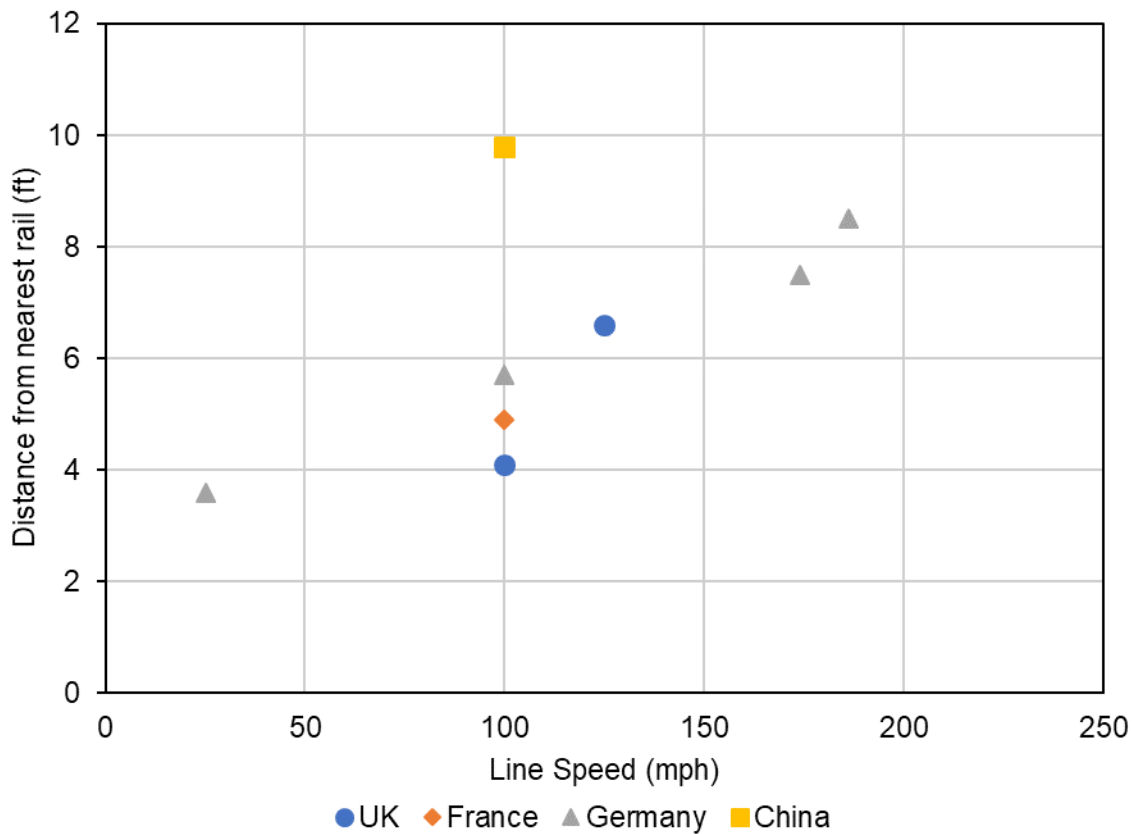


Figure 3-10. Summary of international regulations on safe distances for track-side workers, measured from the nearest rail (from [91])

3.5.3 Members of the Public near Open Track

Internationally, access to HSR lines by the public is usually restricted by fences or other physical barriers to prevent trespasser strikes and vandalism. In this report, it is assumed that new HSR lines in the U.S. would have similar protection. The distance from the track to the fence is typically governed by factors including, but not limited to, the space needed for equipment, track formation, foundations, drainage, etc. These distances are usually greater than the distance at which the train slipstream could cause a significant risk to the public. Therefore, there is usually no need to consider additional mitigation for slipstream effects for people outside the fence. However, information is provided in Section 3.6.5 regarding assessment and mitigation for cases where it might be required.

3.5.4 Loading of Objects and Structures Near the Track

Structures alongside the track should be designed to resist the loading induced by the train slipstream as well as ambient winds. Structures close to the track that have a significant area facing along the track will experience the greatest load. The magnitude of this load is proportional to the square of the air speed.

Wayside structures will be loaded during every train passage, and therefore an assessment of the risk of fatigue damage should also be completed.

3.6 Assessment

The objective of an assessment of slipstreams is usually to determine the safe distance at which a person can stand in order to mitigate aerodynamic risks for a particular train type and speed.

The slipstream conditions that lead to a given risk of accidents are not known; therefore, the safe distance cannot be calculated from consideration of the impacts. Instead, distances are based on operations with a satisfactory safety record. As well as aerodynamic considerations, the definition of a safe standing distance should also consider other factors, for example noise levels, the potential for a fright reaction from the sudden approach of a train, and the possibility of tripping toward the train.

In most cases, assessment would be simply a case of selecting appropriate safe standing distances and/or speed limits as described in Sections 3.6.3 to 3.6.5.

For situations not covered by this guidance, an expression for estimating slipstream speeds is provided in Section 3.6.2. More reliable results can be obtained by full-scale testing, with the same rolling stock and where relevant, platform dimensions as in the proposed operation. In order to maintain compatibility with existing data for HSTs, it is recommended that the procedure for determining velocity coefficients should be aligned with the TSI method, which is used across Europe and China. This is described in Sections 2.6 and 3.3.2.

3.6.1 International Assessment Criteria

Acceptable maximum slipstream air speeds for passengers and track-side workers are not consistently specified in international regulations. More than 20 potential air speed limits were identified in the FRA High-Speed Rail Aerodynamic Assessment and Mitigation Report [49]. Note that the slipstream air speed processing method is a key element of all these criteria and they cannot be compared with each other (or with measured values) unless the processing method is the same in both cases. None of the criteria described below are recommended for use in the U.S.

Chinese regulations [100] require that people (including track workers and passengers) should not be exposed to instantaneous slipstream speeds exceeding 14 m/s (32 mph). The use of an instantaneous air speed without applying any filtering or moving average is different from practice in other countries and may cause difficulties when comparing this criterion with measured data like that shown in Figure 3-2.

British and German recommendations [90] suggest a maximum 1-second moving average slipstream air speed of 17 m/s (38 mph) for track workers.

For passengers at platforms, a lower air speed limit is appropriate, as they may include elderly or infirm people who are more vulnerable to the effects of turbulence in the slipstream. Japanese [136] and British [90] recommendations specify safety limits of 9 m/s and 11 m/s respectively (20 and 25 mph respectively).

The European TSI includes performance criteria for maximum slipstream air speeds induced by trains at heights of 0.2 m (8 in) and 1.4 m (55 in) above TOR, in relation to safety of track-side workers and passengers at platforms, respectively. The maximum slipstream air speeds of 22 m/s (50 mph) and 15.5 m/s (35 mph) specified for the rolling stock compliance tests are sometimes taken as safety limits for people, but there is no reliable basis for doing this, and these speeds would exceed those experienced by trackside workers and passengers at platforms under typical international practice.

3.6.2 Estimation of Slipstream Air Speed for Baseline Trains

Safe distances for people on platforms, track workers, and members of the public near open track are presented in Sections 3.6.3 to 3.6.5. In situations where the designer requires an approximation of the maximum slipstream air speed (for example, to estimate the slipstream load on a track-side sign) the expression provided in this section may be used.

Figure 3-11 shows an approximation of the maximum slipstream air speed at different distances from the track for the Baseline Trains described in Section 2.3.2. Also shown in the figure are data from a selection of the scale model and full-scale tests from a number of references. For clarity, the data in the figure includes only a subset of the data from Baker [6] (which included multiple HST models), obtained by excluding certain older, less aerodynamic HSTs which are now superseded by more recent designs. Only the data from Baker [6] is fully consistent with the TSI method for assessing the velocity coefficient.

Note that the curve in Figure 3-11, while providing a conservative upper limit on the relevant available data, gives only a rough approximation for informing early design and is not expected to fully represent the broad range of different trains that may be used in practice. Also, due to the chaotic and turbulent nature of the slipstream, individual measurements of slipstream air speed will vary widely.

The curve is described by the equation:

$$c_v = 0.23 k_p \left(\frac{y}{w} \right)^{-1.2} \quad \text{Equation 3-2}$$

Where:

c_v = Velocity coefficient for maximum slipstream air speed on open track, calculated according to the “TSI method” as described in Section 3.3.2;

k_p = Platform factor (0.7 for high platforms greater than 0.55 m (22 in) above TOR, 1.0 for low platforms and open track);

y = Distance from the track centerline; and,

w = Train width, in the same units as y .

Equation 3-2 is based on the sketched curve in EN 14067-4 [33] that provides an estimate of maximum slipstream air speed as a function of distance from the train. The exponent of -1.2 is consistent with the curve in EN 14067-4 [33]. However, the curve

recommended in this manual has been scaled down to account for the improved aerodynamic performance of the Baseline trains over the older, less aerodynamic HSR rolling stock which is allowed for in the EN 14067-4 curve.

Figure 3-11 and Equation 3-2 apply to trains that meet the criteria for the U.S./Euro and U.S./Asian Baseline Trains. The platform factor is included as an approximation of the effect of high platforms, based on limited data, and should not be relied on in place of full-scale testing to evaluate slipstream air speeds for passengers at platforms.

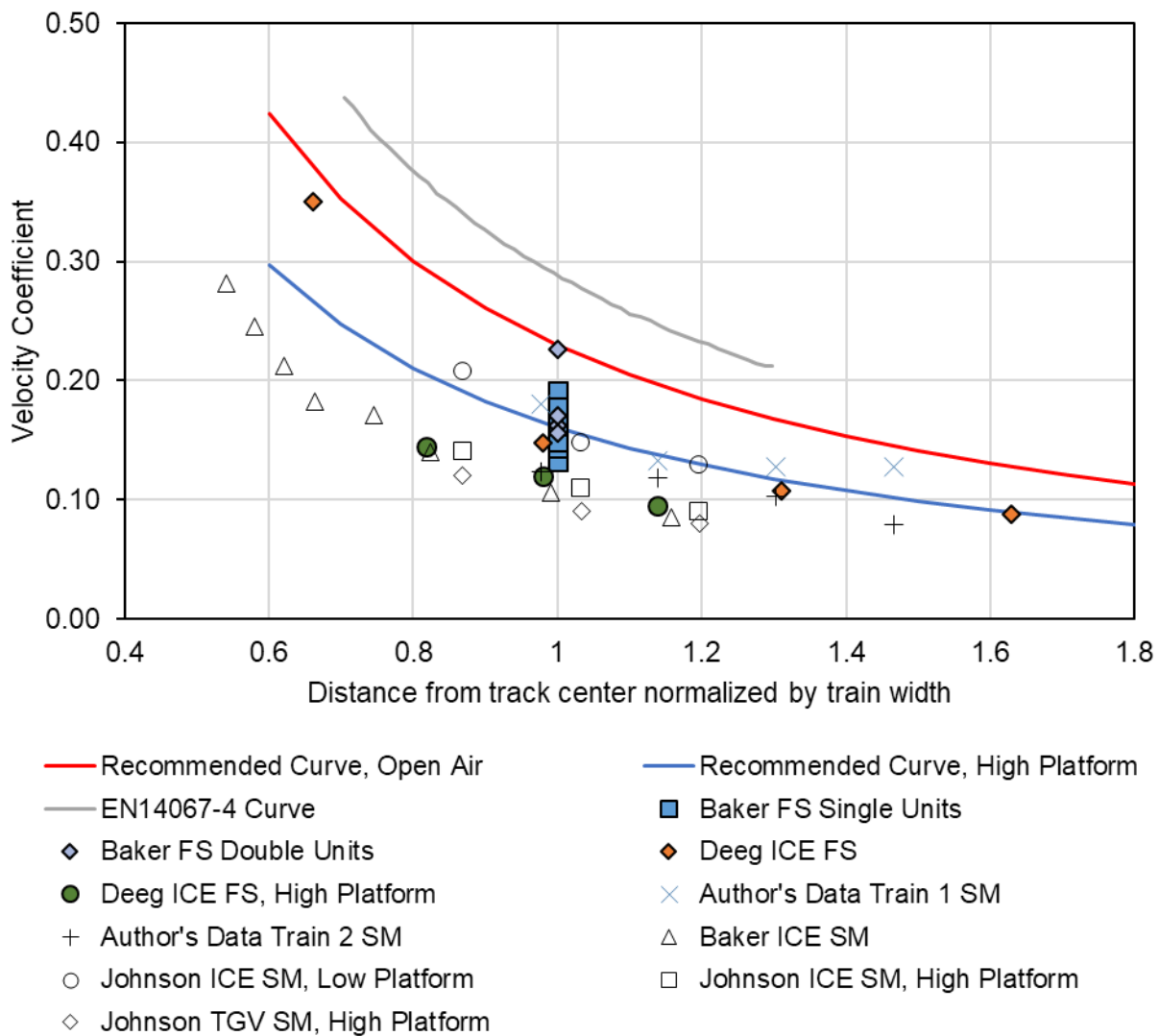


Figure 3-11. Approximate variation of velocity coefficient with distance from track center on open track for Baseline Trains, overlaid on full-scale data from Baker [6] and Deeg [23], (marked FS, with solid markers) and scale-model data from Baker [7], Johnson & Holding [82] and the authors' own tests (marked SM, with outline markers)

3.6.3 Assessment for Passengers at Platforms

Operators are recommended to limit train speeds at platforms to 125 mph (200 km/h) for HSTs and incorporate safety markings at 5 ft (1.5 m) from the edge of platform in line with international practice. This applies to high platforms, defined by a height greater than 0.55 m (22 in) above TOR (typically platforms at 48 in above TOR in the U.S.), and to HSTs that satisfy the Baseline Train requirements in Section 2.3.2. Based on Equation 3-2, this practice implies a maximum slipstream air speed of approximately 20 mph (9 m/s) for both U.S./Euro and U.S./Asian Baseline trains, which is in line with international recommendations for platform safety as cited in Section 3.6.1.

For low platforms (platforms of height less than 0.55 m (22 in) above TOR – typically 8 in or 15 in above TOR in the U.S.), speed limits and/or safe standing distances should be selected such that the maximum slipstream air speed experienced by passengers is limited to 20 mph for consistency with international practice on high platforms.

Where the train speed is known, the safe distance from the edge of a low platform, D , may be calculated using Equation 3-3:

$$D = w \left[\left(\frac{V_L / V_T}{0.23k_p} \right)^{-\frac{1}{1.2}} - 0.5 \right] \quad \text{Equation 3-3}$$

Where:

D = Safe distance from the platform edge;

V_L = Limiting maximum slipstream air speed (20 mph);

V_T = Train speed, in the same units as V_L ;

w = Train width, in the same units as D ; and,

k_p = Platform factor (0.7 for high platforms, 1.0 for low platforms).

For a train speed of 125 mph (200 km/h) alongside a low platform, Equation 3-3 results in a safe standing distance of 8.3 ft (2.5 m) for U.S./Euro Baseline trains, and 9.4 ft (2.9 m) for U.S./Asian Baseline trains.

Where the marked safe distance from the platform edge is fixed, the maximum train speed may be calculated using Equation 3-4:

$$V_T = \frac{V_L}{0.23k_p \left(\frac{D}{w} + 0.5 \right)^{-1.2}} \quad \text{Equation 3-4}$$

For a standing distance of 5 ft from the edge of a low platform, Equation 3-4 results in a maximum line speed of 87 mph (140 km/h) for U.S./Euro Baseline trains, and 82 mph (130 km/h) for U.S./Asian Baseline trains.

Equation 3-3 and Equation 3-4 have been derived from Equation 3-2 assuming, conservatively, that the side of the train is aligned with the platform edge. These equations may be used also for other situations not covered above, for example to determine the safety marking distance for high platforms for train speeds other than 125 mph.

For trains which do not satisfy the Baseline Train requirements, full-scale testing will be necessary (see Section 3.6.6). Full-scale testing would be used to determine the velocity coefficient at a range of distances from the train, to identify the combination of train speed and distance which achieve a maximum slipstream air speed no greater than 20 mph (9 m/s).

Where operators require train speeds at platforms higher than those determined from the recommendations above, platform screen doors or barriers may be used to protect passengers from the effects of train slipstreams.

As described in Section 3.4.1, there is potential for injury and death if wheeled conveyances are set rolling by a train slipstream and collide with the train or fall off the edge of the platform after the train has passed. Operators may wish to consider further mitigation measures such as warning signs or announcements informing passengers of the risk to strollers and wheelchairs from slipstreams and to prompt users of wheelchairs and strollers to apply brakes when trains are approaching.

Although the scope of this report is limited to high-speed operations, readers should also be aware that the aerodynamic risks to the occupants of strollers and wheelchairs may be greater with less aerodynamic trains, such as conventional passenger trains and, especially, freight trains. For a given train speed, these less-aerodynamic trains generate higher slipstream air speeds for a longer period of time, resulting in a greater likelihood of a stroller or wheelchair being set in motion. Reduced speed limits on platform tracks are appropriate for these types of trains, with the limit for freight trains lower than that for conventional passenger trains.

3.6.4 Assessment for Trackside Workers

Internationally, it is not common to permit track workers to be present while the line is running at full speed to minimize the risk to their safety. However, there may be occasions when a visual track inspection or other maintenance activity requires work adjacent to tracks with operational trains.

To determine aerodynamic minimum safe distances for workers, the maximum slipstream air speed is estimated for an existing operation with substantial safe operational experience. In this report, the maximum slipstream air speed is based on the regulations for trackside workers in the UK, working alongside live tracks with a line speed of up to 125 mph (200 km/h). Applying Equation 3-2, the maximum slipstream air speed in the UK operation is 32 mph (14 m/s). The objective of the guidance given below is to prevent track-side workers from being exposed to slipstream airflow speeds greater than this.

Aerodynamic minimum distances are presented in Figure 3-12 and Table 3-2 as one element of operational safety for track-side workers. The distances are calculated using Equation 3-2, such that estimated maximum slipstream air speed is no more than 32

mph (14 m/s), assuming Baseline Trains, see Section 2.3.2. This approach results in recommendations which are more conservative than regulations in France and Germany but consistent with U.K. guidance.

The selection of the place of safety and other protective measures will be decided by operators based on multiple safety considerations, but in any event, the authors recommend that the distance should be no less than the aerodynamic minimum presented below.

For operations with trains which are less aerodynamic than the Baseline Trains, full-scale testing is required to identify the distance at which the maximum slipstream air speed does not exceed 32 mph (14 m/s).

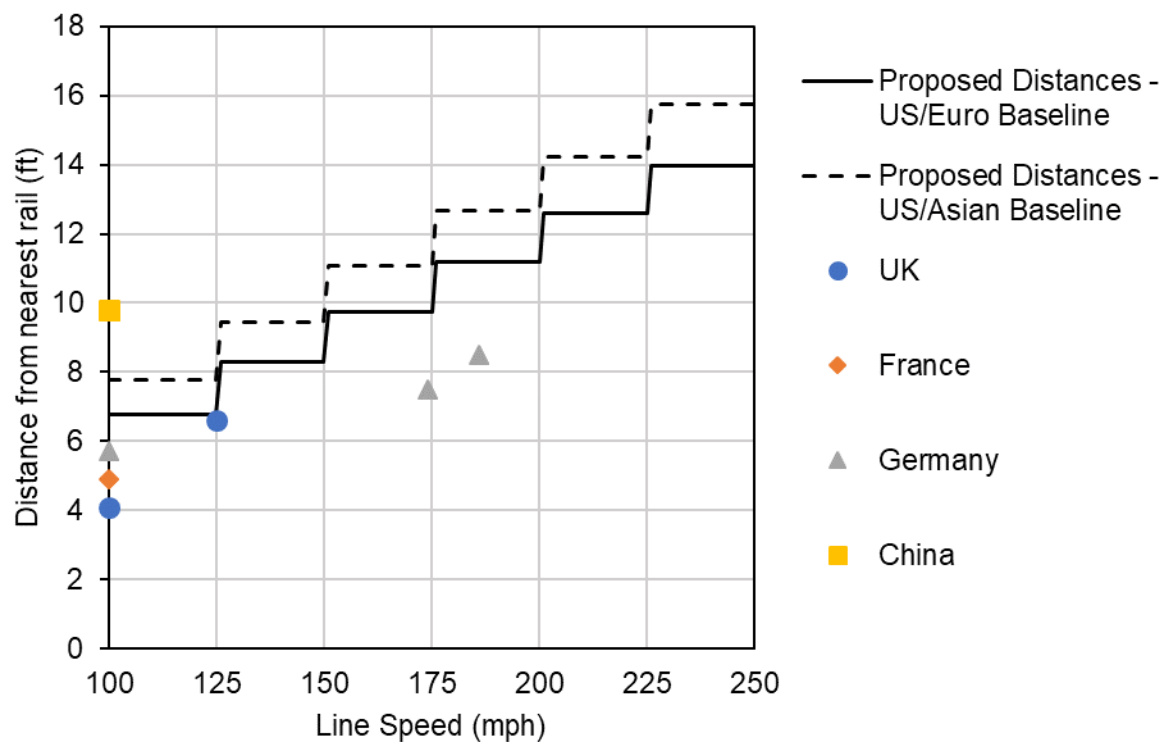


Figure 3-12. Aerodynamic minimum distances from nearest rail for track workers, with international regulations (from [91])

Table 3-2. Aerodynamic minimum distances for track workers

Design speed (mph)		Aerodynamic minimum distance to nearest rail for track workers			
		U.S./Euro Baseline		U.S./Asian Baseline	
mph	km/h	ft	m	ft	m
Up to 125	Up to 200	6.8	2.1	7.8	2.4
126-150	201-240	8.3	2.5	9.4	2.9
151-175	241-280	9.7	3.0	11.1	3.4
176-200	281-320	11.2	3.4	12.7	3.9
201-225	321-360	12.6	3.8	14.2	4.3
226-250	361-400	14.0	4.3	15.7	4.8

3.6.5 Assessment for Public near Open Track

As noted in Section 3.4.2, slipstream-related risks to the public near open track are not usually a governing consideration in the design of HSR. However, these risks could potentially exist, and may be assessed using the information presented here. Operators would likely weigh the perceived risks against the costs of providing mitigation and might consider limiting mitigation to places where vulnerable people are more likely to be present.

It is not appropriate to apply the aerodynamic minimum distances for track workers given in Section 3.6.4. Lower slipstream air speed limits (and therefore increased distances from the track) are appropriate for members of the public who may be more vulnerable to slipstream effects and less aware of the risks from approaching trains than track workers.

To assess aerodynamic risks to the public near open track, first determine the distance between the track center and the closest point at which the public can approach the ROW (typically the barrier or fence that prevents public access to the ROW). It is assumed here that the barrier or fence is completely porous and does not impede airflow. The distance should then be compared with the aerodynamic minimum distances in Table 3-3. If the actual distance is less, people standing in that position would be exposed to a stronger slipstream effect than people standing on platforms under conditions known to be generally safe based on international experience.

The distances in Table 3-3 are calculated using Equation 3-2 such that the estimated maximum slipstream air speed is no more than 20 mph (9 m/s), thus providing the same low level of aerodynamic risk as for passengers on platforms; see Section 3.6.3. Note that this is potentially a conservative approach and the impacts of slipstream air speeds greater than 20 mph are not known.

Where the distance to the fence is less than in the table, and there is a particular risk of vulnerable people being present, e.g., a sidewalk immediately outside the fence, operators may wish to consider providing solid or semi-porous barriers to protect people from slipstream effects. Alternatively, the aerodynamic impacts could be mitigated by

placing the fence or barrier further from the track, although increased real estate costs might make this solution unattractive.

Table 3-3. Distance to track center for people near open track to achieve slipstream safety equivalent to that at a platform

Design speed (mph)		Distance to track center for platform-equivalent slipstream speeds near open track			
		U.S./Euro Baseline		U.S./Asian Baseline	
mph	km/h	ft	m	ft	m
Up to 125	Up to 200	13.1	4.0	15.1	4.6
126-150	201-240	15.4	4.7	17.4	5.3
151-175	241-280	17.4	5.3	19.7	6.0
176-200	281-320	19.7	6.0	22.3	6.8
201-225	321-360	21.7	6.6	24.3	7.4
226-250	361-400	23.6	7.2	26.6	8.1

3.6.6 Assessment Using Test Data

Where the operator needs to determine safe standing distances from trains which do not meet the aerodynamic requirements of the Baseline Trains, full-scale testing is required to determine the maximum slipstream air speeds at the relevant locations.

For example, although not within the scope of this report, the slipstream induced by freight trains is typically considerably wider, with higher air speeds at a greater distance than from a HST traveling at the same speed. Therefore, the risk from freight train slipstreams should be assessed separately from that of HSTs.

Full-scale tests can be carried out at lower speeds than the full line speed and velocity coefficients determined at relevant locations for assessing the slipstream risk. Any significant obstructions (e.g., platforms) should be included in the full-scale tests.

To identify a safe distance from the train, a series of measurements should be taken at a number of distances from the side of the train, and processed using the TSI Method described in Sections 3.3.1 and 2.4.1 to determine the maximum velocity coefficient at each distance. The velocity coefficients should then be multiplied by the proposed line speed to identify the predicted maximum slipstream air speed at each distance from the track. The distance at which the maximum slipstream air speed is reduced to 20 mph (9 m/s) for passengers or public, or 32 mph (14 m/s) for track-side workers, can then be identified.

3.7 Examples

3.7.1 Select Required Safe Standing Distance Based on Speed

Question

U.S./Asian Baseline HSTs will operate on a new railway at 210 mph. What is the aerodynamic minimum distance from the nearest rail to a place of safety for trackside workers?

Methodology

Select the appropriate track spacing from [Table 3-2](#).

Inputs

HST speed, V_T 210 mph (340 km/h)

Calculations

From Table 3-2, the aerodynamic minimum safe distance from the nearest rail for U.S./Asian HSTs at speeds between 200–225 mph is 14.2 ft (4.3 m).

Result

The aerodynamic minimum safe distance from the nearest rail is 14.2 ft (4.3 m).

3.7.2 Determine Maximum Passing Speed for Platform

Question

U.S./Euro Baseline HSTs of width 10.0 ft (3.0 m) will pass through an existing station with low platforms (8 in above TOR), where passengers can stand 5 ft (1.5 m) from the edge of the platform (10 ft from the track center). What is the maximum speed that trains should pass through the station?

Methodology

Due to the low platform, the standard speed limits from Section 3.6.3 cannot be used directly.

Equation 3-4 may be used to determine an appropriate maximum train speed, to ensure the maximum slipstream air speed experienced by passengers on platforms does not exceed 20 mph (9 m/s).

Inputs

Train width, w	10.0 ft
Distance from platform edge, D	5 ft
Maximum slipstream air speed, V_L	20 mph
Platform factor, k_p	1.0 (low platform)

Calculations

Maximum train speed (from Equation 3-4)

$$\begin{aligned} V_T &= \frac{V_L}{0.23 k_p \left(\frac{D}{w} + 0.5 \right)^{-1.2}} \\ &= \frac{20}{0.23 \times 1.0 \left(\frac{5}{10.0} + 0.5 \right)^{-1.2}} \\ &= 87 \text{ mph} \end{aligned}$$

Result

The train speed through the station should be limited to 87 mph (140 km/h). If higher speeds are required, the standing distance for passengers should be increased, or platform screens should be provided.

4 Pressures on Wayside Structures

4.1 Introduction

As an HST passes stationary structures, such as wayside signs, noise or wind barriers, or buildings, the train exerts an aerodynamic pressure on these structures.

While this report does not make recommendations for the structural design of the vast array of potential structures, this section does provide a means for predicting the magnitude and nature of the pressure loading, which may be used by structural engineers to assess each structure on a case-by-case basis.

Pressure loadings imparted to other trains are covered in detail in [Section 5](#).

This section includes:

- Aerodynamic principles and key influencing factors
- Impacts on structures
- Methods for predicting and assessing the pressure loads
- Example calculations

4.2 Aerodynamic Principles and Phenomena

As a moving train pushes air out of the way, it causes a zone of high-pressure air just in front of the train nose and a zone of low-pressure air immediately behind the nose. The situation is reversed at the tail of the train, where there is a zone of low-pressure air just ahead of the tail of the train, and a zone of higher pressure immediately behind the tail – see [Figure 4-1](#).

These zones of high and low pressure move with the train, resulting in rapid pressure pulses experienced by structures, objects, people, or other trains close to the passing train. The tail pressure pulse is generally smaller in amplitude than the nose pressure pulse. In addition to the nose and tail of the train, pressure pulses are generated at the coupler of nose-to-nose coupled trains and smaller pressure pulses are generated at each inter-car gap.

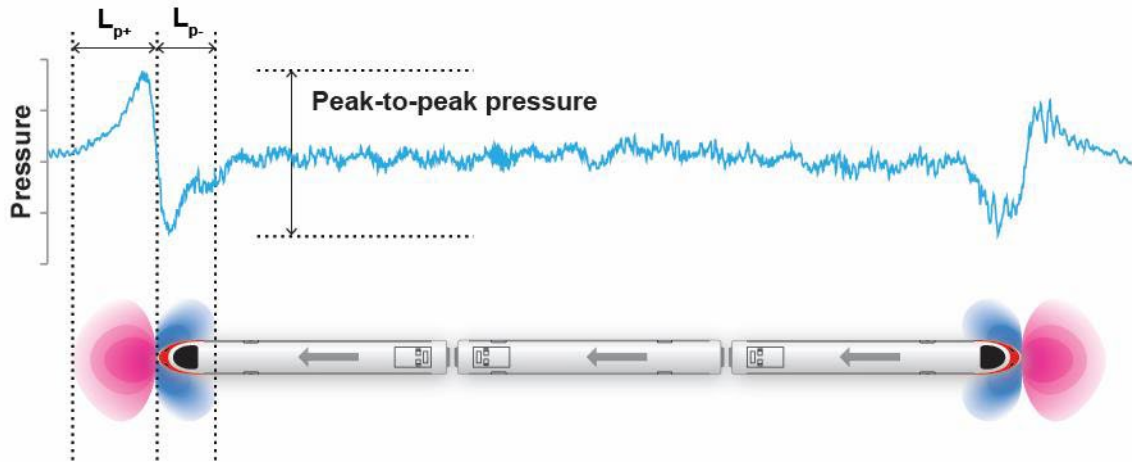


Figure 4-1. Pressure near the nose and tail of a train (In the lower image, red represents zones of high pressure, and blue represents zones of low pressure.)

The tendency of a particular train shape to generate pressure loading on wayside structures can be described by a **pressure coefficient** c_p :

$$c_p = \frac{\Delta p}{\frac{1}{2} \rho V_T^2} \quad \text{Equation 4-1}$$

Where:

Δp = Peak-to-peak pressure;

V_T = Train speed; and,

ρ = Air density.

This equation requires consistent units, see Section 2.7 (SI units recommended).

Several sources (e.g., Chinese regulators) recommend a correction factor for compressibility effects at speeds over 350 km/h (220 mph), called a **Mach number correction**: see [49]. However, the correction increases the predicted pressure by only 6 percent at a speed of 250 mph (and by a lesser amount at lower speeds). In the interests of simplicity, this correction is not recommended for use with the assessment methods described in this section.

Apart from the Mach number effect, the pressure coefficient remains constant as the train speed varies. Therefore, experiments may be performed at lower speeds and the results extrapolated to higher speeds.

Trains capable of high speeds have well-designed aerodynamic shapes, resulting in lower pressure coefficients. Thus, the effects of the higher speeds are mitigated to some extent by streamlined designs.

4.3 Influencing Factors

Pressure pulses are very repeatable, unlike slipstream velocity measurements, which have high variability. If the same train passes the same measuring position at the same speed a number of times, the pressure pulses will typically be within around 2 to 5 percent of each other.

4.3.1 Train Speed

The magnitude of the pressure pulse is proportional to the square of the speed of the train through the air (i.e., the train speed plus any headwind). In principle, when applying the assessment methods outlined in Section 4.6.2, the headwind speed should be added to the train speed. However, in practice, the headwind speed is unknown during design. For determining *maximum design loads*, these should be based on the highest credible combination of train speed and wind speed at that location (see also Section 6). For fatigue design, where the *typical loading* is used rather than the maximum, headwind speed is usually not considered.

4.3.2 Train Dimensions and Aerodynamic Performance

The magnitude of the pressure pulse is dependent on the aerodynamic properties of the train. High-speed trains tend to be more streamlined than conventional passenger and freight trains. Therefore, traveling at the same speed, the magnitude of the pressure pulse generated by HST is smaller than that from a conventional train.

The lateral extent of the pressurized zone around the nose and tail of the train is expected to be approximately proportional to the width of the train. Therefore, a wider train results in a wider zone of high pressure at the nose and tail of the train.

4.3.3 Confinement by Surroundings

If the track is partially enclosed, for example, by walls on one or both sides of the track, the pressures are increased due to the zone of high pressure being confined [61].

4.3.4 Length along Track

The along-track extents of the high- and low-pressure zones move with the train, depend on the shape of the nose and tail, and are insensitive to train speed. Thus, the length of the high-pressure zone at the nose of the train (typically 40 to 50 ft; 12 to 15 m) does not change significantly at speeds between 125 and 250 mph.

Because the length of the high-pressure zone is constant, the time taken for the high-pressure zone to pass over a certain point on a wayside structure is proportional to the inverse of train speed. The higher the speed, the shorter the time for the high-pressure zone to traverse that point. For example, the duration of the high-pressure loading is halved at 250 mph compared to 125 mph.

4.3.5 Distance from the Track

The pressure applied to the surface of a structure reduces approximately with the square of the distance from the track center. Figure 4-2 shows the variation of the pressure with distance from the track center, based on the formulae given in EN 14067-

4 [33]. The plotted pressure represents the **area-averaged** value. That is, the average pressure applied over the extents of the pressure pulse, rather than a local peak value.

For buildings more than approximately 20 feet from the track center, the pressure pulse is unlikely to be a concern for structural design, although it may still be capable of causing some minor impacts (e.g., rattling windows).

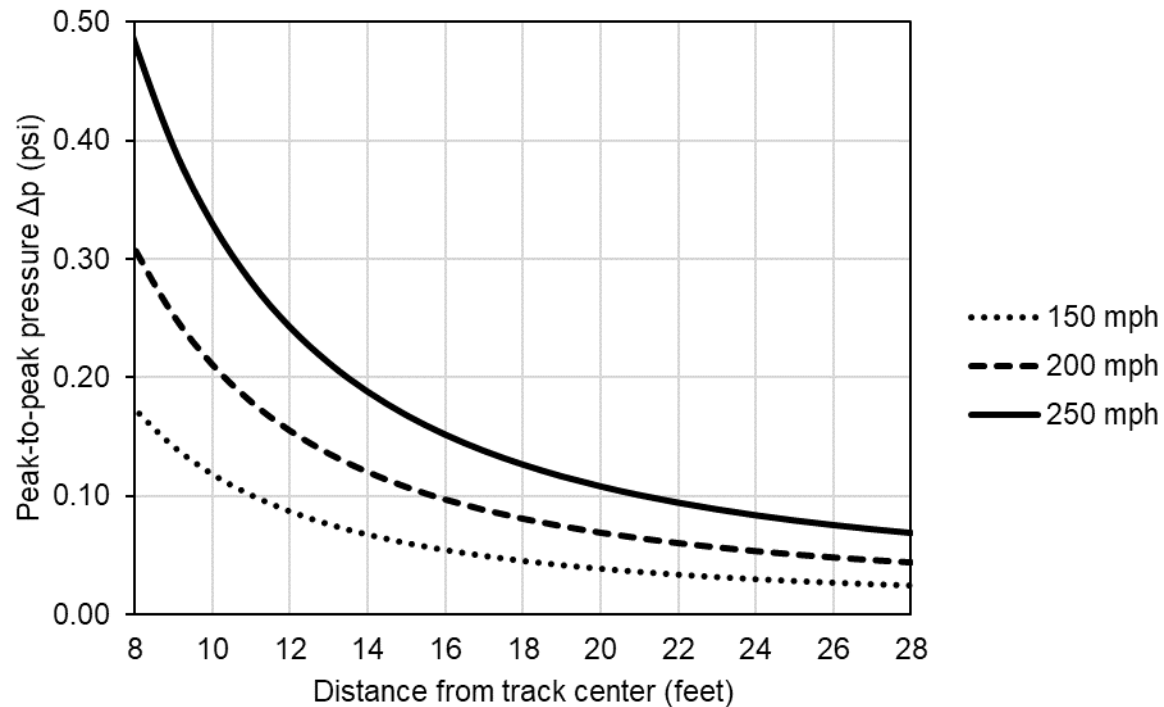


Figure 4-2. Magnitude of area-averaged pressure pulse on vertical surface as function of distance from track center for a streamlined HST [31]

4.4 Impacts

Principal impacts of the pressure pulses:

- The potential for damage to wayside structures (described below)
- The effects on other trains; see Section 5

4.4.1 Impacts on Structures

New structures close to the track should be designed with sufficient strength and fatigue resistance to withstand the pressure load from passing trains. The load is dynamic and is repeated at least twice every time a train passes, and therefore any design should consider how the loading impacts vibration and fatigue performance. In existing operations, reported impacts include:

- Fatigue failure of noise barriers after only a few months of operation [71]
- Fatigue failure of wayside signs and station wall finishing materials [92]
- Loosening of screws on structural elements [135]

- Rattling of windows, shutters, and doors of residential buildings close to the track [134]

In the case of noise barriers, their distance from the track is a compromise between the need for stronger (and potentially more expensive) barriers if placed closer to the track, versus reduced efficiency in attenuating noise when placed farther from the tracks.

Where a new ROW passes very close to existing structures, these may need to be strengthened to withstand the pressure loads or demolished. The same considerations arise when operating speeds on existing railroads are to be increased.

4.4.2 Impacts on Trains

The pressure pulse from an HST also acts on trains on neighboring tracks. The impacts and appropriate mitigation measures are considered in detail in Section 5.

4.4.3 Impacts on People

The pressure pulse from the train is considered to be too rapid to cause a person standing near the track to fall over. The pressure pulse is therefore generally considered less problematic for people than slipstream effects.

There is unlikely to be an aural discomfort effect because the pressure pulse passes very quickly and returns to zero. This is different from the situation with pressure waves in tunnels where a rapid step-like change to a different pressure would be perceived as uncomfortable; see Section 7.

4.5 Mitigation Methods

Mitigation is best achieved by designing the structures to resist the loading. The magnitude and duration of the loading may be estimated using the formulae given in Section 4.6.2.

4.6 Assessment

4.6.1 Assessment Objective

The objective of the assessments is to predict the pressure loads on structures alongside tracks. This will provide the loads to be used for an assessment of the strength of the structure and identify whether any structural mitigation is required.

4.6.2 Assessment Methods: Formulae for Design

Internationally, the formulae adopted in the European Standards EN 1991-2 [37], EN 14067-4 [33] and UIC leaflet 779-1 [77] are typically used to predict loads on wayside structures. All these standards contain the same guidance in different forms. Chinese design codes [99] provide similar information, adapted to Chinese rolling stock. The German standard for noise barrier design, Ril 804.5501 [25], contains more detailed formulae which provide a more accurate representation of the pressure pulse including its horizontal and vertical distribution, the effect of barrier height, and the relative sizes of the pulses from nose, tail, and nose-to-nose coupling.

The formulae described in Sections 4.6.2.1 through 4.6.2.5 are based on the European formulae, with an adaptation to account for operations using the larger U.S./Asian Baseline trains.

The loads described in this section are approximated by a square wave form, as shown in Figure 4-3. This is consistent with EN 14067-4, except that this manual recommends an increased along-track length of the pressure pulse. Recent experience in Germany [71] has indicated that the 5 m (16 ft) length recommended in EN 14067-4 may be non-conservative in terms of the impulse applied to wayside structures. This is of particular relevance to relatively flexible structures, such as noise barriers, where the dynamic response is important in assessing the fatigue life. This manual recommends an increase in the along-track length of the pressure pulses from 5 m (16 ft) to 12.5 m (41 ft), which results in an impulse which is similar to that derived from the recommendations in the German standard Ril 804.5501 [25].

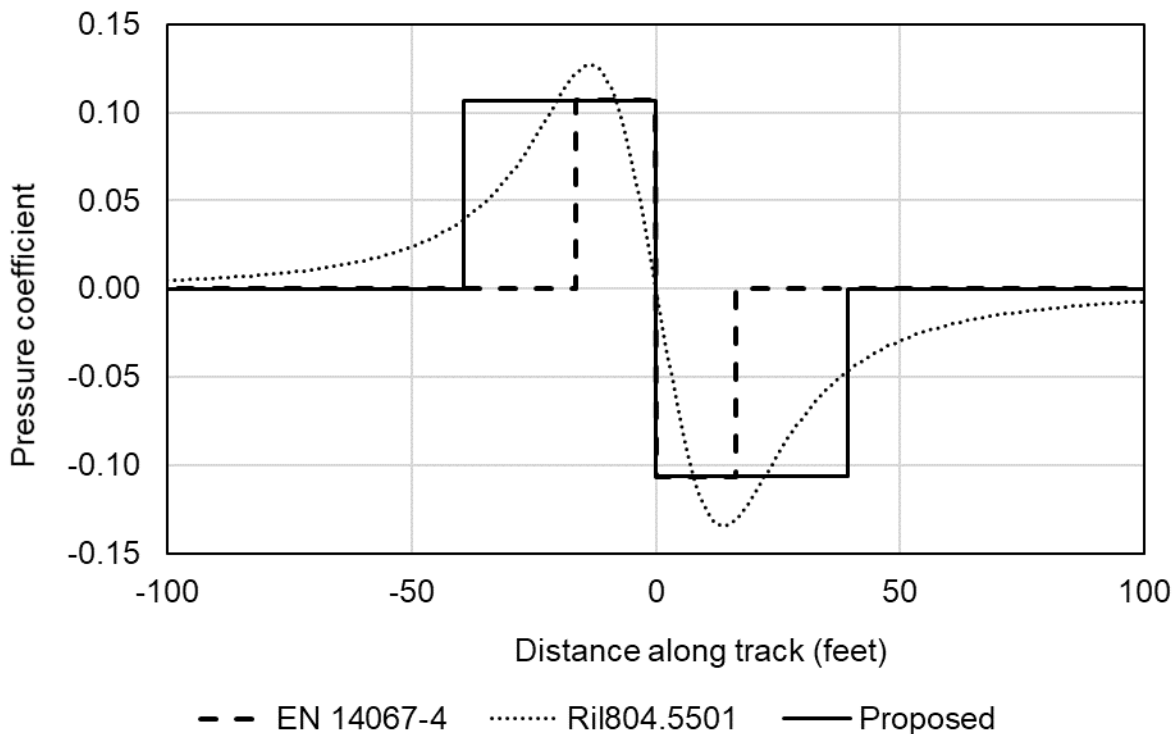


Figure 4-3. Comparison of the pressure distribution on wayside structures inferred from the formulae in EN 14067-4, Ril804.5501, and this report

If the trainsets are known in advance, scale model experiments or CFD analysis can be performed to measure the actual form of the pressure pulse and confirm the suitability of these formulae for the trains on any new operation.

Unless noted otherwise, these formulae give the area-averaged pressure, not the peak value. To estimate the maximum loading on a small area of a structure, use a factor of 1.3 to convert from area-averaged to localized peak value.

4.6.2.1 Vertical Surfaces

For a vertical surface such as a noise barrier or wall parallel to the track, the pressure distribution is idealized as shown in [Figure 4-4](#).

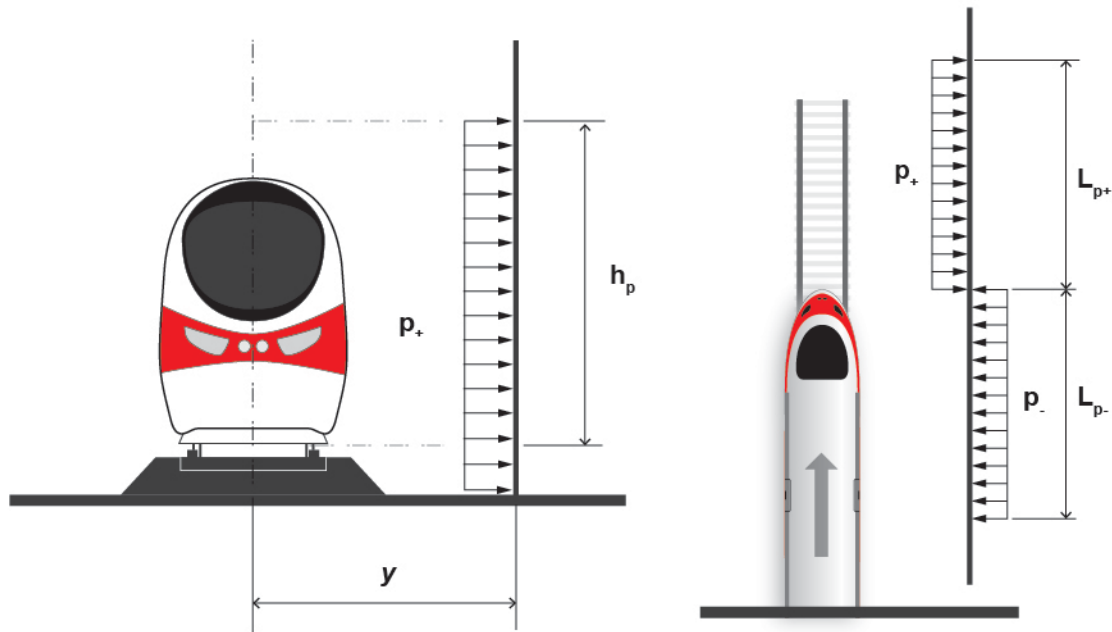


Figure 4-4. Idealization of pressure pulse on a vertical wayside structure

The lengths of the positive and negative pressure pulses, denominated L_{p+} and L_{p-} in [Figure 4-4](#), are assumed to be 41 ft (12.5 m). The loading is assumed to apply uniformly from ground level to a height h_p , taken as 16.4 ft (5 m) above TOR, or to the top of the structure if less than 16.4 ft (5 m) above TOR.

The magnitude of the pressure pulse on a vertical surface may be calculated as:

$$p_+ = p_- = k_{ap} k_t \left[\frac{2.5}{(y/k_d + 0.25)^2} + 0.02 \right] \times \frac{1}{2} \rho V_T^2 \quad \text{Equation 4-2}$$

Where:

p_+ , p_- = Amplitude of positive/negative pressure pulse (Pa);

k_{ap} = 1.0 for area-averaged pressure or 1.3 for localized peak pressure;

k_t = Train shape factor (1.0 for freight trains, 0.85 for conventional passenger trains or 0.6 for streamlined HST) ¹;

k_d = Factor to account for train dimensions (1.0 for U.S./Euro Baseline, 1.13 for U.S./Asian Baseline) ²;

y = Distance from center of track (m) ³;

ρ = Density of the air (typically taken as 1.225 kg/m³); and,

V_T = Train speed (m/s).

This equation requires SI units.

Notes:

1. More accurate values of k_t for particular trains may be derived from moving-model scale model testing, full-scale testing, or CFD analysis.
2. This assumes that the pressure field scales with the width of the train, taking the widths of the two train types as 118 in (3.0 m) for U.S./Euro and 134 in (3.4 m) for U.S./Asian.
3. [Equation 4-2](#) is valid for $y > 2.3$ m (7.5 ft) for U.S./Euro Baseline Trains or $y > 2.6$ m (8.5 ft) for U.S./Asian Baseline Trains.

4.6.2.2 Horizontal Surface above Track

Equation 4-3 may be used for flat horizontal structures, such as bridge decks above the tracks. The load should be applied across a width W_p , which is taken as 66 ft (20 m) for U.S./Euro Baseline Trains, 74 ft (22.6 m) for U.S./Asian Baseline Trains, or the width of the structure if less than these values.

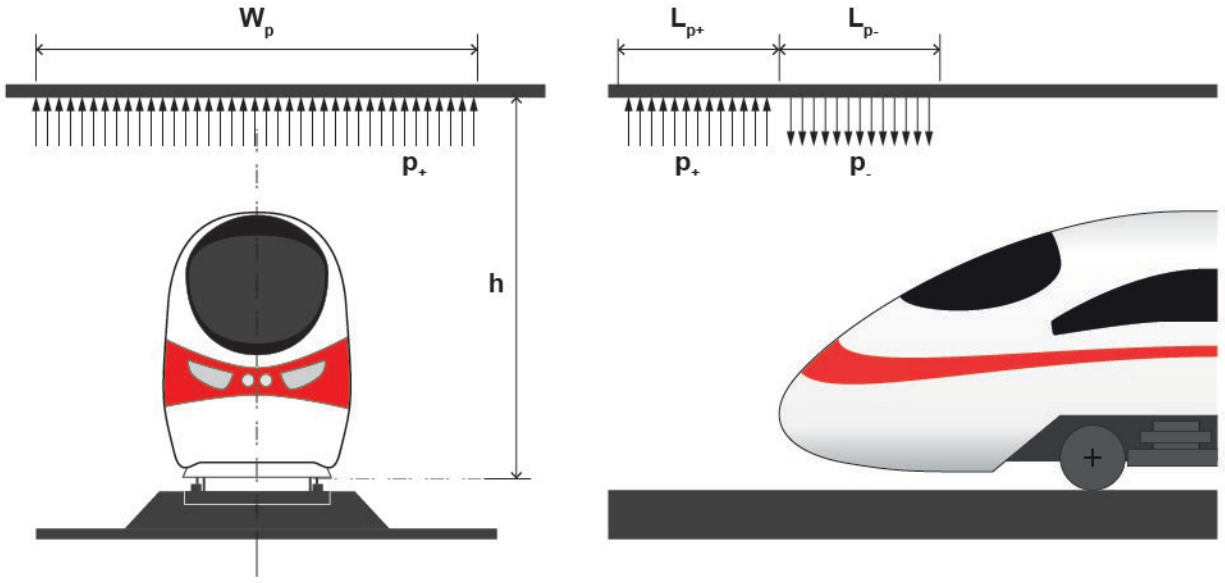


Figure 4-5. Idealization of pressure pulse on a horizontal structure above the track²

$$p_+ = p_- = k_{ap}k_t \left[\frac{2.0}{(h/k_d - 3.1)^2} + 0.015 \right] \times \frac{1}{2} \rho V_T^2 \quad \text{Equation 4-3}$$

Where:

h = Distance above TOR (m).

Other variables are as defined in Equation 4-2.

This equation requires SI units.

² L_p is 41 ft (12.5 m), W_p is 66 ft (20 m) for U.S./Euro Baseline Trains, or 74 ft (22.6 m) for U.S./Asian Baseline Trains, or the width of the structure if less than these values.

4.6.2.3 Horizontal Surfaces at Trackside

For horizontal structures close to the track, such as platform canopies, without a blockage caused by a supporting wall or a train on a parallel track, Equation 4-4 may be used. In this case, the pressure is assumed to vary as a function of lateral distance from track centerline (denoted y in Equation 4-4 below).

This equation is valid for canopies that begin at least 6.6 ft (2 m) from the track centerline for U.S./Euro Baseline Trains or 7.4 ft (2.3 m) for U.S./Asian Baseline Trains. For structures that extend closer to the track centerline, see Section 4.6.2.2. For cases with a supporting wall or a train on a parallel track; see Section 4.6.2.4.

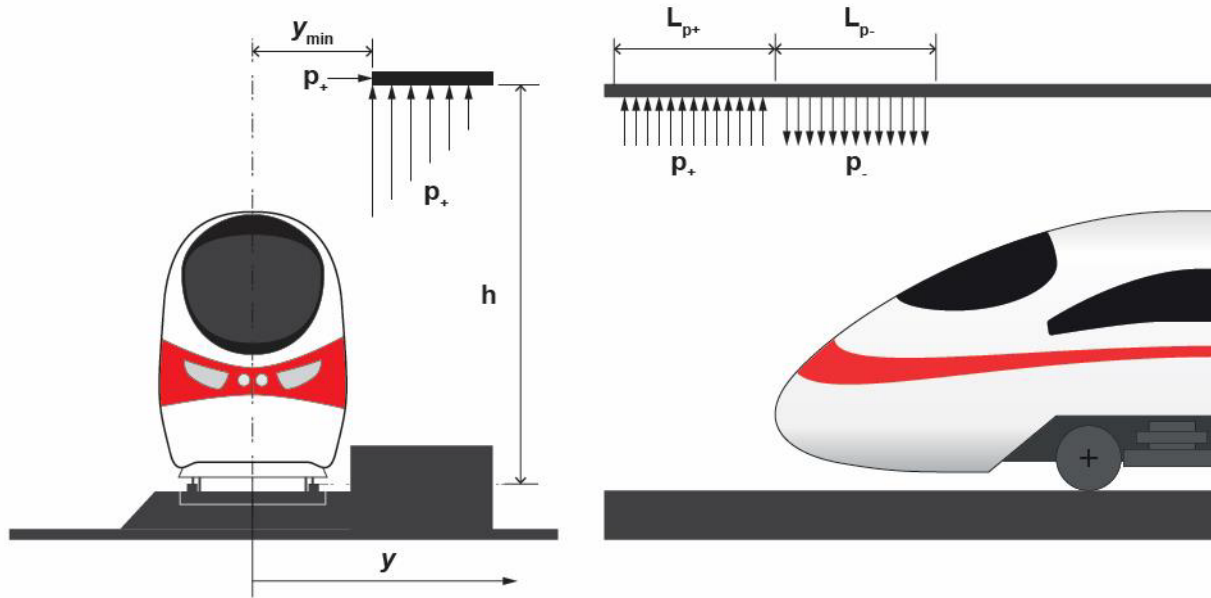


Figure 4-6. Idealization of pressure pulse on a horizontal structure above and to the side of the track³

$$p_+(y) = p_-(y) = k_t k_{ap} \frac{7.5 - h/k_d}{3.7} \left[\frac{1.5}{(y/k_d + 0.25)^2} + 0.015 \right] \times \frac{1}{2} \rho V_T^2 \quad \text{Equation 4-4}$$

Where:

h = Distance above TOR (m); and,

y = Distance from center of track (m).

Other variables are as defined in Equation 4-2.

This equation requires SI units.

³ Applicable if $y_{min} \geq 6.6$ ft (2 m) and h is in the range 12.5-24.6 ft (3.8-7.5 m) for U.S./Euro Baseline Trains, or $y_{min} \geq 7.4$ ft (2.3 m) and h is in the range 14.1-27.8 ft (4.3-8.5 m) for U.S./Asian Baseline Trains.

4.6.2.4 Mixed Vertical and Inclined or Horizontal Surfaces at Trackside

This category covers structures with a vertical and inclined or horizontal part and includes cranked noise barriers, platform canopies with a vertical wall or screen below, or canopies with a train standing on a parallel track. For these structures, [Equation 4-5](#) below may be used.

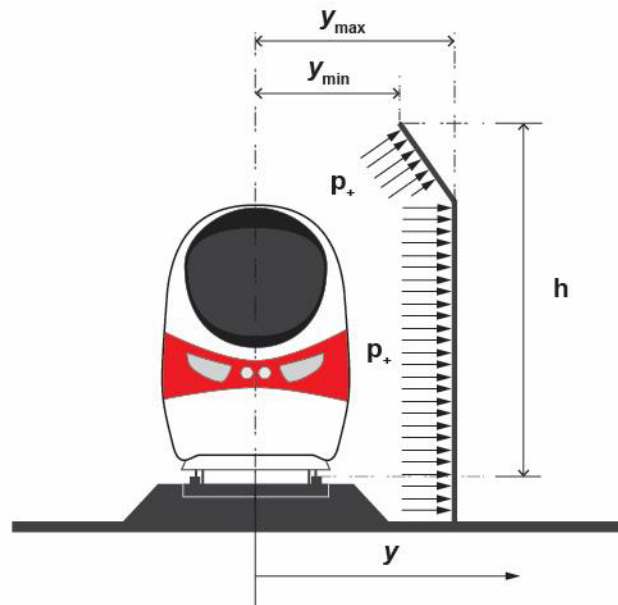


Figure 4-7. Idealization of pressure pulse on mixed vertical and inclined or horizontal structure at track-side

The loads on these structures should be calculated as for a vertical surface (using [Equation 4-2](#)) with the distance from track center defined as:

$$y = 0.6y_{min} + 0.4y_{max} \quad \text{Equation 4-5}$$

For U.S./Euro Baseline Trains, if y_{max} is greater than 19.7 ft (6.0 m), calculate the pressure with y_{max} equal to 19.7 ft (6.0 m).

For U.S./Asian Baseline Trains, if y_{max} is greater than 22.2 ft (6.8 m), calculate the pressure with y_{max} equal to 22.2 ft (6.8 m).

4.6.2.5 Surfaces Enclosing Track

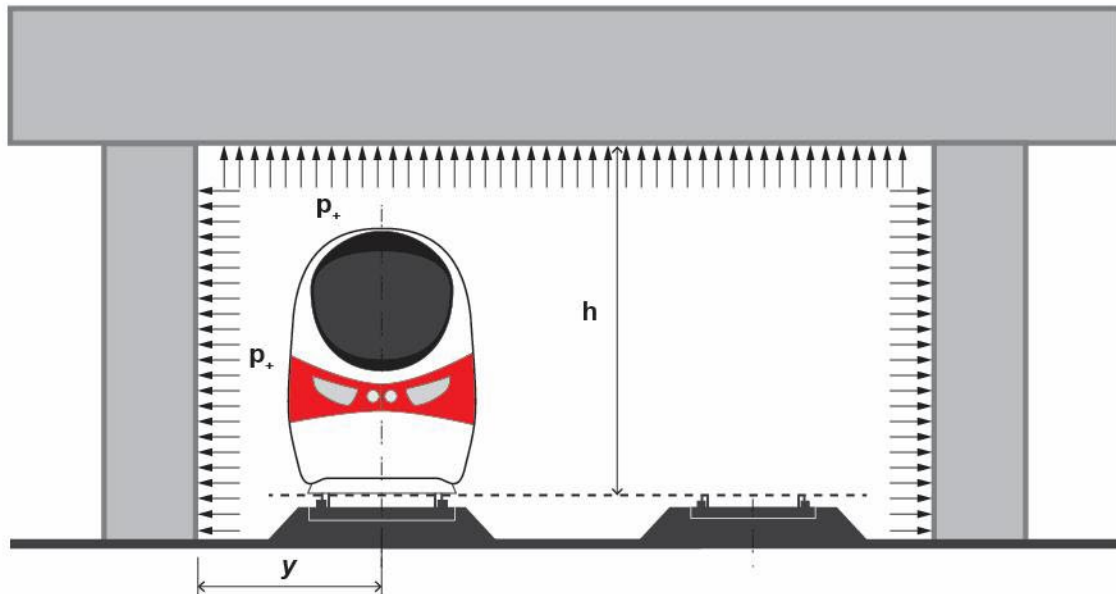


Figure 4-8. Idealization of pressure pulse on a structure enclosing the track

A structure enclosing a track, such as a bridge, is depicted in [Figure 4-8](#). For structures of length less than 66 ft (20 m), the equations for vertical and horizontal surfaces as defined in [Equation 4-2](#) and [Equation 4-3](#) should be used with the calculated pressure multiplied by:

- 2 for loads on vertical surfaces
- 2.5 for loads on horizontal surfaces enclosing one track
- 3.5 for loads on horizontal surfaces enclosing two tracks

EN 1991-2 [\[37\]](#) recommends applying these pressures uniformly over the full extents of the vertical and horizontal surfaces with no specified limits on the width or height of the structures. For very large enclosures, this may be overly conservative and a more detailed assessment (using scale model testing or numerical analysis) may be appropriate.

For structures longer than 66 ft, in addition to the pressure pulse effects described above, pressure waves should be considered; see the guidance in [Section 7](#).

4.6.2.6 Duration of Pressure Pulse

The spatial length of the positive and negative pressure pulses is constant and moves with the train. The pressure pulses are approximated as square waves, as shown in [Figure 4-3](#) and [Figure 4-4](#). The duration of the positive and negative phases Δt_{p+} and Δt_{p-} are therefore:

$$\Delta t_{p+} = \Delta t_{p-} = \frac{L_{p+}}{V_T} \quad \text{Equation 4-6}$$

Where

L_{p+} = Length of the high-pressure zone (12.5 m); and,

V_T = Train speed (m/s).

This equation requires consistent units, SI units recommended.

4.6.3 Dynamic Analysis of Flexible Structures

The rapid change from positive to negative pressure as a train passes can cause relatively flexible wayside structures, such as noise or wind barriers, to respond dynamically, with the potential for a large number of stress cycles for each train passage. If not considered during design, this could lead to eventual fatigue failure of these structures.

For assessment of these flexible structures, a transient dynamic analysis of the structure is required, including the pressure pulse moving across the structure at the train speed, to determine the response and number of stress cycles for each train passage. Alternatively, static design methods that include allowance for dynamic enhancement effects may be found in UIC 779-1 Appendix A [\[77\]](#).

The simplified square-wave form of the pressure pulse described in this manual is appropriate for initial assessment of the dynamic response of wayside structures. More detailed load time histories may be obtained from scale model testing or from the German standard Ril 804.5501 [\[25\]](#), which provides detailed mathematical formulae for estimating the spatial distribution of pressure, including the variability with height. Fatigue life of noise barriers is covered further in [\[71\]](#), which describes recent cases where fatigue failure has occurred.

Fatigue testing of components of structures is recommended to understand their potential design life under repeated loading. With particular regard to fatigue of wayside structures, any structural assessment should consider the following effects:

- Pressure pulses will be applied two to three times per train passage, corresponding to the nose and tail of the train, and the nose-to-nose coupling where two trains are coupled together, passing the point in question (see [Figure 4-9](#)).
- Each pressure pulse causes a dynamic response of the structure. Resonant effects may lead to higher stresses than would occur if the loading were applied statically.

- Dynamic response of the structure can cause each component to experience many stress cycles per applied pressure pulse.
- The pressure pulses caused by the inter-car gaps are typically only 10 percent of the size of the nose pressure pulse, but if the frequency at which the cars pass is close to a resonant frequency of the structure, a resonant response may build up.
- The dynamic response of structures such as noise barriers can be significantly influenced by flexibility in the foundations.
- Over the lifetime of a structure, the total number of loading cycles arising from the above effects can be extremely large.

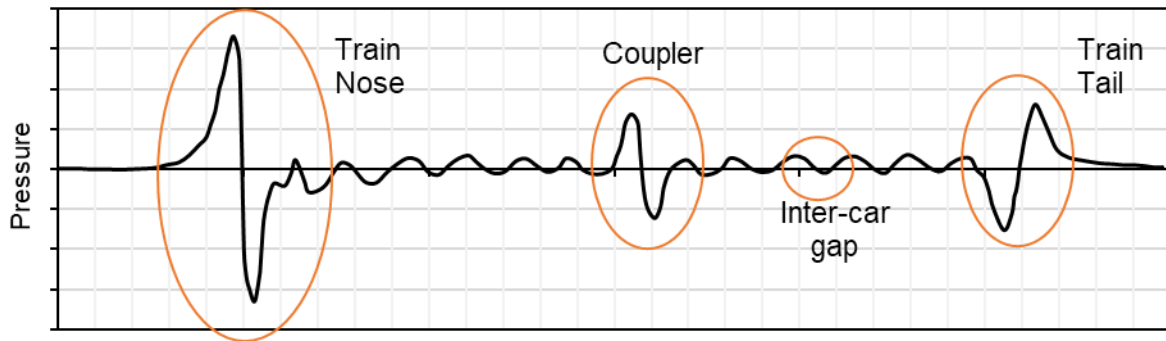


Figure 4-9. Typical form of pressure pulse from two trains coupled together, based on data from [71] and [72]

As well as ensuring the structures have sufficient strength and stiffness, it may be desirable to incorporate damping in the design.

Where necessary and practicable, the distance between the track and the structures may also be increased to reduce the loads.

4.6.4 Assessment Methods for Pressure Pulse Far from the Track

When considering structures further from the track, structural damage becomes less likely because the pressure magnitude reduces. However, other impacts (such as rattling windows) may still occur, and the same equations (such as Equation 4-2) may be used to predict the pressure magnitude at greater distances from the track.

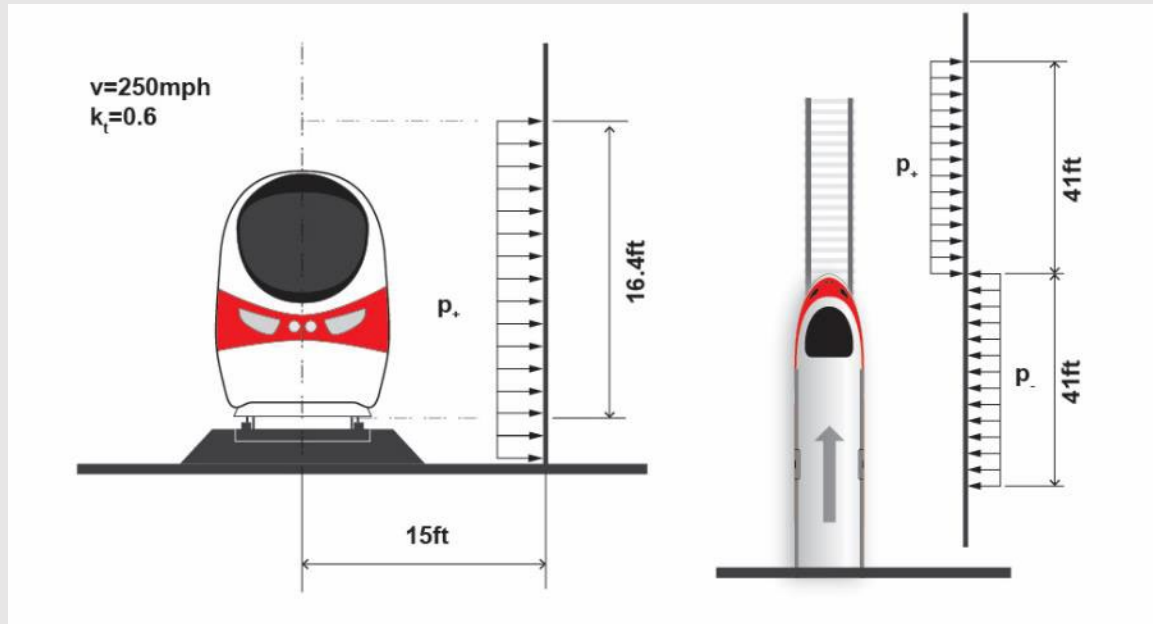
4.7 Example Calculations

4.7.1 Example 1

Question

A new noise barrier is to be erected 15 ft (4.6 m) from the track centerline. Well-streamlined U.S./Euro Baseline Trains will pass the barrier at 250 mph.

Estimate the magnitude and duration of the positive and negative parts of the area-averaged pressure pulse (p_+ and p_-) on the noise barrier.



Methodology

The pressure on the noise barrier can be estimated from [Equation 4-2](#), using values for the U.S./Euro Baseline Train.

The duration of the positive and negative pressure pulses can be estimated from [Equation 4-6](#).

Inputs

Distance to track centerline, y	15 ft (4.6 m)
Train speed, V_T	250 mph (400 km/h, 111.1 m/s)
Air density, ρ	Use standard value 1.225 kg/m ³
Train shape factor, k_t	0.6 (well-streamlined high-speed train)
Peak factor k_{ap}	1.0 (pressure distributed over large surface)
Train size factor, k_d	1.0 (U.S./Euro Baseline Train)
Length of pressure pulse, L_{p+}	41 ft (12.5 m)

Calculations

Equation 4-2:

$$\begin{aligned} p_+ &= k_{ap} k_t \left[\frac{2.5}{(y/k_d + 0.25)^2} + 0.02 \right] \times \frac{1}{2} \rho V_T^2 \\ &= 1.0 \times 0.6 \times \left\{ \frac{2.5}{(4.6/1.0 + 0.25)^2} + 0.02 \right\} \times \frac{1}{2} \times 1.225 \times 111.1^2 \\ &= 572.8 \text{ Pa} \\ &= 0.083 \text{ psi} \end{aligned}$$

Equation 4-6:

$$\begin{aligned} \Delta t_{p+} &= \frac{L_{p+}}{v} \\ &= \frac{12.5}{111.1} \\ &= 0.11 \text{ s} \end{aligned}$$

The magnitude and duration of the negative pulse is assumed to be equal to that of the positive pulse.

Result

The estimated pressure pulse magnitude is ± 0.083 psi, and the duration of both the positive and negative parts of the pressure pulse is 0.11 s.

These would form the input to a dynamic analysis of the barrier, see Section 4.5. For fatigue design, the number of cycles caused by one pressure pulse should be multiplied by 2 per train passage for single trains, or by 3 per passage where two trains are coupled together.

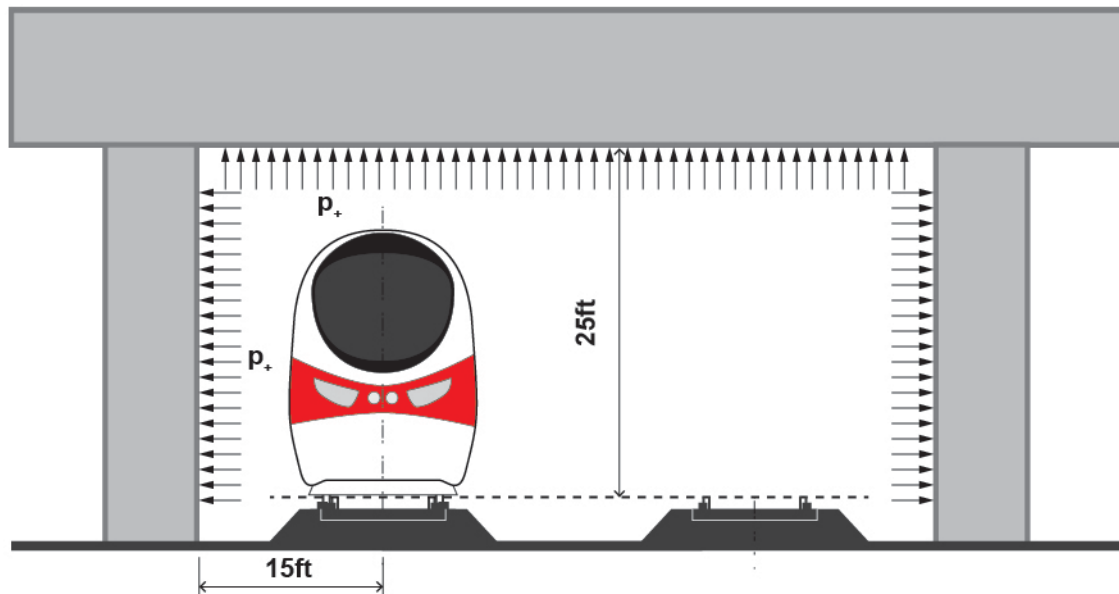
4.7.2 Example 2

Question

A new high-speed service is to operate well-streamlined, U.S./Euro Baseline Trains at a speed of 200 mph on an existing railroad. The track passes under an existing road bridge. The length of track passing under the bridge is 30 ft. The dimensions and track layout under the bridge are shown below.

What is the area-averaged pressure on the roof and side wall (nearest the train) of the bridge?

What would the maximum allowable train speed be if the pressure on the roof were to be limited to 0.120 psi by structural concerns?



Methodology

For a structure enclosing the track of length less than 66 ft, the load on vertical walls can be calculated from [Equation 4-2](#) with an additional pressure multiplier of 2 (see [Section 4.6.2.5](#)).

Because the structure encloses both tracks, the load on the horizontal roof can be calculated from [Equation 4-3](#) with an additional pressure multiplier of 3.5 (see [Section 4.6.2.5](#)).

The maximum allowable speed can be determined by noting that pressure is proportional to speed squared.

Inputs

Distance to track centerline, y	15 ft (4.6 m)
Distance above TOR, h	25 ft (7.6 m)
Train speed, V_T	200 mph (322 km/h, 89.4 m/s)
Air density, ρ	Use standard value 1.225 kg/m ³
Train shape factor, k_t	0.6 (well-streamlined high-speed train)
Peak factor k_{ap}	1.0 (pressure distributed over large surface)
Train size factor, k_d	1.0 (U.S./Euro Baseline Train)

Calculations

Load on vertical wall: Equation 4-2 with additional multiplier of 2

$$\begin{aligned}\Delta p_+ &= 2 \times k_{ap} k_t \left[\frac{2.5}{(y/k_d + 0.25)^2} + 0.02 \right] \times \frac{1}{2} \rho V_T^2 \\ &= 2 \times 1.0 \times 0.6 \times \left\{ \frac{2.5}{(4.6/1.0 + 0.25)^2} + 0.02 \right\} \times \frac{1}{2} \times 1.225 \times 89.4^2 \\ &= 741.8 \text{ Pa} \\ &= 0.108 \text{ psi}\end{aligned}$$

Load on roof: Equation 4-3 with an additional pressure multiplier of 3.5

$$\begin{aligned}p_+ &= 3.5 \times k_{ap} k_t \left[\frac{2.0}{(h/k_d - 3.1)^2} + 0.015 \right] \times \frac{1}{2} \rho V_T^2 \\ &= 3.5 \times 1.0 \times 0.6 \times \left\{ \frac{2.0}{(7.6/1.0 - 3.1)^2} + 0.015 \right\} \times \frac{1}{2} \times 1.225 \times 89.4^2 \\ &= 1169.5 \text{ Pa} \\ &= 0.170 \text{ psi}\end{aligned}$$

The pressure is proportional to speed squared. Therefore, the maximum allowable speed can be calculated as:

$$\begin{aligned}V_{T,max} &= 200 \times \sqrt{\frac{0.120}{0.170}} \\ &= 168 \text{ mph}\end{aligned}$$

Result

The estimated pressure pulse magnitude is ± 0.108 psi on the vertical walls, and ± 0.170 psi on the roof.

To limit the load on the roof to 0.120 psi, the maximum speed should be limited to 168 mph.

5 Train-to-Train Aerodynamic Effects

5.1 Introduction

When a HST passes another train on a neighboring track, the same phenomena that result in pressure loading of wayside structures (see Section 4) also result in a pressure force being applied to the neighboring train.

This force is typically experienced as a jolting of the neighboring train and may result in disturbance or discomfort for passengers. In most new high-speed railroads, the impacts of aerodynamic interaction between HSTs are mitigated simply by selecting an appropriate track spacing from guidance tables.

Where HST share ROW with other types of trains, like freight or older passenger trains, the force exerted has the potential to cause damage to the trains or dislodge loose items. Numerical studies [72] suggest that these forces could lead to the derailment of freight trains, although no documented cases of this are known.

In shared ROWs, or where sufficient space is not available to use the track spacing from the guidance tables, further assessment may be required to determine if the loads experienced by neighboring trains would be greater or less than those experienced by the same trains on existing railroads elsewhere. Determination of the acceptability of any impacts is not part of this report.

The phenomena described in this section occur both in the open environment and in tunnels containing more than one track. Track spacing tables are assumed to apply to both environments, even though the aerodynamic interactions may be stronger in tunnels.

This section includes:

- Aerodynamic principles and key influencing factors
- Impacts on passenger comfort
- Impacts on other trains
- Mitigation of impacts – by selecting appropriate track spacing
- Methods for calculating the magnitude of the load on passing trains
- Assessment methods when track spacing cannot be increased
- Example calculations for determining track spacing

The FRA has recently released literature reviews, draft guidance, and summary reports of hazards associated with HSR operations adjacent to conventional tracks [46][47][48]. The aerodynamic hazards and mitigations mentioned in these reports are covered in this guidance manual.

5.2 Aerodynamic Principles and Phenomena

This report refers to an **acting train**, which exerts a force on an **observing train** as they meet or pass. The observing train may be stationary or moving. The pressure pulse is caused by the acting train forcing air out of its path, resulting in a zone of high pressure around the nose of the train, immediately followed by a zone of low pressure (see also Section 4). Other aerodynamic impacts from passing trains (for example, the effect of the slipstream of the acting train on the observing train) are usually negligible for HSTs.

5.3 Influencing Factors

The magnitude of the pressure pulse primarily depends on:

- The speed of the acting train
- The cross-sectional dimensions and aerodynamic performance of the acting train
- The width of the observing train and the track spacing, which determines the distance to the side of the observing train (Figure 5-1).

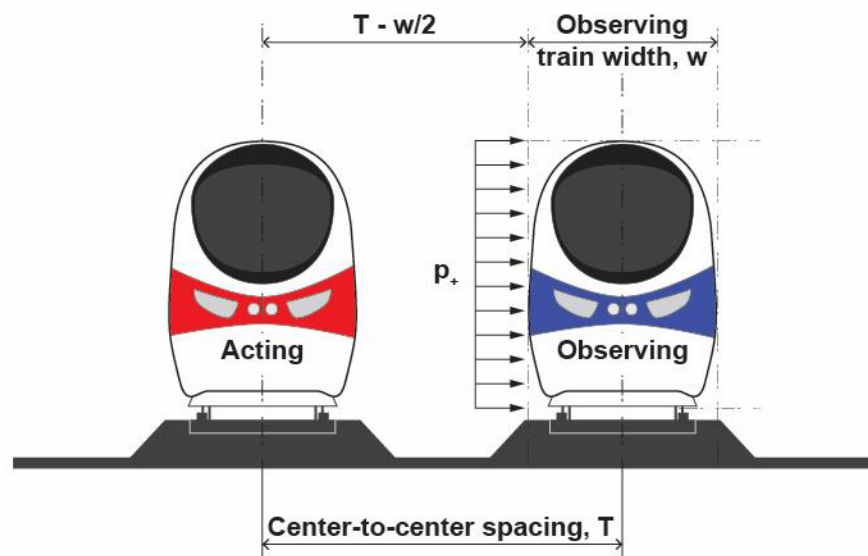


Figure 5-1. Key dimensions for train-to-train aerodynamic effects

5.3.1 Train Speed

The magnitude of the pressure pulse is proportional to the square of the speed of the acting train through the air (i.e., the acting train speed plus any headwind). Therefore, a doubling of train speed results in a four-fold increase in the pressure pulse magnitude (see Figure 5-2).

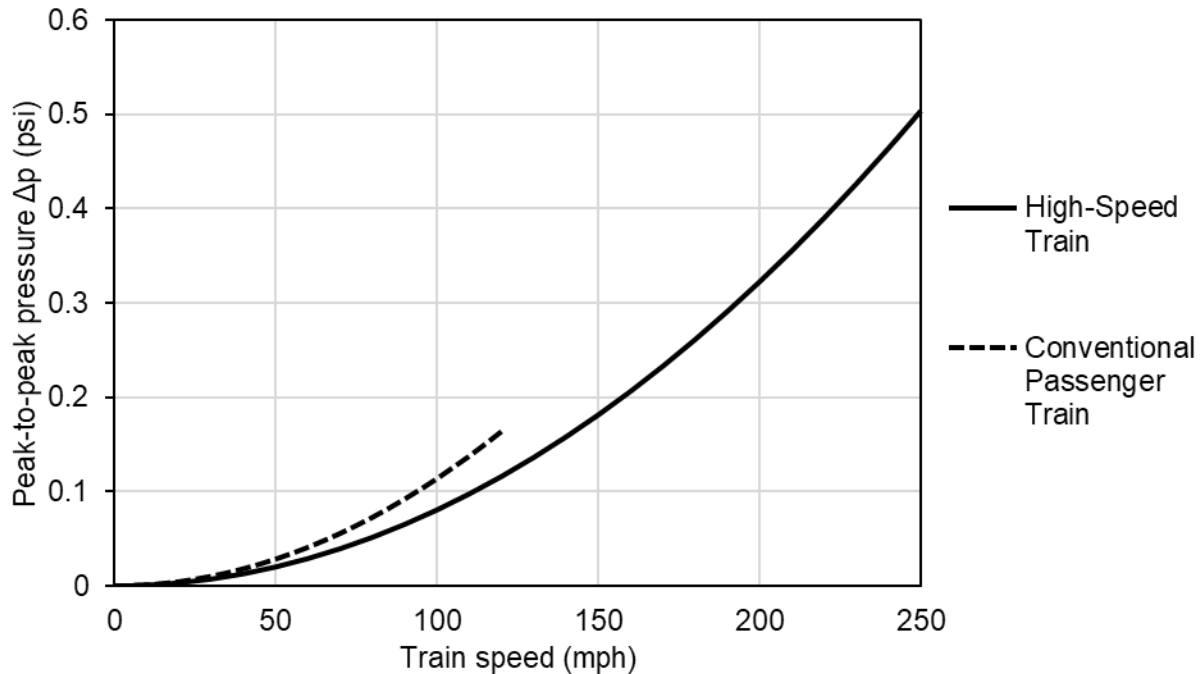


Figure 5-2. Variation of pressure pulse magnitude with train speed for track spacing of 13 ft (4.0 m) and train width 10 ft (3.0 m)

The closing speed of the two trains is less relevant. For modern high-speed trains, as described in Section 3, the streamlined form of the trains induces a slipstream air speed that reduces rapidly with distance from the train (see Figure 5-3). As such, the motion of the observing train cannot create a significant headwind effect on the acting train and, therefore, makes little difference to the magnitude of the pressure pulse caused by the acting train.

Full-scale measurements have shown that the difference in pressure between a stationary observing train and an observing train traveling at the same speed as the acting train may be 10 to 25 percent [96][141], equivalent to a 5 to 12 percent increase in acting train speed. In the calculations presented in Section 5.6.3, no allowance for this effect is included. However, as these equations are intended to be used for comparing HSR operations on a like-for-like basis rather than to determine absolute pressure values, this omission does not affect the conclusions of the assessments.

Aerodynamic impacts may be more severe in cases of trains traveling in the same direction rather than opposing directions [72] because the pressure is applied on the observing train for a longer time, resulting in a greater impulse. However, for the purposes of the assessment methods and mitigation described in this report, there is no need to distinguish whether the trains are traveling in the same or opposing directions.

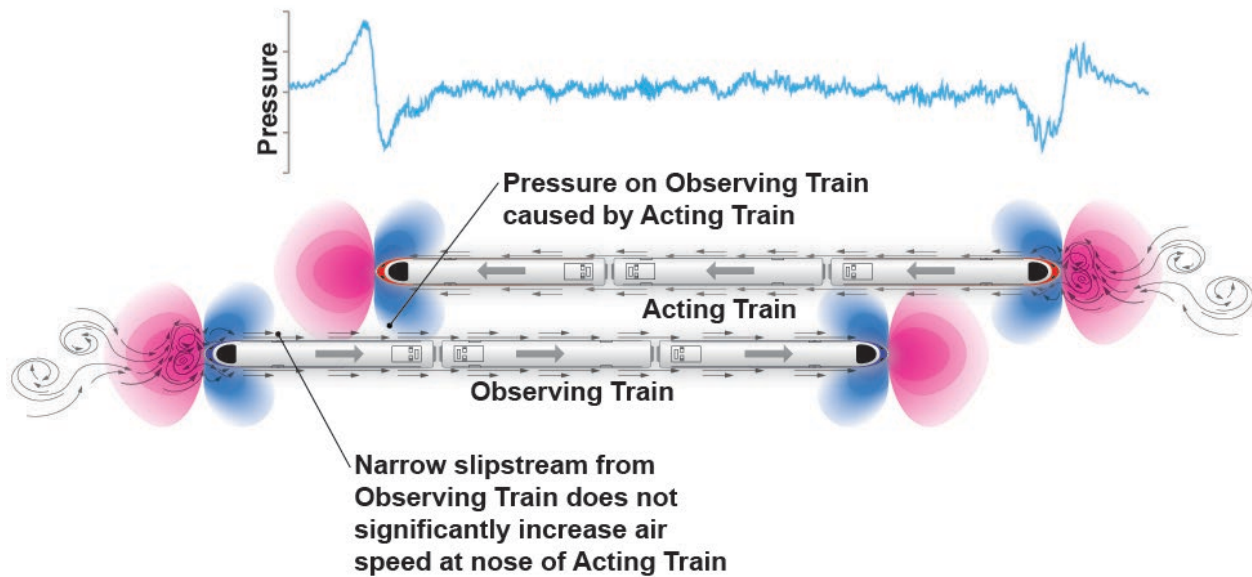


Figure 5-3. Pressure pulses exerted by an acting train on an observing train

5.3.2 Train Dimensions and Aerodynamic Performance

The magnitude of the pressure pulse is dependent on the aerodynamic properties of the train. HSTs tend to be more streamlined than conventional passenger and freight trains. Therefore, traveling at the same speed, the magnitude of the pressure pulse generated by a HST is smaller than that from a conventional train.

The lateral extent of the pressurized zone around the nose and tail of the train is expected to be approximately proportional to the width of the train. Therefore, a wider train results in a wider zone of high pressure at the nose and tail of the train.

5.3.3 Confinement by Surroundings

If the track is partially enclosed, for example by walls on one or both sides of the track, the pressures are increased due to the zone of high pressure being confined.

5.3.4 Track Spacing

The pressure around the nose of the acting train is highest at the surface of the acting train and reduces with increasing distance from the acting train. Therefore, the pressure pulse experienced by the observing train is reduced where there is a greater distance between the tracks (see [Figure 5-4](#)).

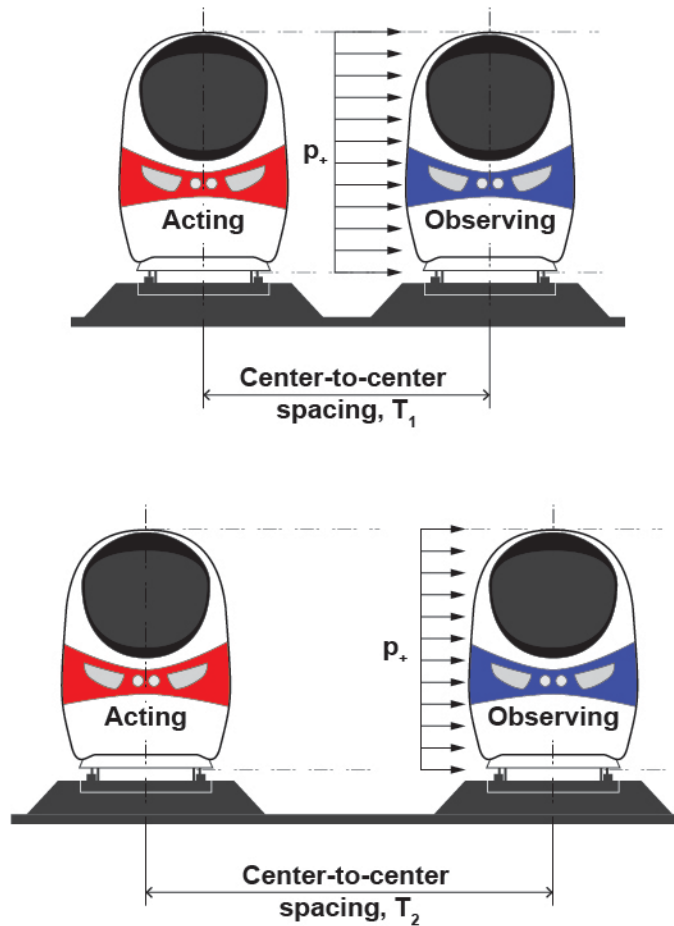


Figure 5-4. Illustration of pressure pulse magnitude reduction with increased track spacing

The magnitude of the pressure pulse is approximately inversely proportional to the square of the track center-to-center spacing ([Figure 5-5](#)). Thus, doubling the track spacing reduces the magnitude of the pressure pulse by a factor of approximately four.

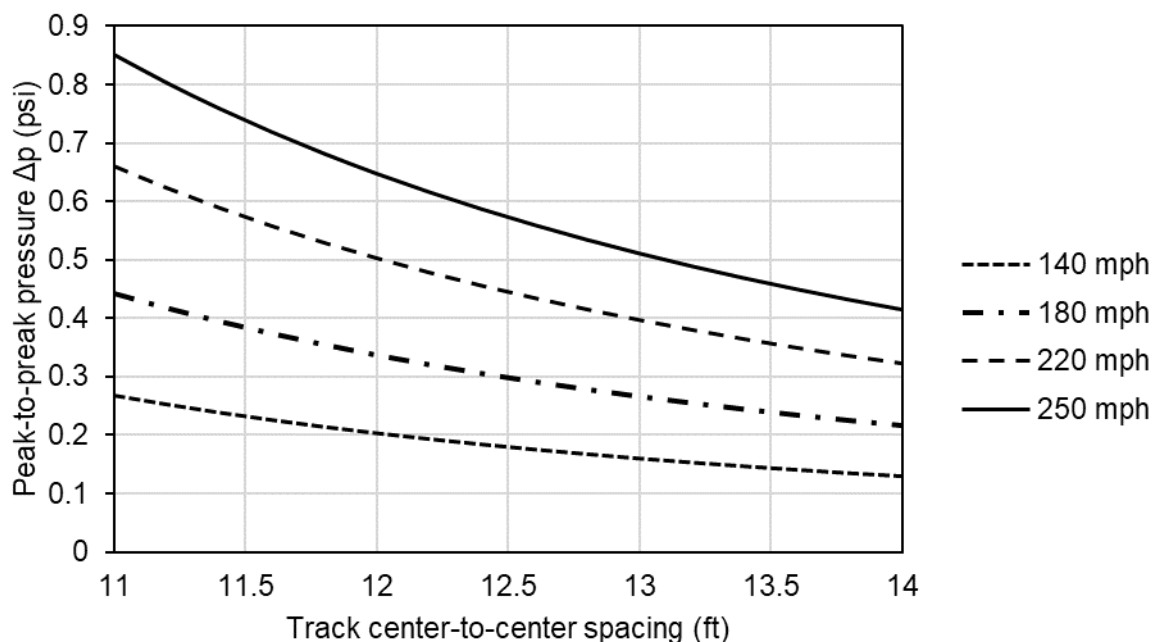


Figure 5-5. Variation of pressure pulse magnitude with track spacing for a HST of width $w=10$ ft

5.4 Impacts

5.4.1 Impacts on HSTs

Known impacts of aerodynamic interactions between HSTs primarily relate to passenger comfort. For example, the sudden arrival of the pressure pulse may cause a jolting motion in the observing train. There may also be noticeable flexing of the sides of the cars and potential for fatigue damage to train bodywork or more serious damage such as window blow-out. However, in practice HSTs are designed to resist this loading and operators are unlikely to need to consider it provided that recommendations regarding track spacing are followed.

5.4.2 Impacts on Conventional Passenger and Freight Trains

HSTs meeting or passing conventional passenger and freight trains on adjacent tracks at high speed could potentially cause a number of aerodynamic impacts on the conventional vehicles. These include window breakage or blow-out, fatigue damage to railcar doors and body structure, fabric or other lightweight covers being damaged or torn off, or bulk cargos being blown out of open gondola cars. The authors cannot state for certain that no aerodynamic impacts will occur in practice, however these impacts are not expected to be problematic in the U.S. for the following reasons:

- Tier III equipment is limited to 125 mph in shared ROWs. The aerodynamic impacts of HSTs on conventional passenger or freight vehicles will likely be no worse than the aerodynamic impacts from non-HST vehicles with speeds up to 125 mph.

- The NEC (Tier II) operates at speeds above 125 mph on shared ROWs but has a long history of operation without reported aerodynamic impacts on conventional vehicles. Given the unique characteristics of operations in the NEC, any further speed increase there should be subject to a route-specific risk assessment.
- Tier III may operate at speeds above 125 mph in corridors shared with conventional ROW, but the separation between the HSR tracks and the conventional tracks will likely be large enough to mitigate aerodynamic interactions as a by-product of other considerations such as ROW protection.

Additional caution is advised in case of planning a new line, or speed increases on an existing line, where double-stacked container trains may be passed by HSTs. Numerical modelling [72] has suggested that, in extreme circumstances, double-stacked containers may be at risk of derailment when passed by HSTs at speeds lower than 125 mph.

It is not common practice in other countries for HSTs to share a tunnel with conventional traffic, but where this does occur, the aerodynamic impacts on conventional passenger and freight vehicles can potentially be much more severe than in open air, as described in Sections 7.4.5 and 7.5.8. This situation is not expected to occur in the U.S., except where speeds are too low for aerodynamic impacts to be of concern.

5.5 Mitigation Methods

5.5.1 *Mitigation for Dedicated HSR ROW: Recommended Minimum Track Spacing*

In the design of new high-speed railroads, mitigation of aerodynamic impacts between trains is achieved by providing sufficient center-to-center track spacing for the anticipated operating conditions. European [38] and Chinese [99] HSR regulations mandate minimum center-to-center track spacings based on line speed. Where two tracks share the same tunnel, the mandated minimum center-to-center track spacing is the same as in open air.

The proposed aerodynamic minimum center-to-center track spacings for the U.S./Euro and U.S./Asian Baseline Trains are summarized in Table 5-1. These spacings are the same as European and Chinese practice, respectively, for speeds up to 215 mph (350 km/h), and thus are based on successful operation experience. The existing European and Chinese standards do not cover speeds higher than 215 mph. For higher speeds, the track spacings have been calculated such that the pressure pulse at 250 mph is no worse than that under existing regulations at 215 mph.

A comparison of the proposed aerodynamic minimum track spacings against European and Chinese standards is shown in Figure 5-6.

Table 5-1. Aerodynamic minimum center-to-center track spacing for HSTs

Design speed (mph)		Aerodynamic minimum center-to-center track spacing for HST-to-HST			
		U.S./Euro Baseline		U.S./Asian Baseline	
mph	km/h	ft	m	ft	m
Up to 155	Up to 250	13.0	4.0	15.1	4.6
156–185	251–300	13.8	4.2	15.7	4.8
186–215	301–350	14.8	4.5	16.4	5.0
216–250	351–400	16.6	5.1	18.9	5.8

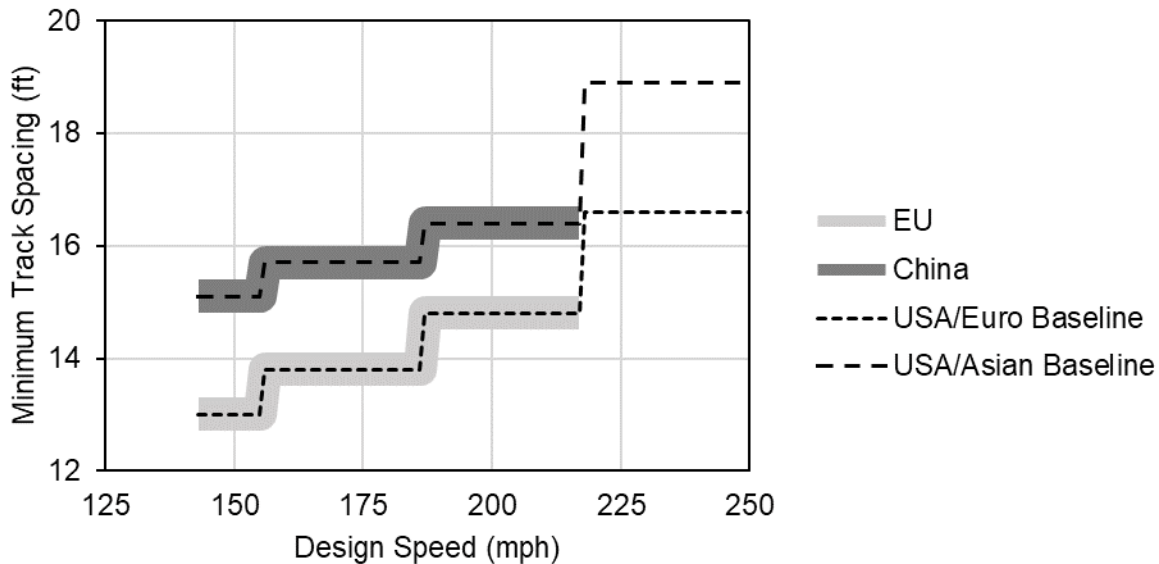


Figure 5-6. Proposed aerodynamic minimum center-to-center track spacing for HST-to-HST and existing European and Chinese regulations

Legal requirements and other drivers may lead operators to provide wider track spacing than the aerodynamic minimum values given in this manual. [Figure 5-7](#) shows the legal minimum center-to-center distances for main tracks by state, from Table 28-3-3 of the AREMA Manual for Railway Engineering [\[3\]](#).

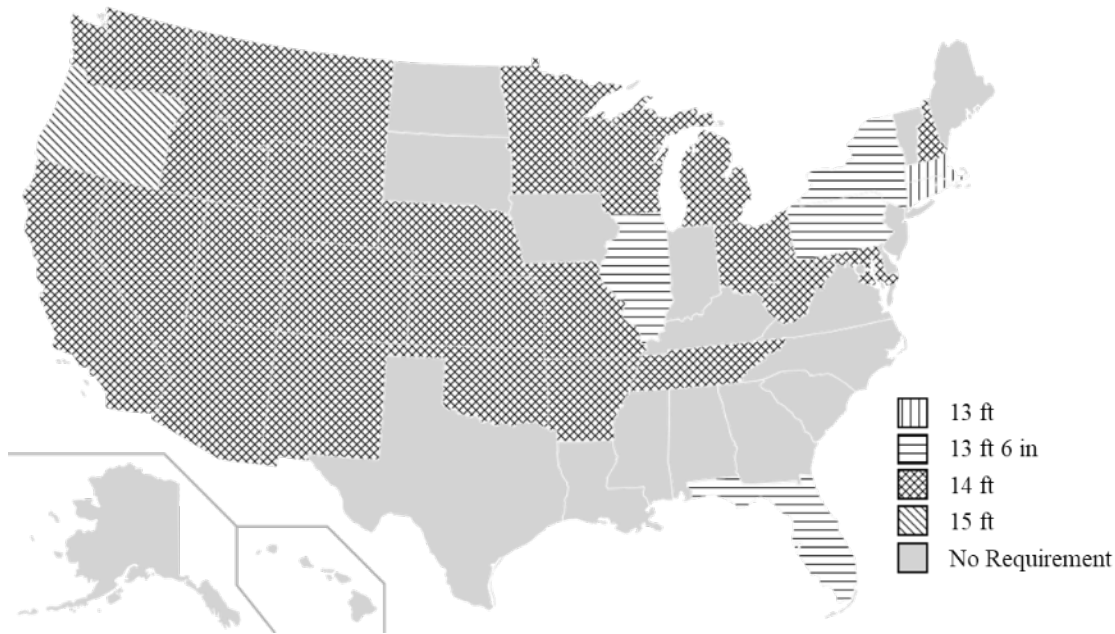


Figure 5-7. Map of legal minimum track spacing for US states⁴

The proposed aerodynamic minimum center-to-center track spacings can be used in two ways to find the maximum speed at which aerodynamic interactions between trains will be no worse than in international HSR operations: either in the design of new railroads to determine the necessary track spacing; or with existing railroads. For example, if the existing track separation is 14 ft, speeds of up to 185 mph would be in line with international practice,;see [Figure 5-6](#).

Note, the spacing guideline is based on regulations and design criteria for international HSR systems with a history of non-problematic operation. These recommendations may be conservative and the impacts of trains passing at higher speeds or closer track spacings are not quantifiable. For example, in the NEC, trains operate at speeds up to 150 mph, with center-to-center spacing as low as 12 ft. This is less than the aerodynamic minimum spacing proposed above based on international experience, but there have been no known safety issues due to aerodynamic interactions between passing or meeting trains.

For track spacing less than is recommended in [Table 5-1](#), the designer should assess any impacts by full-scale testing. Full-scale testing is required to identify impacts, such as damage to windows or passenger discomfort, that are not well-predicted by model scale or CFD-based assessments.

⁴ Outline U.S. map by Theshibboleth
[https://commons.wikimedia.org/wiki/File:Blank_US_Map_\(states_only\).svg](https://commons.wikimedia.org/wiki/File:Blank_US_Map_(states_only).svg)

5.5.2 Mitigation for Shared ROW and Shared Corridors

Mitigation measures for the aerodynamic impacts of HSTs on conventional trains might include larger track spacing than for dedicated HSR tracks and/or speed restrictions. There is no consistent international approach to determining the required track spacing for shared ROWs. Methods of estimating minimum track spacing or maximum speed of HSTs to prevent unacceptable train-to-train aerodynamic impacts in shared ROW are proposed in Section 5.6. Speed restrictions based on operational experience are described in [14][142]. However, for the reasons given in Section 5.4.2, these measures are not expected to be necessary in the U.S.

In shared corridors, a wall or other barrier is sometimes provided between HSR and conventional tracks. This is typically driven by ROW protection for derailment situations rather than aerodynamics but would provide aerodynamic mitigation as an additional benefit.

5.5.3 Design of Rolling Stock

Rolling stock manufacturers design high-speed trains to withstand the loads that are expected to be experienced during operation. The governing load case for design may be the pressure changes experienced in tunnels, although trains passing in open air are also considered due to the potential for a very large number of pressure cycles over the lifetime of the train.

The aerodynamic form of rolling stock may also be designed to reduce the pressure pulses generated by the nose and tail to reduce the loads on passing trains.

5.6 Assessment

5.6.1 Assessment Objectives

Assessment is not required for exclusive HSR ROWs where track spacing conforms with Table 5-1. In other cases (for example, ROWs shared with conventional trains), the objective of the assessment is to determine either the appropriate track spacing or the maximum speed, such that aerodynamic interactions between trains in the new operation will be no worse than in an existing non-problematic operation with the same trains.

5.6.2 Assessment Principles

The governing aerodynamic phenomenon considered in this assessment is the nose/tail pressure pulse, not the slipstream.

An equation is provided from which the pressure pulse magnitude on an observing train can be calculated; see Section 5.6.3 below. This will be used as the basis for comparing the level of train-to-train aerodynamic impacts in different operations. The observing train must be of the same type in both cases, because the magnitude of pressure pulse at which impacts become problematic varies from one train type to another.

If required, the pressure pulse magnitude can be calculated for a range of train speeds and track spacings, enabling calculation of the tradeoff between higher train speed and greater track spacing.

5.6.3 Calculation of Pressure Pulse Magnitude

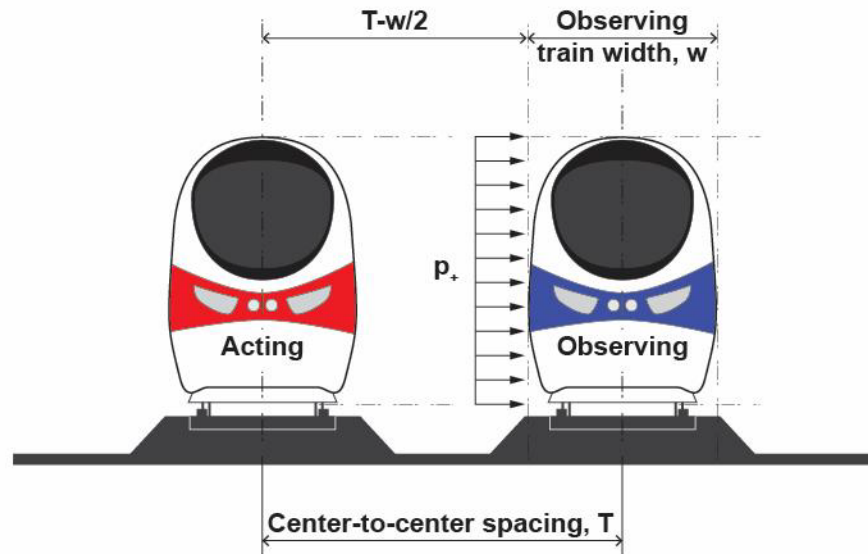


Figure 5-8. Relevant dimensions in pressure pulse calculation for trains meeting

The magnitude of the area-averaged pressure pulse on the observing train may be calculated using [Equation 5-1](#), adapted from EN 14067-4 for pressures on vertical surfaces adjacent to the track [\[33\]](#). In this equation, the distance to the vertical surface (the side of the observing train) is expressed in terms of track spacing and train width.

$$p_+ = p_- = k_t \left[\frac{2.5}{\left(\frac{T - w/2}{k_d} + 0.25 \right)^2} + 0.02 \right] \times \frac{1}{2} \rho V_T^2 \quad \text{Equation 5-1}$$

Where

p_+/p_- = Amplitude of positive/negative pressure pulse (Pa)

k_t = Train shape factor of acting train (1.0 for freight trains, 0.85 for conventional passenger trains or 0.6 for streamlined HST) ¹

k_d = Factor to account for dimensions of acting train (1.0 for U.S./Euro Baseline, 1.13 for U.S./Asian Baseline) ²

T = Center-to-center track spacing (m)

w = Width of observing train (m)

ρ = Density of the air (kg/m³)

V_T = Speed of acting train (m/s)

This equation requires SI units.

Notes:

1. For purposes of design, k_t may be taken as 1.0 for freight trains, 0.85 for passenger trains, or 0.6 for aerodynamically shaped high-speed trains. More accurate values of k_t may be derived from moving-model scale model testing, full-scale testing, or computational fluid dynamics (CFD) analysis based on the shape of the particular train.
2. This assumes that the pressure field scales with the width of the train, taking the widths of the two train types as 118 in (3.0 m) for U.S./Euro and 134 in (3.4 m) for U.S./Asian.

5.6.4 Assessment by Comparing New and Existing Operations

Where a proposed HST is larger or less aerodynamic than either of the U.S. Baseline Trains or where HSTs pass adjacent to conventional or freight vehicles in a shared ROW, there are no existing international regulations or guidance which can be directly adopted in the U.S.

The tolerance of conventional rail vehicles to aerodynamic loading is likely to vary widely between particular vehicle types, and quantitative data are not usually available. Full-scale physical testing to obtain that data is difficult and expensive.

However, using the known history of safe operation on conventional lines offers the possibility to carry out approximate comparative assessments. This would answer the question, “Is the proposed new HSR/conventional operation likely to generate a higher or lower pressure pulse magnitude on the conventional vehicle than the existing conventional/conventional operation which has satisfactory performance?”

The steps involved in this comparative assessment would be:

- For the existing conventional/conventional operation with history of safe operation, note the train type, speed, and center-to-center track spacing.

- Use [Equation 5-1](#) to estimate the pressure pulse magnitude occurring in the existing operation.
- Use [Equation 5-1](#) to estimate the pressure pulse magnitude occurring in the proposed new operation.
- If the pressure pulse in the new operation is the same or lower, then the aerodynamic impacts are expected to be no worse than in the conventional operation.
- If necessary, the calculation could be repeated with greater track spacing or lower speed for the new operation.

Note that [Equation 5-1](#) is an approximation, useful for comparing the pressure pulses in two operations. Any conservative or non-conservative aspects of the equation would likely affect the calculations for both operations equally and therefore are not expected to bias the conclusions of the assessment.

5.6.5 Assessment by Full-Scale Testing

If it is not possible to compare against existing operations or existing regulations, train-to-train aerodynamic interactions should be assessed using full-scale testing.

In situations where space is restricted or where the tracks already exist and will not be moved, it may not be possible to provide the track spacing suggested by the above method. The question then becomes whether the aerodynamic impacts can be tolerated or, if not, what speed restrictions need to be established.

For example, if the line speed for a particular route were to be increased, the increase in pressure exerted by the HSTs on adjacent trains can be calculated, but there is not a pre-determined value at which the increased pressure will result in unacceptable impacts (such as damage to windows or passenger discomfort). In this case, full-scale testing, including all train types involved in train passing scenarios, would be the most reliable method to determine a limiting value at which impacts do not occur. Methods for full-scale testing are presented in [Section 2.4.1](#).

5.7 Examples

5.7.1 Select Required Track Spacing Based on Speed

Question

A new railroad is to be designed in Oregon, with US-Euro HSTs traveling at 200 mph. What is the recommended center-to-center track spacing to be used?

Methodology

Select the appropriate track spacing from [Table 5-1](#), and cross-check against the relevant legal minimum for the state from [Figure 5-7](#).

Inputs

HST speed, V_T 200 mph (320 km/h)

Calculations

From [Table 5-1](#), the aerodynamic minimum center-to-center track spacing for US-Euro HSTs at speeds between 186-215 mph is 14.8 ft (4.5 m). However, from [Figure 5-7](#), the legal minimum track spacing in Oregon is 15 ft.

Result

The minimum center-to-center track spacing is 15 ft (4.6 m).

5.7.2 Estimating Required Track Spacing Based on Existing Reference Operation

Question

A conventional passenger railroad operates adjacent to freight lines at 80 mph and a track spacing of 14.0 ft without unacceptable aerodynamic impacts when the passenger trains meet freight trains. The freight trains have a width of 10.5 ft.

If a new high-speed railroad, with trains which travel at 125 mph, is to operate adjacent to freight lines carrying the same freight trains, with a track spacing of 18 ft, will the pressure experienced by the freight trains be less than or greater than that on the existing railroad?

Methodology

Use [Equation 5-1](#) to calculate the pressure pulse amplitude for the conventional railroad and the proposed new railroad.

Inputs

Air density, ρ Standard value **1.225 kg/m³**

Observing train width, w **10.5 ft (3.2 m)**

Conventional Railroad

Existing center-to-center spacing, T_{conv} **14 ft (4.3 m)**

Conventional train speed, $V_{T,conv}$ **80 mph (130 km/h, 36 m/s)**

Conventional train shape factor, $k_{t,conv}$ **0.85** (see notes under [Equation 5-1](#))

Train size factor, k_d **1.0** (U.S./Euro Baseline Train)

HSR Railroad

Proposed center-to-center spacing, T_{HST} **18 ft (5.6 m)**

HST speed, $V_{T,HST}$ **125 mph (200 km/h, 56 m/s)**

HST shape factor, $k_{t,HST}$ **0.6** (see notes under [Equation 5-1](#))

Train size factor, k_d **1.0** (U.S./Euro Baseline Train)

Calculations

Using [Equation 5-1](#),

$$\begin{aligned}\Delta p &= 2k_t \left[\frac{2.5}{\left(\frac{T - w/2}{k_d} + 0.25 \right)^2} + 0.02 \right] \times \frac{1}{2} \rho V_T^2 \\ \Delta p_{conv} &= 0.85 \left[\frac{2.5}{\left(\frac{4.3 - 3.2/2}{1.0} + 0.25 \right)^2} + 0.02 \right] \times 36^2 \\ &= 338 \text{ Pa} \\ \Delta p_{HST} &= 0.6 \left[\frac{2.5}{\left(\frac{5.6 - 3.2/2}{1.0} + 0.25 \right)^2} + 0.02 \right] \times 56^2 \\ &= 298 \text{ Pa}\end{aligned}$$

Result

At center-to-center track spacing of 18 ft, the pressure experienced by the freight trains from HSTs at 125 mph is expected to be less than that from the conventional trains at 80 mph and 14 ft center-to-center track spacing.

6 Crosswinds

6.1 Introduction

Strong crosswinds have been known to cause derailment and overturning of trains, resulting in loss of life and serious injuries to passengers and crew. This section sets out the methods of assessing and mitigating these risks. This report concentrates on HSR, but crosswinds are a potential threat to all rail operations.

Crosswind safety needs to be considered by rolling stock manufacturers during the design of vehicles, and also by operators, especially when planning new routes or when introducing new rolling stock or increasing speeds on existing routes. This document is aimed primarily at operators rather than railcar manufacturers and therefore more attention has been focused on the route safety aspects and the influence on safety of infrastructure choices. However, the vehicle-related issues are also summarized to help operators understand the information provided to them by manufacturers and to assist with specifying rolling stock.

In addition to derailment or overturning of trains, high winds can cause overhead catenary damage and other important safety concerns such as fallen trees or debris on the track. This report does not include assessment methods for these risks. Nevertheless, operators will need to have appropriate procedures in place to mitigate them.

This section includes:

- Aerodynamic principles relevant to crosswind safety and key influencing factors
- Impacts on safety caused by wheel unloading leading to derailment or overturning
- Mitigation by providing wind barriers
- Mitigation by operational methods such as stopping trains when high winds are forecast
- A summary of assessment methods for crosswind stability of railcars
- A method for route safety assessments
- Example calculations

6.2 Aerodynamic Principles

A **crosswind** is any wind that is not blowing directly parallel to the track. A train subjected to crosswinds experiences a lateral force along the exposed side of the train that results in a tendency for the train to tip to one side. Depending on the shape of the railcar, vertical force (lift) and a moment about the railcar axis may be generated in addition to the lateral force. The combined effect of the aerodynamic forces and moments may be expressed as a moment about the leeward rail, M_A in [Figure 6-1](#), which is commonly called the **tipping moment**. The weight of the vehicle creates a rotating action in the opposing direction to the tipping moment (to restore the train to equilibrium) called the **restoring moment**, M_R (also shown in [Figure 6-1](#)).

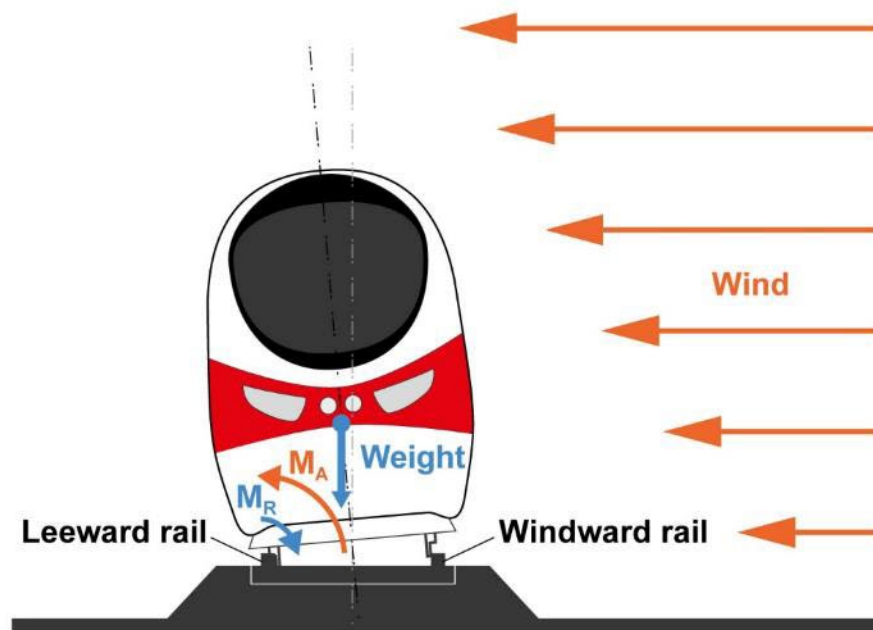


Figure 6-1. Crosswinds generate forces and moments that can cause derailment or overturning

6.2.1 Relevant Wind Speed Measurements

Accidents are typically caused by gusts, rather than by steady wind. It can take as little as 1 to 3 seconds for a train to be derailed or overturned by a wind gust, therefore the most relevant measure of wind is the maximum wind gust speed measured over a 1-to-3-second timeframe. In the U.S., weather forecasts often predict the **wind gust speed**, which is measured over 3 seconds and is relevant to the risk of accidents. Sometimes forecasts quote **sustained wind speed**, which is averaged over 1 minute and is less relevant.

6.2.2 Definitions of Critical Wind Speed and Critical Gusts

In crosswind risk assessments, the **critical wind speed** can be thought of as the speed of a wind gust that would almost cause the train to tip over. It is defined in Europe as the wind gust speed causing the windward wheels of the most vulnerable railcar to be unloaded by 90 percent (that is, the wind exerts 90 percent of the force required to initiate tipping). This report takes the definition as 85 percent unloading instead of 90 percent for compatibility with U.S. regulations governing track geometry defects, 49 CFR 213.333 [145]. This adds a further level of conservatism to the risk calculation compared with the European system. The occurrence of a gust at the critical wind speed does not necessarily mean that the train will derail or overturn, only that the stated level of wheel unloading will occur. The critical wind speed is unique to a particular train design and depends on its shape, weight, suspension behavior, and other considerations. Wind gusts with a speed of at least the critical wind speed will be called **critical gusts** in this report.

6.2.3 *The Need for a Probabilistic Approach to Assessment*

Wind gusts are a random phenomenon. Their exact speed cannot be predicted in advance. Some locations are windier than others, making it more likely that a critical gust will occur. However, even in the least windy places and no matter how high the critical gust speed, there is still some chance that a critical gust will occur. Crosswind safety assessments are concerned with calculating the probability of occurrence of a critical gust and ensuring that the probability is acceptably low – by applying mitigation measures if necessary. Unless the entire railroad alignment is in a tunnel, the risk of a critical gust occurring cannot be eliminated completely.

6.2.4 *Probabilistic Description of Wind Gust Speeds*

Wind gust speeds may be described in terms of how often they are expected to occur in a given location. The faster the wind gust speed, the less often it occurs. The frequency of occurrence is described by the **Mean Recurrence Interval (MRI)**. For example, if the 10-year MRI wind gust speed is 71 mph, then a wind gust of 71 mph or greater is expected to occur on average once every 10 years; in any one year, there is a 1-in-10 chance of such a gust occurring. At the same location, the 100-year MRI wind gust speed may be, say, 92 mph. Thus, gusts of 92 mph or more are expected to occur on average once every 100 years. In this location, gusts of at least 71 mph are 10 times as frequent as gusts of at least 92 mph.

The probabilistic assessment approach involves calculating the MRI of a critical gust. The lower the MRI, the more frequently critical gusts are expected to occur, the higher the risk of crosswind-induced accidents, and the more likely that mitigation measures will be required.

6.2.5 *Wind Angles and Interaction with Train Speed*

In this report, the wind that an observer standing on the ground would feel in the absence of any trains is called the **natural wind**. The speed and direction of the natural wind are described relative to the ground. A moving train experiences an **apparent wind** consisting of the combined effects of the natural wind together with the headwind from the train's motion through the air. These are shown in the vector diagram in [Figure 6-2](#), in which the speed and direction of the natural wind relative to the ground are labelled V_w , and β_w respectively, the train's velocity is labelled V_T , and the speed and direction of the apparent wind are labelled U and β , respectively. U is sometimes called the **crosswind speed** and β is called the **yaw angle**. The apparent wind has a greater magnitude and a more head-on direction than the natural wind, as shown in [Figure 6-2](#).

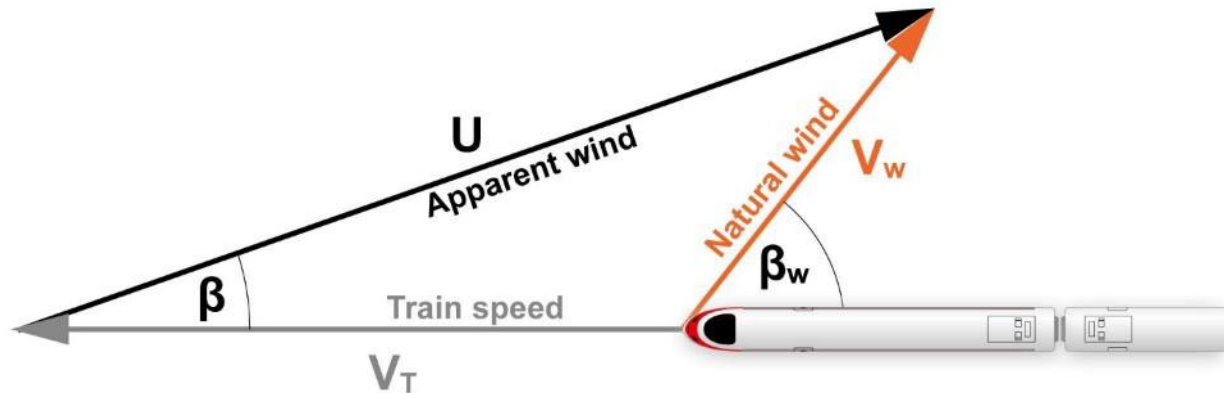


Figure 6-2. Natural wind, V_w , and apparent wind, U , relative to a moving train

It is the apparent wind (resulting from the combined effect of train motion and natural wind), and not only the natural wind itself, which causes the forces and moments that result in a tipping action on the railcar. When testing train shapes in a wind tunnel or by CFD analysis, the train model does not move and the wind in the test (or analysis) represents the apparent wind. However, when the results of such tests are presented as **Characteristic Wind Curves (CWCs)** (see Section 6.2.8), the apparent wind required to cause unloading of the windward wheel has been broken down into a combination of train speed and natural wind speed and angle using vector diagrams like Figure 6-2. Critical wind speeds refer to the natural wind speed V_w and are specific to a given train speed and a given natural wind direction.

One might intuitively expect that since the motion of the train causes only a headwind and a train cannot be overturned by a headwind, the speed of the train would play no part in determining the natural wind speed that can overturn the train – but this is not the case. Consider the two situations shown in Figure 6-3. The natural wind is the same in both cases. In case (b), the train speed is twice that of case (a). The apparent wind in case (b) has a greater speed and a more head-on direction than case (a). Which of the two cases offers greater potential to overturn the train? On one hand, the direction of the apparent wind in case (a) is more side-on. On the other hand, the apparent wind in case (b) has a greater speed. The balance between these two effects depends on the aerodynamic characteristics of the railcars and experiments consistently show that case (b) causes greater tipping effect than case (a). In other words, if the natural wind stays the same, *the tipping tendency of the train increases with increasing train speed.*

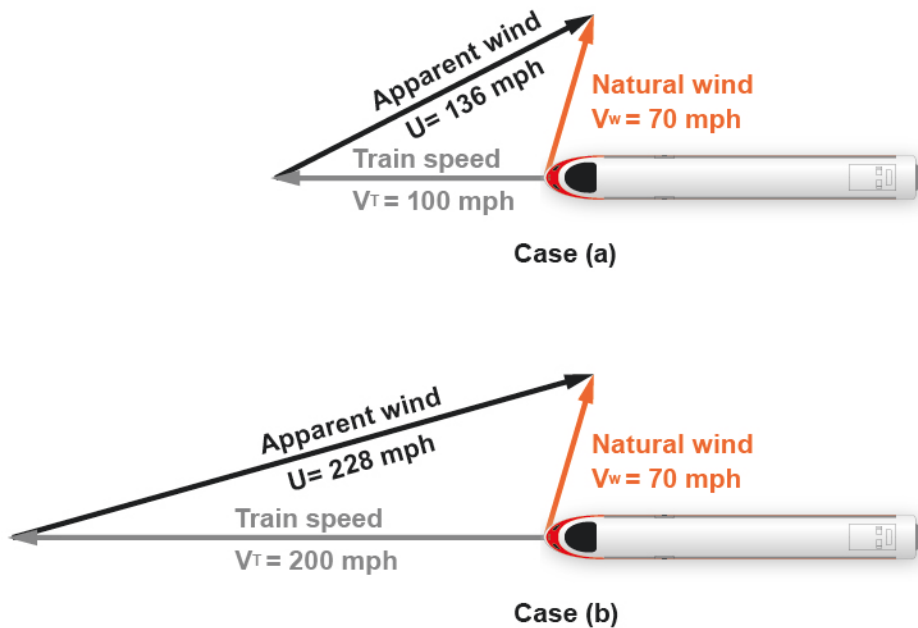


Figure 6-3. Influence of train speed on apparent wind

A corollary of the above is that, for a given natural wind direction, *the greater the train speed, the lower the critical (natural) wind speed*. An example is shown in Figure 6-4 – in both cases (c) and (d), the natural wind is at the critical wind speed for the stated train speed, according to the reference CWCs given in Figure 6-6.

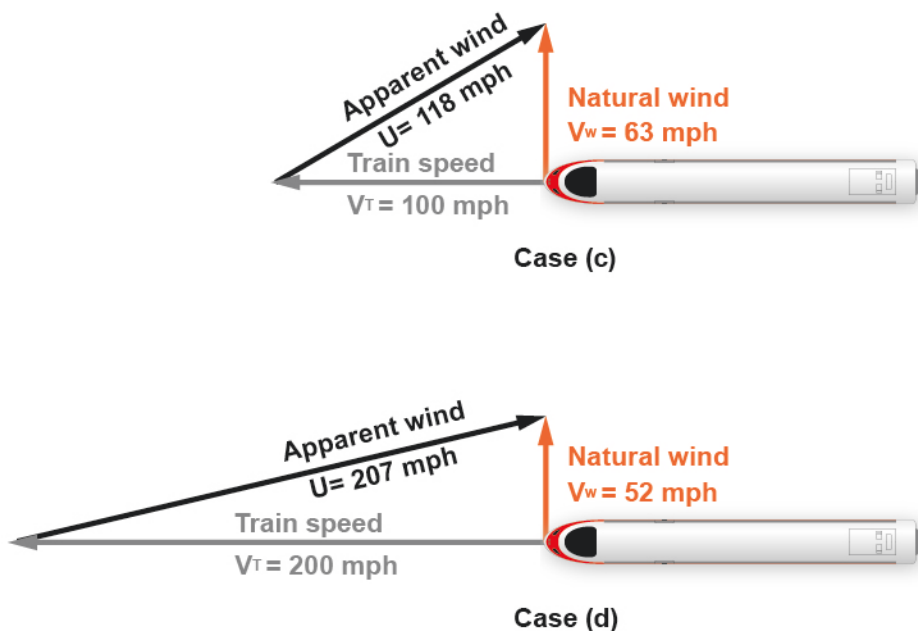


Figure 6-4. Two combinations of train speed and natural wind speed resulting in a critical wheel unloading condition

6.2.6 Unbalanced Lateral Acceleration in Curves

When a train negotiates a curve, a centrifugal acceleration pushes the train toward the outside of the curve. To counteract this effect, the track may be **superelevated** with the outer rail being higher than the inner rail. The train speed at which the superelevation in a given curve exactly balances out the centrifugal acceleration is called the **balance speed**. Alternatively, it can be said that **balanced superelevation** is required to cancel out centrifugal acceleration at a given train speed.

If the train is traveling faster than the balance speed, there is an insufficient superelevation to balance the centrifugal effect, leading to an **unbalanced lateral acceleration** tilting the train toward the outside of the curve. In a given curve and at a given train speed, the difference between the balanced superelevation and the actual superelevation is called **cant deficiency**. When the train is traveling below the balance speed, an unbalanced lateral acceleration tilts the train toward the inside of the curve. In this case, the difference between the balanced superelevation and the actual superelevation is called **cant excess**.

Either cant deficiency or cant excess will result in partial unloading of the wheels on one side of the train. If a wind gust blows in the same direction as the unbalanced lateral acceleration, the two effects can combine to cause the train to tip; see [Figure 6-5](#). Therefore, in an unbalanced condition, the 85 percent-wheel unloading can be reached at a lower wind gust speed than in a balanced condition. For this reason, the unbalanced lateral acceleration (or, alternatively, cant deficiency/cant excess) on any curves along the route is one of the inputs to the crosswind route risk assessment.

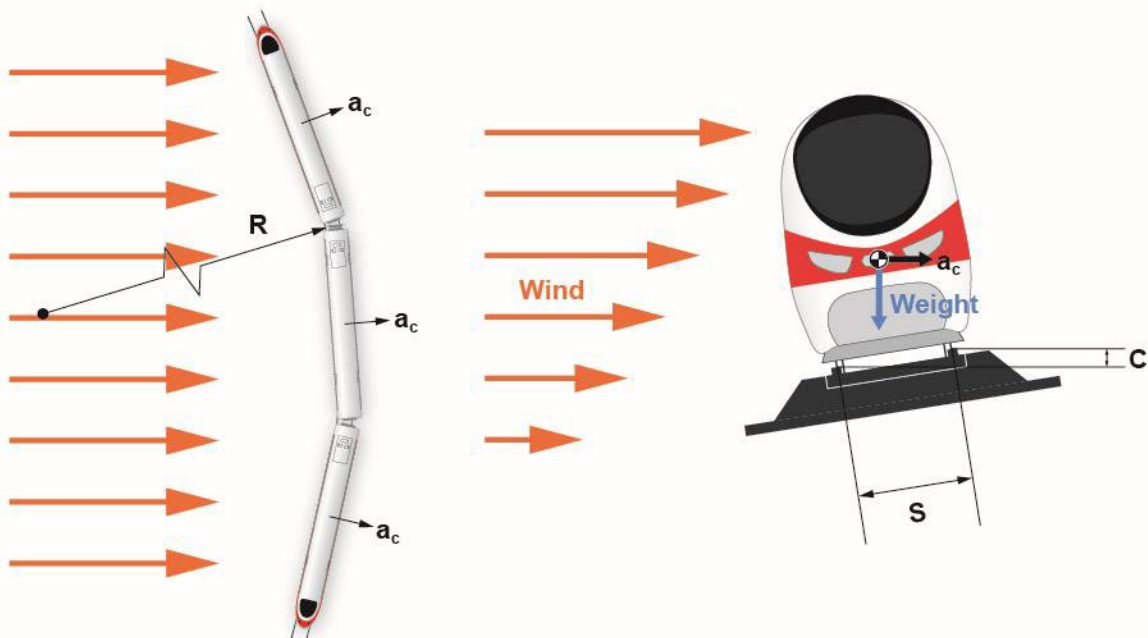


Figure 6-5. In curves, the tipping effect from unbalanced lateral acceleration can add to the tipping effect from wind

Unbalanced lateral acceleration may be calculated as follows:

$$a_c(\text{in } g) = \frac{V_T^2}{Rg} - C/S \quad \text{Equation 6-1}$$

Where:

a_c = Unbalanced acceleration in units of g ;

V_T = Train speed;

R = Curve radius;

C = Superelevation (height difference outer rail minus inner rail);

S = The track width (center-to-center distance between left and right rail); and,

g = The acceleration due to gravity.

Consistent units must be used with this equation, see Section 2.7.

If the cant deficiency is known, then the unbalanced acceleration may be calculated from Equation 6-2:

$$a_c(\text{in } g) = \frac{C_D}{S} \quad \text{Equation 6-2}$$

Where:

C_D = Cant deficiency = $C_{BAL} - C$;

C_{BAL} = Balanced superelevation; and,

a_c , C , g , S are defined as for Equation 6-1.

C_D and S must be in the same units as each other.

Note that the unbalanced lateral acceleration can either decrease or increase crosswind stability depending on whether the wind is blowing in the same direction or the opposite direction to the unbalanced lateral acceleration. Furthermore, although unbalanced lateral acceleration usually acts toward the outside of the curve, it can act toward the inside of the curve if the train speed is slower than the balance speed. However, the assessment method described in this manual uses a source of wind speed data that does not include wind direction information. The assessment conservatively assumes that the wind is always in the worst-case direction, adding to the unbalanced lateral acceleration rather than cancelling it out.

6.2.7 Track Geometry Perturbations

Perturbations of track geometry (such as those caused by natural degradation on ballasted track) can create a tipping effect on trains that could potentially add to the tipping effect from crosswinds. The critical wind speed would be lower in the presence of such perturbations and a rigorous risk assessment would consider this. However, apart from cant deficiency effects in curves, the risk assessment method set out in this study ignores track geometry perturbations for the following reasons:

- Typically, HSTs in the U.S. will only operate on dedicated track while at high speeds and that track will be maintained to a set of standards which restrict the amount of wheel unloading due to track geometry perturbations.
- Significant track geometry perturbations are likely to affect only a small proportion of the length of the route in total. The probability of a critical wind gust occurring precisely at the same time as a train reaches such a track geometry perturbation is likely to be very small.
- It would be overly conservative to reduce the CWCs uniformly by an amount that allows for the maximum allowable track geometry perturbation being present at all times.

6.2.8 Characteristic Wind Curves

As has been explained in Section 6.2.5, the critical wind gust speed varies with train speed. A **CWC** is a set of critical wind gust speeds graphed or tabulated against train speed. The wind gust speed referred to is the natural wind speed, not the apparent wind speed. A CWC is specific to a particular vehicle design or it may be a **Reference CWC** used as an acceptability criterion for rail vehicles. The critical wind speed varies with natural wind angle relative to the track, and CWCs are sometimes given for multiple wind angles. The most commonly presented CWCs are for a 90-degree wind angle, taken as the worst case. Furthermore, since critical wind gust speed is reduced in the presence of unbalanced lateral acceleration (see Section 6.2.6), CWC tables usually contain CWCs for multiple levels of unbalanced lateral acceleration. Example CWCs are shown in Figure 6-6.

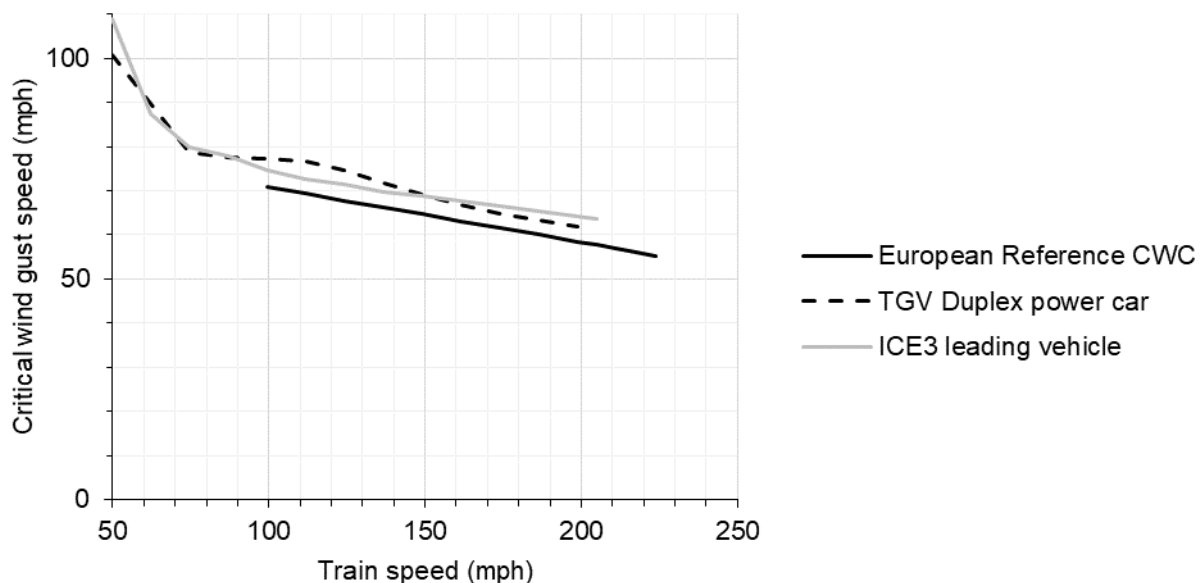


Figure 6-6. CWCs for 90-degree natural wind angle and zero unbalanced lateral acceleration: Reference CWC from [35]; data for European trains TGV and ICE3 from [109]

CWC exceedance means that a train experiences a wind gust of a speed greater than the critical gust speed listed in the CWC. This does not necessarily imply that an accident will occur. CWC exceedance is a necessary but not sufficient condition for overturning. Acceptability of calculated risks may be expressed as an expected number of CWC exceedances per year, either for the whole route or per mile.

6.2.9 Force and Moment Coefficients

Aerodynamic loads vary with speed squared – and in the context of crosswinds, it is the apparent wind speed squared (the term “apparent wind” is defined in Section 6.2.5). This general rule can be used to extrapolate experimental or analytical results from one apparent wind speed to another. For this reason, aerodynamic forces and moments may be expressed as non-dimensional force and moment coefficients (c_F representing the Coefficient of Force, c_M representing the Coefficient of Moment). The forces, moments and coefficients are all functions of yaw angle (β).

$$c_F(\beta) = \frac{F(\beta)/A}{\frac{1}{2}\rho U^2} \quad \text{Equation 6-3}$$

$$c_M(\beta) = \frac{M(\beta)/AH}{\frac{1}{2}\rho U^2} \quad \text{Equation 6-4}$$

Where:

β = Yaw angle;

F = Aerodynamic force;

M = Aerodynamic moment,

A = Area of the side of the vehicle;

H = Height of the side of the vehicle;

ρ = Air density; and,

U = Apparent wind speed (crosswind speed) as defined in Section 6.2.5.

These equations require consistent units, see Section 2.7.

The aerodynamic coefficients are found numerically or experimentally for a given vehicle shape at different yaw angles, resulting in coefficients that are functions of yaw angle. Of these coefficients, the side force and roll moment coefficients are presumed to be the most important.

6.2.10 U.S. Wind Climate

It is useful to understand the different mechanisms that cause strong winds so that appropriate action can be taken with regard to monitoring of weather alerts. Strong wind gusts may be caused by any of the following wind mechanisms:

- **Extra-Tropical Depressions** are the areas of high and low atmospheric pressure observed in weather reporting. These drive the wind climate across the

majority of the U.S. Storms caused by extra-tropical depressions include the blizzards experienced in the Northeast, known as Nor'easters.

- **Hurricanes** typically form over large bodies of warm water such as the Caribbean Sea. These storms have a low-pressure center call the “eye” surrounded by rapidly rotating winds. They have the potential to generate some of the strongest winds experienced in the U.S. There are well developed forecasting models for hurricane activity and national alerts and monitoring can always be anticipated.
- **Thunderstorms** can generate very strong winds close to ground level, especially if a **downburst** occurs. A downburst is a jet of air that is forced downwards by the thunderstorm, hits the ground, and fans out horizontally at very high speed. Because thunderstorms are a localized phenomenon, the most likely source of advance warning is from local weather alerts.
- **Tornados** typically form over land. A tornado consists of a narrow, violently rotating column of air that extends from the base of a thunderstorm to the ground. Although there are areas that are more at risk of tornados, this does not preclude occurrence in other locations. [Figure 6-7](#) shows the relative probability of tornado occurrence across the U.S. Being a localized phenomenon, local weather alerts represent the most likely source of advance warning.
- **Downslope Winds** occur when air flows over high mountain ridges with steep slopes. These types of winds are referred to by many different names, such as the Rocky Mountain Chinook and the Santa Ana winds in California. This phenomenon can cause strong wind speeds in local areas; for example, a narrow patch of land adjacent to the slope of the mountain. Many of the locations susceptible to this type of wind are shown below in [Figure 6-7](#) in the hatched areas described as “Special Wind Regions.” Downslope winds are less predictable than other types.
- **Sea-Land Circulations**, also known as sea-breezes, occur as a result of the difference in temperature between land and sea. The effect of this circulation can have impact relatively far inland. The direction of the wind is reversed at night compared to during the day. This phenomenon is less likely to generate strong gusts than the above mechanisms.

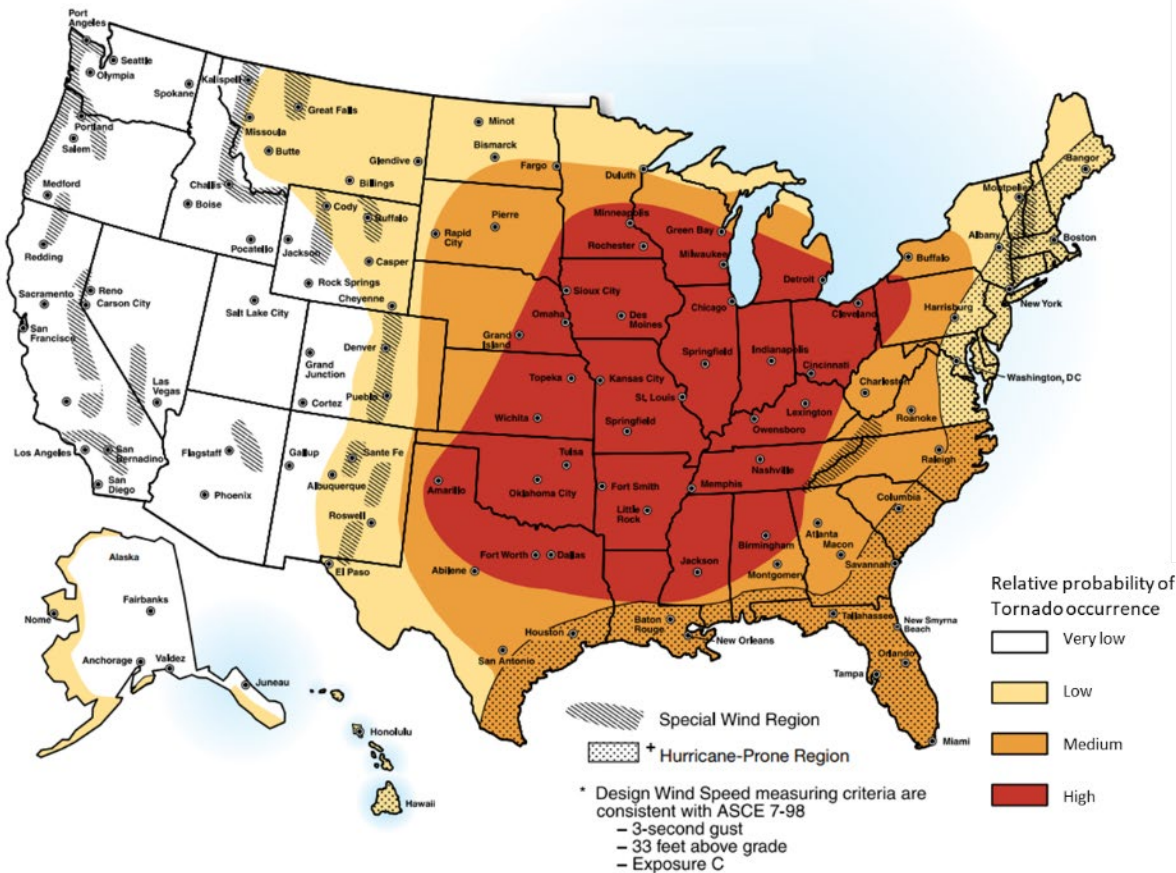


Figure 6-7. Map showing occurrence of tornados and hurricanes, and "Special Wind Regions," associated with Downslope Winds; image from [42]

6.3 Influencing Factors

6.3.1 Wind Gust Speed

Measured over a period of 3 seconds or less, wind gust speed is a primary influencing factor. The frequency with which a wind gust of the critical speed occurs in a given location determines the calculated risk in that location.

6.3.2 Wind Direction

The assessment method set out in this report takes no account of wind direction. This is a simplification arising from the fact that the most readily accessible wind data in the U.S. does not include directionality information. In reality, the wind direction does influence the forces and moments experienced by the train, and thus, influences the risk of overturning. The worst-case wind direction is usually at about 80 to 90 degrees to the track, depending to some degree on the aerodynamics of the railcars.

The **prevailing wind direction** means the direction from which the wind blows most frequently. In most locations, the non-prevailing directions are associated with lower wind gust speeds. For example, the 10-year MRI gust speed in a non-prevailing direction may be 80 percent of the 10-year MRI gust speed in the prevailing direction. If

the prevailing wind direction were directly along the track, then the assessment method set out in Section 6.6.2 will over-estimate the risk.

6.3.3 Train Speed

As described in Section 6.2.5, the critical wind speed reduces (and the risk of tipping increases) with increasing train speed. The relationship between train speed and critical wind speed is not a simple one – it depends on the aerodynamic characteristics of the vehicle and is expressed in CWCs. Furthermore, the consequences of a derailment or overturning accident are likely to be more severe if the train is traveling at higher speed.

6.3.4 Aerodynamic and Other Characteristics of Vehicles

The force and moment coefficients depend on the *dimensions and shape of the train*. For example, given the same height, railcars with arc-shaped roofs are more stable under crosswinds than cars with flat roofs [73].

The *leading vehicle* is usually the most vulnerable vehicle in a train, partly due to aerodynamic lift effects around the nose.

The *weight of the vehicle* provides the restoring moment resisting the tendency to tip in crosswinds. The heavier the vehicle, the more resistant to overturning. The weight of the leading vehicle is especially relevant. Trains with a heavy locomotive may therefore be more resistant to overturning than trains with distributed power systems.

The *train suspension* influences the tendency of the train to tip. For a train with a softer, more flexible suspension, the restoring moment from the train's weight is reduced by lateral displacement and roll of the vehicle suspension because the weight of the train is no longer central between the wheels. There may also be a dynamic suspension response when a wind gust builds up rapidly, such that the railcar overshoots the lateral movement that would have occurred if the gust had built up more gradually. Counteracting this, when a sudden wind gust occurs, it takes time for the mass of the railcar to respond, potentially offering an increase in stability. These points are accounted for in the calculation of CWCs for rail vehicles if the Multi-Body Simulation (MBS) method is used.

6.3.5 Unbalanced Lateral Acceleration

As described in Section 6.2.6, the critical wind gust speed is reduced in the presence of unbalanced lateral acceleration when the train passes around a curve, because the tipping effect of curving adds to the tipping effect of the wind. This statement conservatively presumes that the wind is blowing in the same direction as the unbalanced acceleration.

6.3.6 Surface Roughness and Effect of Height

Wind is slowed down at ground level by friction. Different types of terrain offer different levels of friction, described as **surface roughness**, which may be thought of in terms of the average height of obstructions to the wind. In cities and suburbs, buildings slow the wind significantly. In open country, vegetation (trees, grass, crops, etc.) provides an

intermediate level of surface roughness. Its frictional effect is less than that of city buildings because the vegetation is lower than the buildings. The lowest surface roughness occurs when wind blows over open water or very flat ground, such as mud or salt flats.

Because of the ground friction effect, the higher above ground, the faster the wind speed. Where a railroad is suspended above ground level, for instance on a viaduct, it will be exposed to stronger winds (see [Figure 6-8](#)).

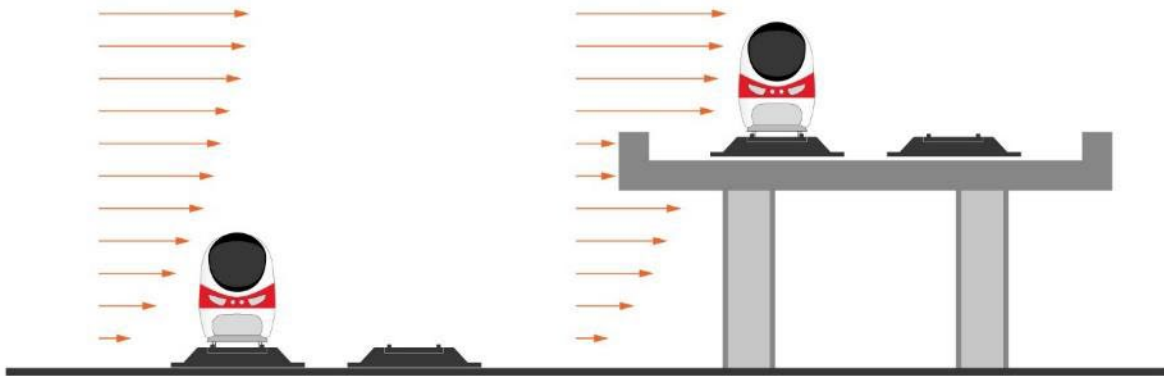


Figure 6-8. Trains exposed to stronger winds on viaducts due to greater distance from the ground

6.3.7 Wind Effects from Infrastructure Features

Wind accelerates as it passes over an embankment and slows down in a cutting (see [Figure 6-9](#)). Walls and fences provide protection from the wind depending on their height and porosity. In crosswind safety assessments, speed-up factors (or slow-down factors) are applied to the wind gust speeds to account for these effects.

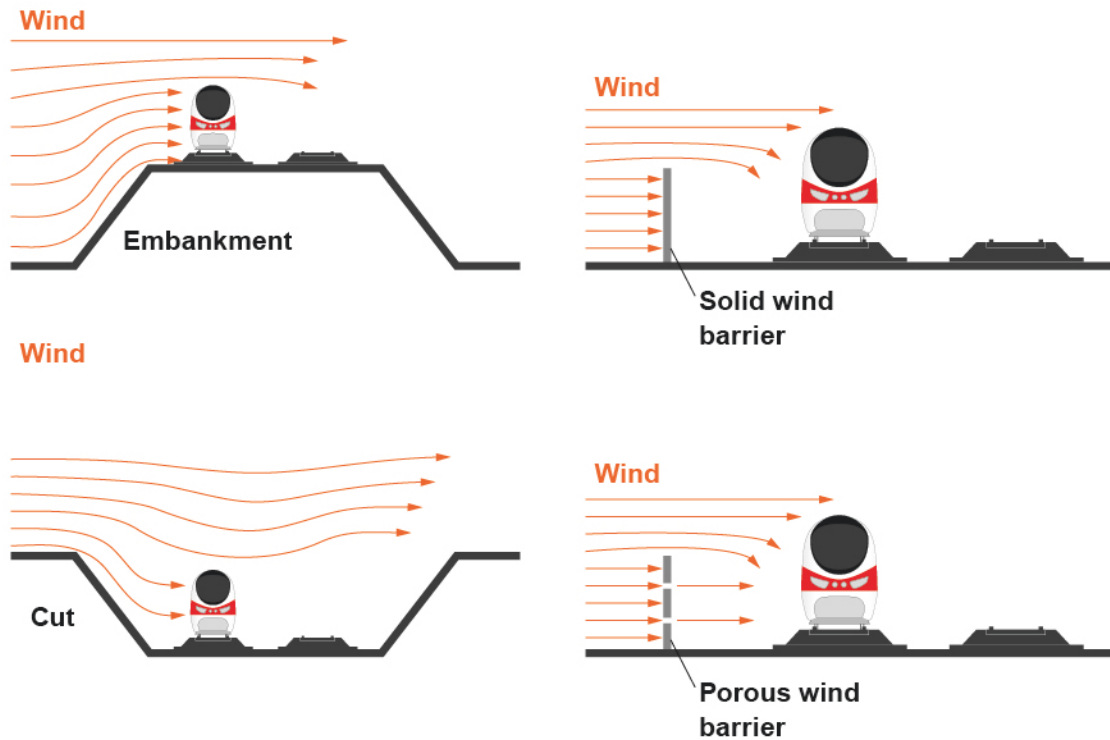


Figure 6-9. Effects on wind of embankments (top left), cuttings (bottom left), and solid or porous barriers (top right and bottom right, respectively)

6.3.8 Wind Effects from Topography

Wind can be funneled through steep-sided valleys or blocked by steep hills near the track, as illustrated in [Figure 6-10](#). These effects are difficult to allow for in assessments and may require case-by-case analysis using CFD or long-term site wind speed measurements.

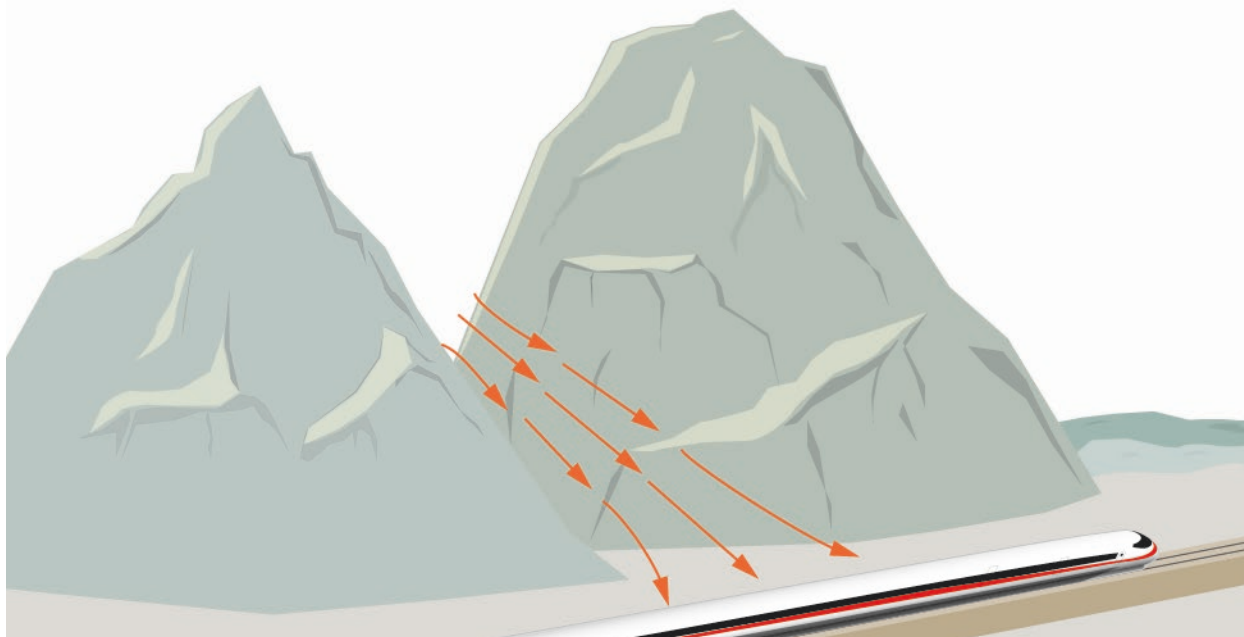


Figure 6-10. Wind can be strengthened by funneling through steep-sided valleys

6.4 Impacts

6.4.1 Derailment and Overturning

Strong crosswinds are known to cause derailment and overturning of trains due to unloading of the wheels on the windward side of the train. This is the principal focus of crosswind safety assessments. Wind-induced train accidents, some of them fatal, have occurred in many locations, including China, Japan [54], Belgium, Switzerland, France, Denmark, and Austria. Examples may be found from an internet search using the term “wind blows train off track.”

Crosswinds could potentially cause derailment due to **flange climb**, when a wheel flange climbs up the gauge side of the rail under the influence of high lateral and/or low vertical wheel load. Flange climb derailment could occur at a different wind speed than overturning. However, internationally, crosswind assessments for HSR assume that overturning is the critical mechanism rather than flange climb.

6.4.2 Impacts on Freight

Crosswinds are a threat not only to high-speed passenger trains but also to all other traffic, including freight trains. Freight vehicles are outside the scope of this report, but note that unloaded freight railcars can be more vulnerable than passenger cars. High box cars and double-stacked container cars are especially vulnerable to overturning due to their large lateral surface area, bluff/blunt shape, and high centers of wind pressure and gravity [2]. When empty, the situation is exacerbated because there is less weight to resist the tipping action.

6.4.3 Overhead Catenary System Damage

The contact wire may be displaced laterally by strong winds (sometimes referred to as **blow-off**) and end up trapped under the pantograph, causing wires to be torn down and/or damage to the pantograph. Winds may also damage the overhead catenary system directly, leading to wires or other debris on the track. These issues are not specific to HSR and can affect any rail system with an overhead catenary.

6.4.4 Accidents Caused Indirectly by Crosswinds

Crosswinds may dislodge railcar components or cargos and displace them laterally, potentially exceeding the limits of the dynamic envelope and hence leading to the risk of collision with wayside structures, platforms, or other trains. A fatal accident of this type occurred in Denmark in 2019 [16]. Accidents can also be caused by collisions with trees, catenary wires, cargos, or other objects that have been blown onto the tracks.

These types of accidents are not covered by the assessment methods set out in this section. Risks to HSR operations from displaced cargos can be reduced by segregating HSR tracks from freight tracks.

6.4.5 Previous Wind-Induced Accidents in the U.S.

Incidences of wind-induced train accidents in the US are available from the FRA Accident/Incident database [43] beginning in 1992 with two wind-related accident causes (“tornado” and “extreme wind velocity”).

From 1992 to 2013, tornados accounted for 57 reportable railroad accidents in the U.S., none of which involved passenger trains. During the same period, extreme wind velocity accounted for 356 reportable accidents, 13 of which involved passenger trains. In none of these 13 cases did the passenger trains derail. In three cases, the damage to the train was caused by catenary wire damaged by high winds. The remainder encompassed carbody damage caused by falling trees and small windblown objects [49].

6.5 Mitigation Methods

There are three main ways of preventing crosswind-induced train accidents:

- Designing rolling stock such that crosswind effects are minimized, or selecting rolling stock with suitable crosswind stability for the intended route
- Erecting wind barriers along the track
- Operational methods such as placing permanent speed restrictions at wind hot-spots, temporary speed restrictions during periods of high winds, or shutting down train operations altogether if very high winds are expected

6.5.1 Rolling Stock Design

The aerodynamic shape of the train may be designed to improve crosswind stability. Trains with a heavier leading vehicle are less prone to the risk of rollover from crosswinds. While this report is not intended to address matters of train design, system

operators may desire to understand the CWC data related to crosswind-resistance when selecting rolling stock for particular routes.

6.5.2 Wind Barriers

Wind barriers (or fences) may be constructed alongside the track at locations where the route risk assessment shows an unacceptably high risk of overturning – for example, on embankments or viaducts in exposed locations (see Figure 6-11). Barrier heights are usually defined as height above TOR. Wind barriers are typically 10 to 13 ft (3 to 4 m) high and may be solid or porous. Typical noise barriers are also effective wind barriers, provided they are at least 10 ft high. Low barriers up to around 6.5 ft (2 m) high are sometimes used for noise mitigation, but with regard to wind they are at best ineffective and can even make the situation worse by redirecting the wind against the upper part of the train, thus increasing the tipping effect on the train.

Barriers do not need to be very close to the train to be effective. Barriers can still block the wind even if they are 25 ft (7.5 m) away, provided they are tall enough. If barriers are placed too close to the track, the train may be buffeted by turbulent air between the train and the barrier. For this reason, barriers are sometimes placed 10 to 15 ft (3 to 4.5 m) from the track center.



Figure 6-11. Main wind protection structures along the Lanxin Railway II [17]. (a) Subgrade wind barriers; (b) bridge wind barriers; (c) wind-proof tunnels

6.5.3 Speed Restrictions Applied Permanently at Crosswind “Hot-Spots”

It may be necessary to set reduced speed limits at locations such as viaducts where wind speeds are high on a regular basis. The British West Coast Main Line has speed restrictions on some curves due to high wind exposure combined with uncompensated lateral acceleration [83].

6.5.4 Mitigation for Overhead Catenary System Blow-Off

Blow-off is generally mitigated by controlling the motion of the contact wire – for example, by reducing the spacing between the supporting structures and/or increasing tension. The ability to prevent blow-off through pantograph design is limited by the need to minimize drag, lift, and aerodynamic noise.

6.5.5 Speed Restrictions Applied Temporarily

Internationally, operational rules based on forecast or measured wind speeds are common for both HSR and non-HSR operations. Some of these are shown in Table 6-1 below. These rules are applied to mitigate a number of wind-related risks such as catenary damage, catenary blow-off, collisions with fallen trees, or debris on the line, and are not necessarily sufficient to mitigate risk of overturning or derailment.

Table 6-1. Examples of operational mitigation for crosswind risk

Wind speed		Train speed limit			
Gust speed	Sustained speed	Japan HSR [66][87]	China HSR (less windy locations) [20]	Amtrak [106]	Britain ¹
34 mph (15 m/s)	-	-	185 mph (300 km/h)	-	-
45 mph (20 m/s)	-	16 mph (25 km/h)	125 mph (200 km/h)	-	-
56 mph (25 m/s)	-	Suspend operations	75 mph (120 km/h)	-	-
61 mph ³ (27 m/s)	50 mph (22 m/s)	-	-	60 mph (95 km/h)	-
67 mph (30 m/s)	-	-	Suspend operations	-	-
70 mph ² (31 m/s)	-	-	-	-	50 mph (80 km/h)
73 mph ³ (33 m/s)	60 mph (27 m/s)	-	-	Suspend operations	-
90 mph (40 m/s)	-	-	-	-	Suspend operations
Notes: 1. Information from private communication. 2. Either 70 mph gusts or gusts over 60 mph occurring for at least a 4-hour period. 3. Most countries base their criteria on wind <u>gust</u> speed, while Amtrak uses <u>sustained</u> wind speed. Wind gust speeds are typically around 1.2 to 1.25 times greater than the sustained wind speed; to enable comparison of Amtrak's criteria with others, values for sustained wind speed have been converted to gust speed using a factor of 1.22.					

Such restrictions may be applied manually – for example, in response to national or local weather forecasts, or automatically in response to wind gusts recorded by track-

side monitoring equipment. An example of an automatic system is the French TGV Mediterranean high-speed line [58], equipped with a network of anemometers that measure the wind speed. The system is integrated with the signaling system and slows trains automatically when high winds are recorded.

In China, maximum train speeds are reduced in response to wind speeds detected by track-side monitoring stations [20]. The Chinese Code for Design of High-speed Railway [99] lists detailed requirements for positioning of weather monitoring stations. However, China Railway operates several routes in perennially windy regions, where applying the standard wind-based speed restrictions would make daily operations difficult or impossible. In these regions, speed restrictions are tailored to the characteristics of different routes and different types of railcars, based on the results of CFD simulations, wind tunnel tests, and dynamic models. Different speed restrictions apply to sections with and without wind barriers [18].

Trackside monitoring of wind conditions is recommended, especially in higher-risk locations where winds are generally stronger or may be less predictable, such as in steep valleys, canyons, and mountain passes. In the U.S., this would include “special wind regions” affected by downslope winds.

Operational mitigation measures such as those described above can cause serious difficulties for operations unless planned with sufficient advance notice. For example, if operations are suddenly suspended, trains and their passengers may be stranded between stations; and, after the restrictions are lifted, trains or crew may be in the wrong place to begin the next day’s journeys. These aspects may need to be considered when deciding between wind barriers or operational mitigation measures.

When developing operational procedures for high wind conditions, operators may wish to consider risks from trees or other debris blown onto the tracks, risk of catenary damage, as well as derailment and overturning. Operating at low speed gives drivers time to brake if they see that the track is blocked. This is sometimes the governing consideration in deciding operating speeds under high wind conditions.

Operating at low speed also mitigates the risk of overturning to a significant extent because the critical wind speed increases when train speed reduces; thus, there is a band of wind gust speeds that are unsafe for full speed operation but safe for low speed with regard to overturning. The consequences of a derailment or overturning accident may also be reduced when operating at low speed.

6.6 Crosswind Risk Assessment

The overall purpose of an assessment is to evaluate the risk of crosswind-induced accidents and to identify locations along a route where mitigation is required. Safety depends on the combination of the rail vehicle’s tolerance of crosswinds with the conditions along the particular route. A full assessment would calculate risk for the vehicle/route combination. In practice, assessment is usually done in two separate parts:

- Railcar manufacturers perform *rail vehicle assessment*. Vehicles are assessed to calculate the CWCs. Acceptance procedures may require that a vehicle must

be at least as safe in crosswinds as a **Reference Vehicle** defined by **Reference CWCs**.

- Operators and route planners perform *route risk assessment*, assuming that the trains will have the characteristics of the Reference Vehicle. Any difference between the actual train's CWCs and the Reference CWCs is an additional safety margin. A route risk assessment may be used to quantify the risk associated with the whole route, and/or to identify the highest-risk locations along the route (**risk hot-spots**), enabling overall risk to be reduced by applying mitigation at those locations. Operators should decide acceptability of the calculated risks. This is described in Section [6.6.3.13](#).

6.6.1 Rail Vehicle Assessment

Rail vehicle assessment is undertaken by railcar manufacturers and is not a primary focus of this report. No recommendations are given. A summary is provided here to assist operators with specifying rolling stock and to understand the information provided by manufacturers.

The aim of rail vehicle crosswind safety assessment is to derive the CWCs. This is done in two steps:

- Measurement of aerodynamic forces and moments at different wind angles, usually by wind tunnel testing on a reduced-scale model and/or CFD analysis
- Calculation of the CWCs using the aerodynamic forces measured in the first step and an assumed wind gust profile. This is often done using a dynamic MBS model, but simpler methods may also be used.

6.6.1.1 Measurement of Aerodynamic Forces and Moments

Aerodynamic forces and moments may be measured by wind tunnel testing on a reduced-scale model or by CFD analysis. Wind tunnel testing has limitations – in particular, the model train is not moving relative to the ground, which has some influence on the results – but nevertheless it represents a reliable, practical way of obtaining the aerodynamic forces and moments. CFD analysis is a useful method of assessing different proposed designs and may be performed instead of wind tunnel testing if suitably validated and if appropriate modeling techniques are used. The validation should include comparison against wind tunnel results.

A typical wind tunnel test setup is shown in [Figure 6-12](#). The wind in the wind tunnel represents the *apparent wind* (see Section [6.2.5](#)), and the angle of the wind relative to the train is the *yaw angle*. The test is repeated at a range of yaw angles.

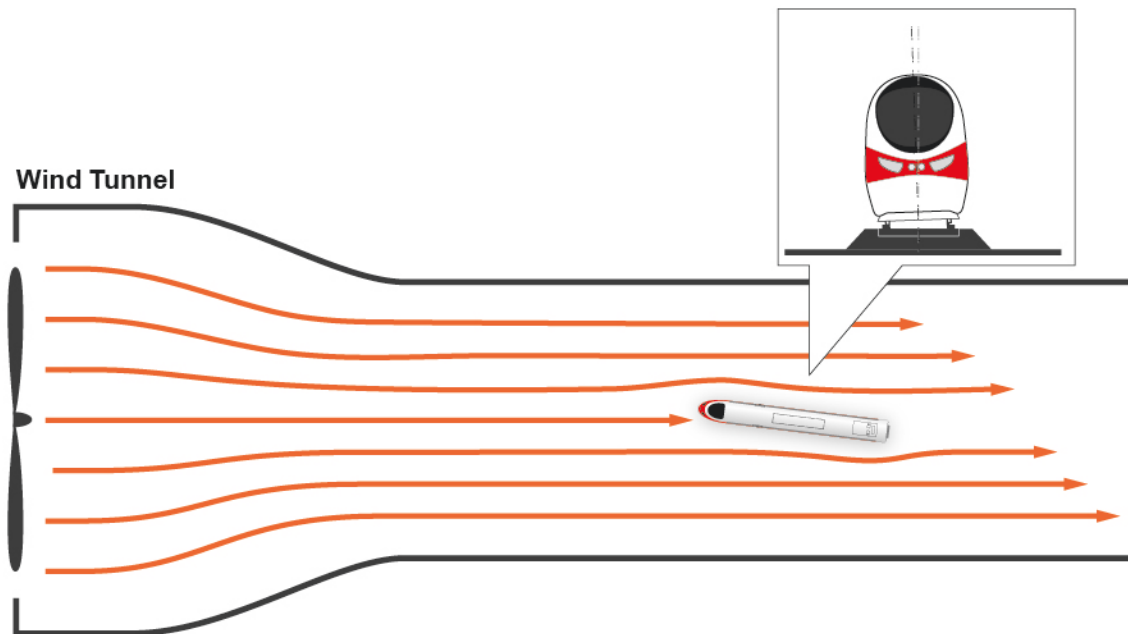


Figure 6-12. Wind tunnel test setup for measuring aerodynamic coefficients relevant to crosswind stability

Internationally, there are well-established guidelines for this type of testing [35]. It is important to understand what ground condition was modelled in the wind tunnel or CFD simulation. Current practice is for tests to be carried out with a standard ground shape representing a 2.7 ft (0.825 m) high ballast shoulder, called **Single Track Ballasted Rail simulation (STBR)**. Even if the actual railroad will be constructed with slab track or a different ballast detail, this standard ground shape should still be used in wind tunnel testing to enable like-for-like comparisons with other vehicles and with Reference CWCs.

Results of wind tunnel tests or CFD analysis are usually presented as force and moment coefficients (terms defined in Section 6.2.9). In assessments, the coefficients are assumed to hold a constant value which applies irrespective of train speed, and for time-varying wind as well as constant wind.

6.6.1.2 Calculation of CWCs

Most railcar manufacturers use a dynamic MBS model to evaluate critical wind speed. The model of the train includes the masses and inertias of the carbody, trucks, wheelsets, and other components together with the suspension and other items linking them together. The standard method of modelling the wind gust is to make the model train pass through a jet of air that has the speed profile described in the European Standards [35] as a “Chinese Hat” (Figure 6-13), such that the forces are applied to one car after another as they pass through the jet. The forces and moments to be applied to each point along the length of the MBS model are calculated from the wind speed of the model gust at that particular point together with the coefficients derived from wind tunnel tests or CFD as described in Section 6.6.1.1 above. The analysis is repeated with different wind gust speeds until the relevant wheel unloading criterion is reached (90

percent unloading in the European system). Next, the wind angle is changed and the process is repeated. Unbalanced lateral accelerations may be applied to the model in addition to the wind.

The standard wind gust profile used in the MBS simulation results in, approximately, a 0.5-second gust being applied to each vehicle. In the U.S., data for 3-second gusts are more widely available than for 0.5-second gusts. To maintain compatibility between the CWCs and the wind gust data, the route assessment method described in Section 6.6.2 includes a correction factor for gust duration.

The above procedure is used to find the apparent wind gust speed at which the critical unloading condition is reached, at each apparent wind direction (yaw angle) tested. These results can then be expressed as combinations of train speed with natural wind speed and direction, which form the CWCs.

Alternative, simpler methods are permitted in the European standard such as quasi-static tipping analysis using a three-mass model. The three masses represent the railcar, trucks, and wheelsets. The intention of the model is to capture the lateral displacement of the carbody when under lateral load from wind, which reduces the restoring moment (M_R in Figure 6-1). The wind gust is taken as a static load. Details are given in Section 5.4.2 of the European standard [35].

The advantage of the MBS method is that the dynamic response of the railcars is included, while the advantage of the quasi-static method is its simplicity. The MBS method also potentially enables assessment of the effects of crosswinds on wheel-rail interaction-related derailments such as flange climbing, rail rollover, or track panel shift. Railcar manufacturers usually already have MBS models of their vehicles for other purposes, so the additional effort involved in the MBS method may not be excessive.

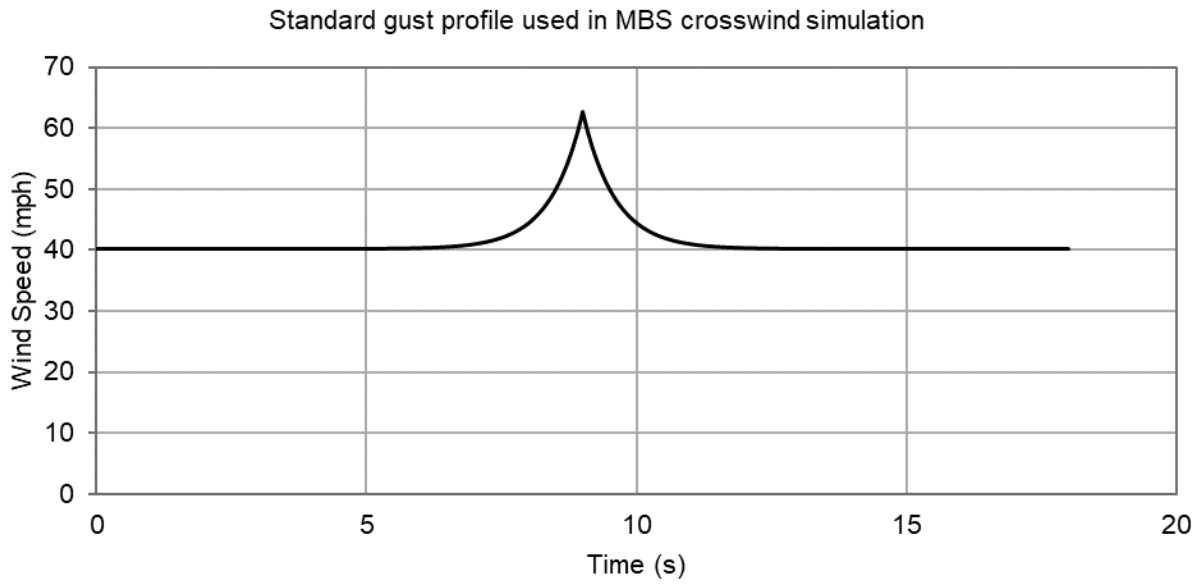


Figure 6-13. Example of the standard wind gust idealization as seen by a railcar passing through the gust [35]

6.6.2 Route Assessment Methods – Overview

Assessment of crosswind risk for a railroad route can take two forms:

- A **probabilistic route assessment** calculates the risk in terms of the probability, or recurrence interval, of a train on the route experiencing a critical wind gust. This method is described in Section 6.6.3.
- A **wind speed threshold assessment** calculates the forecast or measured wind speed at which operations should be halted or subject to speed restrictions in order to prevent unacceptable risk of a train experiencing a critical wind gust. This method is described in Section 6.6.4.

The reason for two separate methods is that it is not possible to account for wind-dependent operational restrictions in the probabilistic calculation, whereas operational restrictions are an important tool in reducing risk. For example, the probabilistic calculation would include the risk of a train being overturned by a hurricane, but in reality, the trains would not be running when a hurricane is approaching. Nevertheless, each method has its advantages, and several of the assessment steps are common to both methods.

The following process is recommended:

1. Start with the probabilistic route assessment. Use the results to identify risk hot-spots where it is beneficial to provide wind barriers.
2. Repeat the probabilistic assessment with the wind barriers included at the selected locations.

3. Proceed to the wind speed threshold assessment (re-using the results of the steps in the probabilistic assessment that are common to both methods). Use the results of the threshold assessment to check the wind speeds at which operational restrictions should be deployed.

Both assessment methods provided below use elements of the British system of route assessment [118], combined with the European CWC method of quantifying the stability of trains [35] adapted for American conditions and input from the American Society of Civil Engineers' (ASCE) Standard 7 [4]. This approach has been necessary because no single source provides a complete methodology suitable for American conditions.

6.6.3 Probabilistic Route Assessment

The objectives of a probabilistic route assessment are, firstly to identify risk hot-spots along the route where mitigation measures such as wind barriers need to be provided, and secondly to determine whether the route as a whole presents an acceptable level of risk. This report does not state what level of risk should be considered acceptable; that decision is left to operators.

Where possible, the authors recommend benchmarking the calculated risk in the following manner. A route assessment is performed for an existing route with a good safety record in similar wind conditions (see Section 6.6.3.13), using the same calculation method. The objective of the assessment of the existing route is to establish a threshold for what level of risk (as calculated by this method) can be considered acceptable. The advantage of benchmarking in this way is to reduce the influence of any conservative or non-conservative aspects of the assessment because these affect both assessments (for the new operation and the existing safe operation) equally.

The steps are shown in overview in Figure 6-14, with descriptions of each step given below:

1. Input data are gathered in a table covering the whole route (see Section 6.6.3.1).
2. The table is used to subdivide the route into segments, such that all the input data are the same within a segment.
3. The risk within each segment is calculated as follows:
 - a. From ASCE 7 Hazard Tool⁵ available online, obtain the wind gust speeds for 10, 20, 50 and 100-year recurrence intervals (see Section 6.6.3.3).
 - b. Correct the gust speeds for height, terrain type, infrastructure effects, and any fences or barriers (see Sections 6.6.3.6 and 6.6.3.7).
 - c. Use the CWCs of the selected trains, or alternatively the reference CWCs provided in this report, to read off the critical wind speed according to the train speed and any unbalanced lateral acceleration (see Section 6.6.3.8).

⁵ This material may be found at <https://asce7hazardtool.online/>. This material may be downloaded for personal use only. Any other use requires prior permission of the American Society of Civil Engineers.

- d. Combine results from the previous two steps to find the probability or recurrence interval of the critical wind speed being exceeded (Section [6.6.3.9](#)).
 - e. Calculate the number of times per year that the critical wind speed will be exceeded when there is a train in the segment (Section [6.6.3.10](#)).
- 4. The route risk is calculated by adding together the risk for all the segments (Section [6.6.3.11](#)).

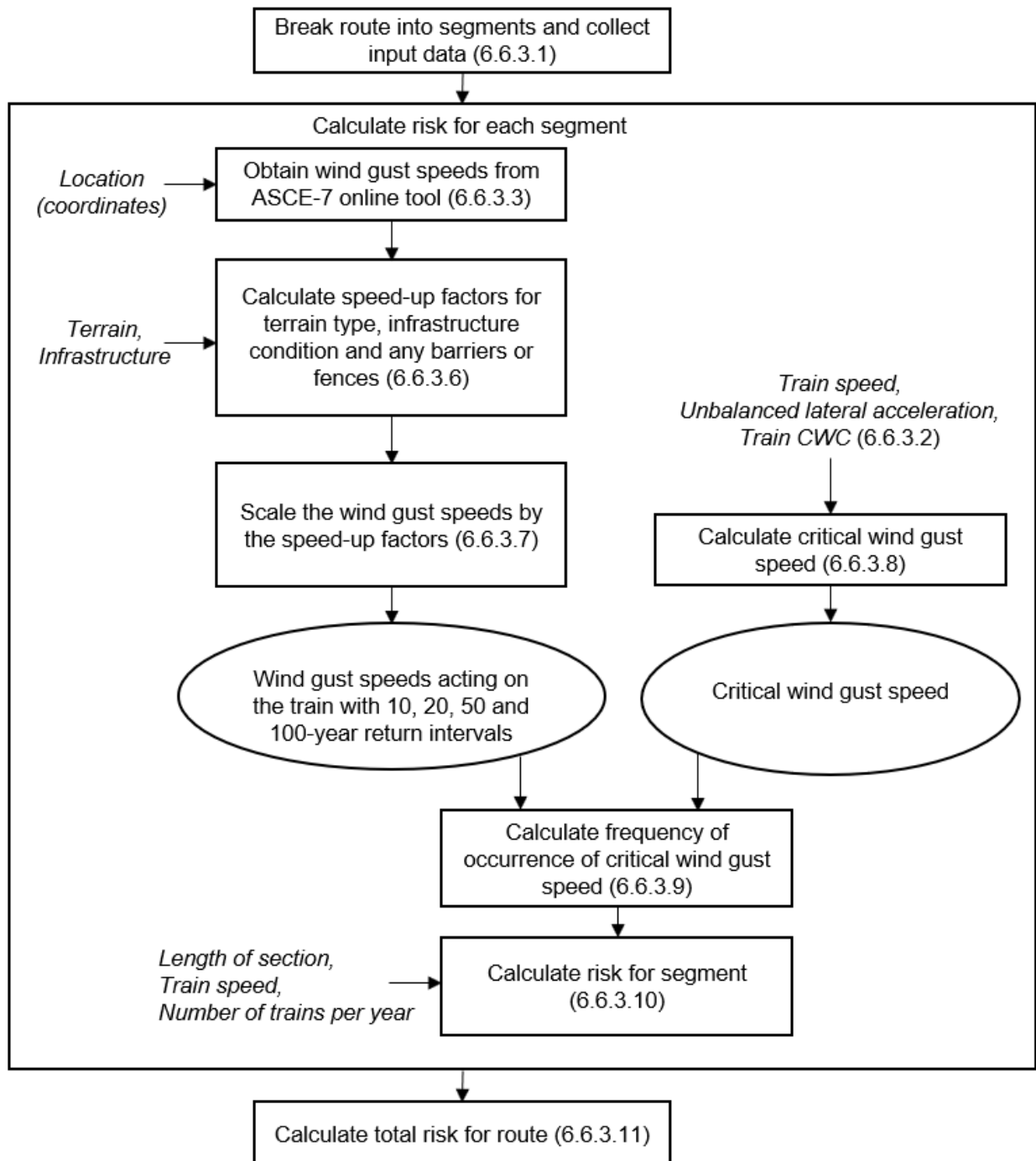


Figure 6-14. Probabilistic route risk assessment overview

6.6.3.1 Input Data to Be Collected

The required input data explained in [Table 6-2](#) should be gathered for the whole route. The route should be divided into **segments**. A segment is a length of route within which the input data for the risk calculation are treated as being the same.

Table 6-2. Input data required for crosswind route assessment

Item	Explanation
Milepost start, milepost end	Route segments will be demarcated by milepost. Pick milepost values where the input data below changes.
Map coordinates (latitude and longitude)	Location definition for obtaining wind data from the ASCE 7 Hazard Tool.
Train speed, to nearest 10 mph. Record separately for each track if different.	Affects critical wind speed. The higher the train speed, the lower the critical wind speed. This point is explained in Section 6.2.5 .
Terrain type B, C or D (see descriptions in Table 6-4)	The terrain type describes the degree of exposure to the wind. For example, in urban areas the wind is slowed by buildings.
Infrastructure type: At Grade, Embankment, Viaduct, Cutting or Tunnel (see Table 6-6) Height/depth of embankment, viaduct, cutting, etc., to nearest 5 ft	The wind speeds up over an embankment and slows down in a cutting; on a viaduct the railroad is exposed to faster winds because it is further from the ground, and the slowing effect of the ground is lost. No calculations need to be performed for route segments in tunnels.
Presence of walls, noise barriers, fences, etc., alongside the track and their porosity (see Section 6.6.3.6)	Barriers protect trains from the wind. More porous barriers let more wind through.
Topography (hills/valleys etc.)	Note the presence of any topographic features that might funnel the wind, for example mountains or valleys with slopes exceeding 10 percent that are close enough to influence the local wind conditions at the track. If in doubt, consult a wind engineering practitioner.
Unbalanced lateral acceleration to nearest 0.01g, or cant deficiency/excess to nearest 0.5 in	Applies on curves where the superelevation of the track does not balance the acceleration due to curving. If the wheels are already partially unloaded for this reason, less wind is needed to reach the critical 85 percent unloaded condition. To calculate unbalanced lateral acceleration, either the curve radius and superelevation will be needed, or else the cant deficiency, see Section 6.2.6 .

Typically, segments are 0.1 to 1 mile long but can be longer or shorter. Working along the route from one end, find the points where any of the input information changes (such as train speed, embankment height, etc.). For simplicity, segments may be

chosen such that not all the input data are exactly the same throughout the segment, but in that case the most conservative value of each input parameter should be noted, i.e., the value that leads to the highest calculated risk. Record the information in a table, in order of milepost. An example is given in [Table 6-3](#). Each row in the table represents a segment of the route. The risk will be calculated separately for each segment.

Table 6-3. Example input data collection for crosswind route safety assessment

Milepost start/end (miles)	Lat, Long	Train speed (mph)	Terrain type	Infrastructure type, height/depth (ft)	Barrier, porosity	Cant deficiency (in)
0 to 3.0	29.425, -98.494	50	B	At grade	no	0
3.0 to 4.6	29.425, -98.444	60	C	5 ft embankment	yes, 0%	0
4.6 to 5.1	29.425, -98.368	80	C	10 ft embankment	no	0
5.1 to 5.2	29.425, -98.283	100	C	20 ft viaduct	no	0
5.2 to 5.45	29.425, -98.197	100	C	10 ft embankment	no	2
5.45 to 6.8	29.424, -98.106	130	C	5 ft embankment	no	0

The service pattern will be required for the risk calculation; namely, how many trains pass through the route segment per hour on average.

6.6.3.2 Obtain CWCs

CWCs for the train will be required, as described in [Section 6.2.8](#). These may be obtained from the train manufacturer for a specific train type, noting that for American conditions based on compatibility with 49 CFR 213.333 [\[145\]](#), the critical event is defined as 85 percent wheel unloading, not 90 percent as used in other countries, and thus the manufacturer may need to re-calculate the CWCs. Alternatively, the Reference CWCs below may be used, though, these will likely give a more conservative result than CWCs for actual HSTs. The Reference CWCs for use in the U.S. are based on the European Reference CWCs [\[35\]](#) but re-worked for 85 percent wheel unloading. They are provided below in the form of an equation and also plotted as a graph (see [Figure 6-15](#)). The European Reference CWCs are shown in [Figure 6-15](#) for comparison. The difference between the European and U.S. CWCs is due to the level of wheel unloading taken as critical (85 percent for U.S., 90 percent for Europe).

CWC formula for U.S.:

$$u_{g,CWC} = 80.8 - 0.126V_{T,mph} - 151a_C$$

Equation 6-5

Where:

$u_{g,CWC}$ = CWC critical wind gust speed in mph;

$V_{T,mph}$ = Train speed in mph; and,

a_C = Unbalanced lateral acceleration in g (referred to as ULA in Figure 6-15).

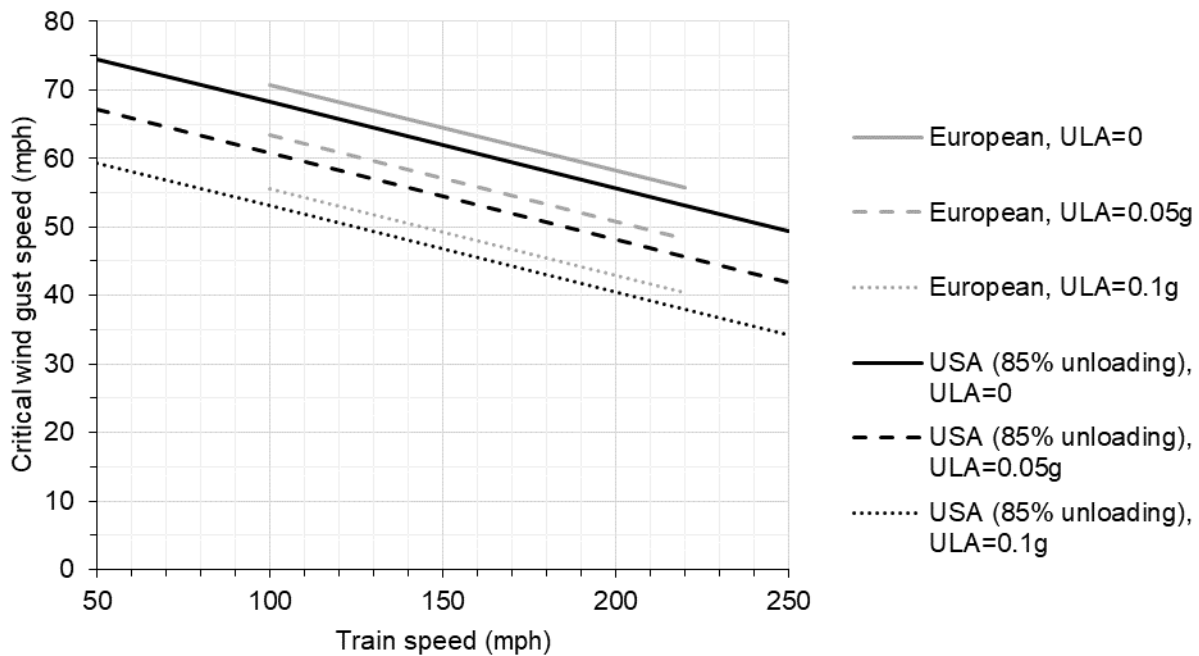


Figure 6-15. Reference CWCs for U.S. compared to European CWCs from EN 14067-6:2018 [35]. ULA means unbalanced lateral acceleration

Sections 6.6.3.3 through 6.6.3.10 describe the calculations to be performed on each segment of the route.

6.6.3.3 Obtain Wind Gust Speeds

ASCE Standard 7 [4], hereafter referred to as **ASCE 7**, sets out the minimum design loads for buildings and other structures and is also suitable for deriving wind climate input data for HSR crosswind route safety assessments.

ASCE provides the online **ASCE 7 Hazard Tool**, which can be used to determine key hazard parameters, including wind speeds. The ASCE 7 Hazard Tool is available to use free of charge with limited functionality, or through individual or corporate subscription, and can be found at: <https://asce7hazardtool.online/>. The limited functionality is sufficient for determining wind speed at a given location. The instructions included within this section are current at the time of writing.

Select the guest option to access the tool.

1. On the initial menu (see [Figure 6-16](#)):
 - a. Input the location of interest. This can be done in three ways: entering the full address of a nearby building or landmark, entering the latitude and longitude coordinates, or directly selecting the location on the map.
 - b. The latest version of the ASCE 7 Standard should be selected. At the time of writing, this is ASCE/SEI 7-16.⁶
 - c. The next step is to select the Risk Category, which for the purpose of this guidance manual relates to the MRI of the evaluated wind speed. Risk Category I should be selected. This is the lowest risk category and corresponds to a 300-year recurrence interval, the shortest available among the standard options.
 - d. Ignore inputs related to soil type – these are not relevant here.
 - e. Select the load type “Wind,” along with the units of interest. Since this assessment method uses wind speeds in mph, “US customary” units are recommended.
 - f. Select “View Results.”
2. The following information is provided: location elevation, location latitude / longitude and the 3-second gust wind speed at 33 ft above the ground in open country for the Risk Category selected (in this case, 300-year).
3. Select the “Details” button: see [Figure 6-17](#). Note the 3-second gust wind speeds for 10-, 25-, 50-, and 100-year recurrence intervals. These wind speeds will be referred to as $u_{g,ASCE-7,10year}$, $u_{g,ASCE-7,25year}$, etc. The output also states whether the location is in a hurricane region.
4. By selecting ‘Overlay’, wind hazard contours are overlaid onto an area map (see [Figure 6-18](#)). This can be useful when assessing how the wind hazard varies at different points along the route.
5. The results can be downloaded by selecting the “Full Report” button. The summary report includes a map of the location with elevation and coordinates, as well as the wind hazard results, data source, date accessed, and additional notes about the data. If other hazards were considered in the analysis, the report would include results for each parameter.

⁶ This material may be found at <https://www.asce.org/product.aspx?isbn=9780784414248>.

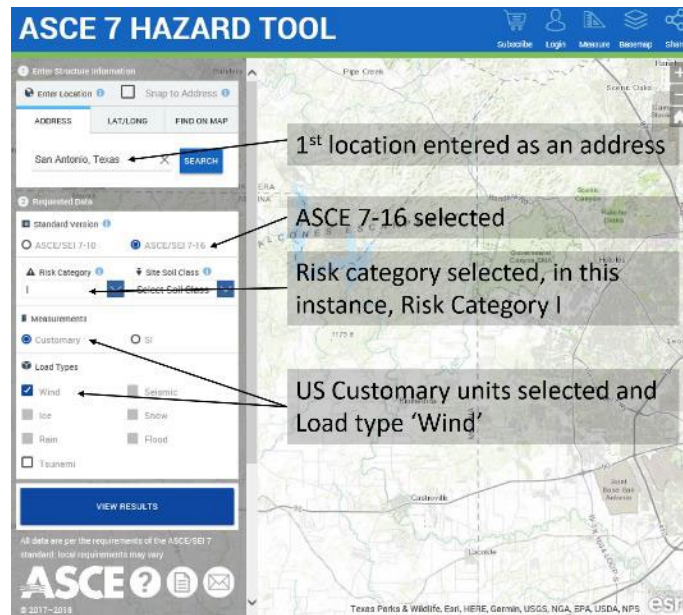


Figure 6-16. Screenshot of ASCE 7 Hazard Tool – entering location, risk category, and hazard type (with permission from ASCE)

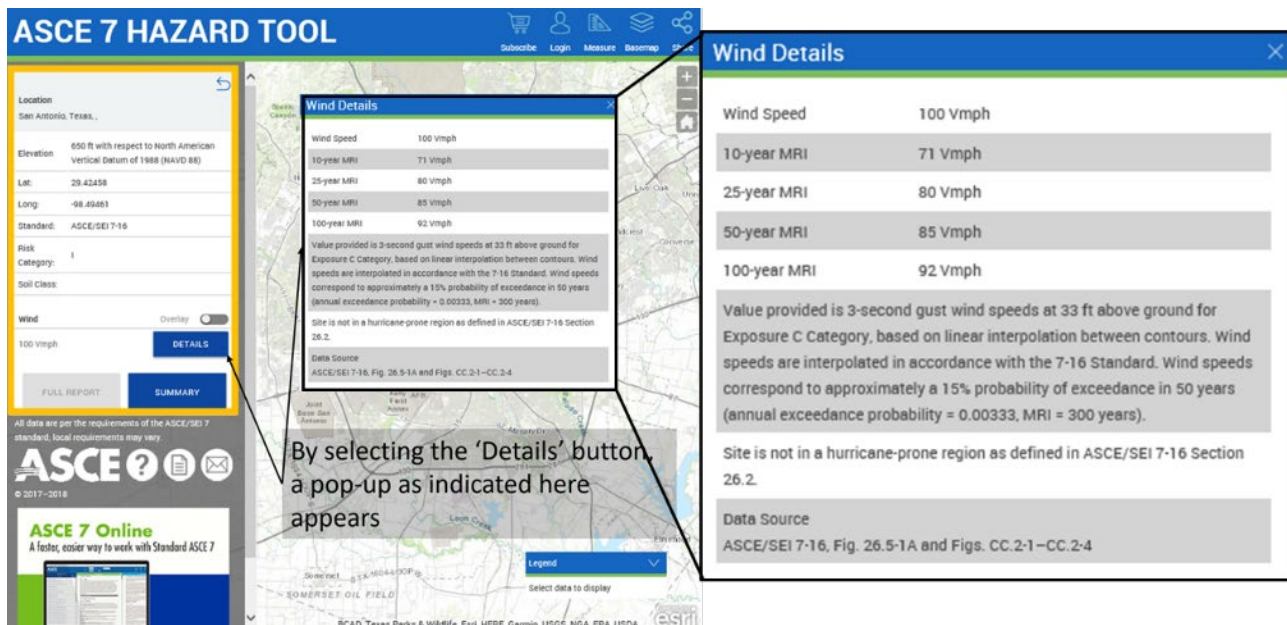


Figure 6-17. ASCE 7 Hazard Tool – obtaining gust wind speeds from the "Details" button (with permission from ASCE)

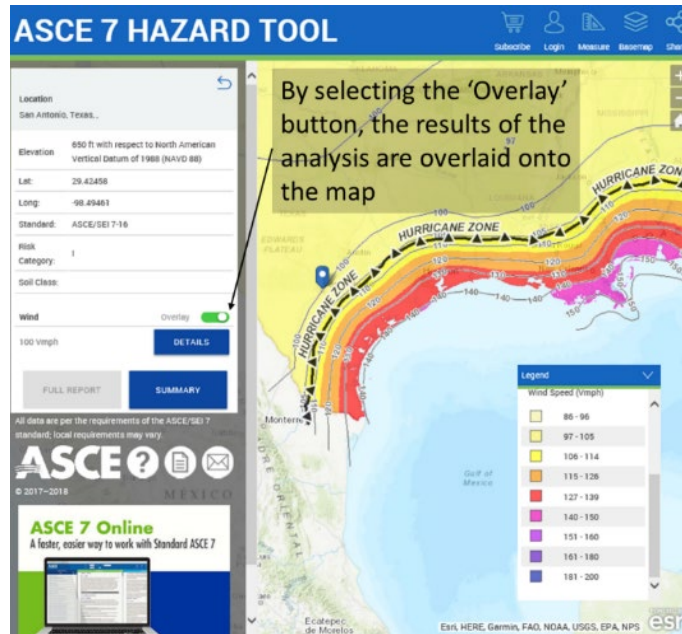


Figure 6-18. ASCE 7 Hazard Tool – "Overlay" function (with permission from ASCE)

6.6.3.4 Wind Gust Speed Recurrence Intervals – Types of Wind Included

The wind speeds and their recurrence intervals derived from the ASCE 7 Hazard Tool include gusts caused by all the wind mechanisms given in Section 6.2.10 except for tornados. The risks calculated during the assessment therefore include risks from hurricanes and thunderstorms. There is no way to make the risk calculation allow for operational choices such as stopping all trains when a hurricane is forecast in the area. The calculated risk should be considered an over-estimate for regions where the wind gust speed recurrence intervals are dominated by situations in which the trains would not be running.

As tornados are excluded from the wind gust data in the risk assessment, operators should take additional steps to prepare for these events. Information about this is given in Section 6.8.

6.6.3.5 Situations Where Caution is Required

For certain regions of the U.S., the actual wind gust speeds may be substantially higher than the values indicated by the ASCE 7 Hazard Tool. This includes:

- The **special wind regions** defined by ASCE 7.
- Any other regions where mountains or valleys may concentrate the wind acting on the railroad.

When selecting basic wind gust speeds in these regions, or if there is doubt about whether a particular location falls into this category, expert advice should be sought.

6.6.3.6 Speed-Up and Slow-Down Factors: Gust Duration, Terrain, Height, and Infrastructure

The wind gust speeds derived from ASCE 7 apply to 3-second gusts at 33 ft above the ground over open country and need to be modified in order to arrive at the wind gust speeds acting on the train. Obtain the following factors:




- **Gust duration factor, K_{gd}** , taken as 1.05, to convert from the speed of a 3-second gust to a 0.5 second gust, which is more compatible with the method by which rolling stock manufacturers determine the Characteristic Wind Curves. The value of the factor has been calculated from information given in Section 26.5 of ASCE 7.
- **Height and terrain factor, K_{zt}** , from [Table 6-4](#), selecting the terrain type from [Table 6-5](#). Wind is slowed down near the ground surface, but this effect varies according to the size of the obstructions to wind flow such as buildings or vegetation. Open water or very flat ground such as mud or salt flats provide the least surface resistance. For ROWs at-grade, the wind speed acting on the train is taken 10 ft (3.0 m) above ground level. In the assessment, K_{zt} is the factor by which the wind speed at 10 ft is less than the speed at 33 ft. The rougher the ground, the lower the value of K_{zt} .
- **Infrastructure factor, K_i** , from [Table 6-6](#), representing wind speed-up or sheltering effects caused by railway infrastructure such as embankments and cuttings. See notes below [Table 6-6](#).
- **Barrier factor, K_b** , from [Table 6-7](#), representing the sheltering effect of any walls, noise barriers, wind fences, etc. alongside the track.

Table 6-4. Height and terrain factor K_{zt}

	Terrain type		
	B	C	D
K_{zt}	0.71	0.88	0.98

The values of K_{zt} in [Table 6-4](#) have been derived from the height-dependent exposure coefficients in Table 26.10-1 of ASCE 7, extrapolated to 10 ft above ground, and adapted to wind speed factors rather than pressure factors by taking the square root. Engineering judgment has been used to provide an interpretation of the data suitable for this application. Not all of the stipulations in ASCE 7 have been included; for example, ASCE 7 does not recommend extrapolating to heights below 30 ft for Terrain Type B or below 15 ft for Types C and D, but if that requirement were applied, it would distort the relative risks to HSTs for the different terrain types.

Table 6-5. Selection of terrain type

Terrain Type	Description	Example
B Urban, suburban, or wooded	Urban and suburban areas, wooded areas, or other terrain with numerous, closely spaced obstructions that have the size of single-family dwellings or larger. To count as terrain Type B, these conditions must prevail in the 60-degree sectors on both sides of the track (see Figure 6-19) for a distance greater than 1,500 ft.	
C Open country	Open terrain with scattered obstructions that have heights generally less than 30ft. This category includes flat, open country, farm land, prairie (including shortgrass prairie), grasslands. Terrain Type C should be selected whenever Types B or D do not apply.	
D Water or smooth flat ground	Flat, unobstructed areas with insignificant vegetation, or water surfaces. This category includes smooth mud flats, salt flats and unbroken ice. To count as terrain Type D, these conditions must prevail for at least 5,000 ft in at least one direction within the 60-degree sectors (see Figure 6-19). Additionally, if this condition is not met at the location in question but <u>is</u> met at any position within 600 ft of the location in question, terrain Type D should be selected.	

Note:

Terrain images used with permission from ASCE from Minimum Design Loads and Associated Criteria for Buildings and Other Structures, ASCE 7-16 Commentary [\[4\]](#).

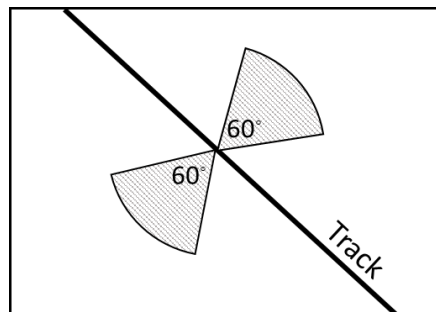

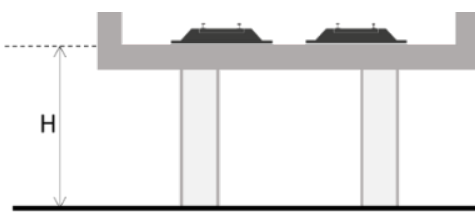

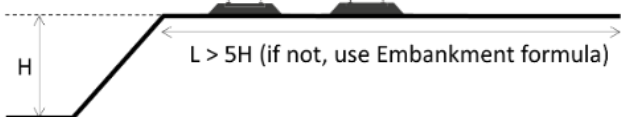

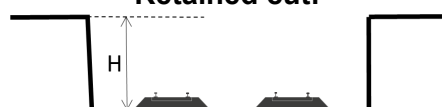


Figure 6-19. Sectors for assessment of terrain type

Table 6-6. Infrastructure factor K_i . Choose one of the options below. See notes in Section 6.6.3.6 above and below this table.

Infrastructure type/Diagram/Notes	K_i			
At Grade:  Flat ground (less than 1-in-6 gradient) within 300 ft of the tracks	1.0			
Viaduct:  Wind can pass under and over the structure. Valid for heights up to 200 ft.	K_i for Terrain Type			
	H (ft)	B	C	D
	0	1.00	1.00	1.00
	10	1.17	1.11	1.09
	20	1.27	1.18	1.15
	30	1.35	1.22	1.18
	40	1.40	1.26	1.21
	50	1.45	1.29	1.24
	60	1.48	1.31	1.26
	100	1.60	1.39	1.32
	150	1.69	1.45	1.37
	200	1.76	1.49	1.40
Embankment:  Slope angle between 1-in-1.5 and 1-in-3	H (ft)	K_i		
	0	1.0		
	10	1.18		
	20	1.28		
	30	1.36		
	40	1.42		
	50	1.48		
	60	1.55		
Escarpment:  $L > 5H$ (if not, use Embankment formula) Slope angle between 1-in-6 and 1-in-1.5. If slope is less than 1-in-6 use At Grade. If tracks are not close to the edge of the escarpment, formula will be conservative.	H (ft)	K_i		
	0	1.0		
	10	1.17		
	20	1.24		
	30	1.30		
	40	1.36		
	50	1.40		
	60	1.43		
Cutting:  Slope angle between 1-in-1.5 and 1-in-6. If slope is less than 1-in-6 use At Grade.	H (ft)	K_i		
	0	1.0		
	10	0.82		
	20	0.53		
	≥ 34	0.0		
Retained cut:  Near-vertical sided cut with walls close to the train	H (ft)	K_i		
	0	1.0		
	5	0.82		
	10	0.53		
	≥ 17	0.0		
Tunnel	0.0 (no calculation required)			

In all cases shown in Table 6-6, ballast or track slab structure can be up to 3 ft (0.9 m) high above the surrounding terrain.

Factors are provided in Table 6-6 for a limited range of situations. Where the infrastructure in question does not fit any of the categories shown in Table 6-6 or is outside the stated limitations (for example, viaducts over 200 ft [60 m] high or embankments with sides steeper than 1-in-1.5), specific investigations such as wind tunnel tests or CFD analysis will be required. It is more important to obtain accurate values of K_i for exposed locations, i.e., locations where the value of K_i is expected to be high, rather than for sheltered locations where a low value is expected. Specialist advice should be sought with regard to defining the investigations. These should include details such as ballast shoulder and representative infrastructure and should compare the wind speed for the investigated infrastructure against the wind speed for the at-grade condition.

The values for K_i in Table 6-6 have been derived in the following manner.

- For viaducts, embankments, and escarpments, the factors are based on data in [118]. This source has been preferred over similar data in ASCE 7 (which is applicable to buildings on an escarpment, for example) because [118] is specific to railway applications.
- For retained cuts, no information is provided in ASCE 7 or [118]. The factors were derived from engineering mechanics calculations, with some conservative assumptions.
- For cuttings, factors are provided in [118], but these are considered over-conservative by the authors of this report. The factors provided are based on engineering judgment together with the calculations for retained cuts and are expected to be somewhat conservative.

Note that the outcomes of assessments are usually insensitive to the exact value of factors expressing a sheltering effect (such as cuttings). Risks are dominated by exposed locations, not sheltered ones.

The barrier factor K_b applies if there is a fence or wall of height at least 10 ft (3 m) above TOR, located 10 to 15 ft (3 to 4.5 m) from the track centerline on both sides of the track, as shown in Figure 6-20. The porosity of the barrier is defined as the area of gaps or holes divided by the total area of the fence or wall, as seen when looking toward the track from the side. Thus, a solid wall has a porosity of zero, while a chain-link fence has a porosity close to one. The barrier factor does not depend on whether the railroad is at grade, on an embankment, or a viaduct. Note that the barrier should not be placed too close to the side of the train, as the train may be buffeted by turbulence between the train and the barrier. A typical position is around 12.5 ft (3.8 m) from the track centerline.

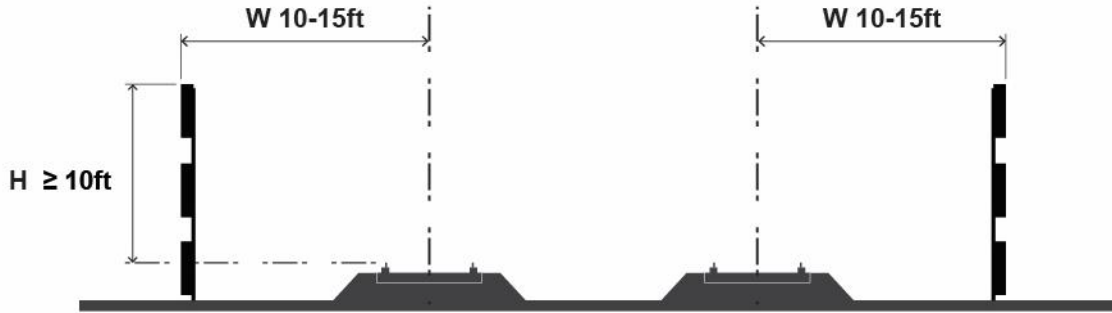


Figure 6-20. Qualifying dimensions for applying the barrier factor K_b (height measured from TOR)

Table 6-7. Barrier factor K_b

Porosity	K_b
0 (solid wall)	0.45
0.25	0.75
0.5	0.9
1.0 or no barrier	1.0

The factor K_b may be obtained from [Table 6-7](#) for barriers satisfying the qualifying dimensions in [Figure 6-20](#), interpolating linearly for porosity values not shown in the table. Barriers shorter than 10 ft or further than 15 ft from the track may still be effective, but the wind speed factor K_b will need to be obtained from wind tunnel experiments or CFD analysis. Note that low barriers (up to about 7 ft) high can sometimes make the situation worse by redirecting wind against the upper part of the train, and K_b would then be greater than one. Different researchers have obtained different results regarding the effectiveness of different barrier designs, heights, and distances from the track – the approach given above is approximate.

The values of K_b in Table 6-7 have been derived from test results in [\[75\]](#) and data given in [\[118\]](#).

6.6.3.7 Applying the Gust Duration, Height, Terrain, and Infrastructure Factors

The four wind gust speeds derived from ASCE 7 should be multiplied by the speed-up factors K_{gd} , K_{zr} , K_i and K_b to obtain the wind gust speeds acting on the train:

$$K_{su} = K_{gd}K_{zr}K_iK_b \quad \text{Equation 6-6}$$

$$u_{g,Train,10year} = K_{su}u_{g,ASCE-7,10year} \quad \text{Equation 6-7}$$

$$u_{g,Train,25year} = K_{su}u_{g,ASCE-7,25year} \quad \text{Equation 6-8}$$

$$u_{g,Train,50year} = K_{su}u_{g,ASCE-7,50year} \quad \text{Equation 6-9}$$

$$u_{g,Train,100year} = K_{su}u_{g,ASCE-7,100year} \quad \text{Equation 6-10}$$

6.6.3.8 Calculating the Critical Wind Speed

The critical wind gust speed, $u_{g,crit}$, is obtained from a CWC graph or equation for the particular train speed and the unbalanced lateral acceleration applicable to the route segment, see Section 6.6.3.2. Unbalanced lateral acceleration may be calculated from Equation 6-1, see Section 6.2.6. The unbalanced lateral acceleration for use in the CWC calculation should be treated as positive, no matter whether there is cant deficiency or cant excess.

6.6.3.9 Calculating the MRI of the Critical Wind Speed

The MRI of the critical wind gust speed $u_{g,crit}$ is calculated using two wind gust speeds with known recurrence intervals R_1 and R_2 years, here called $u_{g,Train,R1}$ and $u_{g,Train,R2}$. These are selected from the four wind gust speeds $u_{g,Train,T}$ (where $T=10$ -year, 25-year, 50-year, and 100-year) calculated in Section 6.6.3.7. The selection logic is given in Table 6-8. Note that the ASCE Hazard Tool does not give wind gust speeds for MRIs below 10 years. However, the equations given below are assumed to remain valid for MRIs outside of the 10- to 100-year range; so, for example, the MRI of the critical wind gust speed can be calculated from the 10-year and 25-year MRIs even if $u_{g,crit}$ is less than $u_{g,Train,10year}$.

Table 6-8. Selection of MRIs R_1 and R_2

Condition	R_1 (years)	$u_{g,Train,R1}$	R_2 (years)	$u_{g,Train,R2}$
If $u_{g,crit} < u_{g,Train,25year}$	10	$= u_{g,Train,10year}$	25	$= u_{g,Train,25year}$
If $u_{g,Train,25year} \leq u_{g,crit} < u_{g,Train,50year}$	25	$= u_{g,Train,25year}$	50	$= u_{g,Train,50year}$
If $u_{g,Train,50year} \leq u_{g,crit}$	50	$= u_{g,Train,50year}$	100	$= u_{g,Train,100year}$

For reference, the relationship between two wind gust speeds ($u_{g,1}$, $u_{g,2}$) and their corresponding MRIs (R_1 , R_2) is given in Equation 6-11, in which γ is a constant chosen to fit the known data. This equation has been rearranged into Equation 6-12 through Equation 6-14 for use in the next steps.

$$\left(\frac{u_{g,1}}{u_{g,2}}\right)^2 = \frac{\gamma + \ln(R_1)}{\gamma + \ln(R_2)} \quad \text{Equation 6-11}$$

Next, calculate k and γ :

$$k = \frac{u_{g,Train,R1}}{u_{g,Train,R2}} \quad \text{Equation 6-12}$$

$$\gamma = \frac{\ln(R_1) - k^2 \ln(R_2)}{k^2 - 1} \quad \text{Equation 6-13}$$

The MRI R_{crit} of the critical wind gust speed $u_{g,crit}$ can now be calculated:

$$R_{crit} = e^{\left(\left(\frac{u_{g,crit}}{u_{g,Train,R1}}\right)^2(\gamma + \ln(R_1))\right) - \gamma} \quad \text{Equation 6-14}$$

As an alternative to the equations above, [Figure 6-21](#) provides an approximate method to find R_{crit} for cases where $u_{g,crit} < u_{g,Train,10year}$. The Figure is used as follows:

- Calculate k as above;
- Calculate the ratio c per [Equation 6-15](#). This is the x-axis value on the graph:

$$c = \frac{u_{g,crit}}{u_{g,Train,10year}} \quad \text{Equation 6-15}$$

- Select the line on the graph with the next value of k above the actual value (e.g., if $k=0.82$, select the line for $k=0.85$); and,
- Find R_{crit} , the y-axis value corresponding to the x-axis value of c .

The calculated value of R_{crit} is an approximation based on known data for certain MRIs, usually 10 and 25 years. The further from these known data points, the less accurate the calculated value of R_{crit} and the greater degree of error in the risk calculation. In particular, if the calculation gives an R_{crit} less than two years, it should be treated as unreliable. Nevertheless, the risk calculation is still valid for identifying which route segments have the highest risk. This applies whether it was derived using the equations above, or from [Figure 6-21](#).

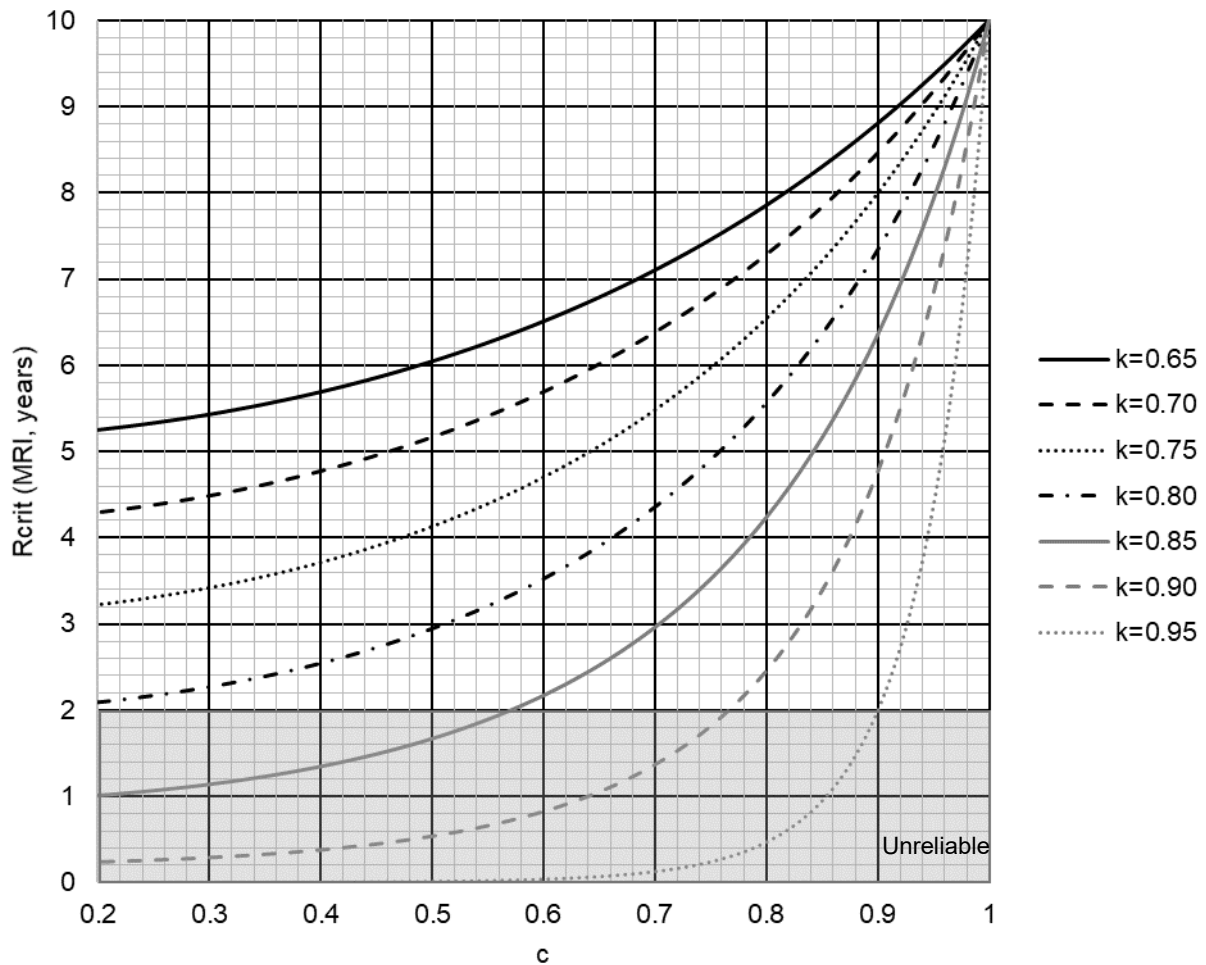


Figure 6-21. Approximate method to determine R_{crit} for cases where $u_{g,crit}$ is less than $u_{g,Train,10year}$

6.6.3.10 Calculate the Route Segment Risk

The probability of a **critical wind gust** (that is, a gust strong enough to cause at least 85 percent wheel unloading of the most vulnerable vehicle) is $1/R_{crit}$ per year. A critical wind gust is also called a **CWC exceedance**.

The probability of a train being present in the segment at any given time, P_t , is given by:

$$P_t = \frac{LN}{V_{T,mph}} \quad \text{Equation 6-16}$$

Where:

L = Length of the segment in miles;

N = Average number of trains per hour = number of trains per year / 8760; and,

$V_{T,mph}$ = Speed of the train in mph.

The **annual segment risk** P_S , defined as the expected number of times per year that a critical wind gust will occur at the same time as a train is present in the segment, is given by:

$$P_S = \frac{P_t}{R_{crit}} \quad \text{Equation 6-17}$$

Where:

R_{crit} = MRI of critical wind gust calculated from [Equation 6-14](#).

The degree to which the risk to the operation is concentrated in particular route segments may be evaluated by comparing the segment risks on a per-mile basis. The **annual segment risk per mile**, P_{spm} , is given by:

$$P_{spm} = \frac{P_S}{L} \quad \text{Equation 6-18}$$

6.6.3.11 Add Up the Segment Risks Across the Whole Route

The **total route risk**, P_R , defined as the expected number of times per year that any train on the route will experience a wind gust strong enough to cause 85 percent wheel unloading (CWC exceedance), is given by adding up the annual segment risks (P_S) for all the route segments.

6.6.3.12 Alternative Risk Metrics – Risk per Train Passage

The annual risks described in [Section 6.6.3.10](#) are calculated for the whole operation. The more frequent the trains, the more likely it is that a train will be present in the route segment at the instant when a critical gust occurs, and therefore the higher the annual risk for the operation. Alternative risk metrics can be calculated on a per-train basis. These metrics are independent of the frequency of trains. They are provided here because risk per train passage (or risk per train per mile) may be preferred by some operators for compatibility with existing risk criteria.

The **segment risk per train passage**, P_{spT} , defined as the probability of a critical gust occurring during the time it takes for a train to pass through the route segment, is given by:

$$P_{spT} = \frac{L}{8760 R_{crit} V_{T, mph}} \quad \text{Equation 6-19}$$

Where:

L = Length of the segment in miles;

$V_{T, mph}$ = Speed of the train in mph; and,

R_{crit} = MRI of critical wind gust calculated from [Equation 6-14](#).

The **segment risk per train per mile** for the route segment, P_{spTm} , is given by:

$$P_{SpTm} = \frac{P_{SpT}}{L} = \frac{1}{8760R_{crit}V_{T,mph}} \quad \text{Equation 6-20}$$

The **total route risk per train**, P_{RpT} , defined as the probability that a critical gust will affect a train while it passes from one end of the route to the other, can be calculated by adding up the segment risk per train (P_{SpT}) for all the route segments.

6.6.3.13 *Evaluating the Outcomes of a Crosswind Route Assessment*

The outcomes of a Crosswind Route Assessment may be evaluated on a whole route basis, either by comparing the Route Risk against a reference acceptable risk, or against Route Risk calculated in the same manner for an existing route with a good safety record running in a similar wind climate (a **reference operation**). The latter is recommended where a suitable reference operation exists with sufficient input information to perform an assessment; this comparative approach to risk is preferred because the approximations and assumptions in the assessment method affect the results equally for both routes.

The results of the assessment can reveal risk hot-spots, which are the route segments for which the risk per mile is greatest. This is a useful outcome even when the acceptability of the overall route risk cannot be determined (due to, for example, lack of a benchmark of acceptable risk). A comparison of segment risks can inform decisions about the provision of mitigation, such as wind barriers.

This report does not specify what level of risk should be deemed acceptable. That decision is left to operators. Internationally, acceptability criteria and the manner in which they are expressed differ across different countries. Examples are:

- In Britain, risk has historically been calculated in terms of annual probability of fatality for a passenger who uses the route 500 times per year (250 return journeys). The tolerable probability of fatality due to overturning in crosswinds was set at 10^{-7} per year [117]. This approach is now superseded by a principle that mitigation measures should be provided unless it can be shown that the costs are grossly disproportionate to the safety benefits [118]. Benefits may be expressed as an annual reduction of fatalities, monetized using an assumed value of preventing a fatality.
- In Germany, risk is expressed as the expected number of CWC exceedances per year calculated per 2 km (1.24 miles). The calculation method uses a 2 km moving average. The acceptable risk value reduces with increasing train speed, on the basis that overturning or derailment at high speed is more likely to lead to fatalities. For high-speed operations, the limit applied in the German method is around 10^{-4} exceedances per year per 2 km [143].

Note that the above risk criteria are not proposed for use in the U.S. – that is a decision for American operators. They are given only as examples of practices in other countries.

6.6.3.14 *Incorporating Permanent Mitigation Measures in the Assessment*

Wind barriers may be added at risk hot-spots along the route, as revealed by the route assessment. The calculations are then repeated with the barrier factor applied in the relevant segments; see Section [6.6.3.6](#).

The influence of permanent speed restrictions on risk may be evaluated by recalculating risk with different train speeds for the affected segments.

Temporary operational restrictions conditional on wind conditions are covered in Section [6.6.4](#).

6.6.3.15 *Conservative and Non-Conservative Elements of the Probabilistic Route Assessment Method*

The assessment method recommended above is conservative in several aspects:

- Extreme wind events such as hurricanes are included in the wind gust speed recurrence intervals from ASCE 7, even though trains would likely not be operating by the time winds reached hurricane speeds; operations are normally suspended when exceptionally high winds are forecast or detected by track-side monitoring equipment, see Section [6.5.5](#).
- The method assumes that the wind always blows from the worst-case direction, which is approximately perpendicular to the track; and in the case of curves, the method assumes that the wind is blowing in the same direction as the unbalanced lateral acceleration. To reduce the level of conservatism, it would be necessary to obtain wind directionality data, e.g., for each direction in 30-degree steps around the compass, the percentage of the time that the wind blows from that direction and any difference in the wind strength compared to the prevailing wind direction.
- The Reference CWCs are more conservative than CWCs of many actual HSTs.
- Exceedance of the critical wind gust does not mean that an accident will necessarily occur. First, the critical wind gust speed is determined on the basis of 85 percent wheel unloading rather than 100 percent. Second, it would still be deemed a critical gust if that degree of wheel unloading occurred only for a brief instant in time, whereas, to cause a rollover accident, the wheels need to stay unloaded for long enough for the train to tip over.

The assessment method is potentially non-conservative in that:

- It excludes risks from wind events that are not included in the ASCE 7 data and require local monitoring, such as tornadoes.
- Wind speed patterns may change over time. The wind gust speed values provided in the ASCE 7 Hazard Tool represent the industry's best current understanding of the expected wind conditions, but these may need to be updated as new data emerge.

- The assessment considers only risks arising from derailment and overturning and excludes other wind-related risks such as damage to catenary wire equipment or collisions with trees or other debris on the tracks.

6.6.4 Wind Speed Threshold Assessment (Operational Mitigation Measures Conditional on Wind Speed)

Operators typically apply procedures whereby trains are slowed or stopped when forecast or measured wind gust speeds exceed a given threshold. Such procedures reduce the probability of trains experiencing critical wind gusts, but the reduced probability is difficult to calculate. Instead, non-probabilistic calculations can be used to inform the wind gust speed thresholds for slowing or stopping the trains.

Reducing train speed during high winds (as opposed to stopping the trains completely) can be an effective mitigation measure for overturning risk because the critical wind gust speed rises when train speed is reduced. Thus, there is a band of wind speed that is safe for reduced speed operation but not for full speed operation. The reduced train speed is typically around 50 or 60 mph and may be set at a level that enables drivers to stop if they see fallen trees or debris on the line and/or to match existing operational procedures during strong winds.

The wind gust speed thresholds are typically based on operational experience but should be checked against thresholds calculated from critical wind speeds as described here. Then, the lower of the two sets of thresholds (out of the experience-based ones or the critical wind speed-based ones) may be adopted.

The logic used to derive wind gust speed thresholds is illustrated in [Figure 6-22](#) and outlined below.

1. The route is broken into segments and input data are collected in the same way as for the probabilistic assessment; see Section [6.6.3.1](#). The calculations then proceed segment by segment.
2. The wind speed-up factor for the segment due to terrain, infrastructure, etc., is calculated as described in Section [6.6.3.6](#).
3. The critical wind gust speed $u_{g,crit}$ at the full operating speed is calculated as described in Section [6.6.3.8](#). A further calculation is performed to derive the critical wind gust speed with a reduced train speed such as 50 mph, $u_{g,crit,slow}$; see Section [6.7.1](#) below.
4. These critical wind gust speeds are converted into wind gust speed at the weather station or other measuring position. A safety factor is applied to derive the forecast or measured wind gust speed thresholds at which the trains would be slowed or stopped, $u_{g,thresh,slow}$ and $u_{g,thresh,stop}$ respectively; see Section [6.7.2](#) below.
5. The above process is repeated for each segment. The calculated wind gust speed thresholds will be lower in segments posing higher risk of overturning, for example, where the track is exposed on a viaduct or on a curve with cant deficiency. The overall threshold wind gust speeds for use in triggering

operational restrictions are taken as the lowest values of $u_{g,thresh,slow}$ and $u_{g,thresh,stop}$ for any segment.

6. Additional mitigation measures such as wind barriers may be considered for any segments for which the calculated values of $u_{g,thresh,slow}$ and $u_{g,thresh,stop}$ are particularly low – this is a tradeoff between the cost of providing the barriers versus the frequency with which operational restrictions have to be applied. The method for adding wind barriers to the calculation is the same as for the probabilistic assessment: the effect of the barriers is included in the speed-up factor (see Section 6.6.3.6) and the results for the segment are re-calculated.

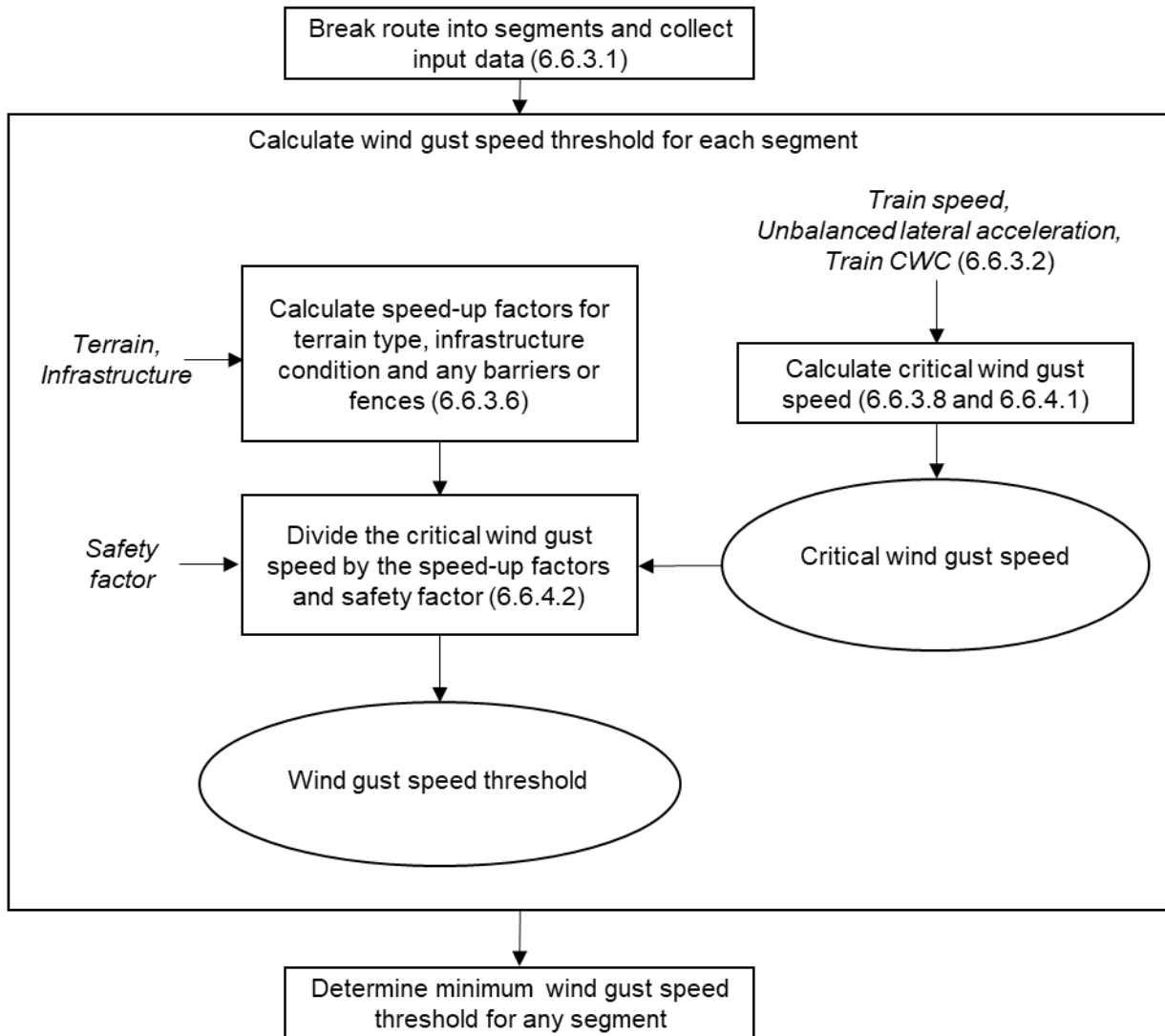


Figure 6-22. Assessment of wind gust speed thresholds for operational restrictions

The above process considers only risk from overturning or derailment due to wheel unloading. There are separate wind-related risks that warrant their own speed restrictions such as risk of catenary system damage and trees, debris, etc., on the line. These risks may already be mitigated by pre-existing operational rules. The final choice

of wind gust speed threshold at which train speeds are restricted or trains are stopped should include all these considerations as well as risk from wheel unloading.

6.6.4.1 Calculating Critical Wind Speeds

The method for calculating Critical Wind Speeds is the same as described in Section 6.6.3.8. When calculating Critical Wind Speed for the reduced operating speed in segments with curves, the unbalanced lateral acceleration should be re-calculated with the reduced speed. Cant deficiency is speed-dependent and may become cant excess at lower speeds. Irrespective of whether the calculations show cant deficiency or cant excess, the unbalanced lateral acceleration is taken as positive when evaluating the Critical Wind Speed from [Equation 6-1](#).

6.6.4.2 Converting Critical Wind Gust Speeds into Wind Gust Speed Thresholds

The wind speed measurements that are used to trigger the operational restrictions could be taken from real-time monitoring by track-side equipment, real-time monitoring by standard weather stations, or from regular weather forecasts. Unless track-side monitoring equipment is provided in every route segment for which the overturning risk is significant, the measured or forecast gust speeds will differ from those experienced by the train due to differences of location, height, terrain, presence of embankments, etc. The calculation for converting from critical wind gust speed at the train to the equivalent gust speed at the measuring point is shown in [Equation 6-21](#) and [Equation 6-22](#).

$$u_{g,thresh,slow} = K_{loc}K_{msu}u_{g,crit} / K_{su}K_s \quad \text{Equation 6-21}$$

$$u_{g,thresh,stop} = K_{loc}K_{msu}u_{g,crit,slow} / K_{su}K_s \quad \text{Equation 6-22}$$

Where:

$u_{g,thresh,slow}$ = Measured or forecast wind gust speed at which trains will be slowed;

$u_{g,thresh,stop}$ = Measured or forecast wind gust speed at which trains will be stopped;

$u_{g,crit}$ = Critical wind gust speed at the normal train operating speed;

$u_{g,crit,slow}$ = Critical wind gust speed at the reduced train operating speed;

K_{loc} = Location factor (converts from ASCE 7 standard gust speed at the route segment location to ASCE 7 standard gust speed at the measurement location);

K_{msu} = Speed-up factor for the measurement point (converts from ASCE 7 standard gust speed to the gust speed actually measured);

K_{su} = Speed-up factor for the route segment from [Equation 6-6](#), see Section 6.6.3.6 (converts from ASCE 7 standard gust speed to gust speed at the train consistent with the rolling stock CWCs); and.

K_s = Safety factor, greater than 1.

For reference, the ASCE 7 standard gust definition is a 3-second gust at 33 ft (10m) above ground of Terrain Type C, while the gust definition consistent with the rolling stock CWCs is a 0.5-second gust at 10 ft (3 m) above ground level, where “ground level” excludes the ballast height.

The methodology below shows how the factors in the above equations may be derived. But, wherever possible, it is preferable to use measurements to derive these values instead. For example, even if permanent track-side monitoring is not envisaged, temporary monitoring stations could be set up for several years in critical locations along the route and the measured wind gust speeds compared against those from the sources that will eventually be used to trigger the operational restrictions.

K_{loc} is intended to represent the ratio between the wind gust speed at the measurement point versus wind gust speed at the route segment, where both are defined as ASCE 7 standard wind gust speed. It accounts for the measurement point being in a windier or less windy location than the route segment. The value used for K_{loc} can be derived by using the ASCE 7 Hazard Tool, see Section 6.6.3.3. Input the location of the weather station and note the 10-year MRI wind gust speed. Repeat for the location of the segment in question. The gust speed for the measurement location divided by the gust speed for the segment gives K_{loc} . If the two locations are close to each other, the Hazard Tool will give the same gust speeds for both locations and hence K_{loc} will be 1.0.

K_{msu} is the speed-up factor for the measurement location. It allows for the effects of terrain, height, etc., being different from those assumed in the ASCE 7 standard wind gust definition. The value used for K_{msu} will depend on the source of the wind gust speed measurements that are used to trigger the operational restrictions. For example:

- If measured by a standard weather station, then K_{msu} is 1.0. This also applies to forecast as well as measured wind gust speeds.
- If measured by a track-side monitoring station, the calculation process is the same as described for K_{su} in Section 6.6.3.6. The wind speed should be measured at least 10 ft (3 m) above ground level.

Note also that if the measurements that trigger operational restrictions come from monitoring stations in the most critical segments, then K_{msu} cancels with K_{su} and it is not necessary to calculate either of those parameters. This situation eliminates any uncertainty associated with the calculation of K_{su} and hence increases the reliability of the risk mitigation measures.

The operator should decide the safety factor K_s to make appropriate reduction of the threshold wind gust speeds in order to reduce risk to a tolerable level. Considerations may include the following:

- Wind conditions that may develop with time.
- The likelihood of a stronger gust occurring than those recently observed due to random chance.
- Any delay between real-time measurement and implementation of the operational restrictions

- Inaccuracy of forecasting and measuring equipment
- Inaccuracy of the calculated speed-up factor due to local effects influencing the measured wind and/or the wind speed at the train.

Several of the above considerations could be informed by measured wind gust data over several years.

The above calculations relate to overturning risk only. The operational procedures for high wind conditions should also consider other wind-related risks such as catenary damage, trees, or debris on the line.

6.7 Route Assessment Examples

6.7.1 Calculation of Route Segment Risk (Probabilistic Method)

Question						
Calculate the segment risk for the route segment with the following input data:						
Milepost start/end (miles)	Lat, Long	Train speed (mph)	Terrain type	Infrastructure type, height/depth (ft)	Barrier, porosity	Cant deficiency (in)
5.2 - 5.45	29.425, -98.197	110	C (Open country)	10 ft embankment	no	1.5

The service pattern consists of two trains per hour in each direction between the hours of 6 a.m. to 9 p.m., and no trains from 9 p.m. to 6 a.m., 364 days per year.

Methodology						
Follow the steps in Section 6.6.3.3 through 6.6.3.10; assume trains with CWC no worse than the Reference CWC given in Equation 6-4.						
The calculation has five main steps:						
Step 1: Obtain wind gust speeds from ASCE 7 Hazard Tool.						
Step 2: Look up and apply speed-up factors to obtain wind gust speeds at 10-, 25-, 50- and 100-year MRI at the train position.						
Step 3: Calculate the Critical Wind Speed.						
Step 4: Calculate the MRI of the Critical Wind Speed.						
Step 5: Calculate the segment risk.						

Step 1	Methodology	
	See Section 6.6.3.3.	
	Inputs	
	Latitude: 29.425 Longitude: -98.197	
	Calculations	
	(performed by the ASCE 7 Hazard Tool)	
	Result	
	10-year MRI = 71 mph	
	25-year MRI = 80 mph	
	50-year MRI = 85 mph	
	100-year MRI = 92 mph	

Step 2	Methodology Obtain speed-up factors from Table 6-4 , Table 6-5 , Table 6-6 , and Table 6-7 ; see Section 6.6.3.6. Apply speed-up factors using Equation 6-5 through Equation 6-9 ; see Section 6.6.3.7.
	Inputs Terrain type: C Infrastructure type & height: 10 ft embankment Barriers: none
	Calculations From Section 6.6.3.6, Gust Duration factor $K_{gd} = 1.05$ From Table 6-4 , Height, and terrain factor $K_{zr} = 0.88$ From Table 6-6 , Infrastructure factor $K_i = 1.18$ From Table 6-7 , Barrier factor $K_b = 1.0$ Calculate overall speed-up factor K_{su} from Equation 6-6 : $K_{su} = 1.05 \times 0.88 \times 1.18 \times 1.0 = 1.09$ Apply the overall speed-up factor to the wind gust speeds using Equation 6-7 through Equation 6-10 : $u_{g,Train,10year} = 1.09 \times 71 = 77.4 \text{ mph}$ $u_{g,Train,25year} = 1.09 \times 80 = 87.2 \text{ mph}$ $u_{g,Train,50year} = 1.09 \times 85 = 92.7 \text{ mph}$ $u_{g,Train,100year} = 1.09 \times 92 = 100.3 \text{ mph}$
	Result MRI gust speeds measured at the train position are: $u_{g,Train,10year} = 77.4 \text{ mph}$ $u_{g,Train,25year} = 87.2 \text{ mph}$ $u_{g,Train,50year} = 92.7 \text{ mph}$ $u_{g,Train,100year} = 100.3 \text{ mph}$

Step 3	Methodology <p>See Section 6.6.3.8. Calculate unbalanced acceleration from Equation 6-2. Calculate critical wind gust speed from the Reference CWC defined in Equation 6-5.</p>
	Inputs <p>Train speed: $V_{T, mph} = 110 \text{ mph}$ Cant deficiency $C_D = 1.5 \text{ inch}$ Track width: $S = 59 \text{ inch}$</p>
	Calculations <p>Equation 6-2:</p> $a_c(\text{in } g) = \frac{C_D}{S} = 1.5/59 = 0.025 \text{ } g$ <p>Equation 6-5:</p> $\begin{aligned} u_{g, crit} = u_{g, CWC} &= 80.8 - 0.126V_{T, mph} - 151a_c \\ &= 80.8 - 0.126 \times 108 - 151 \times 0.025 = 63.2 \text{ mph} \end{aligned}$
	Result <p>Critical wind gust speed $u_{g, crit} = 63.2 \text{ mph}$</p>
Step 4	Methodology <p>See Section 6.6.3.9. Since $u_{g, crit}$ is less than the 25-year MRI wind speed, return periods $R_1 = 10 \text{ years}$ and $R_2 = 25 \text{ years}$ will be used.</p>
	Inputs <p>Wind gust speeds from Steps 2 and 3</p>
	Calculations <p>Calculate R_{crit} using Equation 6-12 through Equation 6-14:</p> $k = \frac{u_{g, Train, R1}}{u_{g, Train, R2}} = \frac{u_{g, Train, 10 \text{ year}}}{u_{g, Train, 25 \text{ year}}} = \frac{77.4}{87.2} = 0.888$ $\gamma = \frac{\ln(R_1) - k^2 \ln(R_2)}{k^2 - 1} = \frac{\ln(10) - 0.888^2 \ln(25)}{0.888^2 - 1} = 1.10$ $R_{crit} = e^{\left(\left(\frac{u_{g, crit}}{u_{g, Train, R1}} \right)^2 (\gamma + \ln(R_1)) \right) - \gamma} = e^{\left(\left(\frac{63.2}{77.4} \right)^2 (1.10 + \ln(10)) \right) - 1.10} = 3.22 \text{ years}$

Step 5	Result <p>The MRI of the critical wind gust speed is 3.22 years.</p>
	Methodology <p>See Section 6.6.3.10.</p> <p>Calculate probability of a train being in the segment at any time from Equation 6-16.</p> <p>Calculate segment risk from Equation 6-17.</p> <p>Calculate segment risk per mile from Equation 6-18.</p>
	Inputs <p>Length of segment: $L = 5.42 - 5.2 = 0.15$ miles</p> <p>Number of trains per year = 2 per hour x 2 directions x 15 hours per day x 364 days per year = 21,840 trains per year</p> <p>Average number of trains per hour: $N = 21,840/8,760 = 2.49$</p> <p>Train speed: $V_T = 110$ mph</p>
	Calculations <p>Equation 6-16:</p> $P_t = \frac{LN}{V_{T, mph}} = \frac{0.15 \times 2.49}{110} = 0.00340$ <p>Equation 6-17:</p> $P_S = \frac{P_t}{R_{crit}} = \frac{0.00340}{3.22} = 0.00106$ <p>Equation 6-18:</p> $P_{spm} = \frac{P_S}{L} = \frac{0.00106}{0.15} = 0.00707$
	Result <p>The expected number of times per year that a critical wind gust will occur at the same time as a train is in this segment of the route (P_S) is 0.00106, or once every 943 years.</p> <p>The annual segment risk per mile is 0.00707.</p> <p>Note that the P_S figures from all the segments of the route should be added up before assessing acceptability of the overall risk.</p>

6.7.2 Calculation of Operational Wind Gust Speed Thresholds

Question

For the route segment in the example above, determine (a) the wind gust speed threshold at which operation speed should be reduced to 50 mph, and (b) the wind gust speed threshold at which operations should be suspended, to mitigate risk of overturning. The wind gust speeds will be measured 33 ft above ground by a standard weather station close to the route segment (not at trackside).

Methodology

Use [Equation 6-21](#) and [Equation 6-22](#); see Section 6.6.4.2.

Inputs

Critical wind gust speed: from Step 3 in example above, $u_{g,crit} = 63.2$ mph

Speed-up factor: from Step 2 in example above, $K_{su} = 1.09$

At the reduced speed of 50 mph, the curve in this segment has cant excess of 1 in. Cant excess is treated the same a cant deficiency in the CWC calculation because the method does not distinguish between overturning toward the center of the curve or toward the outside.

Real-time wind gust speed information at 33 ft above ground is available from a nearby weather station. In this example, a safety factor of 1.3¹ is assumed.

Calculations

The weather station wind gust speed threshold above which operation at the normal speed is no longer advisable is calculated from [Equation 6-21](#). Assume that the weather station is close enough to the route segment that $K_{loc} = 1.0$ and the weather station measures wind gust in the ASCE 7 standard manner so $K_{msu} = 1.0$

$$u_{g,thresh,slow} = K_{loc}K_{msu}u_{g,crit} / K_{su}K_s = 1.0 \times 1.0 \times 63.2 / 1.09 \times 1.3 = 44.6 \text{ mph}$$

For the 50-mph operating speed, calculate the unbalanced lateral acceleration from [Equation 6-2](#):

$$a_c(\text{in } g) = \frac{C_D}{S} = 1.0 / 59 = 0.0169 \text{ } g$$

Calculate the critical wind gust speed at 50 mph from [Equation 6-5](#):

$$\begin{aligned} u_{g,crit,slow} &= u_{g,CWC,50mph} = 80.8 - 0.126V_{T,mph} - 151a_c \\ &= 80.8 - 0.126 \times 50 - 151 \times 0.0169 = 71.9 \text{ mph} \end{aligned}$$

The weather station wind gust speed threshold above which operation at the reduced speed is no longer advisable is calculated from [Equation 6-22](#):

$$u_{g,thresh,stop} = K_{loc}K_{msu}u_{g,crit,slow} / K_{su}K_s = 1.0 \times 1.0 \times 71.9 / 1.09 \times 1.3 = 50.7 \text{ mph}$$

Result

For this particular route segment, the trains should operate at a reduced speed of 50 mph if measured wind gust speeds at the weather station exceed 44 mph, and operations should be suspended if gust speeds at the weather station exceed 50 mph.

The calculation would be repeated for other segments and the lowest wind speed thresholds for any segment would be taken.

Finally, wind speed thresholds would be compared against any existing operational wind speed thresholds, and the lower figures taken.

Notes:

1. Safety factor value used here is an example only. Operators should determine the appropriate value in each case.

6.8 Operational Recommendations

In addition to the risk assessment described above, operators will need to create procedures related to extreme wind events such as thunderstorms, tornados, and hurricanes. The procedures may include the monitoring of national and local weather forecasts and/or track-side wind measurement. The National Oceanic and Atmospheric Administration provides a number of different weather services for the U.S., including forecasts and live weather alerts.

Tornados occur frequently in some parts of the U.S. and have been known to blow rail cars off the track. Weather services issue Tornado Watches when the risk of tornados is high and Tornado Warnings when a tornado has been spotted in the area and the risk is considered severe. Slowing and/or stopping trains during tornado watches and tornado warnings could be considered as methods for mitigating the risks of derailment from tornados. At least one North American freight railroad has a policy of stopping trains in the vicinity of a tornado warning, for the duration of the warning. However if trains were halted in response to every tornado watch, the disruption to services would be considerable. Expert advice should be sought on this topic.

Trackside weather stations connected to the railway communications network and train control systems are recommended for high-speed railways. In this way, the operations control center can receive real-time data for the locations where the stations are located along the route to better inform operational decisions.

7 Pressure Wave Effects Inside Tunnels

7.1 Introduction

This section introduces important considerations when designing HSR tunnels or when planning changes to high-speed operations in tunnels.

When a train enters a tunnel at high speed, it generates pressure waves in the air within the tunnel. Large, rapidly changing air pressures occur inside the tunnel, leading to potential impacts on the comfort and safety of passengers and workers, as well as significant pressure loading on trains, fixed equipment, and structures within the tunnel. Mitigation is principally by selecting a tunnel size appropriate to the train speed and by providing railcars with sufficiently effective pressure-sealing. Pressure wave effects are frequently the governing factor on the size of HSR tunnels and hence may impact significantly on construction costs.

This section includes:

- Aerodynamic principles and phenomena
- Influencing factors
- Impacts on people, trains, fixed equipment, and structures, and on infrastructure design
- A summary of potential mitigation methods
- Assessment methods
- Reference tables for initial sizing of tunnels
- Criteria and considerations to be used in assessments
- Examples and calculations
- Non-aerodynamic issues that may influence the aerodynamic design of tunnels.

7.2 Aerodynamic Principles and Phenomena

A compressive pressure wave is generated by the nose of the train entering the tunnel (sometimes called the piston effect). As the train's nose enters, the air immediately ahead of the train is compressed. Further along the tunnel, the air is still at atmospheric pressure. The boundary between the compressed air and the atmospheric pressure air is called a **pressure wave**. In general, pressure waves are boundaries separating two regions of air that are at different pressures. Pressure waves move (**propagate**) along the tunnel at the speed of sound, which is about 1,130 ft/sec (depending on air temperature, pressure, humidity, and elevation above sea level). Note that the air itself is not moving at that speed, only the boundary between the high pressure and the atmospheric pressure air – just as an ocean wave can cross a whole ocean, while any particular molecule of water simply rises and falls as the wave passes by. The air moves, but only at around 2 to 10 percent of the train speed. This process is illustrated in more detail in [Figure 7-1](#) and described in the text following the figure.

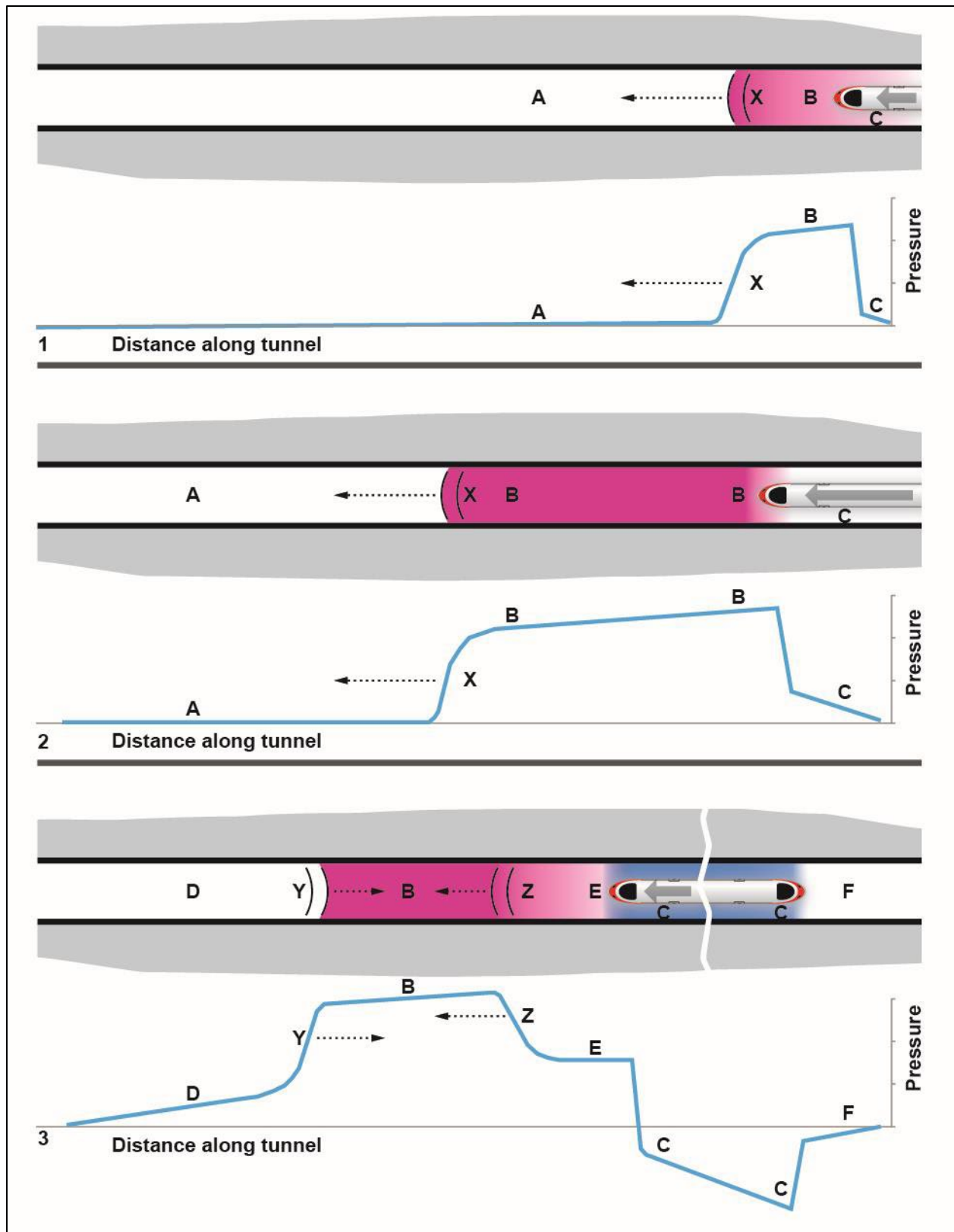


Figure 7-1. Propagation and reflection of pressure waves inside a tunnel

In [Figure 7-1](#), image 1:

- The train's nose has just entered the tunnel.
- The air immediately in front of the nose has been compressed by the so-called piston effect, indicated by a pink color and labeled **B**.
- Further ahead along the tunnel, the air is still at atmospheric pressure (labeled **A**).
- The boundary between the pressurized air and the atmospheric pressure air, labeled **X**, is a **pressure wave**. The wave is moving right to left as indicated by the dashed arrow, at the speed of sound.
- **X** is a **compressive pressure wave**, also called a **compression wave**. If a person were standing in the tunnel, the air pressure would increase rapidly as the wave passed over, with higher pressure in region B versus region A.
- **X** is also referred to as a **nose-entry wave** because it is caused by the train's nose entering the tunnel.

A short time later, the situation is as shown in [Figure 7-1](#), image 2:

- The train has moved a little further into the tunnel.
- Pressure wave **X** has propagated much further along the tunnel.

After the tail of the train enters the tunnel, the situation is as shown in [Figure 7-1](#) image 3:

- The initial compressive pressure wave **X** has reflected at the right-hand end of the tunnel and has now become an **expansion wave**, labeled **Y**, traveling left to right. Pressure waves reverse their type when reflecting at the free end of a tunnel: a compressive wave becomes an expansion wave and vice-versa. An expansion wave reduces the air pressure as it passes.
- The effects of multiple pressure waves add together (they are **superposed**). In this case, wave **Y** is cancelling out most of the positive pressure left behind by the compressive wave **X**, leaving behind a region of air, labeled **D**, at pressure close to atmospheric.
- Although the pressure changes from waves **X** and **Y** have opposite signs (i.e., the pressures mostly cancel out), the two waves cause the air velocity to change in the same direction – towards the tunnel exit in both cases. Superposition applies to air velocity as well as to pressure. The air velocity towards the tunnel exit in region **D** (where the two waves have superposed) is about double the velocity in region **B**.
- When the tail of the train entered the tunnel, it generated another expansion wave, labeled **Z**, traveling right to left, called the **tail-entry wave**. Wave **Z** has a smaller amplitude than wave **X** and only partially cancels out the high pressure left behind by wave **X** – thus, the region labeled **E** has a pressure greater than atmospheric but not as high as region **B**.

- There is a region of very low pressure, indicated by the blue color and labeled **C**, in the air next to the train. The reason for the low pressure is explained in Section 7.2.1 below. This region is sometimes called the **annulus** because it forms a ring of air around the train if seen from the front. This is the pressure that could be experienced by passengers inside the train.
- Behind the train, labeled **F**, the pressure is close to atmospheric. As the train moves further along the tunnel sucking air along behind it, the pressure in region F becomes more negative.

The various pressure waves continue to propagate along the tunnel, reflecting off the ends of the tunnel and passing over the train. Whenever a pressure wave meets a change of resistance in the tunnel (for example, a change of tunnel diameter or part of the tunnel being blocked by a train), a proportion of the pressure wave is reflected back along the tunnel and a proportion continues on, usually with reduced amplitude. Thus, pressure waves tend to fragment and the pattern of waves becomes more complex with time.

Each time a pressure wave passes over an item of equipment in the tunnel, the air pressure on that equipment changes rapidly – a pressure increase for a compressive wave or a pressure decrease for an expansion wave. Likewise, when a pressure wave passes over a point on the train, the pressure on the train (which could be experienced by the passengers inside) changes rapidly. Typical pressure time-histories are shown in Figure 7-2. As may be seen from the complexity of the graphs, this is a subject where computer simulation is the appropriate method of assessment rather than simple equations.

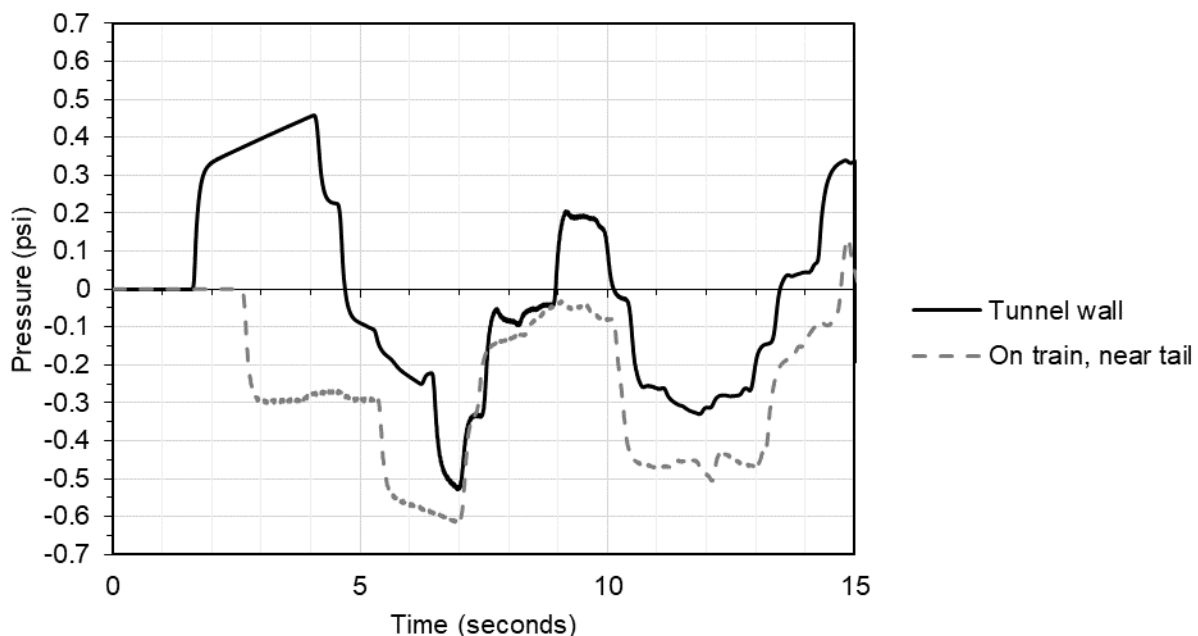


Figure 7-2. Sample pressure time-histories at a point on the tunnel wall and at a point on the train

Pressure change can cause impacts such as discomfort for passengers and crew (see Section 7.4.1), fatigue loading on the train (see Section 7.4.2), and on fixed equipment (see Section 7.4.3).

7.2.1 Conditions in the Vicinity of the Train

The conditions in the immediate vicinity of the train are illustrated in Figure 7-3. These are important because the pressure in the air in the annulus around the train is what passengers and the car bodies are subjected to. The velocity of this air plays a key role in determining the drag on the train. The airflows and pressures described in this section relate to pressure wave effects only, not to any localized flows associated with train slipstreams. For simplicity, the description applies to conditions shortly after the train has entered the tunnel and before the situation becomes complicated by the arrival of reflected waves.

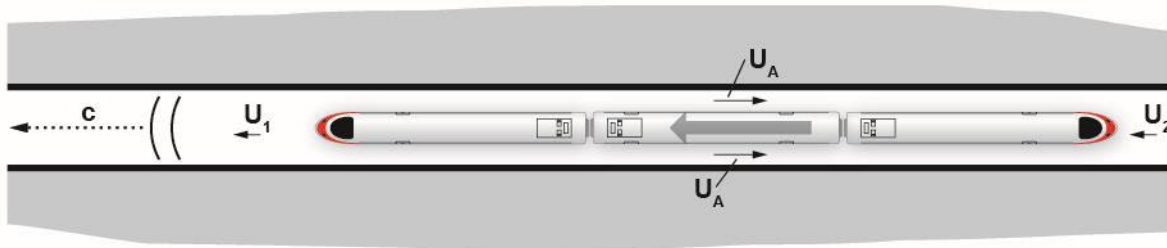


Figure 7-3. Conditions in the vicinity of the train

The train is traveling at speed V_T and the pressure wave propagates at the speed of sound, c . The air behind the nose-entry pressure wave is moving in the same direction as the train, at speed U_1 , typically on the order of 2 to 10 percent of the train speed. Behind the train, air is again moving in the same direction as the train at speed U_2 which is similar to U_1 . Thus, in general, the air is being moved along the tunnel in the same direction as the train, as might be expected. In the annulus around the train, however, the situation is different: air moves *in the opposite direction to the train*, at a speed U_A which is typically greater than U_1 and U_2 . This may initially appear counter-intuitive, but may be understood by the following inter-related considerations:

- Air flows from the high-pressure region ahead of the train to the low-pressure region behind the train.
- As the train moves forward it displaces air. Some of this air is pushed forward along the tunnel (U_1) and some flows past the train (U_A) to help fill in the gap being left behind the train.

Relative to the motion of the train, the air in the annulus is moving at high speed ($V_T + U_A$) leading to high frictional forces along the train. This is the reason why the pressure profile in region C in the graph in Figure 7-1 image 3 is sloping, and is one of the reasons why drag in tunnels is greater than in open air.

Furthermore, it may seem surprising that the pressure in the annulus is lower than the pressure behind the train, as shown in Figure 7-1 image 3. It is a fact of fluid mechanics that, when the velocity of a fluid such as air increases, its pressure reduces; and when

its velocity reduces, the pressure increases. In this case, it is the velocity of the air relative to the train that counts. That velocity increases greatly as the air moves into the annulus from the region ahead of the train, leading to a drop of pressure; and when it reaches the tail, it slows down again, leading to a rise of pressure.

7.2.2 Wave Coincidence Effects

Where two compression waves propagating in opposite directions meet, the pressures add together, potentially resulting in greater impacts than for either of the two waves individually. The same is true for two expansion waves. The increased impacts occur at the position in the tunnel (and at the point in time) where the waves overlap. If this happens to coincide with the train's position in the tunnel, the increased impacts can affect passengers and the train itself. Phenomena of this type will be described in this report as **wave coincidence effects**. Note that a small change in the arrival time of either of the two pressure waves can determine whether the increased impacts affect the train and its passengers or not. For this reason, the relationship between the degree of impact and the influencing factors described in Section 7.3 can be complex.

Of particular interest is the wave coincidence effect arising from the reflected nose-entry wave (Y in Figure 7-1) and the tail-entry wave (Z in Figure 7-1), which can govern some pressure wave impacts in shorter tunnels. It typically reaches a worst-case condition when the tunnel is around four times longer than the train (the exact multiple depends on train speed and other considerations).

7.2.3 Single-track versus Double-track Tunnels

In this report, the term **single-track tunnels** means tunnels where each track has its own separate air space, so that trains and equipment on one track are completely isolated from pressure waves caused by trains on the other track, see Figure 7-4. Single-track tunnels can take the form of two separate tubes with one track in each tube (also called **twin tube** tunnels) or a single structure with an impermeable dividing wall between the tracks. The term **double-track tunnels** means tunnels where two or more tracks are enclosed within the same air space.

For cases where each track has its own separate air space but there are doors or cross-passages between them, the tunnel would still count as single-track if airflow between the tracks is prevented during normal operation (for example, if there are doors between the cross-passages and the tunnel, and these doors are normally kept closed and have minimal leakage). On the other hand, if there are ducts or open cross-passages enabling air to pass from one tube to the other at certain points along the length of the tunnel, this would be a third case. Aerodynamically, it is neither single-track nor double-track but something in between.

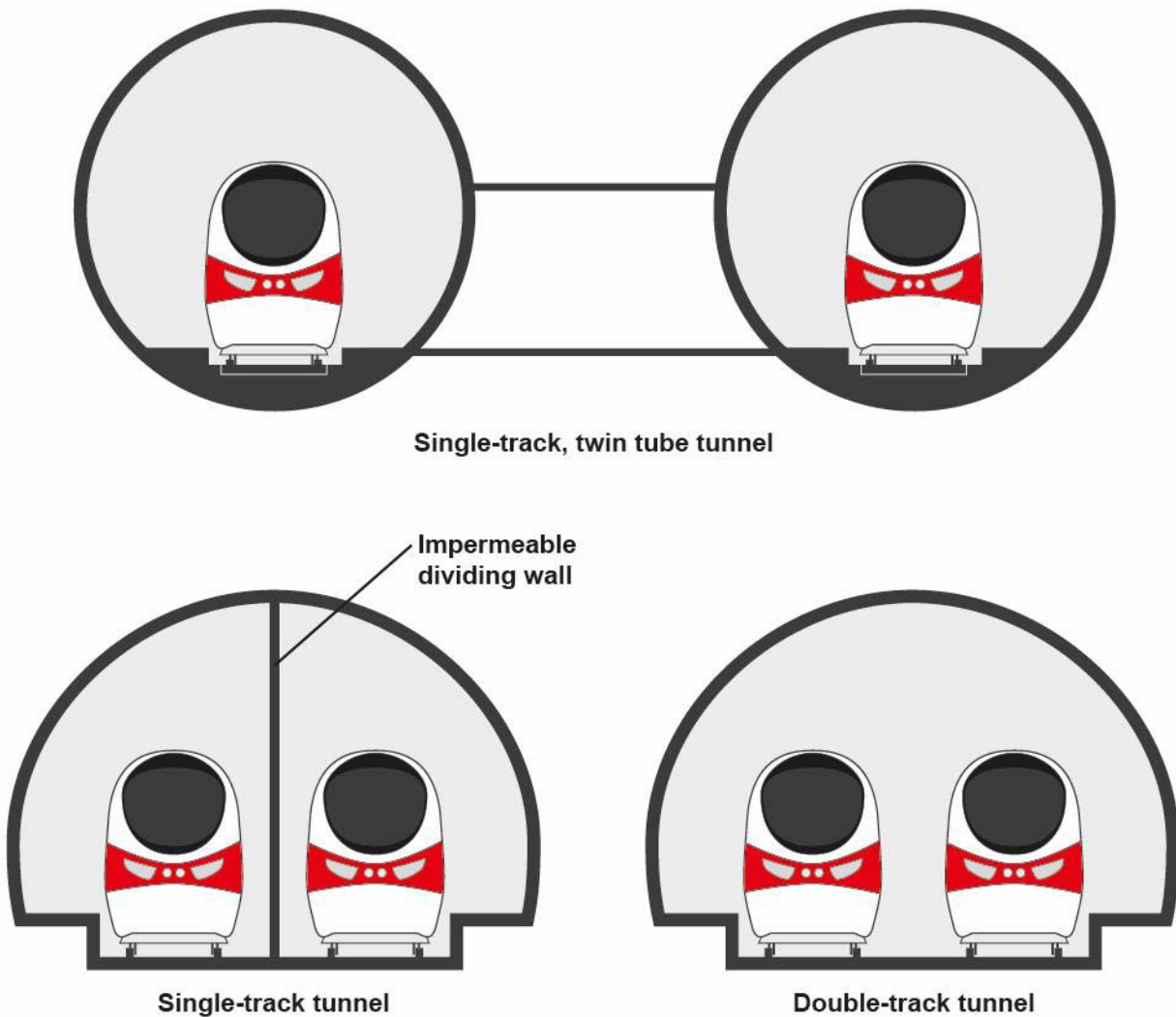


Figure 7-4. Examples of single-track and double-track tunnels, as these terms are used in this report

Historically, most HSR tunnels have been double-track because these tunnels are cheaper to construct, and this is still the case for new tunnels in Japan and China; but in Europe, most new tunnels are now being designed as single-track (twin tube) for fire safety reasons. In the event of a fire, passengers and crew can be evacuated into the other tube which can be kept smoke-free by the ventilation system.

The differences in terms of aerodynamics are:

- Double-track tunnels usually have a greater cross-sectional area than each tube of a single-track tunnel. Therefore, when a train enters the tunnel at a given speed in the absence of any other trains, the blockage ratio is lower and the pressure wave amplitude is smaller.
- In double-track tunnels, complex aerodynamic situations can arise when trains are present on both tracks simultaneously. Each train creates pressure waves

which superpose (add together). The worst-case pressure wave impacts may occur due to an unlucky coincidence of two waves arriving at the same time. This leads to additional complexity in assessments.

- Single-track tunnels can be assessed without considering the effect of trains on the other track because no aerodynamic interaction between them is possible.
- In twin-tube tunnels with leakage between the tubes (e.g., via cross-passages), the leakage influences pressure wave effects and therefore this should be included in assessments. There are similar considerations regarding combinations of trains on both tracks as for double-track tunnels.

7.3 Influencing Factors

7.3.1 Blockage Ratio

Blockage ratio (β) is defined as train cross-sectional area (A_{Train}) divided by the tunnel cross-sectional area (A_{Tun}):

$$\beta = A_{Train}/A_{Tun}$$

Equation 7-1

The tunnel cross-sectional area A_{Tun} is the area of a typical cross section that is occupied by air (and not by solid objects or equipment) in the absence of any trains, as shown in [Figure 7-5](#). A “typical cross section” in this context would show equipment that is present continuously along the tunnel such as cables and walkways, but not equipment or features that are present only at certain points along the tunnel such as fans. Thus, the area occupied by walkways and cables would be excluded from A_{Tun} , while the area that is occupied by fans at certain points along the tunnel would be treated as air (included in A_{Tun}) because, for most of the length of the tunnel, the fans are not present. In the case of double-track tunnels, the blockage ratio is calculated with A_{Train} being the area of one train, even though the tunnel contains more than one track.

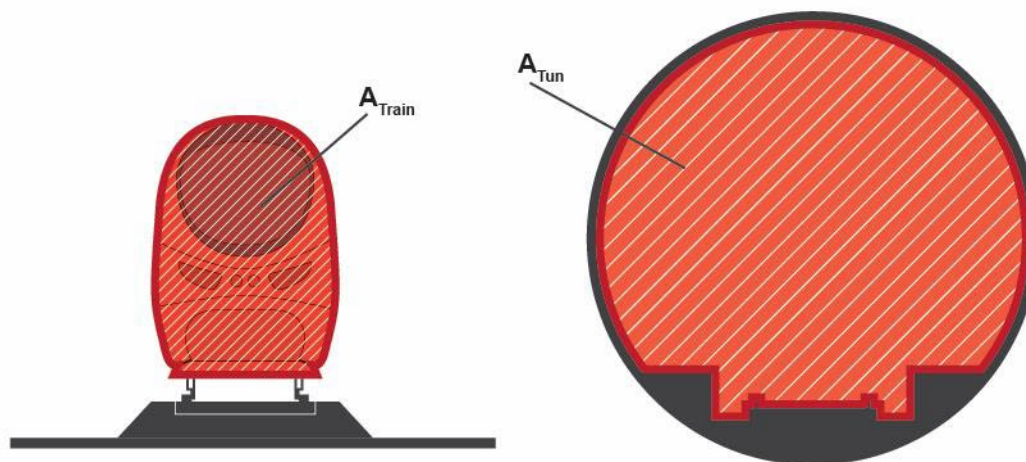


Figure 7-5. Cross-sectional area of train (left) and tunnel (right)

The greater the blockage ratio, the greater the pressure wave amplitude. Typical HSR tunnels have blockage ratios in the range 0.1 to 0.2. In other words, the cross-sectional area of an HSR tunnel is about 5 to 10 times the cross-sectional area of the train. For small changes of blockage ratio, the pressures are approximately proportional to the blockage ratio.

7.3.2 Train Speed

The pressure wave amplitude varies approximately with train speed squared. Due to the complex patterns of superposition of the pressure waves and the effects of train sealing, the pressure changes experienced by passengers and crew do not scale exactly with the amplitudes of the train entry and exit pressure waves, and therefore, they also do not scale exactly with train speed squared. There can even be cases where a reduction of train speed leads to a worse result, due to changes of the wave coincidence effects described in the Section [7.2.2](#).

7.3.3 Tunnel Length

Pressure changes in tunnels occur due to pressure waves and their reflections off the ends of the tunnel. The length of the tunnel influences the pressure changes in three ways:

- Wave coincidence effects (see Section [7.2.2](#)) depend on the time taken for waves to propagate along the tunnel and back. Small changes of tunnel length can sometimes make a big difference to pressure wave impacts, especially in shorter tunnels.
- As a pressure wave propagates along a tunnel, its amplitude reduces due to friction effects. Thus, the longer the tunnel, the smaller the reflected waves and the smaller the wave coincidence effects.
- Longer tunnels offer greater frictional resistance to airflow, leading to the potential for rapid pressure changes when the resistance is suddenly increased or decreased. For example, the longer the tunnel, the more suction builds up behind the train as it moves through the tunnel. When the train exits from the tunnel, the suction is suddenly relieved, leading to a rapid pressure increase that can be experienced by passengers.

7.3.4 Train Length

The length of the train has two influences on pressure waves:

- Longer trains offer more frictional resistance, which contributes to greater pressure wave amplitude, resulting in greater impacts of pressure waves.
- The length of the train governs the time gap between the waves generated by the nose and tail of the train, such as those caused by the train entering the tunnel (nose-entry and tail-entry waves). The time gap influences wave coincidence effects; see Section [7.2.2](#).

For longer tunnels, the first effect is more important. For shorter tunnels, the second effect is more important, and often leads to a worst-case pressure change when the

tunnel length is around four times the train length (the exact multiple depends on the train speed).

When assessing tunnels, it is important to know the maximum and minimum lengths of trains that will use the tunnel. For tunnels shorter than about three to four times the *minimum* train length, the shortest train is likely to be the worst case. For tunnels longer than about four times the *maximum* train length, the longest train is likely to be the worst case. For intermediate tunnel lengths, it is often necessary to try different train lengths to find the worst case.

7.3.5 Air Shafts

Air shafts (sometimes called pressure relief shafts, draft relief shafts, or ventilation shafts) are open cross-passages or ducts linking the tunnel with the atmosphere (see [Figure 7-6](#)). They generally have a beneficial effect on the impacts of pressure waves because some of the pressurized air travels up the shaft and out to atmosphere, instead of along the tunnel. Air shafts can also help reduce drag. The optimum cross-sectional area of a shaft for pressure comfort does not necessarily coincide with the optimum for other purposes, such as ventilation or emergency egress. These considerations are described in [Section 7.5.3](#).

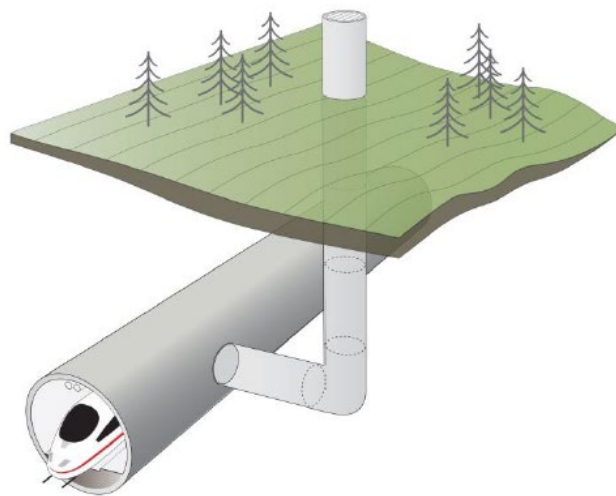


Figure 7-6. Schematic sketch of an air shaft (excludes typical emergency egress and ventilation infrastructure)

7.3.6 Train Aerodynamic Design

The amplitudes of the pressure waves depend partly on the shapes of the nose and tail of the train. A train with a non-streamlined nose creates a slightly bigger pressure wave than a train of the same cross-sectional area with an elongated, streamlined nose. However, among streamlined HSTs, the influence of the nose design on pressure wave amplitude is relatively minor compared to other factors such as speed and blockage ratio. Nose shape, and especially the length of the taper at the nose, can have a strong effect on the *gradient* of the pressure wave, which is important for mitigation of micro-pressure waves (covered in [Section 8.3.6](#)).

The shape of the tail of the train affects the amplitude of the tail-entry wave. Counter-intuitively, a more streamlined tail can generate worse pressure wave effects than a poorly streamlined one, but the influence of the tail (whether well-streamlined or not) is smaller than that of the nose.

Friction on the sides, underbody and roof of a train can add significantly to the amplitudes of the pressure changes in a tunnel, especially for long trains. Compared to friction on the tunnel walls, friction on the train can be more influential because the speed of the air relative to the train is much greater than the speed of the air relative to the tunnel walls. Measures that counteract drag in open air, such as covered inter-car gaps, also reduce friction in tunnels.

7.3.7 Train Sealing

Modern high-speed trains are designed to be pressure-tight, but no train is perfectly sealed. When the pressure increases outside the train, air leaks in slowly, leading to a gradual increase of pressure inside the train. The sealing of the train is beneficial to passenger comfort by slowing the pressure changes inside the train. HSTs are usually considered as a series of separate cars so that air can leak into and out of each car individually. Openly connected cars are considered as a single unit.

Train sealing performance is usually expressed as a **sealing time constant** – the longer the time-constant, the better the sealing. The time constant, τ , is defined such that the rate of change of pressure inside the train, $\frac{dp_i}{dt}$, is given by:

$$\frac{dp_i}{dt} = (p_o - p_i)/\tau \quad \text{Equation 7-2}$$

Where:

$\frac{dp_i}{dt}$ = Instantaneous rate of change p_i ;

p_o = Instantaneous pressure outside the train;

p_i = Instantaneous pressure inside the train; and,

τ = Sealing time constant.

In practical terms, τ is the time it would take for the difference between the pressures inside and outside of the train to reduce by 63 percent (this is a mathematical consequence of the way that τ is defined).

Figure 7-7 shows the pressure time-history inside a train for different sealing time constants when the external pressure undergoes a step change.

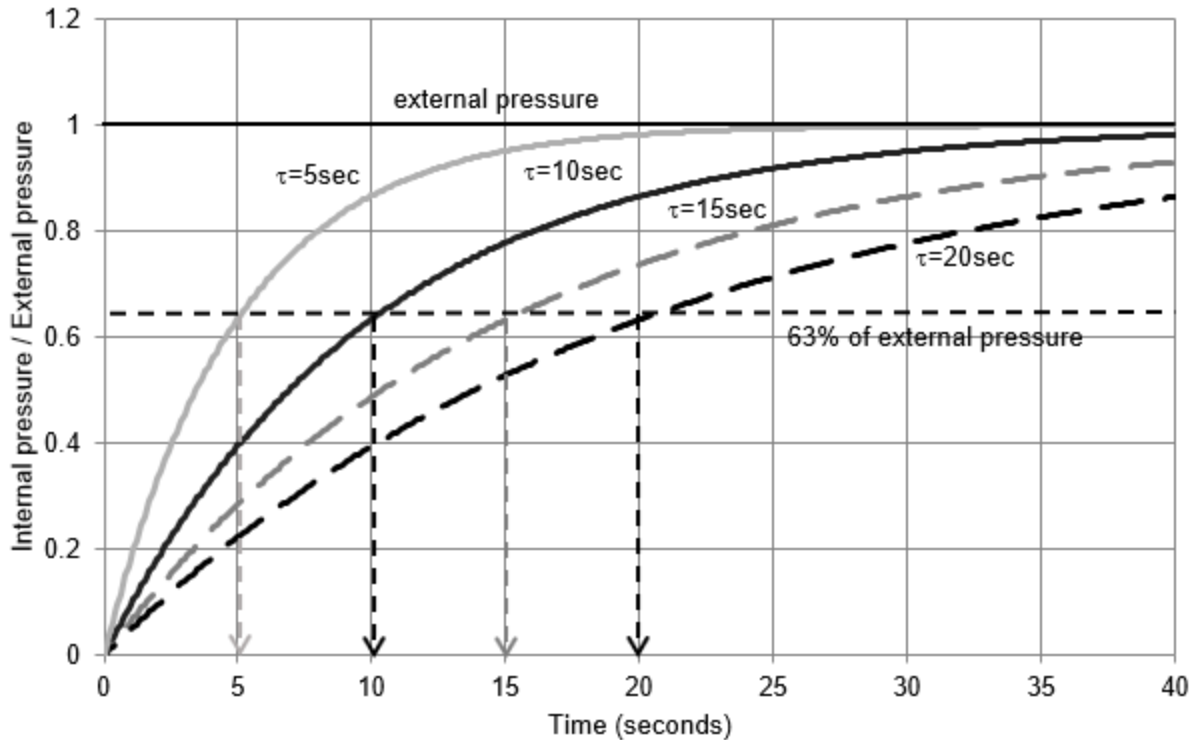


Figure 7-7. Pressure inside a sealed railcar in response to a step change of external pressure, showing influence of time constant τ

Sealing performance can be measured in a static test, as specified in UIC Leaflet 660 [78] in which a single railcar is positively or negatively pressurized and the time it takes for the pressure to pass key values is noted. From these measurements, a **static sealing time constant**, τ_{stat} , may be derived by the railcar manufacturer. However, when the train is in motion, the sealing performance described by the **dynamic sealing time constant**, τ_{dyn} , may be two or even three times lower than the static time constant [79]. It is the dynamic time constant that is relevant for assessments of pressures inside trains in tunnels. The dynamic time constant can be determined only by field tests and cannot be deduced accurately from the static time constant. Furthermore, the time constants for leakage into and out of a railcar may be different from each other. Typical modern HSTs have dynamic sealing time constants in the range 10 to 30 seconds.

The strong influence of sealing on the pressures experienced by passengers is illustrated in Figure 7-8, which shows an example of the pressure changes inside sealed and unsealed railcars as they pass through the same tunnel at the same speed. Passengers in the sealed railcar are subjected to smaller, less rapid pressure changes than passengers in unsealed railcars.

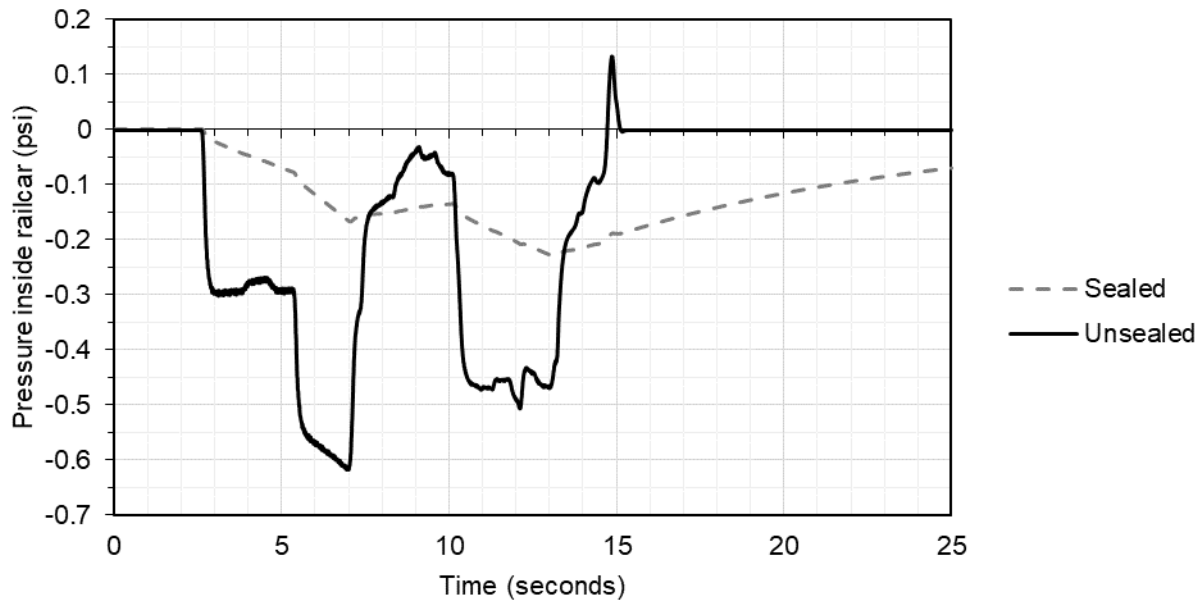


Figure 7-8. Example of pressure changes inside sealed and unsealed railcars during passage through a tunnel

7.3.8 Carbody Shell Compressibility

A sealed carbody is slightly compressible as well as slightly leaky, as indicated in [Figure 7-9](#).

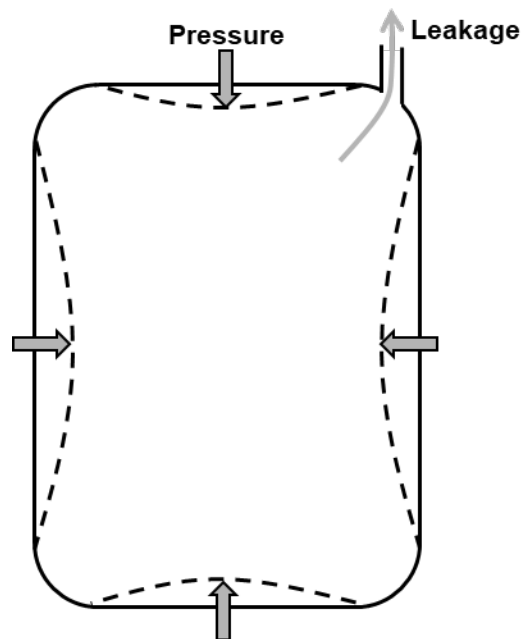


Figure 7-9. Idealization of a railcar as a leaky, compressible box

When an external pressure change occurs, not only does air leak through the sealing system, but the walls and roof of the shells of the carbodies deform slightly. The air inside the carbody is compressed by this movement and thus, a proportion of the external pressure change is experienced immediately inside the railcars, potentially impacting aural comfort. This effect is usually not very significant but could become so if the pressure changes in the tunnel outside the train are large, the cars are well sealed, and a high standard of aural comfort is desired. Carbody design guidance is not a part of this report.

7.3.9 Atmospheric Conditions in the Tunnel

Pressure wave amplitude is proportional to air density. Therefore, pressure wave impacts are increased in cold weather when the air is denser. For example, at 23 °F (-5 °C) the air is 7.5 percent denser than when the temperature is 59 °F (15 °C). Pressure wave amplitude is also increased when atmospheric pressure is higher. Furthermore, the speed of sound, which is the speed at which pressure waves propagate along the tunnel, varies with atmospheric conditions. Further information about this is given in Section [7.6.5.4](#).

Any airflow in the tunnel prior to the train's arrival will influence pressure wave amplitude: a headwind increases pressure wave amplitude; a tailwind reduces it. Airflow in the tunnel can be caused by differences of atmospheric pressure between one end of the tunnel and the other, which may in turn be caused by the natural wind blowing against the hillside at one of the entrance portals. Depending on the natural wind direction relative to the train direction, it could cause either a headwind or a tailwind in the tunnel. This effect tends to be greater in shorter tunnels. Longer tunnels offer more resistance to the flow of air, so the same pressure difference outside the tunnel causes lower airflow speed in a longer tunnel.

The passage of previous trains causes airflow in the tunnel in the direction of travel of the trains. In single-track tunnels this is always a tailwind, and therefore the worst case is obtained by ignoring airflow from previous trains. The airflow speed caused by a previous train decays with time and may be insignificant if there is a long gap between trains.

Pressure decreases at higher altitude, so in a long, inclined tunnel the air pressure varies gradually along the tunnel. As a train passes through the tunnel, the pressure change due to the varying altitude adds to the pressure changes caused by pressure waves.

7.4 Impacts

7.4.1 Impacts on Passengers and Crew

When the air pressure inside the train changes rapidly, passengers and crew may experience discomfort in their ears caused by a pressure difference across the eardrum, resulting in some passengers being reluctant to use the rail service or perceiving the journey experience as low quality. The term **aural comfort** (also called **pressure comfort**) is used in assessments and criteria intended to prevent or mitigate such impacts. Mitigation measures for aural comfort aim to avoid unpleasant effects for

passengers and crew during typical transits through tunnels with the railcar sealing system working as intended.

In extreme cases there would be potential for permanent damage to the ears. **Medical safety** is concerned with avoiding damage to the ears even under worst-case conditions such as failure of a railcar's sealing system. This subject was researched by the European Railway Research Institute [41], leading to the now well-established **Medical Safety Limit**; see Section 7.6.15.1. When designing HSR tunnels, it is important to consider both medical safety and aural comfort.

Discomfort and damage to the ears from pressure changes depend not only on the amplitude of the pressure change, but also on the speed at which the pressure change occurs and on the aural health of the subject. Given sufficient time, the pressure in the middle ear can equalize with the external pressure by venting through the Eustachian tube, thus relieving the net pressure on the eardrum and the associated discomfort. In aircraft after takeoff and before landing, passengers are subjected to pressure changes of around 3 to 4 psi (20 to 30 kPa). These pressure changes are much greater than the pressure changes in rail tunnels but are spread over about 20 to 30 minutes making the impact generally tolerable for most people. In rail tunnels, the pressure changes experienced by passengers are usually less than 0.5 psi (3.4 kPa) but occur over seconds rather than minutes.

Aural comfort is a highly subjective issue. A pressure change that is uncomfortable for one person may be barely noticeable for another. Furthermore, sensitivity to pressure changes may be increased by illness (for example, the Eustachian tube of a person suffering from a cold may be blocked), or by previous trauma to the eardrum.

Aural comfort criteria are informed by experiments in which people are subjected to certain pressure changes and then asked to rate subjectively how uncomfortable each pressure change was. Examples include the *Berlitz study* [12], which used passengers in a train on a German railroad route with many tunnels, and the *Schwanitz study* [127], in which volunteers sat in a pressure chamber and were subjected to pre-determined pressure changes with different amplitudes and rise times. These are referred to in more detail in Section 7.6.15.3.

7.4.2 Impact on HST Railcar Design and Specification

Railcars for HSR should be designed with sufficient pressure-tightness (sealing) to protect passengers and crew from aural discomfort. Due to the sealing system, the air pressure inside the train varies much less rapidly than the air pressure in the tunnel outside the train. This leads to substantial pressure differences across the skin of the railcar every time the train passes through a tunnel. The railcar structure should be designed to withstand this fatigue loading. The railcar manufacturer is responsible for this design.

7.4.3 Impact on Structures and Fixed Equipment Inside the Tunnel

Structures and fixed equipment inside tunnels, such as walls, doors, cabinets, and signs, experience a variety of aerodynamic loading that should be considered in the design and specification, including:

- Pressure waves: relatively large pressure amplitudes develop rapidly when a pressure wave passes by and persist until another wave passes the same point. Positive and negative pressures occur behind compression and expansion waves respectively, leading to significant fatigue loading.
- Nose and tail pressure pulses as trains pass by, as described in Section 4. The pulses are typically of very short duration compared to the pressure wave effects.
- Airflow loading from slipstreams of passing trains, which may be more severe in tunnels than in open air because the tunnel is a confined space.

7.4.4 Impact on Tunnel Design and Construction Cost

The required cross-sectional area of HSR tunnels is frequently governed by pressure wave effects. Larger tunnel cross-sectional area reduces pressure wave amplitude but increases construction cost. The economic consequences of faster train speeds (requiring larger tunnels to mitigate pressure wave effects) should be recognized. See Section 7.5 below for further details.

7.4.5 Impacts Where HSR Tunnels Are Shared with Conventional Traffic

Internationally, dedicated tunnels for HSR are the norm, but HSR tunnels shared with conventional traffic does sometimes occur. Conventional railcars and cargos are unlikely to have been designed to withstand the large pressures generated by HSTs in tunnels. Furthermore, high airflow speeds may be caused by HST slipstreams in tunnels. If HST speeds are not limited within shared tunnels, impacts on the conventional traffic could include window or door blow-outs, structural damage, cargo damage, tarps, or soft covers being torn or blown off, loose cargos being blown out of cars, debris landing on the tracks, etc. Furthermore, conventional passenger railcars may be unsealed or poorly sealed, leading to greater impacts of aural discomfort for the passengers compared to the passengers inside the HSTs. In current practice, speed restrictions are imposed to avoid such problems, potentially leading to impacts on timetabling and journey times.

In the U.S., Tier III HSR will require exclusive ROW when operating at speeds above 125 mph and therefore the possibility of sharing tunnels with conventional (Tier I and freight) traffic will not arise, except at lower speeds than are covered by this report. Current Tier II lines in the NEC have tunnels with mixed traffic but none of these have authorized speeds high enough to fall within the scope of this report.

7.4.6 Impact on Workers Inside Tunnels

This report assumes that workers would not be present inside tunnels during the high-speed operation of trains, and therefore no further details are offered on this subject. If workers were present, aerodynamic risks could include discomfort or injury to the ears from pressure wave effects and noise, or injury from falling due to airflow from trains. The pressure wave effects experienced by track workers would be much greater than those experienced by people inside the train.

Note that pressure waves extend throughout a tunnel system, they are not restricted to the vicinity of the trains that cause them. For example, if one tube of a twin-tube tunnel

were closed for maintenance while operations continued in the other tube, any leakage from tube to tube via cross passages could expose workers to pressure waves with the potential for aural discomfort or damage.

7.4.7 Aerodynamic Impacts at Underground Stations

Where a tunnel emerges into an underground station, pressure waves will be transmitted from the tunnel into the air in the station, potentially causing aural comfort impacts for the passengers on the platforms. Pressure waves in the station could be caused by trains entering or exiting the far end of the tunnel at high speed, even if the speed of the trains at the station end of the tunnel is low. Any trains passing through the underground station at high speed could cause additional pressure changes and airflow effects with potential safety impacts for people on platforms.

Passengers face the additional impact of air velocity due to both slipstreams of passing trains and air pushed along the tunnels by the trains. Airflow from these sources could cause people on platforms to fall and suffer injury or to experience annoyance from dust or trash being blown against them or from hair or skirts being disturbed. They may suffer thermal discomfort if the air from the tunnel is particularly cold or warm (air in the tunnel can be warmed by heat lost from trains, although this is more typically an issue for subway systems than HSR). Similar effects could occur where a tunnel emerges into an open-air station: passengers standing on the platform near the mouth of the tunnel might experience impacts from air being expelled from or sucked into the tunnel.

Station ventilation systems need to be designed to account for the airflows into and out of the station caused by trains. Impacts from high airflow speeds are not limited to platforms but could also affect people walking through access tunnels or riding elevators to or from the platforms.

If trains pass through underground stations at high speed, consideration should be given to pressure pulse effects: signs, tiles, or other finishes may be damaged or dislodged.

Additional information on this topic can be found in the Subway Environmental Design Handbook [\[146\]](#).

7.4.8 Micro-pressure Waves (“Sonic Booms”)

Micro-pressure waves (sometimes called sonic booms) are a by-product of pressure waves in tunnels. These waves and their impacts are described in Section [8](#).

7.4.9 Other Aerodynamic Impacts in Tunnels

A case occurred in Japan [\[27\]](#) involving a particular train type which started swaying laterally as it moved through double-track tunnels. The motion was thought to be caused by turbulence or vortex-shedding on one side of the train which induced the swaying motion. A resonance effect developed in which the turbulence synchronized with the swaying, amplifying both effects. The aerodynamic design of the train and the small gap between the train and the tunnel wall on one side were contributing factors. The problem was solved by modifying the train shape and suspension characteristics.

Since this problem was apparently unique to one type of train, it will not be covered further in this manual.

7.5 Mitigation Methods

Mitigation for pressure wave effects consists of providing a sufficiently large tunnel cross-sectional area, pressure-sealing the trains, providing air shafts, and designing the trains and fixed equipment inside the tunnels to withstand the expected pressure loading. Limiting the speed of trains at the tunnel entry and exit is another effective mitigation measure. There is relatively little scope for reducing pressure wave impacts via aerodynamic design of the train.

7.5.1 Mitigation by Increasing Tunnel Size

The size of HSR tunnels is selected based on consideration of pressure wave effects (and, in some cases, aerodynamic drag; see Section 9.3.5). The larger the tunnel cross-sectional area relative to the area of the train, the lower the pressure wave amplitude for a given train speed, thus reducing all the impacts described in Section 7.4. Therefore, all the impacts of pressure waves can be reduced to acceptable levels by selecting a sufficiently large tunnel size, though this comes at a higher cost.

In general, the higher the design speed at the tunnel entry and exit, the larger the required cross-sectional area. However, there are no hard-and-fast rules, and the designer may choose to trade-off tunnel size against the specification of trains and fixed equipment (e.g., better sealed trains, and more fatigue-resistant trains and fixed equipment may enable a smaller tunnel). The level of aural comfort is also a matter of choice for the operator: smaller tunnels with a less comfortable experience for passengers or larger tunnels with a more comfortable experience.

The additional construction cost for larger tunnels is a strong driver for careful consideration of these tradeoffs early in the design process. Adopting higher-specification trains could lead to increased cost of rolling stock or a more limited choice of manufacturers, while lower comfort standards could impact on the number of passengers using the service and hence on revenues.

Internationally, different countries have adopted different tunnel sizes. In Europe, the specification of the trains for which the tunnels are designed is limited by interoperability considerations. Typical European tunnels for 300 km/h (185 mph) operation have cross-sectional areas of around 90 to 100 m² (969 to 1076 ft²) for double-track, or 60 m² (646 ft²) per tube for single-track tunnels. In contrast, a Japanese double-track tunnel for the same operating speed would be around 62 to 64 m² (667 to 689 ft²), about 40 percent less than the European equivalent. The driver in Japan is that large numbers of tunnels were constructed decades ago for lower operating speeds, and it would be too expensive to re-bore the tunnels. Instead, they set the specification of the trains to achieve the desired performance with the existing tunnels at today's higher speeds – for example, via better levels of sealing and car body structures that tolerate the increased pressures. Additionally, the Medical Safety Limit (described in Section 7.6.15.1), which would have the effect of imposing an upper limit on the speed through these tunnels irrespective of train specification, is not applied in Japan.

Section 7.6.4 provides nominal tunnel sizes for initial concept design.

7.5.2 Mitigation by Choice of Single-Track or Double-Track Tunnel Design

The choice of a single-track or double-track tunnel is likely to be dictated by considerations other than aerodynamics, such as construction cost or fire safety. Both types can be designed such that aerodynamic objectives are met. However, where a choice is available, use of a larger double-track tunnel instead of two smaller single-track tunnels may be considered as a form of mitigation for pressure wave effects. Compared to a single-track tunnel, pressure wave effects are reduced during typical passage through a double-track tunnel when no other trains are present but may be increased in some less common situations when two trains happen to enter the tunnel almost simultaneously. For further information, see Section 7.6.5.6.

7.5.3 Mitigation Using Air Shafts

Air shafts, sometimes called pressure relief shafts or draft relief shafts, are ducts connecting the tunnel to the outside air (Figure 7-6).

The shafts reduce the amplitude of the pressure waves because some of the pressurized air travels up the shaft and out to atmosphere instead of along the tunnel. Typically, air shafts are spaced at 0.5 to 2 miles apart and (if designed mainly to relieve pressure waves) have a cross-sectional area 10 percent to 35 percent of the area of the main tunnel [53][65][151]. As well as mitigating pressure wave effects, air shafts have multiple purposes including reduction of drag, cooling, ventilation during normal operation, smoke control in fires, and emergency evacuation. The optimum cross-sectional area of shaft for these different applications can differ widely – for example, much larger shafts may be required for emergency evacuation than for pressure wave mitigation. It is common practice to design shafts with different parts of the cross-section segregated for different purposes: for example, a large shaft containing a stairwell for emergency evacuation, with a small proportion of its cross section walled off for pressure relief. The emergency evacuation stairwell would be closed off by doors from the tunnel bores during normal operation, while the pressure relief section would be open to the tunnel.

Advantages of air shafts can include:

- Mitigation of pressure comfort issues or permitting a smaller cross-sectional area for the main tunnel while maintaining the same pressure comfort performance
- Reduced aerodynamic drag on the train, thereby reducing power or fuel consumption and/or allowing the desired speed to be attained
- Improved ventilation and control of air temperatures in the tunnel
- Use for smoke ejection in fires
- Use for electricity supply access into the tunnel
- Relatively inexpensive compared with increasing the size of the main tunnel

- Can share space with emergency evacuation shafts (which are much larger) at small additional cost and land take

Disadvantages of air shafts include:

- Noise emissions from the shaft portals into the environment caused by high air speeds within the shafts, and also the noise of the trains themselves. Noise mitigation treatments within the shafts may be necessary in sensitive areas. In some cases, noise restrictions may preclude the use of air shafts altogether.
- The need to protect the shaft portals from vandalism, people dropping objects down the shafts, animals, or birds entering the shafts, etc. These are sometimes achieved by enclosing the shaft portal in a purpose designed building (sometimes called a **headhouse**) [137]. The shaft may exhaust through the roof of the building.
- Micro-pressure waves resulting in audible noises could be emitted from the shaft portals if pressure waves with high gradients are present within the tunnel or could be caused by the train passing the shaft within the tunnel.
- May not be feasible where the tunnel is far below the ground surface or below an urban area.

7.5.4 Mitigation Using Cross-Passages

Cross-passages link the two tubes of a single-track tunnel. They are normally required in single-track tunnels for safety reasons so people can escape into the other tube in the event of a fire or other emergency. Typically, the cross-passages contain doors that are closed during normal operation for fire safety reasons, but it is sometimes possible to reduce pressure wave effects by allowing a percentage of the cross-sectional area to remain open. This is a relatively inexpensive countermeasure, but has some disadvantages:

- Instead of being able to design each tube in aerodynamic isolation, the two tubes are now linked, so pressure wave combinations from trains in each tube should be considered.
- It is often found that a worst-case combination of trains in the two tubes can give a more severe result than the case where the cross-passages are completely closed [137]. Thus, the cross-passages may mitigate pressure wave effects most of the time but make the situation worse occasionally.
- Open cross-passages can cause an effect like a localized crosswind where air blows through the passage onto the side of trains.
- If the cross-passages are kept open during normal operation, there would need to be devices to close them automatically in the event of a fire to prevent smoke reaching the unaffected tube.
- It may be difficult to satisfy all the requirements of pressure wave mitigation, smoke control, ventilation, and drag reduction simultaneously.

7.5.5 Mitigation of Aural Discomfort by Railcar Sealing

Passengers and crew inside trains can be protected to a large extent from pressure changes in the tunnel by the HST sealing system, as described in Section 7.3.7. Modern HSTs can typically achieve dynamic sealing time constants (defined in Section 7.3.7) of 10 to 30 seconds. The need to seal the railcars conflicts with the requirement for fresh air supply and therefore railcars are sealed only when in tunnels. The ventilation systems are designed to shut off the fresh air intakes automatically when entering a tunnel in order to seal the train and protect passengers from pressure changes, then open them again after leaving the tunnel once the interior and exterior pressures have equalized sufficiently. In long tunnels, supply of enough fresh air for the passengers while the intakes are sealed may become an issue. Some HSTs are provided with active fan-driven pressurization systems that keep the interior pressure as constant as possible while the train is in the tunnel [88].

7.5.6 Mitigation by Aerodynamic Design of Trains

The aerodynamic design of the nose and tail of trains has only a minor influence on pressure waves and therefore improved streamlining would not be considered as a mitigation measure. In principle, reducing friction along the length of the train would have a moderately beneficial effect on pressure wave impacts, but most HST designs are already optimized in this respect as part of the regular design process in order to minimize drag, and it would be difficult to achieve further reductions of friction to mitigate pressure wave effects. The adoption of trains with smaller cross-sectional area would be effective, although other considerations such as space for passengers are likely to determine this choice.

7.5.7 Mitigation by Reducing Speed

Reducing the speed of trains is an effective mitigation measure for pressure waves in tunnels. The pressure waves are caused by trains entering and exiting the tunnels and smaller waves are caused by passing air shafts or cross passages inside the tunnels. The speed reduction need only apply at those specific points, not necessarily for the whole length of the tunnel.

7.5.8 Mitigation for Conventional Traffic in Tunnels Shared with HSTs

Internationally, most HSR tunnels are dedicated to HST traffic only. In the few cases where mixed traffic is permitted, speed restrictions are imposed to reduce the risk of damage to the conventional railcars and their cargos or aural discomfort of their passengers. For example, Löetschberg Base Tunnel in the Swiss Alps carries mixed traffic, including passenger, shuttle, and freight trains. A speed limit of 250 km/h (155 mph) applied to passenger trains to avoid aerodynamic impacts on the other train types in the tunnel [14]. The same speed limit was applied in German tunnels with mixed traffic [142].

Suitable speed limits will depend on the blockage ratio and on the particular railcars involved and can only be determined by full-scale testing and/or operational experience.

7.5.9 Mitigation When Line Speed Is to Be Increased in Existing Tunnels

Where the design line speed is to be increased in existing tunnels, an assessment of pressure wave effects should be carried out. If this indicates unacceptable impacts of the higher speed, mitigation measures include:

- Adopting trains with improved sealing performance or reduced cross-sectional area.
- Maintaining the previous line speed when passing the tunnel entrance and exit, even though speed is increased at other points within the tunnel.
- Addition of air shafts
- Increasing the tunnel cross-sectional area by excavating the floor to a lower level.

7.6 Assessment

7.6.1 Assessment Objectives

The objectives of assessment include the following:

- Help design new tunnels – for example, to determine cross-sectional area and requirement for air shafts.
- Prepare the required specifications for HSTs and fixed equipment in tunnels.
- Assess whether proposed new or modified operations might lead to unacceptable aerodynamic impacts.

7.6.2 Assessment of New Tunnels: Rolling Stock Considerations

Before a new tunnel can be designed, the designer needs information about the rolling stock that will use the tunnel and the operating speed through the tunnel. In general, the larger the cross section of the trains, and the faster the operating speed, the larger the tunnel. For new operations it is often necessary to design the tunnels before the rolling stock has been selected, hence the concept of Baseline Trains used in this report as a source of input data; see Section [2.3.2](#).

Note also that the design life of tunnels typically far exceeds the operating lifetime of the rolling stock. A degree of future-proofing of new tunnel designs is appropriate regarding possible future train sizes and operating speeds.

7.6.3 Assessment Methods

Two types of assessment methods are available:

- Tables or graphs of tunnel sizes based on design speed and other input parameters, such as those given in Section [7.6.4](#) of this report. Guidance exists in a similar form in countries such as Germany [\[26\]](#) and China [\[99\]](#).
- Analysis with specialized software. This provides for flexibility to consider all relevant variables and is the recommended method for most assessments. Such

software simulates the generation and propagation of pressure waves in tunnels and can model the particular aerodynamic characteristics of different types of trains and the design features of tunnels such as air shafts and cross passages. With this assessment method, a particular train/tunnel scenario is modelled and the program predicts pressure time-histories at relevant points in the tunnel and the train. These results are then assessed against acceptability criteria and the process is repeated for different values of the input parameters for the tunnel or train. Further details are given in Section 7.6.5.

7.6.4 Nominal Tunnel Sizes for Initial Concept Design

The **Nominal Tunnel Sizes** given in Table 7-1 and Table 7-2 below are intended for initial concept design. Tunnel sizes can simply be taken from the tables, postponing the need for specialized analysis until a later stage in the design process. They provide a level of aerodynamic performance consistent with international HSR practice, but as described below the tables, they are based on certain assumptions and limitations, presuppose certain acceptability criteria, and do not offer full flexibility to consider the tradeoffs. It is strongly recommended that a suitably experienced professional check all tunnel designs for the impacts of pressure waves before committing to construction.

Table 7-1. Nominal Tunnel Sizes for initial concept design: single-track tunnels, area per tube

Train speed (mph)	Tunnel area per tube: U.S./Euro Baseline Trains		Tunnel area per tube: U.S./Asian Baseline Trains	
	ft ²	m ²	ft ²	m ²
125	560	52	611	57
150	603	56	658	61
175	646	60	705	65
200	861	80	939	87
225	1109	103	1209	112
250	1432	133	1562	145

Table 7-2. Nominal Tunnel Sizes for initial concept design: double-track tunnels

Train speed (mph)	Tunnel area: U.S./Euro Baseline Trains		Tunnel area: U.S./Asian Baseline Trains	
	ft ²	m ²	ft ²	m ²
125	861	80	939	87
150	926	86	1009	94
175	990	92	1080	100
200	1367	127	1491	139
225	1787	166	1949	181
250	2207	205	2407	224

The tunnel sizes in the tables above are valid under the following conditions:

- The sizes given are based on considerations related to pressure waves only. Larger sizes may be needed for other reasons, such as space for systems equipment and emergency egress walkways or to mitigate heat build-up or reduce drag. Increasing the tunnel size above that shown in the tables is always beneficial for aerodynamics.
- Trains conform to the Baseline Train properties given in Section 2.3.2. In particular, the trains must have cross-sectional area and length no greater than shown in Table 2-2, they must satisfy the tunnel-entry pressure wave requirements described in Section 7.6.17, and they must be sealed with a dynamic time-constant of at least 10 seconds.
- Aerodynamic performance described in Table 7-3 to Table 7-5 is deemed acceptable by the operator. Trains or equipment that cannot tolerate the pressure loading stated in these tables will require larger tunnels.
- Tunnel length up to 5 miles
- The tunnel sizes also apply to tunnels longer than five miles if air shafts are provided at least every 2 miles and the cross-sectional area of air shafts open to the tunnel during normal operations is no less than 10 percent of the main tunnel area. For single-track tunnels, this stipulation assumes a separate air shaft for each tube. Tunnels longer than five miles without air shafts will require a larger area if they are to provide the same aerodynamic performance.
- In double-track tunnels, the trains on the two tracks travel in opposite directions. If this is not the case, the tunnel sizes do not apply, and the tunnel size should be assessed using one-dimensional analysis.
- In single-track tunnels, if more than one train can be present in each tube at the same time, the guidelines are likely to apply but one-dimensional analysis should

be used to check results for multiple trains in the tunnel versus a single train passage.

7.6.4.1 Derivation of Nominal Tunnel Sizes

Internationally, only Germany [26] and China [99] mandate minimum HSR tunnel sizes for given train speeds. Other European countries set tunnel sizes case-by-case. The Nominal Tunnel Sizes for speeds up to 175 mph (280 km/h) are like those mandated in Germany and China, and are based on operational experience.

Japanese HSR tunnels, which are double-track, predate modern operating speeds and are too small to be consistent with the recommendations for the U.S. in this report. First, the Japanese do not apply the Medical Safety Limit (see Section 7.6.15.1), which would require larger tunnels at current maximum operating speeds. Second, the tunnels require specially designed rolling stock for higher-speed operation which precludes many existing HSTs available internationally. Therefore, the Nominal Tunnel Sizes given above are not derived from Japanese tunnel sizes.

For speeds upwards of 200 mph (for which there is limited international experience of operation in tunnels, especially in single-track configurations), the Nominal Tunnel Sizes were derived such that the aerodynamic performance at these higher speeds is approximately equal to that of the 175 mph condition which is supported by operational experience. In other words, the Nominal Tunnel Sizes for 200 mph and above are made large enough to compensate for the higher speed.

The Nominal Tunnel Sizes are compared against those mandated in Germany and China in Figure 7-10 and Figure 7-11. The dashed lines in these figures labelled as “equal aerodynamic performance,” show the tunnel sizes providing aerodynamic performance approximately equal to the 175 mph baseline condition.

The “equal aerodynamic performance” tunnel sizes for speeds below 175 mph are smaller than the sizes mandated internationally and have not been recommended in this report to maintain a conservative approach. The reasons why these countries select larger tunnel sizes than might seem feasible aerodynamically include space requirements for equipment, walkways, etc.; and, it may be that tunnels with slower line speeds might be used by older HSTs that are less tolerant of high pressures in the tunnel or are less well sealed.

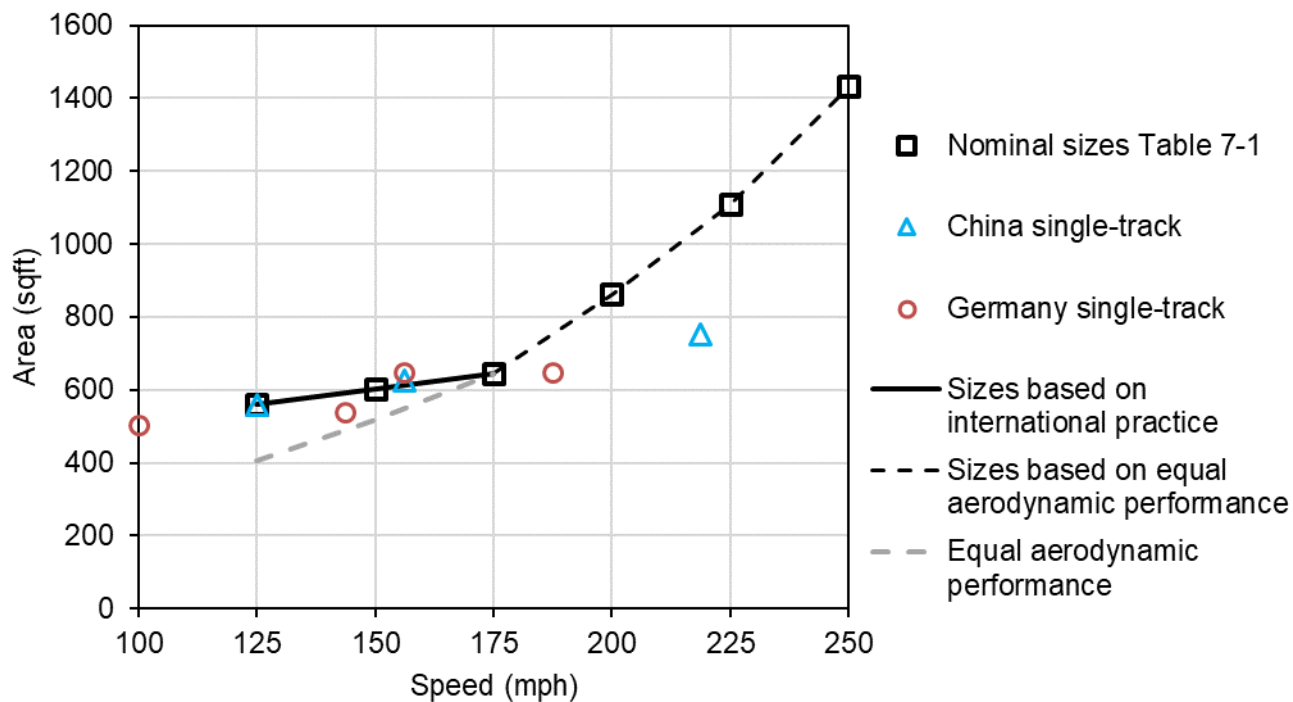


Figure 7-10. Single-track Nominal Tunnel Sizes for U.S./Euro Baseline Trains compared with internationally mandated tunnel sizes

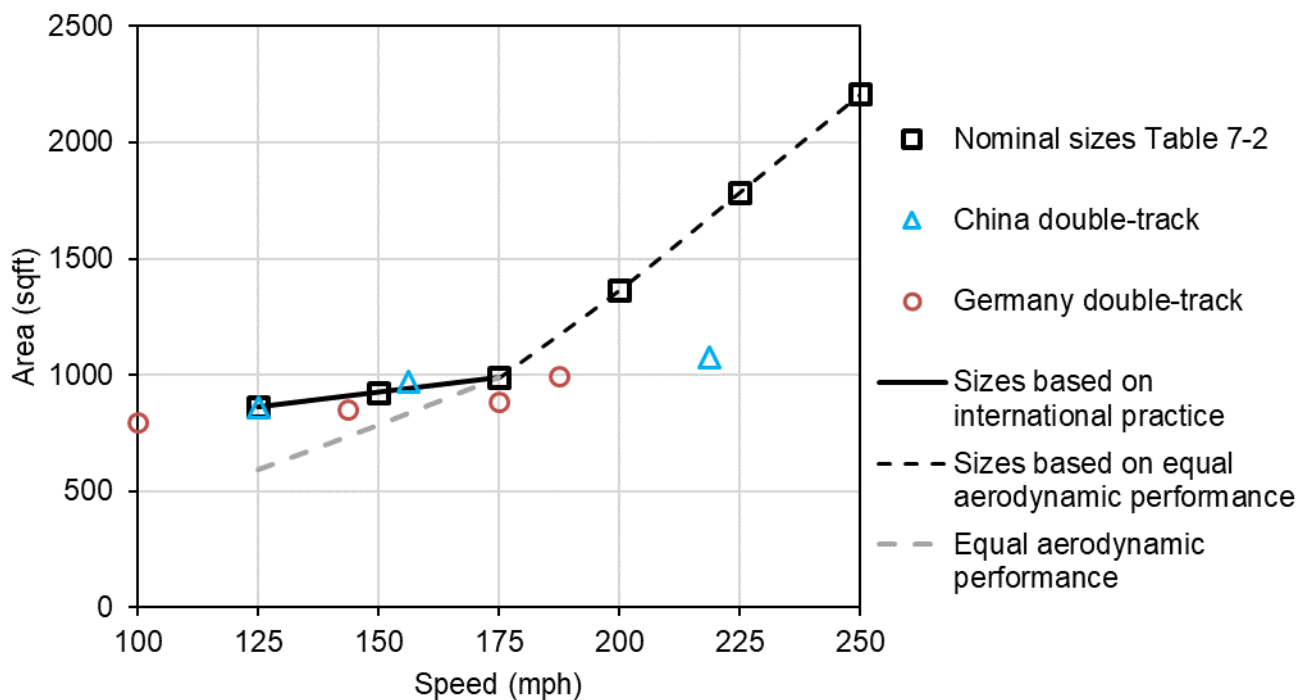


Figure 7-11. Double-track Nominal Tunnel Sizes for U.S./Euro Baseline Trains, compared with internationally mandated sizes

Nominal Tunnel Sizes for U.S./Asian Baseline Trains have been derived by scaling by 12/11 from the U.S./Euro Baseline to preserve the same blockage ratio, assuming the cross-sectional areas of the trains are up to 129 ft² (12 m²) for U.S./Asian and up to 118 ft² (11 m²) for U.S./Euro Baseline Trains.

Because the given tunnel sizes are derived from international HSR practice, it is expected that they will be compatible with HSR equipment available on the international market. The Nominal Tunnel Sizes can be conservative depending on many factors such as tunnel length, train characteristics, tolerable limits on pressures in the tunnel, desired aural comfort levels, and so on. Some of these factors are described in more detail below.

7.6.4.2 Aerodynamic Performance with Nominal Tunnel Sizes and Baseline Trains

The aerodynamic performance with the Nominal Tunnel Sizes is approximately as shown in [Table 7-3](#) to [Table 7-5](#), based on the following assumptions:

- The tunnel size has been selected according to train speed from [Table 7-1](#) for single-track tunnels or [Table 7-2](#) for double-track.
- Baseline Trains (either U.S./Euro or U.S./Asian)
- Standard atmospheric conditions (described in Section [7.6.5.4](#))

Terms used in the tables are explained below:

- **Medical Safety Limit:** Peak-to-peak pressure changes outside the train should be less than 1.45 psi (10 kPa), according to a criterion intended to protect passengers in the event of failure of the train's sealing system. See Section [7.6.15.1](#) for further information.
- **Aural Comfort:** The pressure changes occurring inside the train (when the sealing system is operating normally) are categorized into "Higher Comfort Level", "Lower Comfort Level," or "worse than Lower Comfort Level" as described in Section [7.6.15.2](#).
- **Aural Comfort Index (ACI):** Provides a numerical estimate of the aural comfort performance and is defined in Section [7.6.15.4](#). Lower values correspond to a more comfortable experience for passengers. Values ≤ 1.0 correspond to Higher Comfort Level, 1.0 to 1.5 corresponds to Lower Comfort Level, above 1.5 is worse than Lower Comfort Level.
- **Train dynamic sealing time constant (τ):** Higher values indicate a better-sealed train, see Section [7.3.7](#). Aural comfort data are provided for two time constant values, 10 and 18 s.
- **Pressure (fatigue) load on doors and sealed equipment in the tunnel:** Maximum positive or negative pressure occurring at any point along the length of the tunnel. The figures given relate to pressure waves only (see Section [7.6.13.1](#) for more details) and do not include pressures from the train nose and tail pressure pulses (Section [7.6.13.2](#)) or from air flow along the tunnel (Section [7.6.13.3](#)). As explained in Section [7.6.13.1](#), this loading is relevant only to

equipment or surfaces that separate the air in the tunnel from air at atmospheric pressure, such as sealed cabinets or closed doors leading to cross-passages or emergency access shafts. It is not relevant to signs, signals or other equipment that is fully immersed in the air in the tunnel.

- **Net pressure (fatigue) load on doors between bores:** Assumes trains in both tubes of a twin-tube tunnel and maximum positive pressure in one tube acting on one side of the door simultaneously with maximum negative pressure in the other tube acting on the other side of the door; see Section [7.6.13.1](#).
- **Maximum net pressure (fatigue) load on trains:** the difference between pressure outside the train and pressure inside the train. Net pressure is strongly dependent on the train's sealing performance (better sealing generally causes greater net pressure). The figures in the tables allow for dynamic sealing time constants up to about 50 seconds. For simplicity, the net pressure is quoted in the tables as plus or minus the same pressure. In reality this maximum net pressure occurs with internal pressure greater than external pressure (i.e., the net pressure acts to inflate the train bodyshell), while the maximum net pressure in the other direction (acting to crush the train bodyshell) is usually significantly less. See Section [7.6.11](#) for further information.

Table 7-3. Approximate aerodynamic performance with Nominal Tunnel Sizes and Baseline Trains, train speed 125 mph

125 mph		Single-track tunnel	Double-track tunnel	
			Single train passage	Worst-case trains meeting
Medical Safety Limit Limit 1.45 psi (10 kPa)		Pass 0.51 psi (3.5 kPa)	Pass 0.32 psi (2.2 kPa)	Pass 0.78 psi (5.4 kPa)
Aural comfort	$\tau_{\text{dyn}} = 10 \text{ sec}$	Higher Level ACI 0.8	Higher Level ACI 0.5	Lower Level ACI 1.1
	$\tau_{\text{dyn}} = 18 \text{ sec}$	Higher Level ACI 0.6	Higher Level ACI 0.4	Higher Level ACI 0.8
Maximum pressure load on doors and sealed equipment in the tunnel due to pressure wave effects		$\pm 0.45 \text{ psi}$ ($\pm 3.1 \text{ kPa}$)	$\pm 0.29 \text{ psi}$ ($\pm 2.0 \text{ kPa}$)	$\pm 0.60 \text{ psi}$ ($\pm 4.1 \text{ kPa}$)
Maximum net pressure load on doors between tubes due to pressure wave effects		$\pm 0.90 \text{ psi}$ ($\pm 6.2 \text{ kPa}$)	N/A	N/A
Maximum net pressure load on trains		$\pm 0.40 \text{ psi}$ ($\pm 2.8 \text{ kPa}$)	$\pm 0.25 \text{ psi}$ ($\pm 1.7 \text{ kPa}$)	$\pm 0.56 \text{ psi}$ ($\pm 3.9 \text{ kPa}$)
Notes:				
1. The terms used to quantify aerodynamic performance are explained in Section 7.6.4.2.				

Table 7-4. Approximate aerodynamic performance with Nominal Tunnel Sizes and Baseline Trains, train speed 150 mph

150 mph		Single-track tunnel	Double-track tunnel	
			Single train passage	Worst-case trains meeting
Medical Safety Limit Limit 1.45 psi (10 kPa)		Pass 0.65 psi (4.5 kPa)	Pass 0.41 psi (2.9 kPa)	Pass 1.06 psi (7.3 kPa)
Aural comfort	$\tau_{\text{dyn}} = 10 \text{ sec}$	Lower Level ACI 1.1	Higher Level ACI 0.7	Worse than Lower Level ² ACI 1.6
	$\tau_{\text{dyn}} = 18 \text{ sec}$	Higher Level ACI 0.9	Higher Level ACI 0.5	Lower Level ACI 1.1
Maximum pressure load on doors and sealed equipment in the tunnel due to pressure wave effects		±0.58 psi (±4.0 kPa)	±0.39 psi (±2.7 kPa)	±0.79 psi (±5.4 kPa)
Maximum net pressure load on doors between tubes due to pressure wave effects		±1.16 psi (±8.0 kPa)	N/A	N/A
Maximum net pressure load on trains		±0.51 psi (±3.5 kPa)	±0.34 psi (±2.4 kPa)	±0.71 psi (±4.9 kPa)
Notes:				
<ol style="list-style-type: none"> 1. The terms used to quantify aerodynamic performance are explained in Section 7.6.4.2. 2. The lower comfort level criteria are exceeded only for tunnels longer than four to five times the train length. The exceedances for longer tunnels could be eliminated by increasing the tunnel area (assess case-by-case using one-dimensional computer simulation), but some operators would deem this unnecessary – see description on criteria for double-track tunnels in Section 7.6.15.5. 				

Table 7-5. Approximate aerodynamic performance with Nominal Tunnel Sizes and Baseline Trains, train speeds 175 mph and above

175 to 250 mph		Single-track tunnel	Double-track tunnel	
			Single train passage	Worst-case trains meeting
Medical Safety Limit Limit 1.45 psi (10 kPa)		Pass 0.82 psi (5.7 kPa)	Pass 0.58 psi (4.0 kPa)	Marginal pass 1.33 psi (9.2 kPa)
Aural comfort	$\tau_{\text{dyn}} = 10 \text{ sec}$	Lower Level ACI 1.4	Higher Level ACI 0.9	Worse than Lower Level ² ACI 1.8
	$\tau_{\text{dyn}} = 18 \text{ sec}$	Higher Level ACI 1.0	Higher Level ACI 0.6	Lower Level ACI 1.3
Maximum pressure load on doors and sealed equipment in the tunnel due to pressure wave effects		±0.72 psi (±5.0 kPa)	±0.54 psi (±3.7 kPa)	±1.0 psi (±6.5 kPa) TBC
Maximum net pressure load on doors between tubes due to pressure wave effects		±1.44 psi (±10.0 kPa)	N/A	N/A
Maximum net pressure load on trains		±0.68 psi (±4.7 kPa)	±0.49 psi (±3.4 kPa)	±0.83 psi (±5.7 kPa)
Notes:				
1. The terms used to quantify aerodynamic performance are explained in Section 7.6.4.2.				
2. The lower comfort level criteria are exceeded only for tunnels longer than four to five times the train length. The exceedances for longer tunnels could be eliminated by increasing the tunnel area (assess case-by-case using one-dimensional computer simulation), but some operators would deem this unnecessary – see description on criteria for double-track tunnels in Section 7.6.15.5.				

7.6.4.3 Aerodynamic Performance with Tunnels Larger or Smaller than the Nominal Tunnel Sizes

In this section, the aerodynamic implications of selecting tunnel sizes smaller or larger than the Nominal Tunnel Sizes are described. This information may be used, for instance, when assessing tradeoffs between aerodynamic performance and other considerations such as construction cost or when setting specifications for equipment when the tunnel size is already fixed.

Tunnel sizes larger than shown in Table 7-1 and Table 7-2 will always provide improved aerodynamic performance (i.e., lower pressures, greater passenger comfort), whereas

tunnel sizes smaller than shown in the tables will always result in higher pressures and worse passenger comfort, if all other factors apart from tunnel size remain the same.

For single-track tunnels, sizes smaller than the Nominal Tunnel Sizes are not necessarily unacceptable – this depends entirely on the operator's requirements and choices. For example, one might choose a smaller tunnel, select better-sealed trains to achieve the desired level of aural comfort, and design the fixed equipment to tolerate the increased pressures. The approximate effect of tunnel size on aerodynamic performance with single-track tunnels is shown in [Table 7-6](#) and also in [Figure 7-12](#) through [Figure 7-16](#).

Double-track tunnels smaller than the Nominal Tunnel Sizes for speeds of 175 mph and above are not recommended in general because there is a risk that the Medical Safety Limit would not be met for the worst case of trains meeting or passing within the tunnel. For this reason, tables and graphs similar to those below are not provided for double-track tunnels. However, this depends on the length of the tunnel, and it may be possible to demonstrate acceptable performance for specific smaller tunnels using one-dimensional computer simulations.

Table 7-6. Approximate aerodynamic performance for single-track tunnels smaller than the Nominal Tunnel Sizes for speeds 175 mph and above

175 to 250 mph		Area ratio ¹		
		0.7	0.8	0.9
Factor on maximum pressures compared to Nominal Tunnel Size ²		1.4 to 1.6	1.2 to 1.4	1.1 to 1.15
Medical Safety Limit Limit 1.45 psi (10 kPa)		Pass 1.21 psi (8.4 kPa)	Pass 1.05 psi (7.2 kPa)	Pass 0.92 psi (6.3 kPa)
Aural comfort	$\tau_{\text{dyn}} = 10 \text{ sec}$	Worse than Lower Level ACI 2.2	Worse than Lower Level ACI 1.8	Worse than Lower Level ACI 1.6
	$\tau_{\text{dyn}} = 18 \text{ sec}$	Worse than Lower Level ACI 1.6	Lower Level ACI 1.3	Lower Level ACI 1.1
Maximum pressure load on doors and sealed equipment in the tunnel due to pressure waves		$\pm 1.02 \text{ psi}$ ($\pm 7.0 \text{ kPa}$)	$\pm 0.88 \text{ psi}$ ($\pm 6.1 \text{ kPa}$)	$\pm 0.79 \text{ psi}$ ($\pm 5.5 \text{ kPa}$)
Maximum net pressure load on doors between two bores due to pressure waves		$\pm 2.04 \text{ psi}$ ($\pm 14.0 \text{ kPa}$)	$\pm 1.76 \text{ psi}$ ($\pm 12.2 \text{ kPa}$)	$\pm 1.58 \text{ psi}$ ($\pm 11.0 \text{ kPa}$)
Maximum net pressure load on trains		$\pm 0.95 \text{ psi}$ ($\pm 6.6 \text{ kPa}$)	$\pm 0.82 \text{ psi}$ ($\pm 5.7 \text{ kPa}$)	$\pm 0.75 \text{ psi}$ ($\pm 5.2 \text{ kPa}$)
Notes:				
1. Area of tunnel divided by Nominal Tunnel Size from Table 7-1 for the particular train speed.				
2. The terms used to quantify aerodynamic performance are explained in Section 7.6.4.2 .				

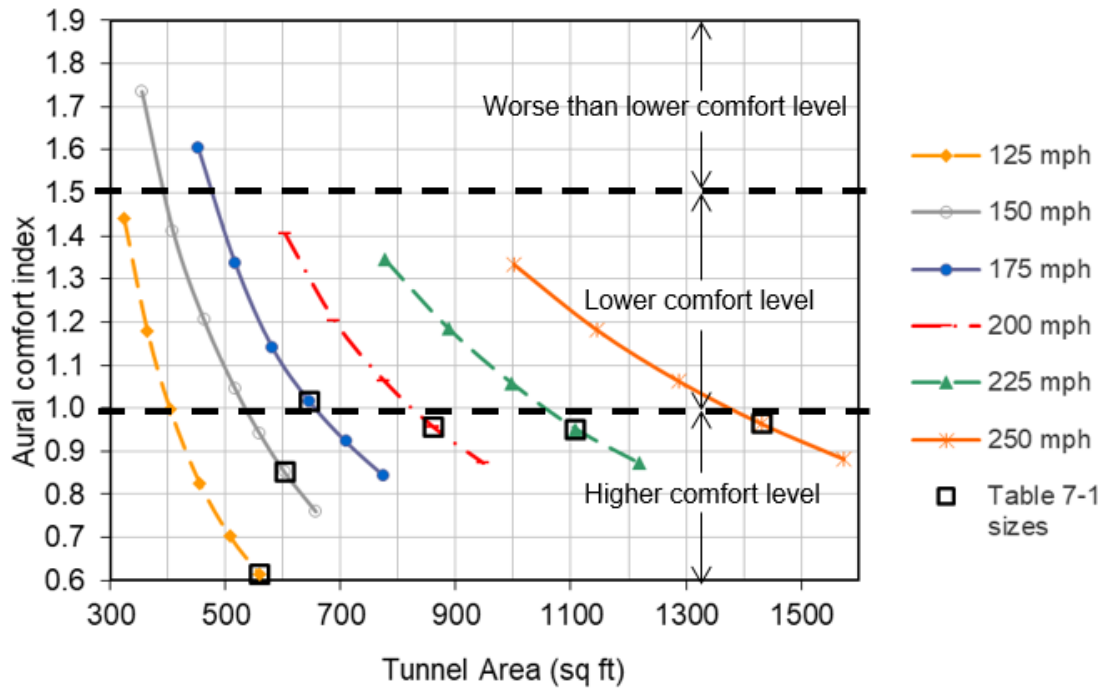


Figure 7-12. Influence of tunnel size on aural comfort performance, 18-second dynamic sealing time constant, single-track tunnel, U.S./Euro Baseline Train. For U.S./Asian Baseline Trains, scale the tunnel area (x-axis) by 12/11. Approximate guideline only

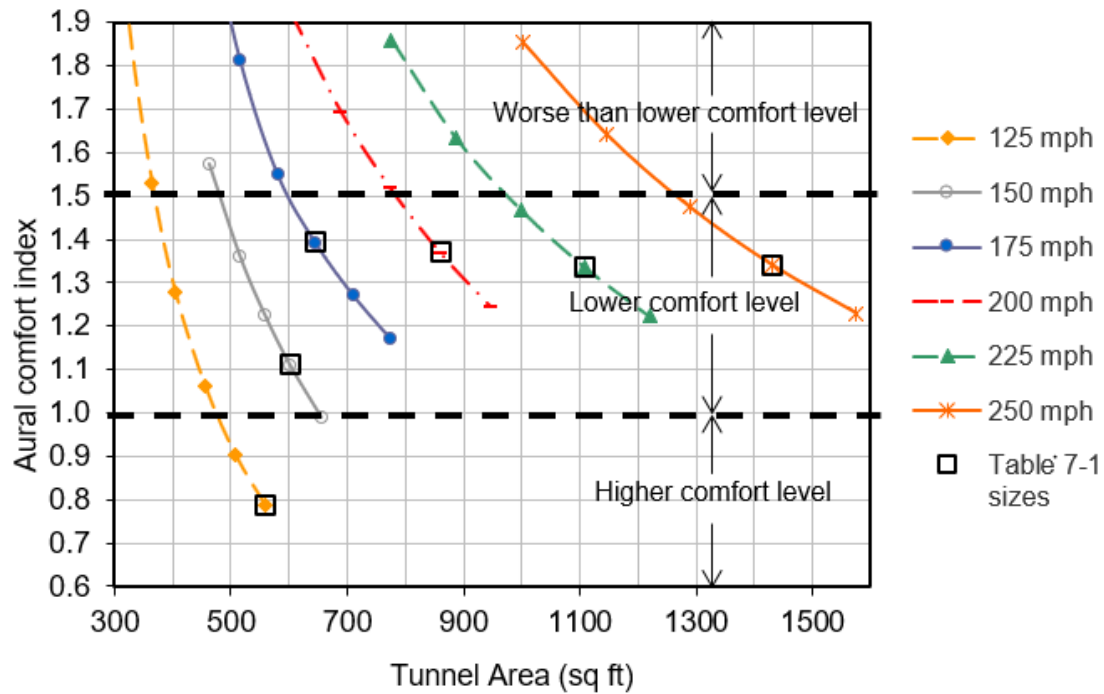


Figure 7-13. Influence of tunnel size on aural comfort, 10-second dynamic sealing time constant, single-track tunnel, U.S./Euro Baseline Train. For U.S./Asian Baseline Trains, scale the tunnel area (x-axis) by 12/11. Approximate guideline only

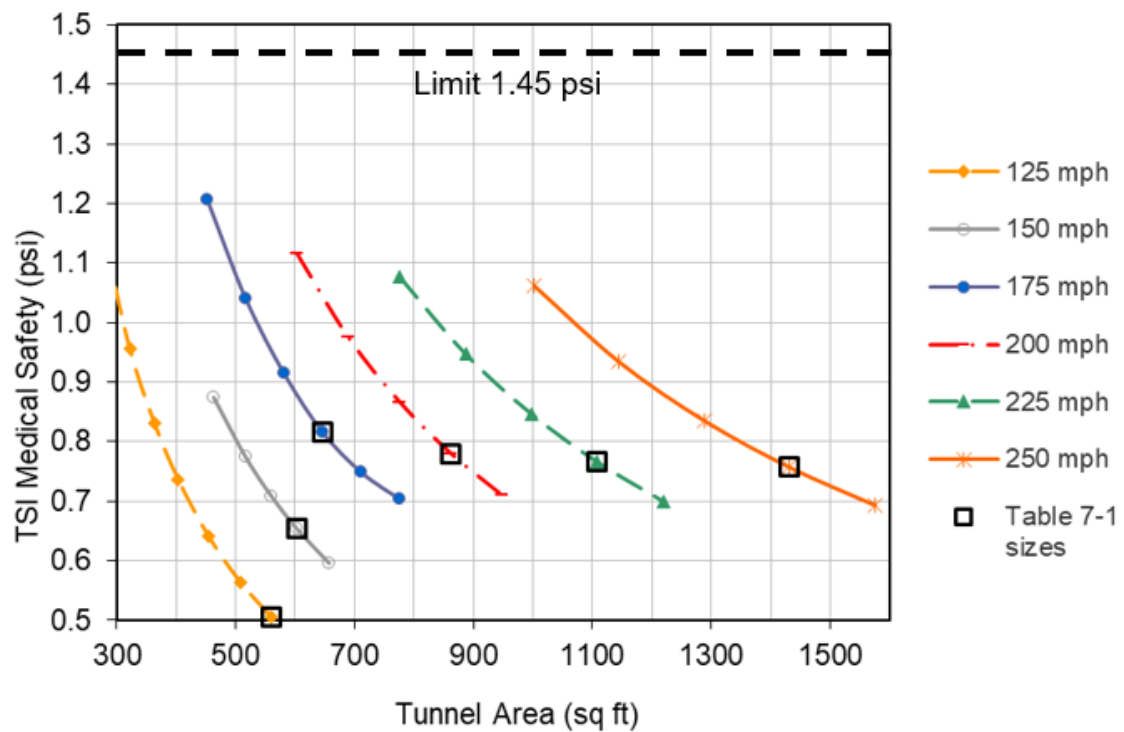


Figure 7-14. Influence of tunnel size on pressure changes compared to Medical Safety Limit, single-track tunnel, U.S./Euro Baseline Train. For U.S./Asian Baseline Trains, scale the tunnel area (x-axis) by 12/11. Approximate guideline only

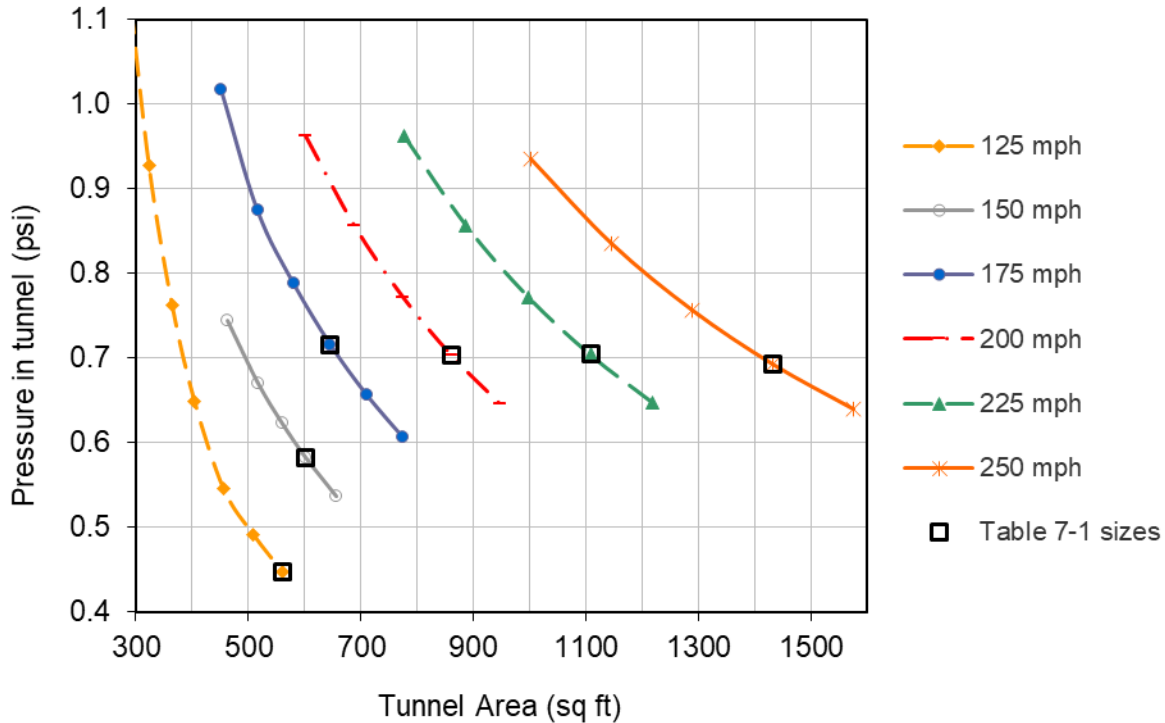


Figure 7-15. Influence of tunnel size on maximum pressure in tunnel, single-track tunnel, U.S./Euro Baseline Train. For U.S./Asian Baseline Trains, scale the tunnel area (x-axis) by 12/11. Approximate guideline only

With regard to the pressures in the tunnel (Figure 7-15), the data points show the maximum absolute value out of the most positive and the most negative pressures. The two pressures are often of very similar magnitude.

With regard to net pressures on the train (Figure 7-16), the data points show the maximum absolute value out of the most positive and the most negative net pressures, but the most negative net pressure (when internal pressure exceeds external pressure, i.e., the net pressure is acting to inflate the train) almost always exceeds the most positive net pressure. Some train manufacturers test to different limits for positive versus negative net pressure.

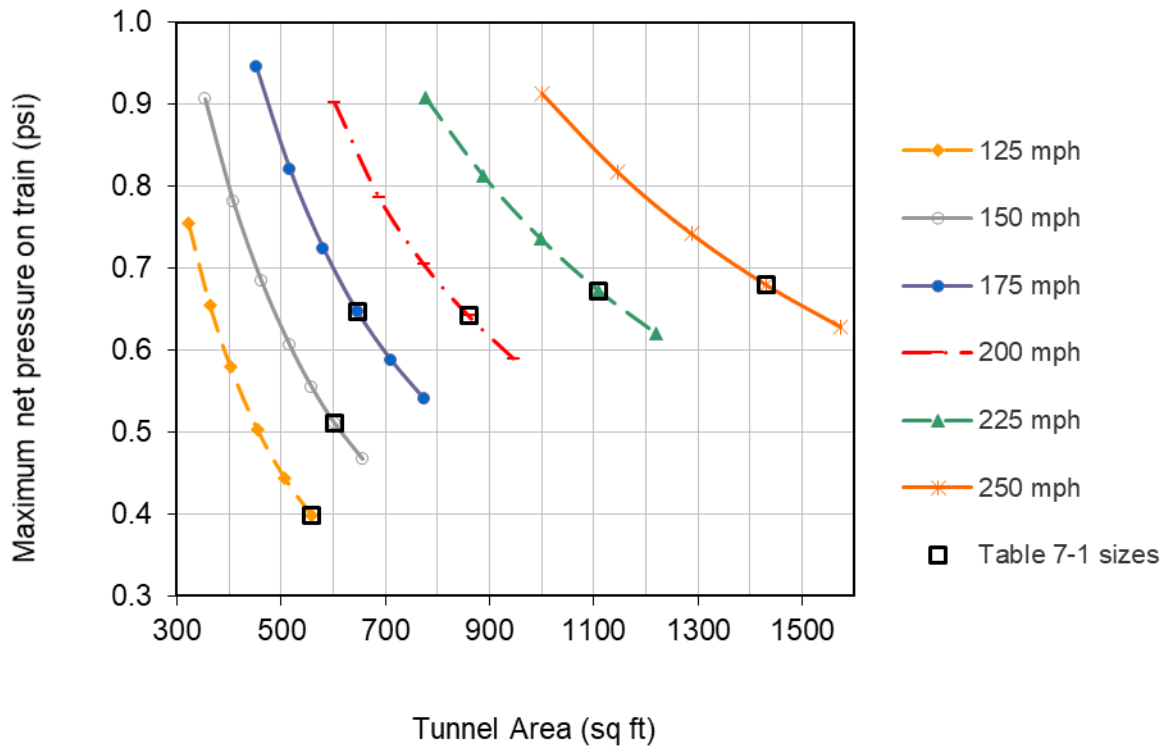


Figure 7-16. Influence of tunnel area on maximum net pressure on the train, single-track tunnel, U.S./Euro Baseline Train. For U.S./Asian Baseline Trains, scale the tunnel area (x-axis) by 12/11. Approximate guideline only

The graphs in the figures above are provided for single-track tunnels only. For double-track tunnels smaller than the Nominal Tunnel Sizes, case-by-case analysis is recommended, because of the risk that the Medical Safety Limit will be exceeded when trains pass or meet within the tunnel.

7.6.4.4 Influence of Tunnel Length on Tunnel Size

Aerodynamic performance depends on tunnel length and train length. The tunnel sizes in [Table 7-1](#) and [Table 7-2](#) are applicable across the range of tunnel lengths up to 5 miles and a range of train lengths up to the maximum stated in [Table 2-2](#), but are likely to be conservative for some combinations of tunnel length and train length.

Furthermore, some of the performance metrics, such as pressure on equipment in the tunnel or aural comfort of passengers, may be more critical than others to a given operator, and these measures have different dependencies on tunnel lengths.

Therefore, it is not possible to offer generic guidelines regarding tunnel size with respect to tunnel length – the size of particular tunnels should be optimized case-by-case using specialized software. However, for tunnels shorter than about twice the train length, all of the measures of interest are reduced, and therefore it is possible to reduce the size of these tunnels without exceeding the limits defined in [Table 7-3](#) to [Table 7-5](#) – see [Equation 7-3](#), which is an approximate description of the envelope of results obtained

from a large number of simulations with different tunnel lengths, train lengths, and train speeds.

$$A_{tun} = A_{baseline} \left(0.65 + 0.175 \frac{L_{tun}}{L_{train,min}} \right)$$

Equation 7-3

Subject to $A_{tun} \leq A_{baseline}$

Where:

A_{tun} = Cross-sectional area of the tunnel;

L_{tun} = Length of the tunnel;

$A_{baseline}$ = Nominal Tunnel Size from [Table 7-1](#) or [Table 7-2](#); and,

$L_{train,min}$ = Length of the shortest train that will use the tunnel.

This equation requires L_{tun} and $L_{train,min}$ to be in the same units as each other.

7.6.4.5 Influence of Train Cross-Sectional Area on Tunnel Size

Pressure wave effects depend strongly on **blockage ratio** (train area divided by tunnel area). If the trains have a smaller cross-sectional area than the values given in [Table 2-2](#), the tunnel area may be scaled down in proportion to train area according to [Equation 7-4](#) so as to keep the same blockage ratios envisaged in [Table 7-1](#) and [Table 7-2](#). This assumes that the smaller train has equivalent aerodynamic performance as the Baseline Trains and specifically that it passes the rolling stock acceptance test described in [Section 7.6.17](#) with a margin to spare.

$$A_{tun} = A_{baseline} \left(\frac{A_{train}}{A_{train,max}} \right)$$

Equation 7-4

Where:

A_{tun} = Cross-sectional area of the tunnel;

$A_{baseline}$ = Nominal Tunnel area from [Table 7-1](#) or [Table 7-2](#);

A_{train} = Actual cross-sectional area of the trains;

$A_{train,max}$ = Maximum cross-sectional area of trains given in [Table 2-2](#).

7.6.4.6 Other Considerations Related to the Nominal Tunnel Sizes

The Nominal Tunnel Sizes may be overly-conservative for tunnels with air shafts, depending on the spacing and size of the shafts and the length of the tunnel. No benefit from air shafts is assumed in the Nominal Tunnel Sizes, other than limiting the pressure wave effects in tunnels longer than 5 miles to be no worse than those in tunnels less than 5 miles long. In reality, air shafts can reduce the impact of pressure waves for tunnels of any length and thereby enable smaller tunnel sizes.

The aerodynamic design of tunnels is a complex task, and it is not possible to offer complete guidance in this report. There are many additional issues to be considered, such as those related to air shafts (see [Section 7.5.3](#)), micro-pressure waves and their

mitigation (Section 8), and drag on the train in tunnels (Section 9.3.5). Furthermore, the required size for any particular tunnel depends on the particular criteria that the operator wishes to achieve and the aerodynamic characteristics (particularly the dynamic sealing time constant) of the available trains. Therefore, users of this report should not rely exclusively on the information herein and should consult a specialist in HSR tunnel aerodynamics before committing to construction.

7.6.5 Analysis Using Specialized Software

Assessment can be carried out using specialized software to simulate the pressure wave effects when a particular train type runs through a particular tunnel at a given speed. The software models the air in the tunnel, which is divided into elements and analyzed in a time-stepping scheme. Pressures in the tunnel and inside the train are predicted by the software, enabling comparison against acceptability criteria. A typical model is shown in Figure 7-17. The figure shows a snapshot in time after the nose of the train has entered the tunnel, with pressure in the air in the tunnel indicated by color (pink being the highest pressure, blue the lowest). The image is stretched vertically so that the train can be seen clearly.

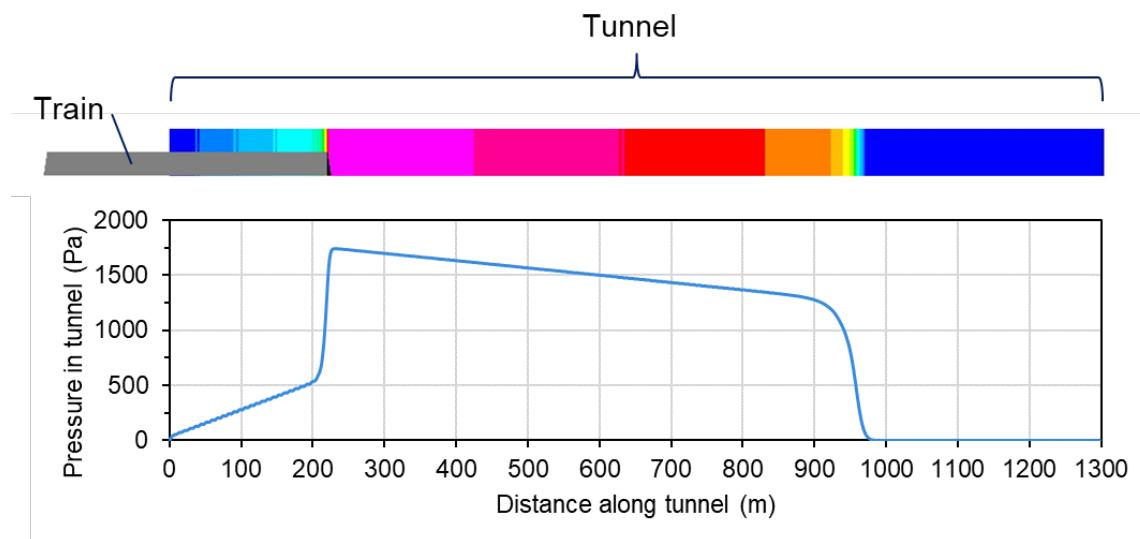


Figure 7-17. Snapshot of an analysis using specialized software. The train has entered the tunnel from the left. Colors indicate pressure in the tunnel. Vertical dimensions are exaggerated in the image

7.6.5.1 Choice of Software

The software is usually one-dimensional and should solve equations of compressible unsteady flow in order to generate the solution. **One-dimensional** means that conditions are assumed to vary only along the length of the tunnel, and not across the width or height, enabling faster solution times than three-dimensional software such as general-purpose CFD programs. **Compressible** means that the density of the air is not treated as constant (the volume occupied by a given mass of air reduces when the pressure increases). **Unsteady** means that the velocity of the air can change with time, i.e., it can accelerate, and the software does not assume steady flow. The

compressible and unsteady aspects of the software's solution scheme are essential for simulation of pressure waves. Software that simulates only incompressible flow, as might be used for ventilation or subway tunnel simulations, is not suitable for pressure wave simulations in HSR tunnels.

Software specialized for the analysis of pressure wave effects in HSR tunnels includes facilities to model the important characteristics of trains and tunnels together with air shafts and other features. Internationally, some operators and consultants use commercially-available software, such as ThermoTun [28], while others develop and maintain their own proprietary software. The authors recommend selecting software that has been validated against experimental data related to pressure waves in HSR tunnels.

Using this type of software requires experience and expertise. As with any complex analytical software, there is a strong risk of faulty inputs resulting in incorrect outputs. Where the results of the simulations will impact on the design of tunnels, the authors recommend specialists be engaged to carry out the analysis. As a minimum, users should model several validation cases themselves and vary the different inputs to understand their influence in order to become familiar with the software before using it to predict the performance of new tunnels.

7.6.5.2 Analyzing Single-Track and Double-Track Tunnels

The description in the following sections applies to both single-track and double-track tunnels: the analysis process is the same for both types, although there are some additional considerations for double-track tunnels, covered in Section 7.6.5.6. Scenarios involving more than one train might be analyzed, such as one train following another through a single-track tunnel, or two trains entering a double-track tunnel simultaneously; and in the latter case, the two trains could be running in opposite directions or in the same direction.

7.6.5.3 Input Data

Some software packages may require input to be provided in a given unit system – for example, SI units. In other cases, any consistent unit system (as defined in Section 2.7) might be permitted. Users should check this in the software documentation.

Input data requirements vary from software to software. Some inputs that might typically be required are shown in Table 7-7 through Table 7-11. Depending on the software, these inputs might have to be typed into a Graphical User Interface or written in a text file in a format defined in the software documentation.

Reference is made in the tables to friction coefficients on the tunnel walls and on the train. There are two different definitions in common use, called the Fanning friction coefficient (defined in Equation 7-5) and Darcy friction coefficient (defined in Equation 7-6). The Darcy coefficient is four times bigger than the Fanning coefficient for the same level of friction.

$$f = \frac{S}{\frac{1}{2}\rho U^2} \quad \text{Equation 7-5}$$

$$\lambda = \frac{4S}{\frac{1}{2}\rho U^2} \quad \text{Equation 7-6}$$

Where:

f = Fanning friction coefficient;

λ = Darcy friction coefficient;

S = Shear stress on the surface, e.g., wall of tunnel, caused by friction from the passing air;

ρ = Density of the air; and,

U = Speed of the air relative to the surface.

These equations require consistent units, see Section [2.7](#).

Table 7-7. Typical input data required by specialized software that predicts pressure wave effects in HSR tunnels – Tunnel data

	Input item	Notes
Tunnel	Length	Input the length of the tunnel.
	Area	Input the cross-sectional area as indicated in Figure 7-5 , or use Nominal Tunnel Size from Section 7.6.4 .
	Perimeter	Used by the software to calculate the surface area of wall for evaluation of friction forces
	Friction coefficient on tunnel walls	Friction on the tunnel walls resists flow of air along the tunnel. Typical Fanning friction coefficients are in the range 0.004 to 0.012. If the software requires Darcy friction coefficients, multiply these values by 4. See friction coefficient definitions provided in Equation 7-4 and Equation 7-5 .
	Loss coefficients at portals	These non-dimensional constants are used by the program to calculate pressure drops when air enters or leaves the tunnel. Usually they have only a minor influence on results. Specialized software may have built-in default values or recommended values given in the documentation. Failing that, users might adopt values typically used in analysis of flow in air ducts or pipes.
	Complex tunnel features	Specialized software can usually model complex tunnel features such as air shafts, cross passages, etc. Input data would typically include the cross-sectional area and length of these features together with any resistances along the air path such as dampers or narrow constrictions through which the air must pass.

Table 7-8. Typical input data required by specialized software that predicts pressure wave effects in HSR tunnels – Train data

	Input item	Notes
Train	Length	Input the length of the train or use Baseline Train data given in Section 2.3.2.
	Area	Input the cross-sectional area, calculated as indicated in Figure 7-5, or use Baseline Train data given in Section 2.3.2.
	Area profile along length of train	Enables definition of tapered nose and tail shapes, locomotive being larger than trailing railcars, etc.
	Perimeter	Perimeter times length gives the surface area of the train for evaluation of friction forces.
	Friction coefficient on train	Friction on the train creates drag and contributes to pressure wave amplitude. Typical Fanning friction coefficients are in the range 0.0025 to 0.005 for streamlined HSTs. If the software requires Darcy friction coefficients, multiply these values by 4 (see friction coefficient definitions provided in Equation 7-4 and Equation 7-5).
	Nose and tail loss factors	Used by the software to calculate pressure drops as air flows over the nose and tail of the train. Lower values indicate better streamlining. Typical values for HSTs in the range 0 to 0.1. Definitions of loss factors may vary from software to software and hence, the typical values may vary. See software documentation for details.
	Dynamic sealing time constant	See definition of sealing time constant in Section 7.3.7. Use dynamic sealing time constant values from train manufacturer, or Baseline Train data given in Section 2.3.2. If the software can model only the pressure in the air outside the train, then the pressure inside the train should be calculated afterwards – for instance, in a spreadsheet using the equations given in Section 7.3.7.
	Train speed	A constant train speed will usually be specified. This might be the planned operating speed or a design speed slightly faster than the intended operating speed to introduce some conservatism. Some software is able to model situations where train speed changes with time.

Table 7-9. Typical input data required by specialized software that predicts pressure wave effects in HSR tunnels – Output data

	Input item	Notes
Output requests	Output points in the tunnel	Positions along the tunnel where pressure time-history should be recorded.
	Output points on the train	Positions along the train where pressure time-history should be recorded. At least three points should be requested; these should be at the front, middle, and rear of the train, but not within any tapering nose or tail regions (see Figure 7-18).

Table 7-10. Typical input data required by specialized software that predicts pressure wave effects in HSR tunnels – Atmospheric data

	Input item	Notes
Atmospheric conditions	Pressure	See Section 7.6.5.4 . Depending on the software, two or three of these need to be provided, with the remainder being calculated automatically by the software.
	Temperature	
	Air density	
	Speed of sound	
	Initial air velocity in the tunnel	Usually taken as zero. See Section 7.6.5.4 .

Table 7-11. Typical input data required by specialized software that predicts pressure wave effects in HSR tunnels – Solution scheme variables

	Input item	Notes
Solution scheme variables	Mesh size, timestep, etc.	The user may be asked to select values for mesh size, timestep, and other parameters that influence the accuracy of the analysis. In general, smaller mesh size and smaller timestep will provide greater accuracy but increase computation times. Users should determine suitable values by a sensitivity study, bearing in mind that the optimum values may vary according to the purpose of the calculation.

A typical train model with output points is illustrated diagrammatically in [Figure 7-18](#). The figure shows three output points for simplicity, but the authors recommend defining a greater number of points, such as one point every 100 ft (30 m) – otherwise, the most severe pressure changes, which could occur at any point along the length of the train, might be missed.

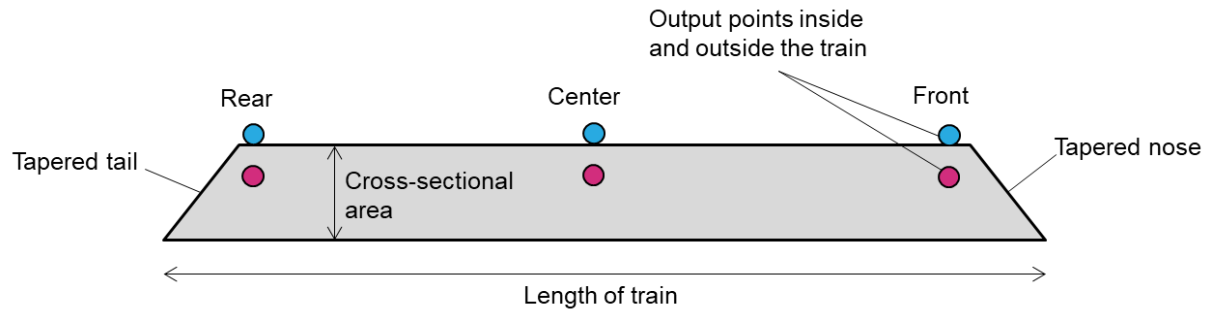


Figure 7-18. Diagrammatic representation of train model used in specialized one-dimensional analysis software

7.6.5.4 Atmospheric Conditions

Atmospheric conditions can have a significant influence on pressure wave phenomena. Pressure wave amplitudes are higher when the air is denser – for example, in cold weather and when atmospheric pressure is high. It is common practice to perform assessments under **standard atmospheric conditions**, defined in [Table 7-12](#). However, if the conditions for the tunnel location are known, it is preferable to use those instead: either annual-average values or worst-case values (high pressure, low temperature) for the tunnel location might be selected depending on the aims of the analysis.

Table 7-12. Standard atmospheric conditions for aerodynamic assessments

Quantity	Value in SI units (for use in assessments)	Approximate value in English units (for reference only)
Atmospheric pressure	101325 Pa	14.7 psi
Temperature	288.15 K = 15 °C	59 °F
Density ¹	1.225 kg/m ³	0.0765 lb/ft ³
Speed of sound ¹	340 m/s	1115 ft/s = 761 mph
Notes:		
1. Density and speed of sound quoted for dry air. These properties vary slightly with humidity.		

The authors recommend including variations of these conditions in a sensitivity study, considering the range of temperatures and atmospheric pressures expected to occur at the tunnel location. Formulae linking the temperature and pressure to density and speed of sound are given in [Equation 7-7](#) and [Equation 7-8](#).

$$c = \sqrt{\gamma R' T}$$

Equation 7-7

$$\rho = P_{atm} / R' T$$

Equation 7-8

Where:

c = Speed of sound in m/s;

γ = 1.4 (adiabatic constant);

R' = 287.05 J/(kgK) (specific gas constant for dry air);

T = Air temperature in Kelvin = Temperature in Centigrade + 273.15;

P_{atm} = Atmospheric pressure in N/m²; and,

ρ = Air density in kg/m³.

Density and speed of sound as calculated by these equations are for dry air. These properties vary slightly with humidity.

SI units should be used in these equations.

The initial airflow speed in the tunnel before arrival of the train is usually taken as zero, but can be included in the analysis for the following reasons:

- If trying to match experimental data (the initial airflow speed should be measured in the experiment)
- If analyzing the effect of multiple trains passing through the tunnel in sequence (the residual airflow caused by one train influences the pressure wave caused by the next train)
- As a sensitivity study to determine the influence of airflow in the tunnel caused by environmental factors

7.6.5.5 Output Data

When the software runs the simulation, it will generate output consisting of pressure time-histories at the requested points in the tunnel and train, such as those shown in [Figure 7-2](#). Depending on the software, it may also output pressure time-histories inside a sealed train, such as that shown in [Figure 7-8](#). The manner in which these pressure time histories are assessed against aural comfort criteria is explained in [Section 7.6.15](#). In some cases, this task may be done automatically by the software.

Some software is capable of outputting other results, such as the air velocity in the tunnel, the resistance force on the train, or the power required to maintain the requested speed.

7.6.5.6 Additional Considerations for Analyzing Double-Track Tunnels

In double-track tunnels, two or more trains may be in the tunnel simultaneously. Each train causes pressure waves. The pressure waves and their impacts will be different in each of the following three example scenarios (these examples assume that the trains

on the two tracks are traveling in opposite directions, but the same principles apply when the trains travel in the same direction):

- A single train passes through the tunnel with no trains present on the other track.
- A train enters the tunnel at one end, and at the exact same moment another train enters at the opposite end.
- A train enters the tunnel at one end, and X seconds later another train enters at the opposite end. Hereafter, this will be referred to as a **relative entry time** of +X seconds.

It will be apparent that there are infinite scenarios similar to the third example above, each with a different value of X (relative entry time) and each scenario will produce a different result. The relative entry time that causes the greatest pressure wave impacts cannot be assessed by inspection, varies from case to case, and depends on what is being measured. It is necessary to model many scenarios with different relative entry times to find the worst case. However, the task is made easier by the fact that the worst case usually occurs somewhere within a predictable range of relative entry times which is related to the time it takes for a pressure wave to propagate the full length of the tunnel, given in [Equation 7-9](#).

$$-4L/c \leq \Delta t_{rel,pmax} \leq 4L/c \quad \text{Equation 7-9}$$

Where:

L = Tunnel length;

c = Speed of sound; and,

$\Delta t_{rel,pmax}$ = Relative entry time causing greatest pressure wave impacts.

This equation requires consistent units, see [Section 2.7](#).

If the tunnel is symmetrical lengthways (with respect to air shafts, cross passages, tunnel cross-sectional area profile, etc.) and the two trains are identical and traveling at the same speed, there is no need to explore both positive and negative relative entry times.

A typical analysis outcome is shown in [Figure 7-19](#). Each point on the graph corresponds to the result from one analysis at a particular relative entry time. The x-axis, **non-dimensional relative entry time**, is defined as the relative entry time divided by the time it takes for a pressure wave to propagate the full length of the tunnel, as shown in [Equation 7-10](#).

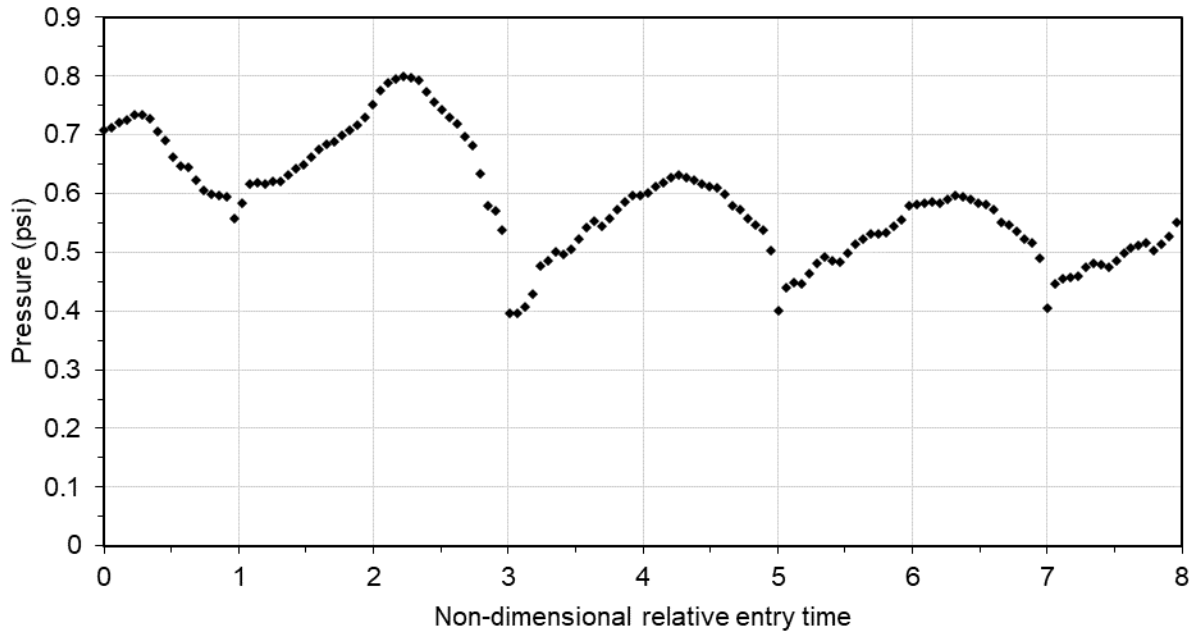


Figure 7-19. Example analysis results for a two-train scenario. Maximum pressure in the tunnel for multiple analyses at different relative entry times

$$\Delta t_{rel,ND} = \Delta t_{rel} / (L/c) \quad \text{Equation 7-10}$$

Where:

$\Delta t_{rel,ND}$ = Non-dimensional relative entry time;

Δt_{rel} = Relative entry time in seconds;

L = Tunnel length; and,

c = Speed of sound.

This equation requires consistent units, see Section 2.7.

It may be observed in Figure 7-19 that the results form a series of peaks at intervals of 2.0 along the x-axis, which corresponds to the time taken for a pressure wave to propagate the full length of the tunnel and back again. The highest peak is usually the first or second one. Equation 7-9 suggests that the maximum should occur at a non-dimensional relative entry time less than or equal to four, which is indeed the case. The example in Figure 7-19 shows maximum pressure in the tunnel; the same principle applies to other results such as pressure changes inside the railcar.

7.6.5.7 Analyzing Tunnels Consisting of Twin Tubes Linked by Cross-Passages

If air can pass from one tube of a tunnel to the other via cross-passages, then trains in one tube influence the pressures in the other tube. Different results will occur for

different relative entry times of trains in the two tubes. Considerations similar to those described above for double-track tunnels apply.

7.6.6 Wave Diagrams

Wave diagrams track the movement of trains and pressure waves through time and can be useful for understanding the outputs of specialized software. The diagrams are made by hand or in spreadsheet software. An example is given in the lower part of [Figure 7-20](#). The y-axis is distance along the tunnel. The entrance and exit of the tunnel are shown at the top and bottom of the diagram, respectively. The blue and red continuous lines indicate the progress of the nose and tail of the train through the tunnel, and the slopes of the lines are equal to train speed in feet per second. The dashed lines show the motion of the pressure waves caused by entry of the nose and tail, and the reflections of those waves; the slope of all the dashed lines is equal to the speed of sound. As an example of how the diagrams may be interpreted, in [Figure 7-20](#) the pressure drop that occurs shortly after 5 seconds (in the rectangle in the upper graph) is caused by the tail-entry wave passing the measurement point (circled in the wave diagram).

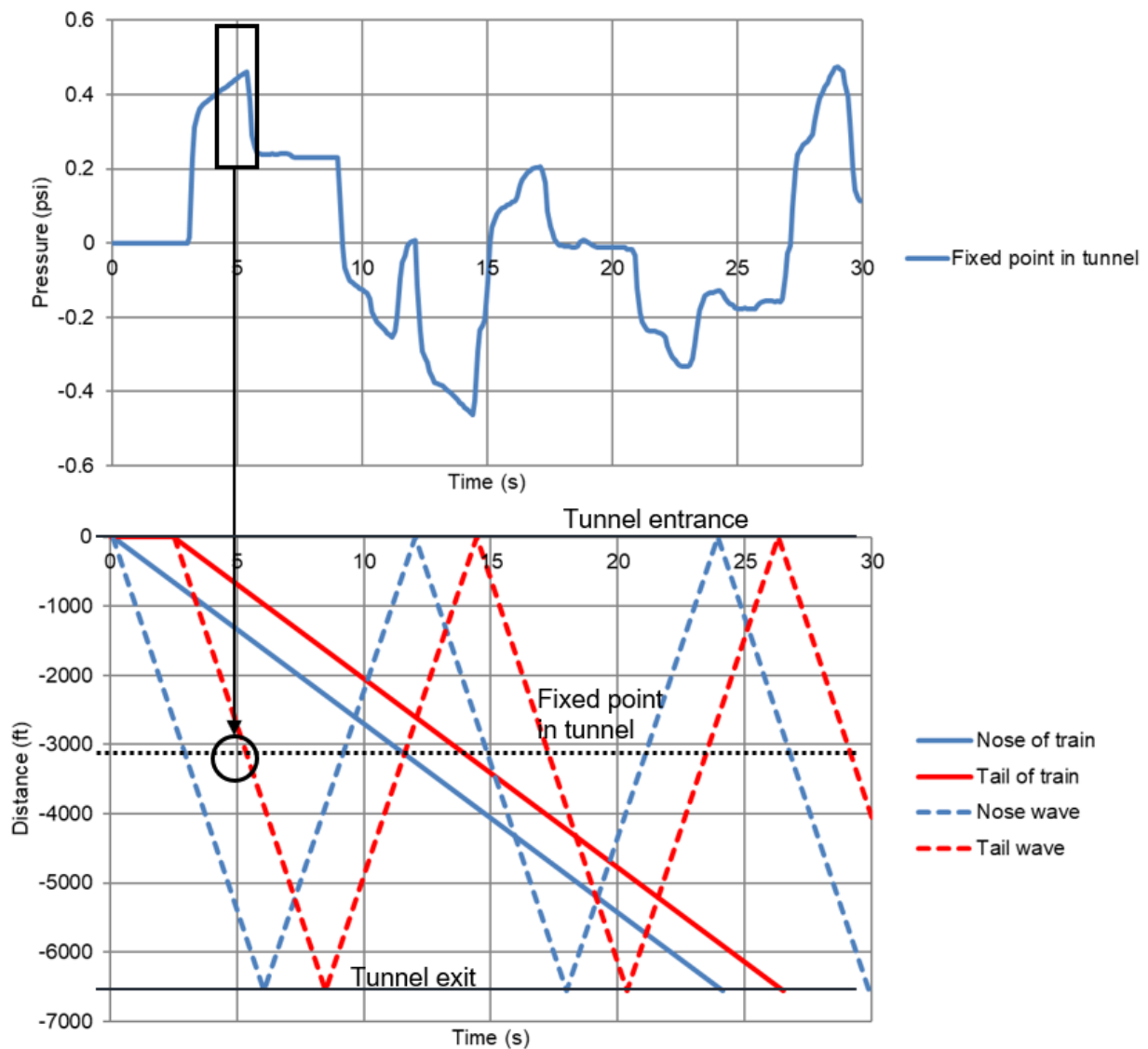


Figure 7-20. An example of a pressure wave diagram (below) used to understand a pressure time-history from one-dimensional software (above)

For simplicity, the wave diagram in [Figure 7-20](#) omits the additional pressure waves created when an existing pressure wave meets the nose or tail of the train. When this occurs, part of the wave is transmitted – it continues propagating in the same direction – and part is reflected. The reflected waves are omitted from the wave diagram in [Figure 7-20](#).

7.6.7 Assessment by 3D CFD Analysis

Three-dimensional (3D) CFD is not commonly used to analyse pressure wave effects since the governing phenomena are essentially one-dimensional. Three-dimensional CFD analysis requires much greater time and effort than specialized one-dimensional

software modelling. Use of 3D CFD for tunnel applications is confined to issues where 3D effects are significant, for example:

- Use by train manufacturers to assess new train designs against acceptance criteria for the tunnel entry pressure wave in the European TSI for HSR rolling stock [39].
- Use by train manufacturers to assess railcar design features to reduce aerodynamic drag in tunnels.
- Assessment of airflow around fixed equipment in tunnels leading to more refined estimates of pressure loading for a given airflow speed.
- Assessment of nose and tail pressure pulse effects and/or slipstream airflow effects in tunnels, leading to more refined estimates of pressure loading on fixed equipment when the train passes by.
- Assessment of trains meeting in tunnels – for example, to estimate pressure loading on conventional trains sharing tunnels with HSR.
- Assessment of any turbulence effects or asymmetrical loading on a train in a tunnel due to proximity to the tunnel wall on one side of the train [27].
- Assessment of pressure wave effects occurring when the train passes irregular tunnel geometry such as changes of cross-sectional area or air shafts.
- Assessment of tunnel entrances designed to mitigate micro-pressure waves; see Section 8.6.2.5.

7.6.8 Assessment by Reduced-Scale Testing

Reduced-scale testing may be used to provide experimental data against which computer simulations can be calibrated and/or as an alternative to CFD analysis to assess situations where 3D effects may be important. Examples of such situations are listed in Section 7.6.7 above. Reduced-scale testing is not generally used as a substitute for one-dimensional analysis because, once validated, the latter is quicker and easier, and the laboratory may not be large enough to accommodate scale models of full-length tunnels.

The trains and tunnels are modelled with their geometry scaled down (for example, 1/25 scale), but the speed of the model train should be the same as the real-life speed, e.g., if the real-life speed is 150 mph then the scale model train runs at 150 mph, not at a scaled-down speed. The measured pressures are then equal to the pressures expected at full-scale. If it is not possible to run the scale model trains at the actual operating speed of the full-size trains, then computer simulation may be used to transfer results to full-scale:

1. A reduced-scale model test is conducted at a lower speed than the real-life speed. The test speed should be as close to the real-life speed as can be achieved by the test facility.
2. A computer simulation of the reduced-scale test is conducted, using the same low speed and with the reduced-scale dimensions for the train and tunnel.

3. Results from the reduced-scaled model experiment are used to calibrate the computer model.
4. The calibrated computer model is then used to simulate a case with the actual operational speed and full-scale dimensions.

7.6.9 Assessment by Full-Scale Testing

Full-scale testing is more difficult and expensive than reduced-scale testing or computer simulation, but it can provide the most reliable data. It might be used in the following circumstances:

- To provide data on phenomena that are difficult to estimate in advance or which depend on small details of the tunnel design – for example, the “damping” of pressure waves during propagation described in [Section 8](#)
- To verify or validate conclusions from reduced-scale testing or computer simulations
- To confirm successful mitigation of anticipated aerodynamic impacts
- To verify conformance with acceptance test requirements
- Existing full-scale test data in publications can be used to validate computer simulation methodologies.

7.6.10 Assessment Considerations for Cross-Passages Linking the Tubes of Single-Track Tunnels

If cross-passages are kept open during normal operations, or if there is significant leakage through the passage doors, air movement from one tube to another may help mitigate pressure wave effects in some scenarios (for example, a train in one bore only), but may present the worst case in other scenarios (for example, when trains enter both tubes simultaneously). The cross-passages should be included in the computer model of the tunnel used to analyze pressure wave effects, and different train scenarios (e.g., trains entering the two bores at different times relative to each other) should be simulated.

If the passages are completely closed during normal operation, which may be required for fire safety reasons, then there will be no air movement from tube to tube, but the doors should be designed to tolerate the net pressure loading arising from pressure wave effects.

7.6.11 Considerations for Assessing Fatigue Loading on Trains

Specialized software can predict the pressure time-histories outside and inside an HST. The difference between these pressures represents the net pressure on the outer carbody. An example net pressure time-history is shown in [Figure 7-21](#). External and internal pressure are measured at the same point along the length of the train – in this case, at the rear. Positive net pressure means that the railcar is being compressed, while negative net pressure means that it is being inflated. In the example shown, the most positive net pressure at this particular point along the train during this passage

through the tunnel is 0.36 psi, the most negative net pressure is -0.46 psi, and the maximum peak-to-peak pressure cycle amplitude is therefore 0.82 psi. The pressures vary along the length of the train. This type of assessment should be performed at multiple points along the length of the train, and for multiple train/tunnel scenarios, to find the worst-case net pressure.

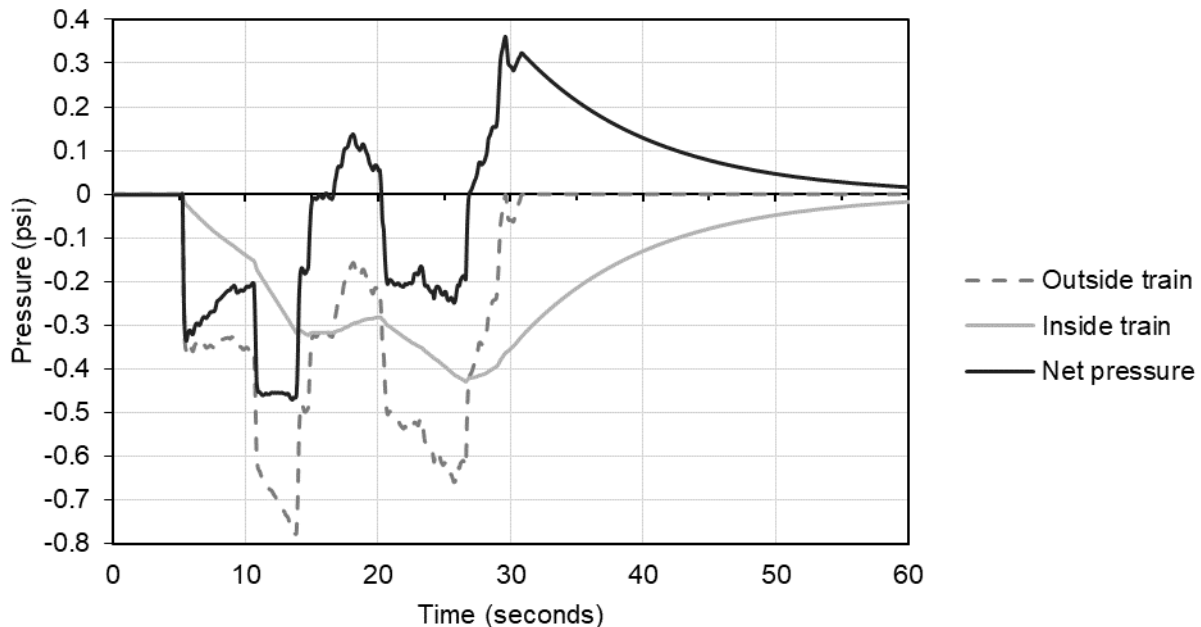


Figure 7-21. Net pressure on a railcar is the difference between external and internal pressure

The net pressure depends on the sealing performance of the train (better sealing usually corresponding to greater net pressure). The dynamic sealing time-constant of the trains may not be known exactly. When performing assessments, taking a high value of the sealing time-constant is usually conservative with respect to fatigue loading on the railcars, whereas taking a low value is always conservative with respect to aural comfort. When assessing fatigue loading, it is recommended to run the simulations multiple times with a range of values for the dynamic sealing time-constant as part of a sensitivity study. The worst case for fatigue is often, but not always, associated with the highest value of sealing time-constant. Stresses in the car body associated with the greatest positive pressure, and with the greatest negative pressure, may need to be checked also. The worst cases for these can sometimes occur with intermediate values of sealing time-constant.

The impact of fatigue loading on railcars depends not only on the maximum net pressures, but also on the number of loading cycles. In the general case it may be necessary to consider all the different tunnel passages expected during the design life of the train (tunnel lengths, train speeds, etc.), and to total up the number of net pressure loading cycles of different amplitudes.

7.6.12 Considerations for Assessing Tunnels Shared by HSTs and Conventional Traffic

Where tunnels are shared by HSTs and conventional traffic, the same methods of analysis by specialized software can be used to assess aural comfort and safety of passengers and crew in the conventional trains as described in this report for HSTs. Conventional railcars may be unsealed, in which case the dynamic sealing time-constant should be set to a low value such as 0.1 second. Different, less stringent criteria for aural comfort may be applied for unsealed railcars, as described in Section 7.4.5, because it is impractical to meet the same high standards of comfort as for well-sealed railcars.

It is difficult to use analysis to assess the possibility of damage to conventional trains and their cargos caused by aerodynamic effects from HSTs (or other conventional trains) passing through tunnels because of a lack of acceptability criteria. Damage could be caused by pressure wave effects or by airflow from trains in tunnels. Each type of railcar and cargo is likely to have a different capacity to tolerate these effects. In practice, where tunnels are shared, the most reliable method may be full-scale testing with the railcar types concerned. It may be necessary to arrive at a suitable speed limit by trial and error, starting with a relatively low speed and monitoring any damage occurring during regular operations. If no damage is observed, the speed limit may be increased. Aerodynamic impacts on trains may include deterioration that occurs gradually over time, such as fatigue damage. It may be desirable to continue operation at the initial lower speed for a long period so that any such damage can be observed.

7.6.13 Considerations for Assessing Aerodynamic Loading on Fixed Equipment in the Tunnel

Aerodynamic loading on fixed equipment in tunnels (doors, cabinets, signs, etc.) arises from three sources:

- Pressures caused by pressure waves.
- Nose and tail pressure pulse
- Airflow along the tunnel caused by pressure waves and train slipstreams.

All these loads should be treated as fatigue loads, considering the number of loading cycles expected within the design life of the equipment. Fatigue loads are generally assessed under expected or average conditions. In addition, ultimate loads may be calculated assuming worst-case atmospheric conditions and train properties.

The three sources of loading and the relevant assessment methods are described in the following sections.

7.6.13.1 Loading on Fixed Equipment from Pressure Waves

Pressure waves form the primary source of aerodynamic loading on fixed equipment in tunnels. The pressure on the equipment changes when pressure waves pass over the equipment and persists until the next pressure wave passes. The pressure should be assumed to fill the tunnel with a uniform spatial distribution, fully immersing any equipment within the tunnel, as shown in Figure 7-22.

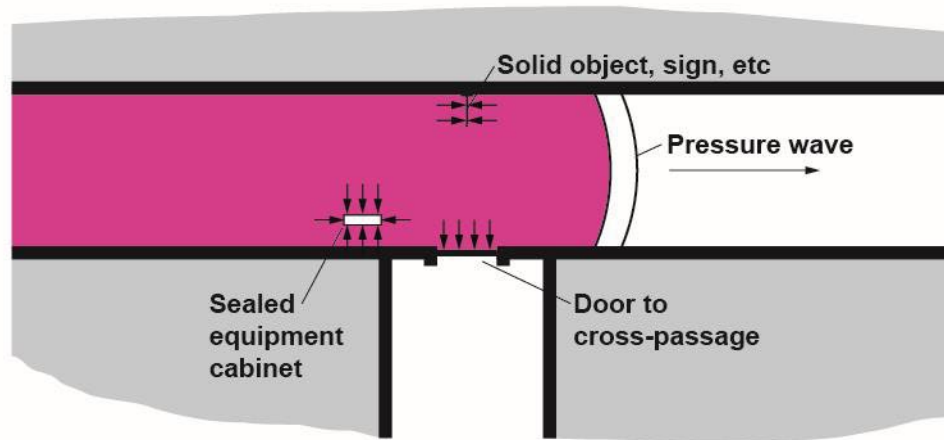


Figure 7-22. Pressure loading from pressure waves (loading shown by black arrows)

The discussion in this section also applies to loading on fixed equipment arising from the low pressure (suction) in the annulus around the train. Although not directly caused by pressure waves, the type of impact on fixed equipment in the tunnel and the assessment methods are the same as for pressure waves. The equipment will be exposed to the suction in the annulus for the time it takes the train to pass by, and this can be the strongest suction applied to the equipment during the whole passage of the train through the tunnel.

The influence of the pressure depends on which surfaces of the equipment are exposed to it, as described below:

- A sealed cabinet experiences the pressure on all its external surfaces, while the air pressure inside the cabinet may be assumed to remain unchanged. Therefore, the calculated pressure of the air in the tunnel should be treated as a load on all the external surfaces of the cabinet.
- A solid object such as a sign made of sheet metal experiences the same pressure on both sides (it is immersed in the pressurized air); therefore, there is no net pressure loading from pressure wave effects.
- For a door between tubes of a single-track tunnel, or between a tunnel and a cross-passage, the air on each side of the door may be subjected to different pressures simultaneously. The assessment should consider the net pressure loading, i.e., the pressure difference across the door, as shown in the examples in [Figure 7-23](#). The pressure in a cross-passage (lower image in [Figure 7-23](#)) will depend on the leakage rate through the doors.

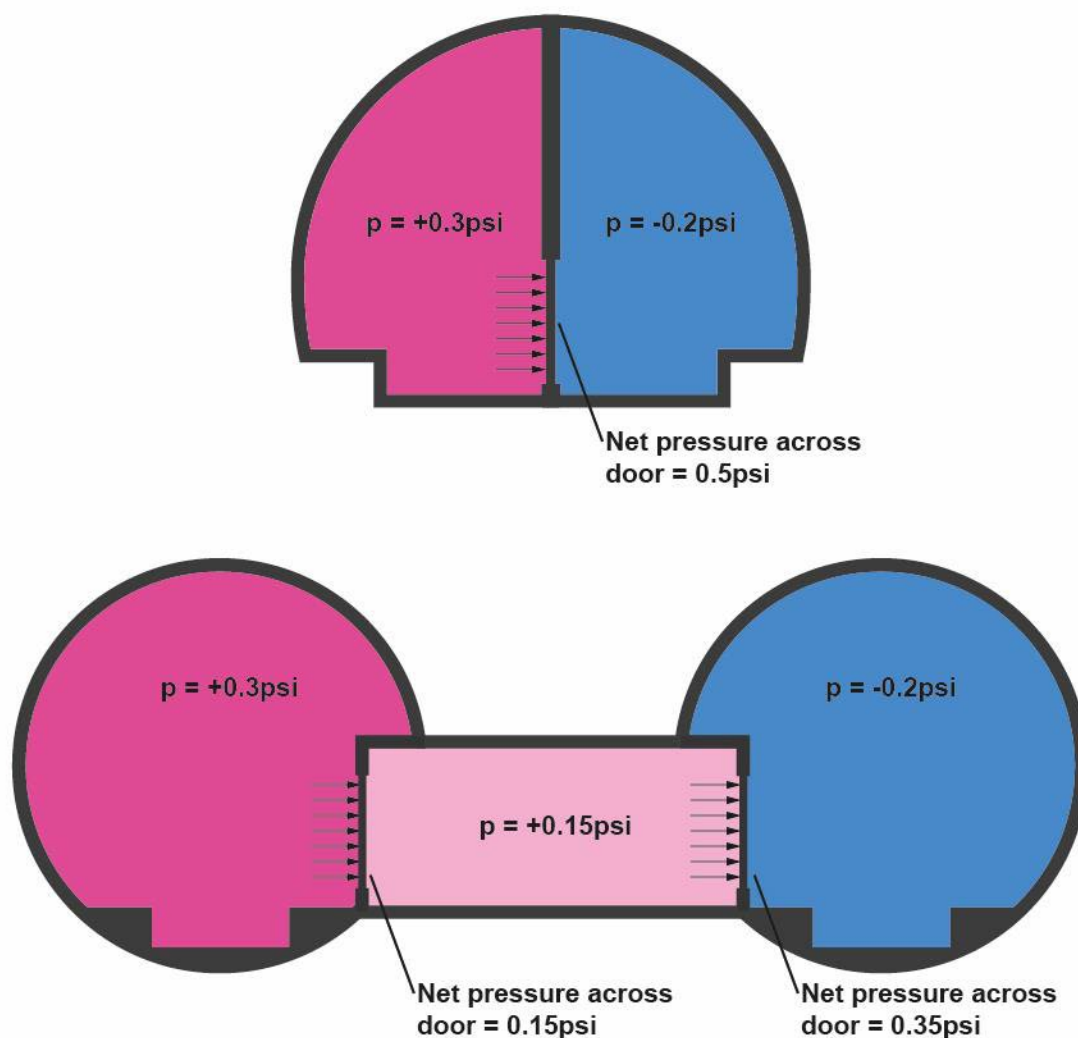


Figure 7-23. Examples of net pressure across doors at a snapshot in time

The pressures caused by pressure waves may be assessed using specialized one-dimensional software, as described in Section 7.6.5. The software should output the pressure time-history at the point along the tunnel where the equipment is located. The negative pressure that occurs while the train passes the equipment will be included in the analysis results automatically – there is no need to perform additional assessment steps to capture this effect. It may be necessary to analyze multiple different train scenarios – for example, different train speeds, types or lengths, and different combinations of trains on each track or in each bore.

The loading from pressure waves should be treated as fatigue loading. Every load cycle uses up some of the fatigue life. In order to design the equipment to tolerate the fatigue loading, the equipment supplier may want to know the number of load cycles of each different amplitude expected during the design life of the equipment (not only the largest pressure cycle). Each train passing scenario may result in multiple pressure load cycles of different amplitudes. Therefore, all the different scenarios resulting in

pressure waves should be considered along with the number of times each scenario is expected to occur during the design life of the equipment.

For the purpose of designing equipment against fatigue loading, the definition of **pressure load cycle amplitude** typically means the pressure difference between a positive pressure peak and a negative pressure peak, without considering whether the two peaks occur one immediately after the other. The biggest pressure load cycle experienced by the equipment is the difference between the greatest positive peak pressure experienced at any time during the life of the equipment, and the greatest negative peak pressure experienced at any time during the life of the equipment. The negative peak could occur hours or days or years after (or before) the positive peak, and yet it would still be considered as part of the same load cycle – see example in [Figure 7-24](#). Techniques such as Rainflow Counting are used to identify all the pressure loading cycles and their amplitudes from pressure load time histories. These methods are not specific to aerodynamics. Their application is a part of rolling stock mechanical design process and is outside the scope of this report.

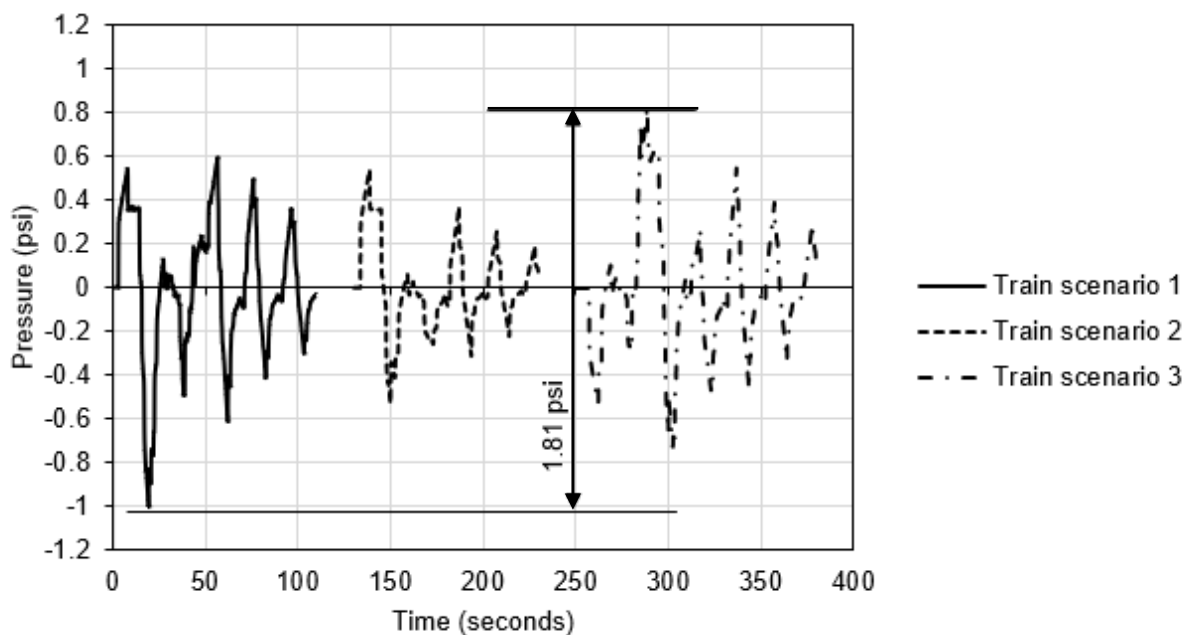


Figure 7-24. Example of maximum pressure load cycle amplitude from multiple train-passing scenarios: Net pressure on a door between bores of a tunnel. Maximum peak-to-peak pressure cycle amplitude is 1.81 psi in this example

7.6.13.2 Loading on Fixed Equipment from Nose and Tail Pressure Pulse

At the nose and tail of the train, high (positive) and low (negative) pressure zones exist that are similar in principle to those described for the open-air case in [Section 4](#), as illustrated in [Figure 7-25](#). These are additional to the pressures described in [Section 7.6.13.1](#). The pressure applied to any object depends on its distance from the track and may be assessed using the same methods as described in [Section 4](#). The loading may be amplified due to the confined situation of the tunnel. In the absence of any well-established guidelines for this, the calculated pressures should be increased by a factor

of two to account for the confinement effect, as per the recommendation for vertical surfaces of enclosed structures in Section 4.6.2.5. Because the pressure pulses are local to the nose and tail of the train, they pass very quickly, and the loading is therefore of very short duration, typically of the order of 0.1 to 0.2 second. Assessments should recognize the possibility of dynamic amplification if the equipment being assessed has resonances at natural frequencies that may be excited by loading of this duration.

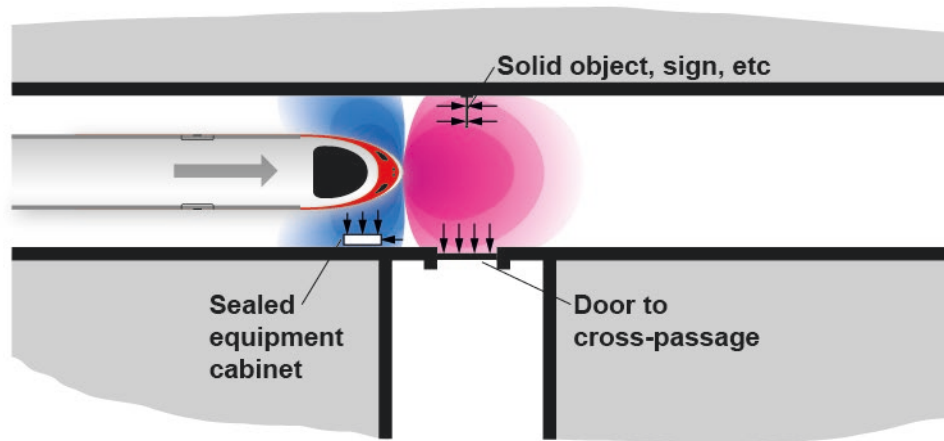


Figure 7-25. The nose and tail pressure pulses apply net pressure to doors and equipment that is sealed and contains air

7.6.13.3 Loading on Fixed Equipment from Airflow in the Tunnel

Airflow in the tunnel arises in two ways, which add together: relatively low speed flows associated with pressure waves, plus stronger localized slipstream gusts as the train passes by. Any equipment (such as signs) offering a surface that impedes this airflow will experience pressure loadings, as shown in Figure 7-26.

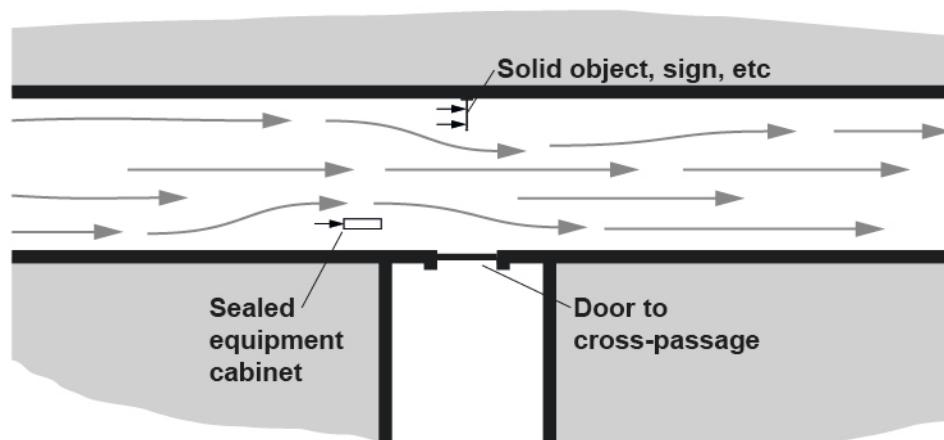


Figure 7-26. Airflow along the tunnel causes pressure loading on surfaces facing into the flow

The airflow speed associated with the initial nose-entry pressure wave (shown as U_1 in Figure 7-3) may be calculated from Equation 7-11. When further pressure waves pass,

each one changes the airflow speed as well as the pressure. Excluding effects that occur in the vicinity of the train, the cumulative effect of multiple pressure waves leads to a maximum airflow speed which is often on the order of two times U_1 for a single train passage through a simple tunnel. A more accurate prediction can be made using one-dimensional software.

$$U_1 = \Delta p / \rho c$$

Equation 7-11

Where:

U_1 = Airflow speed associated with the initial nose-entry pressure wave

Δp = Pressure amplitude of the initial nose-entry pressure wave

ρ = Air density

c = Speed of sound in air

This formula requires consistent units (see definition in Section 2.7).

The airflow speeds associated with pressure waves are typically on the order of 2 to 10 percent of the train speed for HSR tunnels. Because these speeds are usually low compared to the maximum slipstream gust speed as the train passes by, it is the slipstream gusts that are of greater concern in the design of equipment.

Slipstreams in tunnels are similar in character to those in open air in Section 3, consisting of a boundary layer alongside the train and a wake behind it, but compared to the open air case, a stronger slipstream effect is expected in tunnels because the airflow is concentrated into the confined space of the tunnel. Additionally, objects such as signs may be positioned closer to the train than they would be in open air due to the restricted space in the tunnel, and this may increase the loading further. Loading is of short duration and may be subject to dynamic amplification. It should be treated as a fatigue load in the sense that the aim of assessments is to quantify the number and amplitude of loading cycles expected over the lifetime of the equipment.

The airflow speed in the slipstream is highly non-uniform across the cross-section of the tunnel. At the train surface, the flow speed is equal to the speed of the train. The flow speed decays with distance from the train, while further from the train the air can blow in the opposite direction to the train, as explained in Section 7.2.1. Therefore, the airflow speed to which a particular item of equipment will be exposed depends strongly on where it is located relative to the train and the tunnel walls, and these relationships may depend on train shape and numerous other factors. Furthermore, random gusts caused by turbulence as the train passes can occur at any point within the cross-section. Therefore, it is not possible to provide simple guidelines for calculating slipstream airflow speeds with any confidence. Experimental measurements in tunnels have shown speeds in the localized gusts near the train's nose and tail on the order of 50 percent of train speed [68]. As a conservative basis for design, it might be assumed that the maximum airflow speed is equal to the train speed.

7.6.14 Assessment Methods for Underground Stations

Aerodynamic impacts for underground stations are described in Section 7.4.7.

Assessment tools include specialized one-dimensional analysis software and 3D CFD methods. One-dimensional analysis is appropriate for calculating the pressure waves and airflow speed in the tunnel approaching the station. By modelling the station as a length of tunnel with larger cross-sectional area, the amplitude of pressure waves transmitted into the station may be estimated, together with volume flow rates of air into and out of the tunnel. The latter may be useful for ventilation calculations. The airflow from the tunnel will spread out into the station, slowing down as it does so, in a 3D manner that one-dimensional software cannot model. Passengers standing directly in line with the tunnel will feel a different airflow speed compared to people standing further back, including a jet effect when air blows out from the tunnel and a suction effect when air is drawn into the tunnel. Furthermore, there may be turbulence effects near the tunnel opening. CFD would be needed to assess these effects. However, as a conservative upper limit on airflow speed experienced by passengers in the station, the airflow speed *in the tunnel* calculated by one-dimensional software may be used [152].

Guidance on assessing airflow in subway stations is provided in the Subway Environmental Design Handbook [146]. Many of the same considerations apply to underground HSR stations, with respect to airflows in access tunnels, elevator shafts, etc.

7.6.15 Assessment Criteria for Passengers and Crew

The criteria in this section are relevant to assessment using specialized software. The software predicts the pressure wave effects for a particular tunnel design and train scenario. Outputs from the software include pressure time-histories inside and outside the train at several points along the length of the train. The criteria below may be used to decide whether the result should be considered satisfactory, or whether changes to the proposed design are required.

7.6.15.1 Medical Safety Limit

The **Medical Safety Limit**, sometimes referred to as the **TSI 10 kPa limit**, is mandated as a legal requirement in Europe in the TSI Infrastructure [38] and is now also adopted in some other countries. Its purpose is to protect the ears of passengers and crew from damage in the event of failure of the train's sealing system by limiting the pressure changes that are permitted outside the train. The pressure limit derives from research by the European Railway Research Institute [41]. Japan takes a different approach to achieve safety for passengers: It does not apply the Medical Safety Limit or place any other limits on pressure outside the train, but instead focusses on minimizing the risk of failure of the sealing system. There are no records of Medical Safety concerns having arisen in Japanese tunnels.

In the U.S., the Medical Safety Limit is not a legal requirement but is recommended as a basic minimum criterion for tunnels. It may be stated as follows:

The peak-to-peak pressure change occurring on the outside of the train should not exceed 1.45 psi (10 kPa) during the whole duration of the train's transit through the tunnel.

The meaning of “peak-to-peak pressure change” is illustrated by the example in [Figure 7-27](#). Pressure time-histories for three points along the outside of the train are shown. For the front point, the most positive pressure is 0.48 psi and the most negative pressure is -0.49 psi, giving a peak-to-peak pressure change of 0.97 psi. The peak-to-peak pressure changes at the center and rear of the train are 0.93 and 0.79 psi, respectively. The maximum of these is 0.97 psi, which is less than 1.45 psi, so the criterion is met. The example shows only three points along the train for simplicity, but it is recommended that a greater number of points should be taken, as explained in [Section 7.6.5.3](#).

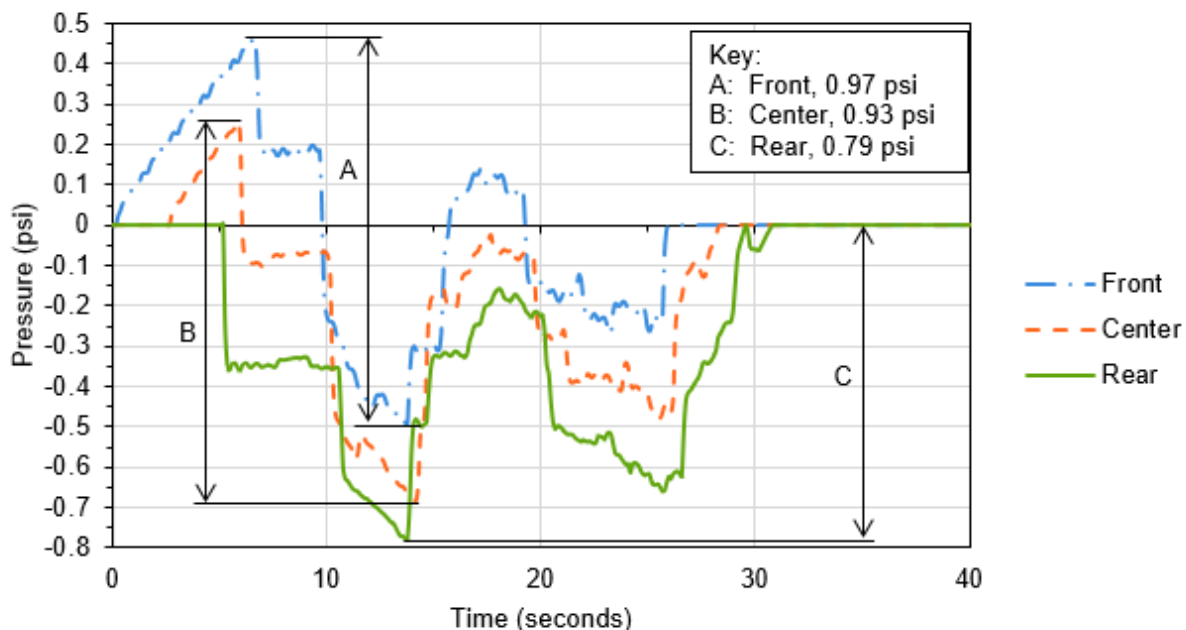


Figure 7-27. Medical Safety Limit assessment from pressure time-histories on the outside of the train

For tunnels in which multiple trains may be present or cause pressure waves simultaneously (e.g., double-track tunnels), the criterion should be satisfied for all feasible combinations of trains.

The criterion relates to pressure change on the *outside* of the train, i.e., the effect of the sealing system is ignored. Passengers inside sealed trains would experience smaller pressure changes than those occurring on the outside of the train. The Medical Safety Limit essentially acts as a backstop, preventing injury in the event of failure of the sealing system (for example, due to breakage of a window).

Assessments are made under standard atmospheric conditions; see [Section 7.6.5.4](#). Unlike the aural comfort criteria, there is no limitation on the time period over which the pressure change is measured.

Since atmospheric pressure changes with altitude, passengers in trains passing through an inclined tunnel will experience small pressure changes (about 0.05 psi for 100 ft of elevation change), just as they would if they were to travel outside a tunnel. Such pressure changes add to those caused by pressure waves, resulting in a larger overall pressure change than in a non-inclined tunnel. The existing European regulations [38] require pressure changes due to altitude to be included in assessments. Thus, in certain cases, an unusually long and steep tunnel could be non-compliant with the Medical Safety Limit, even though an identical non-inclined tunnel would be compliant. In practice, this situation is rare, but can lead to anomalous conclusions from assessments [102]. The upcoming version of the European standard [112] removes the requirement to consider altitude from assessments of train meeting or passing events in double-track tunnels but retains it for single-train passages in all tunnel types.

At present, there is no consensus on whether an inclined tunnel indeed has more potential to damage the ears than an otherwise-identical non-inclined one, or whether the altitude-dependent pressure change is sufficiently gradual that it should not present a practical concern [102]. Until more information from medical experts becomes available, the authors recommend the conservative approach be used, i.e., the total pressure changes including altitude effects must not exceed the Medical Safety Limit.

7.6.15.2 Aural comfort criteria

Aural comfort criteria are not mandatory and are adopted at the discretion of the operator. Providing a higher level of comfort may require a larger tunnel (and hence greater construction cost) or better-sealed trains (and hence greater cost or less choice of rolling stock). Operators may wish to select a comfort level appropriate to the nature of the operation; for example, a greater comfort level for a premium service, or a lesser comfort level for an economy service.

The causes and impacts of aural discomfort are covered in Section 7.4.1.

Criteria are generally set with the aim that no more than a small percentage of passengers would describe the pressure changes as uncomfortable. However, it should be recognized that the impact of selecting one set of criteria or another cannot be quantified exactly. Furthermore, the perception of pressure changes by a population of passengers may depend on their previous experience of rail travel through tunnels.

Two sets of aural comfort criteria for sealed trains are listed in Table 7-13 below as information, with the choice of criteria to be used left to the selection by the rail system operator. Aural comfort criteria vary internationally and those given below draw on multiple sources as described in Section 7.6.15.3 below.

Table 7-13. Proposed aural comfort criteria for U.S. (sealed trains)

Time period	Pressure change	
	Higher comfort level	Lower comfort level
≤1 second	0.072 psi (0.5 kPa)	0.11 psi (0.75 kPa)
≤3 seconds	0.12 psi (0.83 kPa)	0.18 psi (1.25 kPa)
≤10 seconds	0.20 psi (1.4 kPa)	0.30 psi (2.1 kPa)
≤25 seconds	0.33 psi (2.3 kPa)	0.51 psi (3.5 kPa)

The criteria are intended to be applied as follows:

- The pressure changes are those occurring inside the train, as predicted by appropriate specialized software. The simulations should include the effect of the sealing system.
- The criteria should be met at all points along the length of the train, excluding any tapering region at the nose and tail.
- The criteria for all of the four time periods should be met at all times. For example, if the higher comfort level is selected, there should be no 1-second period in which the pressure changes by more than 0.072 psi, and there should be no 3-second period in which the pressure changes by more than 0.12 psi, and there should be no 10-second period in which the pressure changes by more than 0.20 psi, and there should be no 25-second period in which the pressure changes by more than 0.33 psi.
- The time periods are “up to and including,” for example, 10 seconds, means any time-period up to and including 10 seconds long.
- The criteria are intended for sealed trains only. It will not be practical to meet these criteria with unsealed (or poorly sealed) trains because the tunnels would have to be extremely large.

An example pressure time-history inside a sealed train is shown in [Figure 7-28](#) with annotations indicating the maximum pressure changes occurring within the stipulated time intervals.

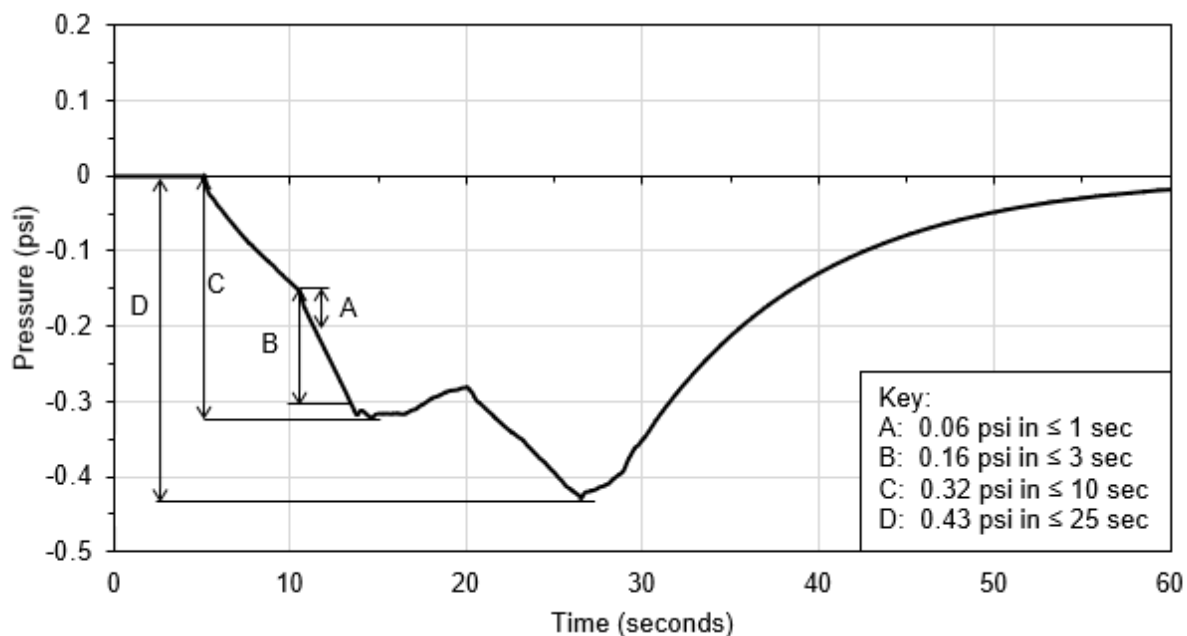


Figure 7-28. Identification of maximum pressure changes for comparison against aural comfort criteria. Example shows pressure at rear of train (see [Table 7-14](#))

The process shown in [Figure 7-28](#) is repeated for each measurement point inside the train. As a minimum, three positions are measured: front, center, and rear of the train. Results are then tabulated and compared against the allowable pressure changes for the desired aural comfort level, as shown in the example in [Table 7-14](#). In this case, the lower level aural comfort criteria are not met, due to the exceedance noted in the [Table 7-14](#) for the 10-second time period.

Table 7-14. Pressure changes compared to aural comfort criteria for the example shown in [Figure 7-28](#)

Time period	Allowable: Lower comfort level	Predicted pressure changes (psi)		
		Front	Center	Rear (Figure 7-28)
≤1 second	0.11	0.05	0.07	0.06
≤3 seconds	0.18	0.15	0.16	0.16
≤10 seconds	0.30	0.23	0.27	0.32 ¹
≤25 seconds	0.51	0.26	0.33	0.43
Notes:				
1. Exceeds allowable value, so this train/tunnel scenario does not achieve the lower comfort level.				

7.6.15.3 *Basis of the Proposed Aural Comfort Criteria*

The aural comfort criteria presented in [Table 7-13](#) draw on sources including UIC leaflets 660 [\[78\]](#) and 779-11 [\[79\]](#), criteria used in the Netherlands [\[86\]](#), and research by Berlitz [\[12\]](#) and Schwanitz [\[127\]](#). China has the same criteria as UIC 660 [\[21\]\[100\]](#). Japanese criteria are not published. [Figure 7-29](#) compares the aural comfort criteria given in [Table 7-13](#) with information from these sources. Some information relevant to the figure is given in the points below.

- The UIC 660 criteria were widely used in Europe in the days when HSR tunnels were double-track and were applied only to single train passages, not combinations of trains on both tracks in the same tunnel. It was not problematic to provide double-track tunnels large enough to pass the UIC 660 criteria. However, now that many new HSR tunnels are single-track, these criteria have been recognized as requiring impractically large tunnels. One of the motivating factors behind the Schwanitz study was to provide evidence on which more appropriate criteria could be founded.
- The UIC 779-11 criteria (also given in Annex B of [\[34\]](#)) are not widely used and are described in the document as a minimum standard fallback in case other criteria are not provided.
- The Netherlands criteria are in two sets: a stricter set for single-track tunnels and single train passages through double-track tunnels, and a less strict set for trains meeting or passing in double-track tunnels.
- In the Berlitz study, passengers in a train on a German railroad route with many tunnels were asked to rate each tunnel based on level of discomfort from pressure changes on a scale of one to seven, with seven being the most uncomfortable, while the pressure changes inside the train were measured. The results of the study were processed to obtain a set of pressure changes that, for an average passenger, would rate 2.5 (Deutsche Bahn's target comfort level).
- In the Schwanitz study, volunteers sat in a pressure chamber and were subjected to pre-determined pressure changes with different amplitudes and rise times. Subjects were asked to rate each pressure change on a scale of 0 to 6, with 6 being the most uncomfortable. The data in [Figure 7-29](#) relates to pressure increases only (decreases were found to be less uncomfortable for the same amplitude and rise time). Rating 2 corresponds roughly to 2.5 percent of people experiencing the pressure change as uncomfortable, while rating 3 corresponds roughly to 15 percent.

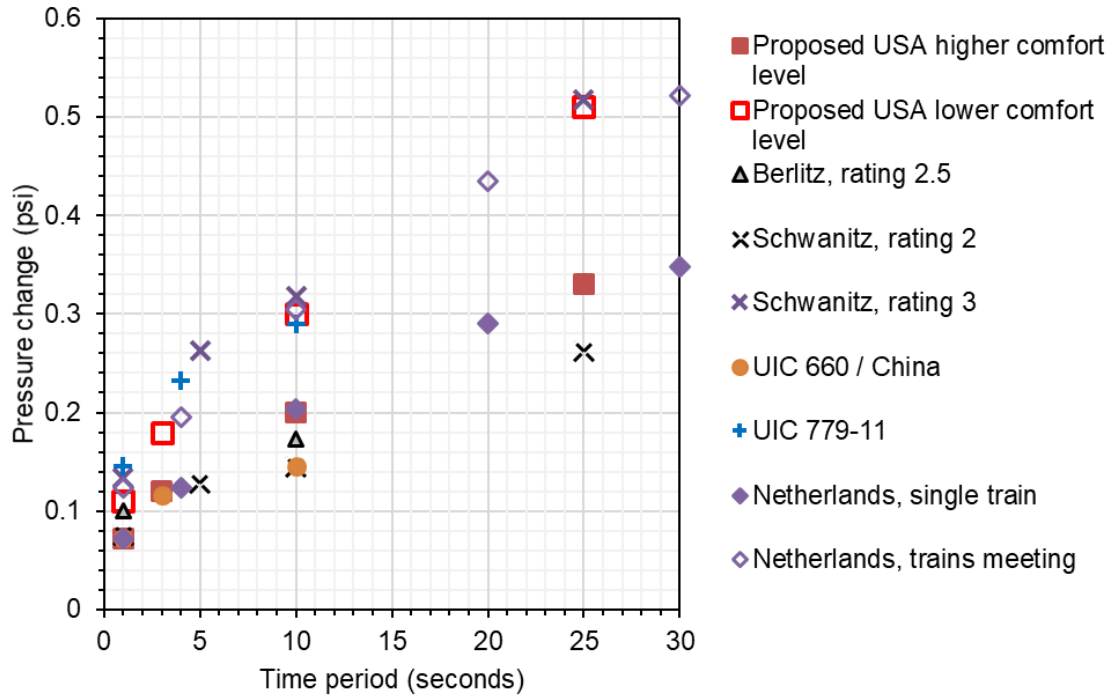


Figure 7-29. Proposed aural comfort criteria for U.S. compared with international criteria and experimental results

As an approximate guide, the proposed Higher and Lower comfort levels correspond to about 5 percent and 15 percent, respectively, of people finding the pressure changes uncomfortable.⁷

7.6.15.4 Aural Comfort Index

It is convenient to define a single parameter expressing the margin by which a given set of pressure changes passes or fails the aural comfort criteria given in Section 7.6.15.2. In this report the **aural comfort index (ACI)** is defined as follows:

$$ACI = \max \left(\frac{\Delta p_{1s}}{\Delta p_{HCL,1s}}, \frac{\Delta p_{3s}}{\Delta p_{HCL,3s}}, \frac{\Delta p_{10s}}{\Delta p_{HCL,10s}}, \frac{\Delta p_{25s}}{\Delta p_{HCL,25s}} \right) \quad \text{Equation 7-12}$$

Where:

ACI = Aural comfort index;

\max = The maximum out of the values of the four expressions in the bracket;

Δp_{ns} = The pressure change occurring in n seconds; and,

$\Delta p_{HCL,ns}$ = The higher comfort limit allowable pressure change in n seconds (Table 7-13).

⁷ Based on data from Schwanitz [127]. Note that the experiments considered only healthy people, whereas those with pre-existing medical conditions affecting the ears, or with illnesses such as colds that cause blockage of the eustachian tubes, are likely to find these pressure changes more uncomfortable.

ACI values are interpreted as follows:

- Lower is better. Higher values mean a more uncomfortable experience.
- The value indicates the size of the pressure changes relative to the higher comfort level criteria, based on whichever one of the four time intervals gives the highest ACI value.
- Less than or equal to 1.0 indicates that the higher comfort level is achieved. For example, 0.8 means that all of the pressure changes were at least 20 percent below the higher comfort level criteria.
- Because the pressure change criteria for the lower comfort level are all 1.5 times the equivalent values for the higher comfort level, an ACI value of 1.5 or less means that the lower comfort level is achieved.

7.6.15.5 *Considerations Relating to Aural Comfort Criteria for Double-track Tunnels*

For double-track tunnels, the pressure changes experienced by passengers depend on if other trains are present in the tunnel and on the timing of entry of the two trains (see Section 7.6.5.6). The worst case is often when two trains enter the tunnel simultaneously from opposite directions, while the more typical case of a single train passing through the tunnel generates significantly smaller pressure changes. In assessing aural comfort, it is common to consider the frequency with which these events are expected to occur. Pressure changes arising from a single train passage with no other trains present may be the most common case and would be assessed against stricter criteria (for example, the “higher comfort level” in Table 7-13), while those arising from combinations of trains that occur only rarely may be assessed against less demanding criteria (for example, the “lower comfort level” in Table 7-13), or even ignored altogether. This avoids the need to provide a larger and more expensive tunnel in order to mitigate rare events that would have little overall impact on passenger perceptions of the railroad.

7.6.15.6 *Additional Considerations Related to Aural Comfort Criteria*

It is common practice to assess aural comfort on the basis of the single most uncomfortable pressure change occurring during passage through a single tunnel, but passenger perceptions of discomfort are also influenced by the number of pressure changes and the time-gap between them; for instance, if there are multiple tunnels within a short distance. According to [148], if a certain pressure change occurs repeatedly at one-minute intervals, it takes about 20 to 30 percent less pressure change to cause the same level of discomfort compared to a single-instance pressure change. This is why stricter limits on pressure changes are more appropriate for subway tunnels than for HSR tunnels. The Subway Environmental Design Handbook [146] recommends limiting the maximum pressure change rate in subway cars to 0.06 psi/sec (0.4 kPa/sec), applicable to any pressure change greater than 0.1 psi (0.7 kPa). When assessing HSR tunnels, it is recommended to reduce the aural comfort criteria pressure changes by 25 percent when the time-gap between tunnels is less than or equal to 1 minute.

Aural comfort criteria used in other countries are described in Section 7.6.15.3.

7.6.15.7 Aural Comfort Criteria for Unsealed Trains

If unsealed (or poorly sealed) HSTs were used on routes with tunnels, a far less strict standard of aural comfort would have to be accepted than for sealed trains (otherwise, the tunnels would have to be extremely large). This situation is unlikely to arise with new HSR rolling stock since all commercially available HSTs are sealed, but it may arise in the case of new operations with existing unsealed HSTs. In the absence of other guidance for unsealed trains, operators may consider applying the criteria for unsealed trains in Annex B of the European standard [34]: 0.44 psi (3.0 kPa) in 4 seconds for single train scenarios, and 0.58 psi (4.5 kPa) in 4 seconds for the worst case two train scenario in double-track tunnels. It should be recognized that many passengers would experience these pressure changes as uncomfortable. Some degree of discomfort for passengers is unavoidable if unsealed trains are used on routes with tunnels.

7.6.16 Assessment Criteria for Fatigue Loading on HSTs

There are no internationally agreed criteria for fatigue loading on trains from pressure in tunnels. China has a guideline pressure limit [21]. In other countries, train manufacturers design the car bodies and the side glazing to their own in-house limits [9] based on experience. In some cases, the railroad operator asks the train manufacturer to design the trains to tolerate whatever pressures they predict will occur in the tunnels.

Care should be taken to distinguish between limits for one-off loading versus limits for fatigue loading – it is the latter which is relevant for pressures in tunnels. The impact on fatigue life of the train will depend not only on the pressure amplitude but also on the number of load cycles (related to number of tunnel transits during the design life of the train). Operators should liaise with the train manufacturer to agree a suitable pressure value for use in tunnel design.

In the absence of information from the manufacturer, the following is offered for purposes of preliminary sizing of tunnels. The pressure limit is similar to one used in China, and within the range of pressure limits from train manufacturers quoted in [9].

The pressure difference between inside and outside of the train should always remain within the range +0.87 to -0.87 psi (+6 to -6 kPa).

In the example shown in Figure 7-21, the maximum positive and negative net pressures at the rear of the train are 0.36 and -0.46 psi, respectively, which are within the limits above and therefore the criterion is met. However, the same checks would need to be carried out for other points along the length of the train.

7.6.16.1 Assessment Criteria for Loading on Conventional Trains and Cargos in Tunnels

There are no criteria for assessing potential damage to non-HST railcars or their cargos from pressure wave effects or airflow from trains in tunnels. Each type of railcar and cargo is likely to have different capacity to tolerate these effects. Car manufacturers and rail operators should determine/select their own criteria.

7.6.17 Criteria for Aerodynamic Performance of Trains in Tunnels

Europe has acceptance criteria for HSTs derived from the pressure wave generated when the train enters a tunnel. This is one of the minimum aerodynamic standards that all European HSTs must meet as part of the interoperability requirement for HSR across Europe. These criteria are not mandatory in the U.S., but operators might wish to consider including this requirement in specifications for new rolling stock. It provides a reference train condition that can be used in the design of tunnels. The U.S./Europe Baseline Train used in this study assumes that the train meets these criteria.

The tunnel entry wave test measures the pressure wave “signature” for a particular train design entering a 63 m² (678 ft²) tunnel at 250 km/h (156 mph). Pressure is measured by an instrument fixed to the wall of the tunnel at point x_p ; see [Figure 7-30](#) and [Equation 7-13](#). The tunnel selected should not be so short that pressure wave reflections from the far end of the tunnel influence the measurements. Depending on train length, this could require a tunnel at least 0.5 to 1.2 miles long. For further information about the test set-up and procedure, see [\[34\]](#).

If a tunnel with the exact specified area is not available for testing, then the test may be performed using a tunnel with a different area and the results transferred to the required tunnel area by computer simulation in the following manner:

1. The tunnel selected for the test should have a cross-sectional area as close as possible to 63 m² (678 ft²).
2. A full-scale test is conducted at 250 km/h (156 mph) using the selected tunnel.
3. A computer simulation of the full-scale test is conducted using the same tunnel size as the test. The simulation methods are described in [Section 7.6.5](#).
4. Results from the full-scale test are used to calibrate the computer model.
5. The calibrated computer model is then used to simulate the same train entering a 63 m² (678 ft²) tunnel at 250 km/h (156 mph).
6. The pressure wave signature from the computer model is compared against the requirements as stated below.

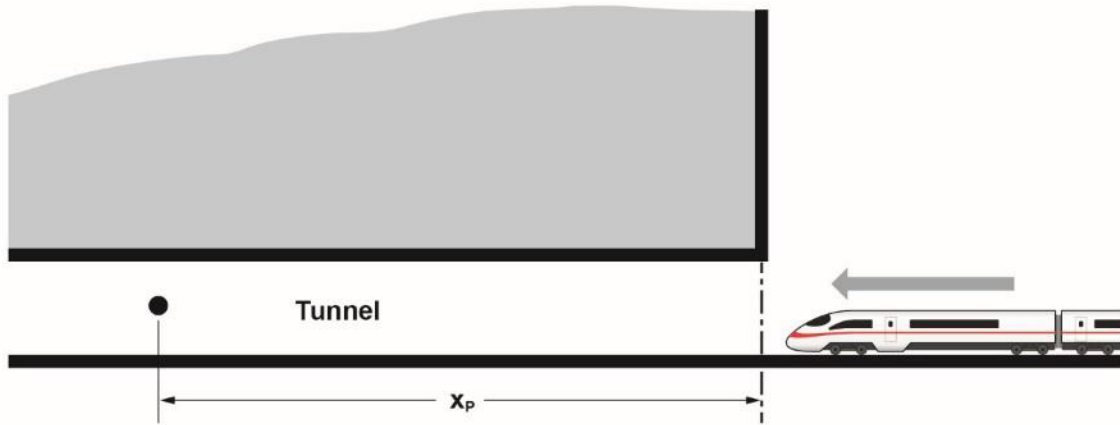


Figure 7-30. Measurement position for tunnel entry wave rolling stock acceptance tests

In [Figure 7-30](#), the dimension x_p is given by:

$$x_p = \frac{cL_{tr}}{c - v_{tr}} + \Delta x_1 \quad \text{Equation 7-13}$$

Where:

c = The speed of sound in air, taken as 334 m/s (748 mph);

L_{tr} = The length of the train;

v_{tr} = The speed of the train; and,

Δx_1 = Between 100 m and 300 m (328 to 984 ft).

When using [Equation 7-13](#), c and v_{tr} must be in the same units as each other (e.g., mph), and x_p , L_{tr} , and Δx_1 must be in the same units as each other (e.g., feet).

The pressure wave signature has the form shown in [Figure 7-31](#), where pressure rise Δp_N is associated with the nose of the train entering the tunnel, Δp_{fr} is caused by the frictional resistance along the length of the train, and pressure drop Δp_T is associated with the tail of the train entering the tunnel. Pressure drop Δp_{Hp} is caused by the train passing the measurement point and is not part of the acceptance criteria. The distance Δx_1 in the above formula is added to ensure that Δp_T is distinguishable from Δp_{Hp} .

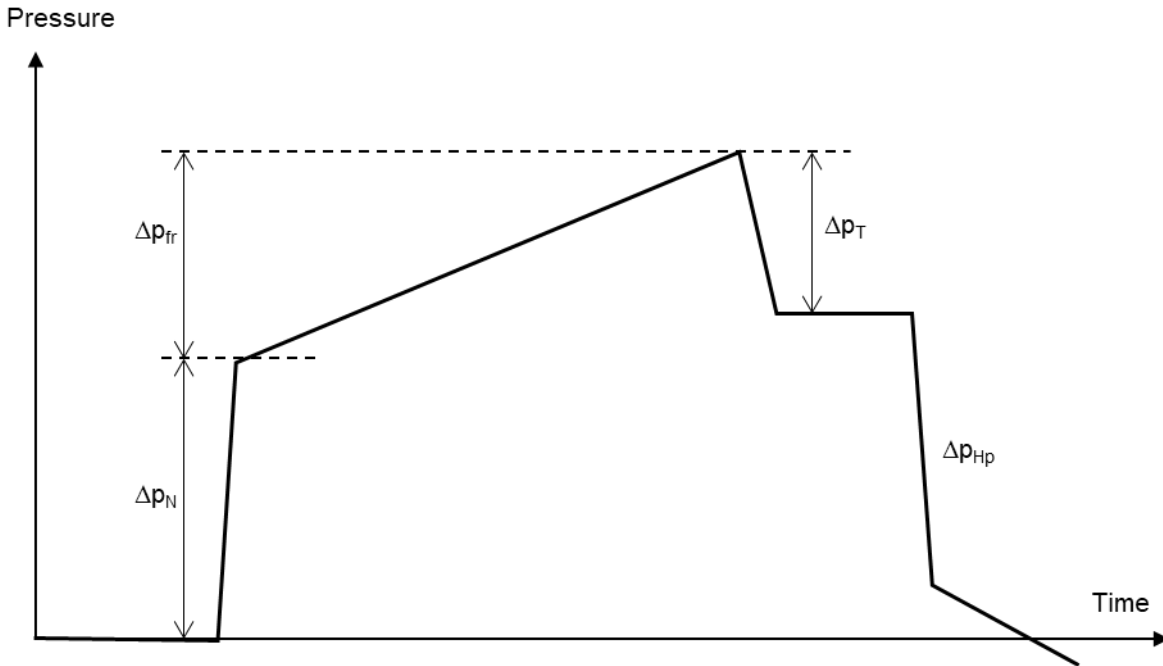


Figure 7-31. Tunnel entry wave “signature”

The acceptance requirements for the train are:

$$\Delta p_N \leq 1600 \text{ Pa (0.23 psi)}$$

$$\Delta p_N + \Delta p_{fr} \leq 3000 \text{ Pa (0.44 psi)}$$

$$\Delta p_N + \Delta p_{fr} + \Delta p_T \leq 4100 \text{ Pa (0.59 psi)}$$

All three requirements must be satisfied. Note that Δp_T is treated as positive in the equation above, even though it represents a reduction of pressure.

This study assumes that U.S./Asian Baseline Trains would pass the above criteria if tested with a 68.7 m² (740 ft²) tunnel, i.e., with the same blockage ratio as a U.S./Euro Baseline Train entering a 63 m² (678 ft²) tunnel.

7.6.18 Assessment Criteria for Fixed Equipment in the Tunnels

There are no assessment criteria for pressures acting on fixed equipment in the tunnels, such as doors, cabinets, etc. However, using specialized software and the considerations described in Section 7.6.13 above, the maximum pressure loading and fatigue cycles can be predicted for a given tunnel design and operating conditions, enabling a dialog with the suppliers of the equipment.

7.6.19 Assessment Criteria for Underground Stations

There are no internationally accepted assessment criteria specifically for HSR underground stations. Criteria can be recommended as follows.

- For slipstreams on platforms (applicable to short-duration “gusts” caused by turbulence), use the same criteria as open air in Section 3.6.1.

- For steady airflow in stations caused by the movement of trains in tunnels, refer to the Subway Environmental Design Handbook [146] which suggests a maximum airflow speed of 12 mph (5.4 m/s) under normal conditions.
- For pressure wave effects, use the same aural comfort criteria as for passengers and crew inside trains in Section 7.6.15.
- For equipment in the stations that may be vulnerable to pressure loading, see Section 7.6.18 above for equipment in tunnels.

7.6.20 Examples

7.6.20.1 Estimating Tunnel Cross-Sectional Area

Question

A new, 1-mile long, twin-tube, single-track tunnel is being designed for a line speed of 190 mph. Estimate the required cross-sectional area. Trains will conform to U.S./Euro Baseline described in Section 2.3.2.

Methodology

Use Nominal Tunnel Size from [Table 7-1](#), interpolating for speed.

The Nominal Tunnel Sizes do not vary with tunnel length, and [Equation 7-3](#) does not apply because the tunnel is longer than twice the minimum length of trains.

Calculations

From [Table 7-1](#), the required tunnel cross-sectional areas for 175 and 200 mph respectively are 646 and 861 ft². Interpolating:

$$\text{Area} = 646 + (861 - 646) \times \frac{190 - 175}{200 - 175} = 775$$

Result

The free cross-sectional area per tube is 775 ft². Onto this should be added the cross-sectional area occupied by solid objects (such as trackbed and equipment that is continuous along the tunnel), to obtain the total internal cross-sectional area of the tunnel.

7.6.20.2 Estimating Net Pressures on Trains in the Tunnel

Question

For the tunnel in the above example, what net pressure load is expected on the trains?

Methodology

For Nominal Tunnel Sizes for 175 mph and above, pressures can be taken directly from [Table 7-5](#).

Result

From [Table 7-5](#), the maximum net pressure on trains is estimated as ±0.68 psi (±4.7 kPa).

7.6.20.3 Estimating Pressure Loading on a Door in the Tunnel

Question

For the above example, estimate the pressure loading on a door leading from one of the tunnel tubes into an emergency escape shaft.

Methodology

The escape shaft is assumed to be at atmospheric pressure. Therefore, the net pressure loading across the door is equal to the pressure in the tunnel.

The pressure loading consists of two parts: loading from pressure waves (see Section 7.6.13.1) and from nose and tail pressure pulses (see Section 7.6.13.2).

Loading from pressure waves can be taken directly from Table 7-5 because the Nominal Tunnel Size for the particular operating speed has been selected. Only the maximum pressure can be estimated by this method, not the numbers of loading cycles of different sizes (which would require assessment by one-dimensional analysis).

The door is a vertical surface parallel to the track, so the loading from the nose and tail pressure pulses can be estimated using Equation 4-2 (Section 4.6.2.1) with a scale factor of 2 to allow for the enclosed situation as recommended in Section 7.6.13.2. SI units will be used for Equation 4-2.

Inputs

The door is located 10 ft (3.0 m) from the track centerline. Therefore, in Equation 4-2, y will be taken as 3.0.

The train factor k_t in Equation 4-2 will be taken as 0.6 (streamlined HST).

The train speed v must be converted from mph to m/s: 190 mph = 84.9 m/s

Calculations

From Table 7-5, the maximum pressure on equipment in the tunnel due to pressure waves is estimated as ± 0.72 psi (± 5.0 kPa).

Using Equation 4-2 for a vertical surface in open air:

$$\begin{aligned} p_+ = p_- &= k_{ap} k_t \left[\frac{A_1}{(y + e_1)^2} + c_1 \right] \times \frac{1}{2} \rho v^2 \\ &= 1.0 \times 0.6 \times \left[\frac{2.5}{(3.0 + 0.25)^2} + 0.02 \right] \times \frac{1}{2} \times 1.225 \times 84.9^2 \\ p &= \pm 680 \text{ Pa} \end{aligned}$$

Apply the factor of 2 as recommended in Section 7.6.13.2 and convert back to psi:

$$p = \pm (2 \times 680) \text{ Pa} = \pm 1360 \text{ Pa} = \pm 0.20 \text{ psi}$$

Add the contributions of pressure waves and nose/tail pressure pulse:

$$p = \pm (0.72 + 0.20) = \pm 0.92 \text{ psi}$$

Result

The estimated pressure load on the doors is ± 0.92 psi.

Note that summing the contributions of pressure waves and nose/tail pressure pulse can be conservative, because the nose/tail pressure pulse does not necessarily coincide with the maximum pressure due to pressure waves.

This method estimates only the maximum loading. To estimate the number of load cycles of different amplitudes, the pressure wave effects would have to be simulated, usually by one-dimensional analysis.

7.7 Inter-Related Considerations

The aerodynamic design of HSR tunnels may be influenced by considerations other than pressure waves, including aerodynamic drag, emergency evacuation, ventilation, and smoke control. The latter three topics are outside of the scope of this report, but are worth noting, as they may limit the aerodynamic design choices or lead to potential aerodynamic impacts that need to be assessed or mitigated.

7.7.1 Drag

Aerodynamic drag is increased in tunnels, as explained in Section 9.3.5. Drag impacts energy costs and may in some cases limit the maximum speed of the train through the tunnel. When considering the aerodynamic design of the tunnel to mitigate pressure wave effects, drag should be considered also. Drag can be mitigated by increasing the cross-sectional area of the tunnel and by providing air shafts.

7.7.2 Emergency Evacuation

It is necessary for tunnels to provide for evacuation in the event of a fire, and this frequently leads to a single-track tunnel design such that people can be evacuated into the other tube in the event of a fire.

National Fire Protection Association standard NFPA 130 [105] requires *either* pedestrian escape routes to the surface no further apart than 2,500 ft (762 m), *or* escape routes to another tunnel tube no further apart than 800 ft (244 m). Even if escape routes to another tunnel tube are provided, local fire departments may additionally require shafts to the surface, typically at intervals of about 0.5 to 1.5 miles (0.8 to 2.4 km), enabling escape from the tunnel and access by emergency personnel.

Where shafts to the surface are needed anyway, the opportunity arises to design them to fulfil a pressure relief function as well as their main emergency access function. In this way, air shafts can be provided to reduce pressure wave impacts and drag at little extra cost.

7.7.3 Ventilation and Smoke Removal

Single-track tunnels are usually designed with ventilation systems that pressurize the non-incident tunnel in the event of a fire to prevent ingress of smoke. For this system to function effectively it is necessary to minimize leakage between tubes and leakage to

the surface by keeping doors at cross-passages and escape shafts closed during normal operation. These doors are part of a compartmentation fire safety strategy, and their natural position is to be closed. As a result, it may not be feasible to use cross-passages to mitigate pressure wave effects during normal operation and it may not be possible to relieve the fatigue loading on doors simply by leaving them open.

The provision of air shafts may be desirable for temperature control and fresh air supply as well as for mitigating pressure wave effects and drag. The same air shafts may also contain fans for emergency smoke control. Different branches of the air shaft system may be provided with controlled dampers, enabling different configurations in normal operation versus emergency mode. Thus, smoke control requirements do not necessarily preclude the use of air shafts for pressure relief during normal operation.

The cross-sectional area of the tunnel may impact ventilation design. For example, the dimensions of the tunnel can be expected to influence the size of fans required for emergency smoke control. It is notable that these smoke control systems are designed with conservative assumptions about leakage or open cross-passage doors to provide a robust system capacity.

8 Micro-Pressure Waves Emitted from Tunnels

8.1 Introduction

Micro-pressure waves (MPWs) emitting from tunnel portals are a by-product of the pressure waves generated by trains inside tunnels. They can cause noise in the environment and sometimes generate loud “sonic booms.” They can also cause doors and windows of nearby houses to vibrate. Where required, mitigation is achieved by providing perforated “hoods” at tunnel entrances. MPW amplitude is even more strongly dependent on train speed than other aerodynamic phenomena. Assessment of MPW issues during design of tunnels becomes all the more important as line speed increases.

The MPW phenomenon is well-understood and methods are available to predict it. The main obstacle to the design of mitigation measures is that the boundaries of acceptability for MPWs are not universally established or agreed upon internationally.

This section includes:

- Description of the relevant phenomena, including how MPWs are caused
- Influencing factors
- Impacts
- Mitigation methods
- Assessment methods, criteria, and examples

8.2 Aerodynamic Principles and Phenomena

The guidance presented in this section assumes that the reader is familiar with the general information on pressure waves given in Section 7.

8.2.1 Overview of the MPW Phenomenon

As described in Section 7.2, when a train enters a tunnel it causes a pressure wave which propagates along the tunnel and, when it reaches the far end, reflects back along the tunnel. An **MPW** is a pulse of air pressure that is emitted from a tunnel portal into the environment whenever any pressure wave inside a tunnel is reflected at the portal. The “micro” in the term refers to the fact that the micro-pressure wave is orders of magnitude smaller than the pressure wave in the tunnel. Every railway tunnel in the world emits MPWs. These are generally at frequencies below the audible range and of such small amplitude that they are rarely noticed. However, MPWs can take the form of audible noise, sometimes called **sonic booms**, which can be very loud. These were first experienced in Japan in 1974 during running tests on the Okayama-Hakata extension of the Sanyo Shinkansen line [107]. Booming noises were heard at tunnel exits and residents complained of rattling windows and shutters.

Unacceptable MPWs are sometimes considered to be a problem unique to long slab track tunnels (because that is the only tunnel type for which they have been reported),

but there is no theoretical reason why they should not occur in short tunnels too, including those with ballasted track as well as slab track.

8.2.2 The Physics of MPWs

The generation and transmission of an MPW take place in four phases (see [Figure 8-1](#)):

1. Generation of a pressure wave inside a tunnel, typically caused by the nose of the train entering the tunnel.
2. As the pressure wave propagates down the tunnel at the speed of sound (approximately 762 mph (340 m/s)) the gradient of the pressure wave may increase, especially in long, slab track tunnels. In ballasted tunnels, the gradient may decrease.
3. When the wave reflects from the tunnel exit, a proportion of the energy is emitted into the surrounding environment as an MPW.
4. The MPW propagates through the air to **receivers** (locations such as homes where people may notice the impacts).

These phases are described in more detail in sub-sections below.

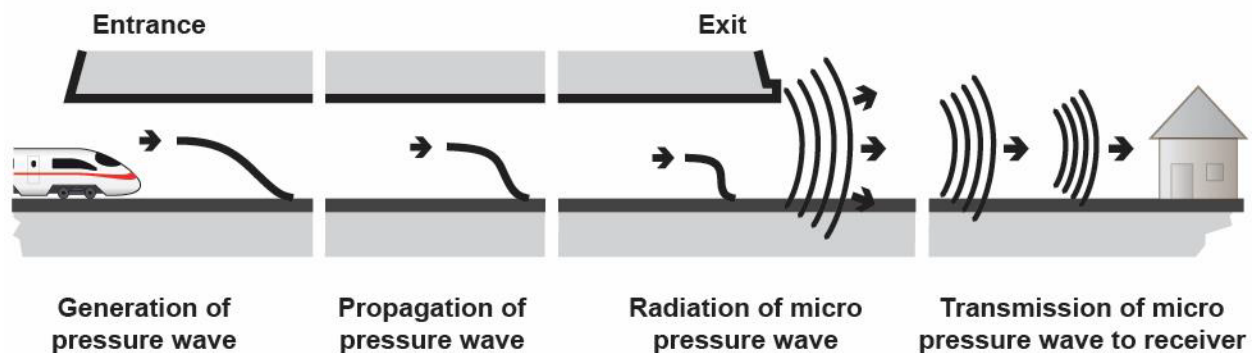


Figure 8-1. Micro-pressure wave generation, propagation, and emission

When considering aerodynamic effects in tunnels, such as aural comfort of passengers, the property of the pressure wave that is of primary interest is its magnitude, i.e., the amount by which the pressure changes when the wave passes. However, for MPW it is the **pressure gradient** that matters most, i.e., the rate at which the pressure increases. The amplitude of the MPW experienced outside the tunnel is proportional to the gradient of the pressure wave inside the tunnel as it approaches the tunnel exit.

The focus of assessments and mitigation is usually on MPWs emitted from tunnel exits caused by reflection of the nose-entry pressure wave after propagation down the tunnel (**nose-entry MPWs**). But MPWs may also be caused by any other event that leads to a steep pressure wave or rapid change of air velocity at an entrance or exit of the tunnel, such as when the train exits from the tunnel or passes an air shaft. Furthermore, each pressure wave undergoes multiple reflections as it propagates back and forth along the tunnel, with each reflection leading to the emission of an MPW. These will be referred to in this report as **secondary MPWs**.

8.2.2.1 Pressure Wave Generation

As the train enters the tunnel, the nose of the train compresses the air in front of it, setting up a pressure wave. This is a 3D process and it takes a finite time to occur, leading to a pressure wave with a finite maximum gradient (not a shock wave, which would have close to infinite gradient). While the pressure wave magnitude is proportional to train speed squared, the gradient is proportional to train speed cubed. For this reason, even relatively modest increases in train speed can result in MPWs becoming a problem even if they were unnoticeable at a lower train speed.

The pressure gradient can be reduced by measures that reduce the pressure wave magnitude, such as increasing the cross-sectional area of the tunnel or decreasing the train speed, or by increasing the time taken for the pressure wave to build up to its full magnitude through modifications to the geometry of the entry portal or the nose shape of the HST.

8.2.2.2 Pressure Wave Propagation

The pressure wave propagates along the tunnel at the speed of sound, in an essentially one-dimensional process. The pressure gradient changes during propagation. It is the pressure gradient when the wave reaches the exit of the tunnel that determines the amplitude of the MPW emitted. Severe cases of MPWs causing loud bangs occur when the pressure wave has become almost infinitely steep, i.e., the back of the wave has almost completely caught up with the front and the wave becomes a shock wave. The pressure gradient changes due to the following competing effects, all of which become more significant for longer tunnels:

- **Inertial steepening** tends to increase the gradient. This occurs because the front of the wave propagates through stationary air, while the back of the wave propagates through air that is moving in the same direction as the wave (and hence the speed of the back of the wave relative to the tunnel is greater). Additionally, the speed of sound in the pressurized air at the back of the wave is slightly greater than in the unpressurized air at the front. Since the back of the wave is traveling faster than the front, the distance between the back and the front reduces, and the pressure wave becomes steeper.
- Friction resists or damps the flow of air down the tunnel and tends to reduce the pressure gradient. Friction may be increased by discontinuities in the surfaces of the walls and track form.
- The presence of ballast tends to reduce the pressure gradient (**ballast effect**). This is due to air being lost from the pressure wave front as it passes into the air spaces between the ballast particles, resulting in the wave being spread over a greater distance.

In slab track tunnels, the inertial steepening process dominates. The pressure wave becomes steeper as it propagates ([Figure 8-2](#)). The longer the tunnel, the more time is available for this process to occur, the greater is the pressure gradient at the tunnel exit, and the greater is the amplitude of MPW emitted.

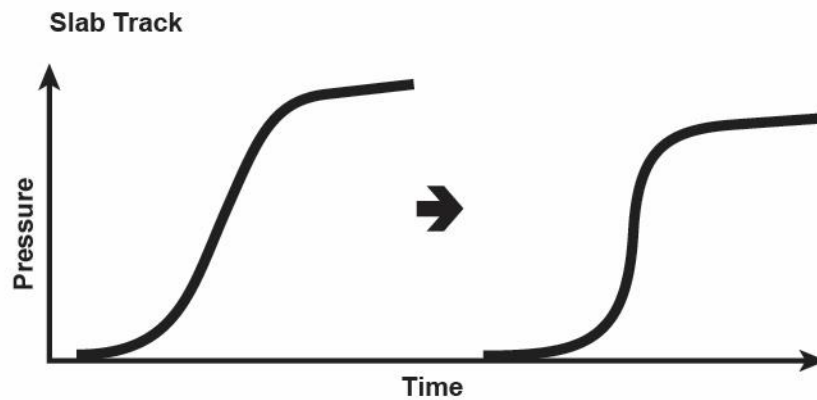


Figure 8-2. Pressure gradient increasing during propagation, typical of slab track tunnels

In long, ballasted track tunnels, the ballast effect usually dominates. The pressure gradient reduction rate, due to the ballast effect, more than cancels out the inertial steepening. The gradient of the pressure wave reduces as it propagates ([Figure 8-3](#)). Therefore, MPW problems have not typically been reported in long ballasted track tunnels. However, it should not be assumed that a tunnel containing ballast will not produce unacceptable MPWs. For example, if the train entry speed is very high (leading to a very high amplitude pressure wave), inertial steepening may occur at a greater rate than can be counteracted by the ballast effect.

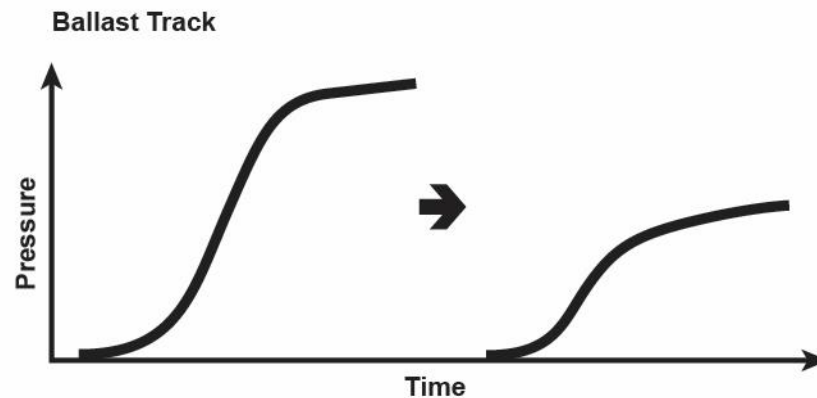


Figure 8-3. Pressure gradient decreasing during propagation, typical of ballasted track tunnels

8.2.2.3 MPW Emission

When the pressure wave reflects at the exit portal, a proportion of the energy is emitted into the environment as an MPW (see [Figure 8-4](#)). When the velocity of the air at the tunnel portal changes (due to arrival and reflection of the pressure wave), the portal acts like a loudspeaker. The amplitude of the MPW is proportional to the rate of change of momentum of the air at the tunnel exit. In practice, this means that it is proportional to the gradient of the pressure wave inside the tunnel as it approaches the tunnel exit (but

before it starts reflecting). It is also proportional to the cross-sectional area of the tunnel. A larger tunnel acts like a larger loudspeaker. This effect partially cancels out the benefit of the larger tunnel in terms of reduced pressure wave gradient.

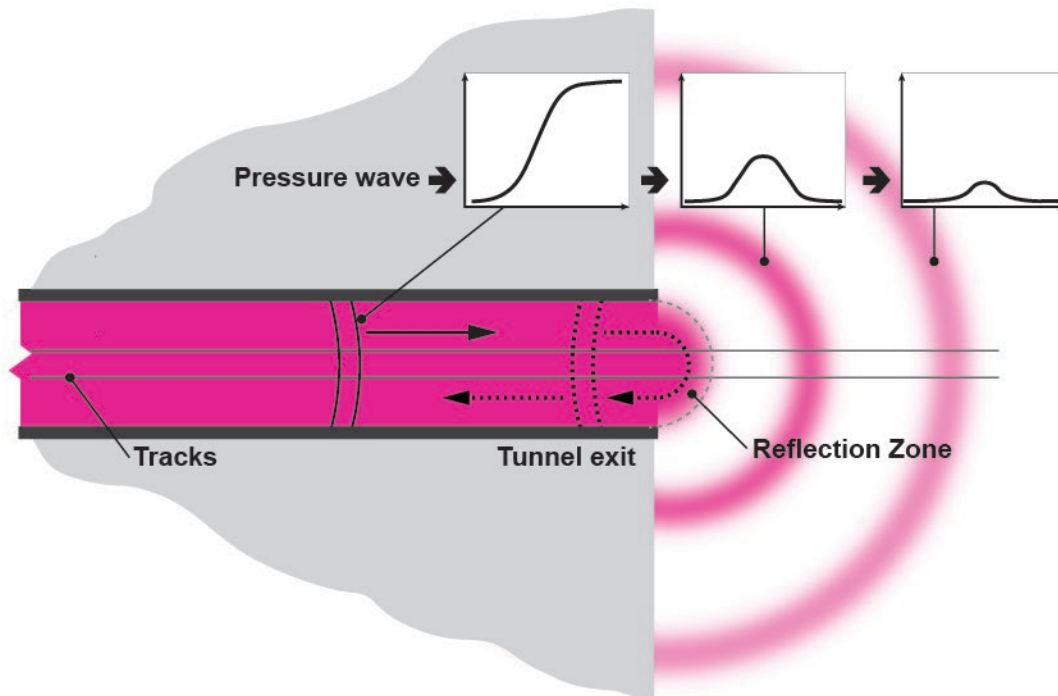


Figure 8-4. Pressure wave reflection and micro-pressure wave emission

8.2.2.4 MPW Transmission

When the MPW is emitted from the tunnel, it radiates out into the environment. The MPW amplitude reduces approximately in proportion to the inverse of distance from the portal. Thus, an observer at 200 ft (60 m) from the portal would experience half the amplitude compared with an observer at 100 ft (30 m) from the portal. The MPW amplitude is also dependent on the shape of the terrain around the tunnel exit. An MPW emitted from a tunnel in a large, vertical cliff-face will be concentrated into a quarter-sphere (see [Figure 8-15\(a\)](#)) bounded by the horizontal ground plane and the vertical cliff-face, while the MPW emitted from a tunnel emerging into almost-flat ground may be spread over almost a half-sphere (see [Figure 8-15\(b\)](#)).

Cuts or other large-scale local topography may funnel the MPW preferentially in certain directions. However, it is thought that MPWs are minimally affected by noise barriers or other objects intervening between the tunnel portal and the receiver if those objects are small compared to the wavelengths of the MPW, which is of the order of 50 to 500 ft (15 to 150 m).

8.2.3 Relationship between Properties of MPW and Noise

An MPW is a pulse of air pressure that may contain higher frequency components superposed on the underlying pulse. The amplitude of the MPW is the maximum air

pressure; this is the property of MPW that is most amenable to assessment. However, it is not the most relevant property to the potential noise impacts. Humans cannot hear frequencies below about 20 Hz (termed **infrasound**), and the sensitivity of our hearing increases greatly as the frequency increases up to around 1,000 Hz. Therefore, it is the higher-frequency components of the MPW that are more likely to be audible and should be of most concern in assessments. An MPW will contain audible noise if (a) wave steepening has occurred inside the tunnel such that the basic pulse of the emitted MPW is very short and sharp, i.e., it is itself high frequency; or (b) if the basic pulse is not audible, but the superposed higher frequencies are audible. When assessing a new tunnel design, situation (a) can be identified more readily than situation (b).

For existing tunnels, audible noise can be measured directly. However, when assessing new tunnels during design, the superposed high-frequency components of MPW cannot be predicted reliably. In this section, MPWs are described in terms of amplitude because that is the property that is most readily assessed. There is an implied assumption that, if the MPW amplitude is sufficiently low, then the high-frequency components of the MPW will be inaudible. Empirical evidence from Japan supports this for the limited range of conditions over which testing has been undertaken. Tunnels without mitigation produced high amplitude MPW with loud noises, but after mitigation was provided, both the MPW amplitude and the audible noise reduced [95]. Thereafter, mitigation was designed for other tunnels to achieve that same low amplitude of MPW that had been shown to correlate with an absence of problematic noise. However, the correlation between MPW amplitude being below a certain level and the absence of audible noise might not always be reliable, because there is not a fixed causal link between them.

8.2.4 Secondary Sources of MPWs

In this report the term **secondary MPWs** means MPWs arising from sources other than the initial entry of the train nose into the tunnel.

8.2.4.1 MPW Phenomena Related to Air Shafts

Air shafts connecting the tunnel to the open air have a beneficial effect on nose-entry MPWs because a proportion of the pressure wave propagates up the shaft instead of continuing along the main tunnel [123]. However, there is also the possibility of adverse impacts for the following reasons:

- MPWs can be emitted from the shaft portals due to wave reflections within the shafts, just as they are from the main tunnel portals. These could have unacceptable impacts in the environment around shaft portals.
- Pressure waves are generated when a train passes a shaft inside a tunnel (**junction waves**) [123]. They cause MPWs at the main tunnel portals and at the shaft portal which could potentially have unacceptable impacts, although no such examples have yet been found in practice at current operating speeds (up to around 180–200 mph). The MPW amplitude arising from junction waves is likely to be greater for higher train speeds and for larger diameter shafts.

8.2.4.2 MPWs Caused by Train Exit with Wave Propagation

Pressure waves are caused when a train exits from a tunnel. These waves propagate back along the tunnel towards the entrance and will result in MPWs when they reflect at the tunnel entrance. Typically, these waves are of lower amplitude (and therefore of less concern) than nose-entry waves, but if mitigation is required for nose-entry waves then it may be necessary to consider them.

8.2.4.3 MPWs Caused Directly by Train Entry/Exit without Wave Propagation

MPWs can be emitted directly from the portals as the train nose or tail enters or leaves the tunnel (**entry/exit waves**) [75]. Because the waves that cause these MPWs have not been transmitted down the tunnel, there is no chance for steepening to occur. These MPWs will be infrasound (which are low and often inaudible frequencies less than 20 Hz). In all cases reported to date, these waves are weaker than the nose-entry MPWs. Evidence from scale model experiments indicates that the waves are strongly directional, with much of the energy being directed into the tunnel rather than out into the environment. Therefore, entry/exit waves are unlikely to require assessment or mitigation if the nose-entry MPWs have already been determined to be acceptable.

8.3 Influencing Factors

The risk of problematic MPWs is increased under any of the following circumstances:

- High train speed
- Long, slab track tunnels
- Tight tunnels (high blockage ratio), especially for long tunnels
- Residential or other sensitive areas near the tunnel exit
- Terrain near the tunnel exit or entrance that funnels the emitted sound toward sensitive areas.

8.3.1 Train Speed

In practice, unacceptable MPWs have been experienced at speeds above about 125 mph (200 km/h).

For a short tunnel and a given train, the amplitude of the MPW is proportional to V_T^3 (where V_T is the speed at which the train enters the tunnel). In longer slab track tunnels there is an even greater impact from V_T because of wave-steepening, as shown in the example in [Figure 8-5](#). Therefore, the difficulty and the expense of designing and constructing tunnels to prevent unacceptable MPWs become much greater as speeds increase from 125 mph (200 km/h) toward 250 mph (400 km/h). When considering an increase of speed on existing lines with tunnels, the possibility of unacceptable MPWs should be assessed even if no MPW problem was experienced at lower speeds.

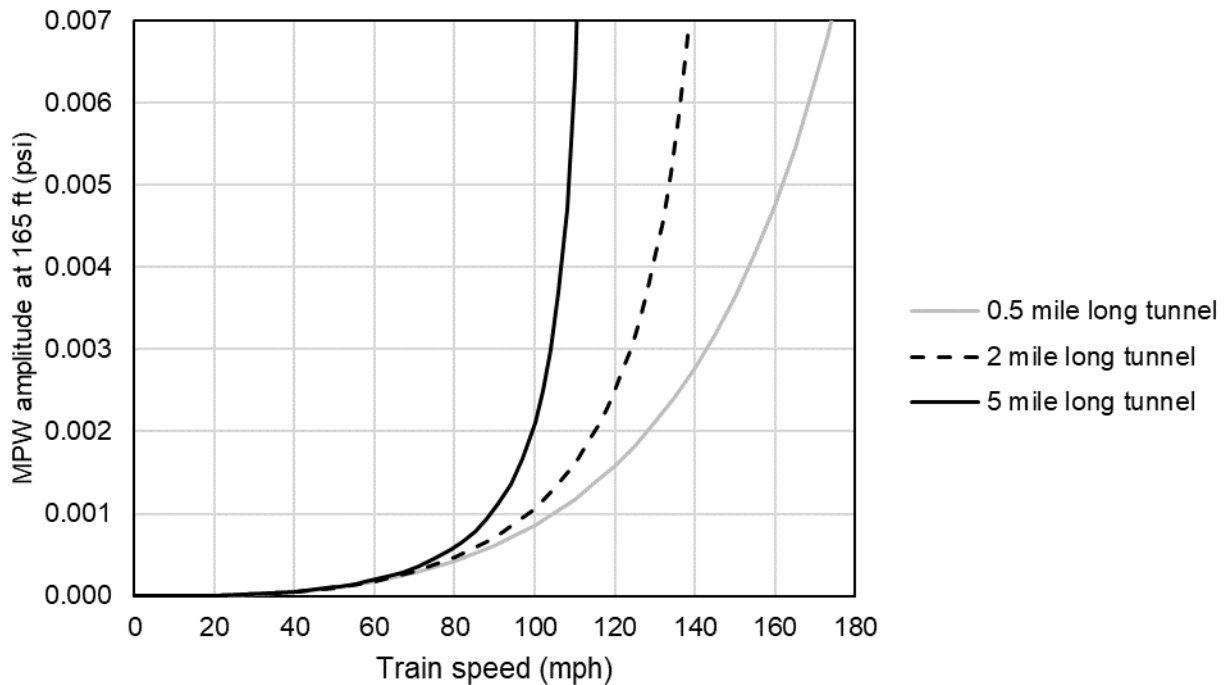


Figure 8-5. Example showing influence of train speed on MPW amplitude

The data presented in [Figure 8-5](#) are intended only to demonstrate the influence of train speed and should not be used for design. They were derived using the method described in [Section 8.6.2.2](#) with the following inputs:

- The tunnel has a cross-sectional area of 646 ft² (60 m²).
- The tunnel has no mitigation measures for MPW.
- The train has a cross-sectional area of 118 ft² (11 m²).
- The other calculation inputs are the same as in [Table 8-3](#).

8.3.2 Pressure Gradient

Not only does the amplitude of the emitted MPW increase with pressure gradient at the tunnel exit, but the rate of inertial steepening also depends on pressure gradient as shown in [Figure 8-6](#) (with gradients given in SI units for compatibility with assessment methods described in [Section 8.6.2](#)). Therefore, anything that increases the initial pressure gradient (such as increased train speed or blockage ratio) can have a very large influence on the amplitude of the emitted MPW. Furthermore, the dependence is not linear, and the pressure gradient can exhibit runaway steepening behavior and become a shock wave.

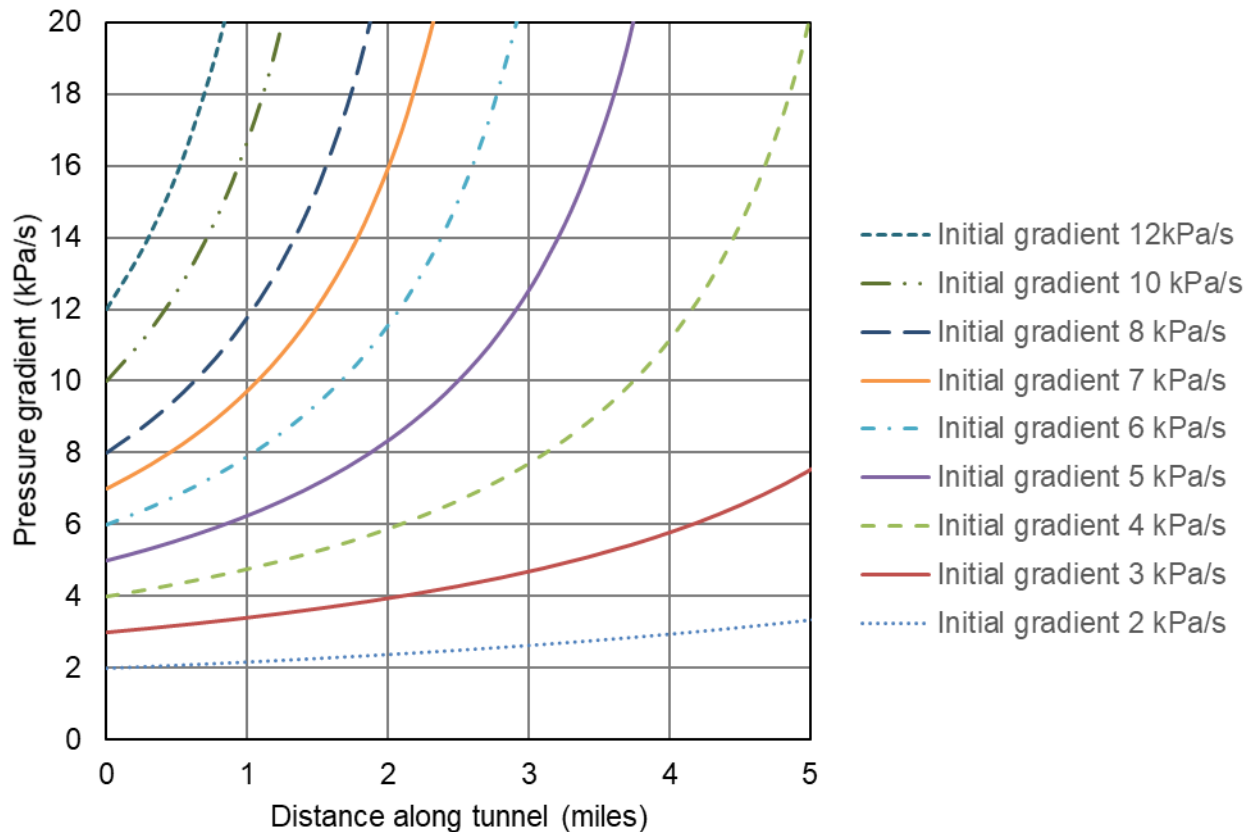


Figure 8-6. Influence of initial pressure gradient on inertial wave steepening.

8.3.3 Tunnel Length

For slab track tunnels, the longer the tunnel the greater the wave-steepening effect and, therefore, the greater the emitted MPW, as shown in [Figure 8-5](#) and [Figure 8-6](#).

8.3.4 Track Bed Type (Slab or Ballasted)

So far, unacceptable MPWs have been reported in the public domain only for long slab track tunnels. Ballast usually resists wave-steepening to a degree that more than compensates the inertial wave-steepening effect, thereby causing the gradient of the pressure wave to reduce rather than increase during propagation along the tunnel. However, impacts of MPWs from ballast track tunnels could potentially occur if the train speed and/or blockage ratio were high enough.

8.3.5 Blockage Ratio

High blockage ratio (defined in [Section 7.3.1](#)) leads to pressure waves of greater amplitude, with two influences on MPW generation:

- The initial pressure gradient is higher (due to greater pressure developing in the same time period).
- The wave-steepening effect is increased.

8.3.6 Train Aerodynamic Design

Trains with long, tapered noses extend the time over which the pressure wave builds up, leading to smaller initial pressure gradient and therefore reduced MPW emission.

8.3.7 Topography Near Tunnel Exit

As described in Section 8.2.3 above, the emitted MPWs can be directed or concentrated by natural or man-made topographical features such as hills, cuts, etc.

8.3.8 Locations of Receivers

In assessing the impacts of MPWs, a key consideration is the distance from the tunnel exit to people, and the distance to sensitive receivers such as residential buildings where the same people may be exposed to the impacts repeatedly. The degree of mitigation required for a given tunnel may be greater if sensitive receivers are close by.

8.4 Impacts

Impacts can potentially occur in the environment around tunnel portals and air shaft portals.

8.4.1 Noise Impacts

People and wildlife near a tunnel exit may hear an unpleasant or startling noise, such as a loud bang or a low booming noise. Annoyance is the most likely impact, especially for people living nearby who are exposed to MPWs repeatedly. Potentially, the noise could be loud enough to damage the hearing of a person standing near to the tunnel exit.

If sufficient steepening has occurred during propagation along the tunnel for the pressure wave to become almost a shockwave (in which the pressure gradient becomes close to infinite), the MPW may be heard as a loud bang and is likely to be audible over a large distance. If a shockwave has not developed, the MPW will likely consist of audible lower frequency noises or inaudible infrasound. Even though infrasound cannot be heard consciously, health impacts such as migraine or disturbed sleep may be caused by repeated exposure – this has been suggested by research into the rhythmic pulsing infrasound from wind turbines [128], but it is not known whether infrasound from MPWs could have the same impacts.

Audible MPW noise can be startling because it can occur without warning before the train itself is audible. For example, for a train speed of 175 mph and a 2-mile-long tunnel, the MPW is emitted about 30 seconds before the train emerges from the tunnel. The “surprise effect” can increase the impact of the noise.

Videos with audible MPWs may be found from internet search engines using the term “sonic boom rail tunnel.”

8.4.2 Vibration Impacts

The MPW consists of a pulse of air pressure that may cause doors or windows to rattle, leading to annoyance for residents. This impact can occur whether the MPW is audible or inaudible.

8.4.3 Impacts on Buildings

The pressure amplitudes and/or durations of MPWs are generally too small for structural damage to be considered as a possibility.

8.4.4 Impacts on People inside Trains

If pressure waves with high gradients are present in the tunnel, when these pass over trains within the tunnel, passengers and crew may be subjected to unpleasant noises [56].

8.5 Mitigation Methods

8.5.1 Tunnel Entrance Hoods

Tunnel hoods are extensions of the main tunnel entrance, usually perforated with holes, the role of which is to reduce the rate at which the pressure wave builds up when the train enters the tunnel. Hoods are the only well-established mitigation method capable of substantial reductions of impacts from MPWs.

8.5.1.1 Hood Layout

For double-track tunnels, the hood is a single structure spanning both tracks. Hoods are required at both ends of the tunnel because trains will enter the tunnel from both ends.

For single-track tunnels, each track on which trains enter the tunnel requires its own hood, although hoods on adjacent tracks may be designed as a single structure with an impermeable dividing wall between the tracks. During normal operation of the railroad, at each end of the tunnel, trains will enter the tunnel on one track and exit on the other track. Whether the exit track requires a hood depends on a number of considerations. Tunnel hoods are sometimes provided on the exit track to allow for “wrong way running” when one of the tracks is closed for maintenance or repairs. Hoods at the exit would also mitigate any MPWs caused when a train running in the usual direction exits from the tunnel. These types of MPWs are described in Sections [8.2.4.2](#) and [8.2.4.3](#).

8.5.1.2 Hood Form and Dimensions

Hoods are usually constructed of concrete or steel. The shape of the cross-section of the hood is not important for aerodynamics and is decided on the basis of cost, ease of construction, or aesthetics. Typically, hoods are parallel-sided with a uniform cross-sectional area between 1.3 and 1.5 times the cross-sectional area of the main tunnel.

Alternatively, but less common in practice, hoods may be funnel-shaped, with the cross-sectional area being larger at the entry portal, tapering down toward the main tunnel. For such hoods, it can be advantageous for the taper to lead to a smooth match with the cross-sectional area of the main tunnel. Hoods of this type are planned for a new high-speed railway in the UK [\[132\]](#).

Typical hoods in use today (for tunnels with train entry speeds up to about 185 mph (300 km/h)) are between 60 and 250 ft (18 to 75 m) long. The required length of hood for a given tunnel depends on the degree of mitigation required and increases strongly

with train speed (assuming that the acceptability criterion and all other conditions remain the same). The required length of the hood may be estimated by calculations, see Section 8.6.

Hoods usually have holes or slots in either the roof, walls, or both, enabling air to escape during the initial build-up of pressure. The optimum size and distribution of the holes is determined by reduced-scale model testing and/or CFD.

8.5.1.3 Example Tunnel Hoods

Steel hoods are sometimes used as a retrofit measure for existing tunnels thanks to rapid construction times [124]. A Japanese steel hood fitted to a double-track tunnel is shown in Figure 8-7.



Figure 8-7. Japanese tunnel entrance hood (steel) – retro-fitted to Ohirayama tunnel, from Maeda et al [94]; reproduced by kind permission of the authors

An example of a concrete hood is shown in Figure 8-8. This 165 ft (50 m) long hood is at the Katzenberg tunnel in Germany, where the line speed is 155 mph (250 km/h) [69]. The hood has slot-shaped holes and is covered with soil and grass, leaving only the rims of the holes protruding. An interesting feature of these hoods is that the holes through which air exits from the tunnel were intentionally built larger than the expected optimum size and covered by sliding plates so that final optimization of the hole size could be achieved by full-scale testing on the finished tunnel [69].

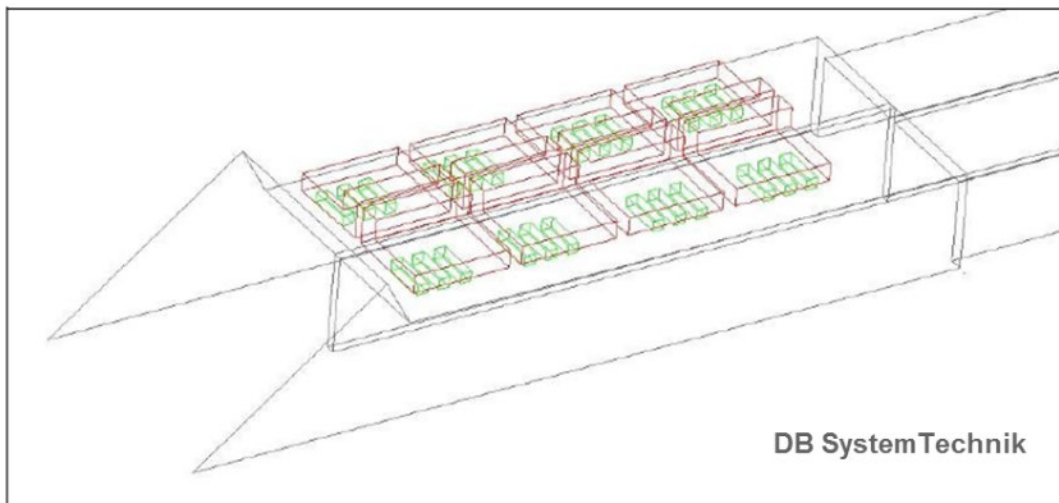


Figure 8-8. Katzenberg tunnel entrance hood, from Hieke et al [69]; photo reproduced with permission of DB Projektbau; schematic drawing with permission of DB SystemTechnik GmbH

Both of the above existing hoods are designed such that they provide the same level of mitigation for trains entering the tunnel on either track.

8.5.2 Tunnel Portal Shape

A small reduction of the pressure wave gradient may be obtained by sloping the entrance portal as shown in Figure 8-9, thus increasing the time over which the pressure wave builds up. This type of entrance is sometimes referred to as a **scarfed portal** or **penne pasta** portal shape. The portal plane is inclined at 45 to 60 degrees to the vertical. The benefit is relatively small (e.g., 10 to 20 percent reduction compared to a vertical portal plane). A scarfed portal cannot provide the same level of mitigation as a hood because the additional length over which the pressure wave builds up is only of the order of 10 to 20 ft, compared to a hood that may be of the order of 150 ft long.

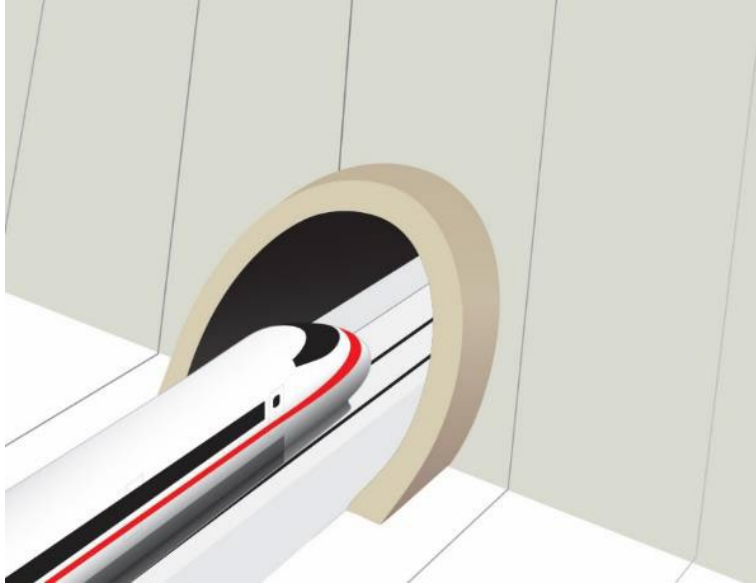


Figure 8-9. Scarfed portal shape

8.5.3 Train Nose Design

The duration of the nose-entry period can be increased (thus reducing the pressure gradient) using a long, tapering nose on the train. Some Japanese Shinkansen trains (see [Figure 8-10](#)) have tapering noses over 40 ft (12 m) long. The purpose of these is to allow trains to run at higher speeds without modifying the existing tunnels and without causing unacceptable MPWs, in cases where the required degree of mitigation is small. Tapered train noses are not a substitute for hoods where more substantial mitigation is required, because the length of the tapering train nose is much smaller than the length of typical hoods and hence the benefit in terms of reduction of pressure gradient is also much smaller.



Figure 8-10. Nose of Shinkansen E5

8.5.4 Acoustic Absorbers

Acoustical track absorbers were used as a retro-fit measure in Euerwang tunnel in Germany after sonic booms occurred during testing [\[24\]\[69\]](#); see [Figure 8-11](#). The absorbers are a commercial product designed to reduce vibration from trains, but also

have the effect of reducing the rate of wave steepening within the tunnel. They were glued to the track slab along the full length of the tunnel.



Figure 8-11. Acoustic absorbers fitted in Euerwang Tunnel, from [69], photographer Peter Deeg, DB Systemtechnik GmbH

The degree of mitigation obtained from this arrangement, although sufficient in this case, was relatively modest and would not suffice for all tunnels. Increased levels of mitigation may be obtainable by increasing the cross-sectional area of absorbers. Other materials may be used to similar effect; for example, promising results have been reported from scale model experiments with porous resin fixed to the tunnel walls [104].

8.5.5 Ballast and Ballast Effect Mitigation Measures

The beneficial effect of ballast, especially in long tunnels, has been well documented [108][55]. Selecting a ballasted track system is therefore a mitigation measure for MPWs in long tunnels. However, the choice of track type is normally governed by other considerations (e.g., cost, construction program, etc.).

Even if the tunnel employs a slab track system, it may be possible to place some ballast within the tunnel if there is sufficient space. Successful experiments along these lines have been performed in Japan [85], but this method has not been used in operational HSR tunnels.

There is no reliable method available to calculate the amount of ballast required; this should be determined by full-scale testing.

Some authors have suggested that the effect of ballast could be replicated by a series of air spaces connected to the main tunnel via small holes [133] but this type of mitigation has not been applied in full-scale operational tunnels.

8.5.6 Speed Restrictions

A very effective method of reducing MPWs is reducing the speed of entry of the train into the tunnel. The speed could increase once the train is inside the tunnel. This mitigation measure has the obvious advantage of having no incremental construction

cost, but the disadvantages of an impact on operations and a small impact on journey times.

8.5.7 Other Beneficial Factors

These could not be described solely as mitigation measures for MPWs because their selection is dictated by other considerations. However, they do offer some side benefits for mitigating MPWs.

8.5.7.1 Air Shafts

Air shafts can reduce passing pressure waves and thereby reduce their gradient. Shafts can therefore be an effective mitigation measure for the nose-entry MPWs. However, new pressure waves arise when trains pass the shafts within the tunnel, with the potential to cause unacceptable MPWs.

8.5.7.2 Closed Side Passages

Closed side passages are short blind tunnels perpendicular to the main tunnel (shown schematically in [Figure 8-12](#)). These are a feature of Japanese HSR tunnel design where they are provided approximately every 1,000 to 1,600 ft (300 to 500 m) along the tunnel. Although their primary purpose is unrelated to MPWs, they help reduce the gradient of the pressure wave as it propagates along the tunnel because some of the pressurized air at the front of the wave passes into the side passages, thus delaying the build-up of pressure downstream [\[55\]](#).

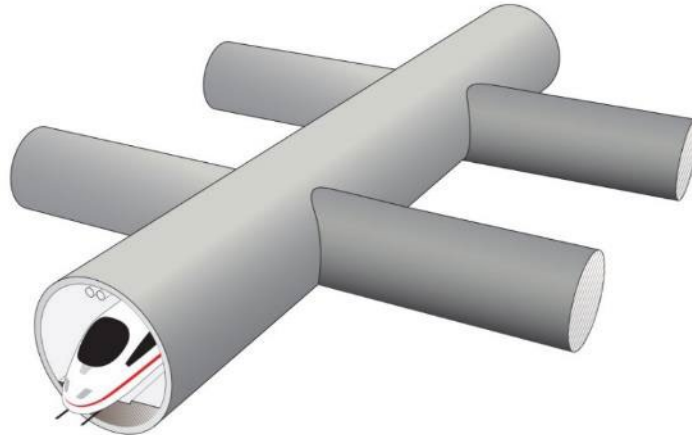


Figure 8-12. Schematic sketch showing closed side passages

8.5.7.3 Train Cross-Sectional Area

If reducing the train cross-sectional area is under consideration for economic or other reasons, the reduction also benefits MPW performance because the pressure in the tunnel is reduced, thus reducing both the initial pressure gradient and the rate at which the pressure wave steepens. For example, a 10 percent reduction of train cross-sectional area could reduce MPW amplitude by around 15 percent or more depending on the length of the tunnel.

8.6 Assessment

8.6.1 Assessment Objectives and Scope

The objectives of assessments for MPW impacts are to determine the following:

- Whether mitigation of MPWs is required for a particular tunnel.
- Which design of mitigation measures will be effective, for example the length and other dimensions of a hood.

8.6.1.1 Types of Tunnels that Should Be Assessed for MPW Impacts

Historically, noticeable MPWs have occurred only in long tunnels equipped with slab track. However, if the train speed and/or blockage ratio were high enough, unacceptable MPWs could occur even in short tunnels and in tunnels with ballasted track for these reasons:

- In a short tunnel, there is little time for the pressure gradient to change. The pressure gradient at the tunnel exit will be almost the same as at the tunnel entrance, whether the tunnel has ballasted track or slab track. The pressure gradient due to train nose entry could be sufficient to cause an MPW problem even in the absence of significant wave steepening.
- In a long, ballasted track tunnel, if the pressure wave gradient is high enough, the inertial steepening rate might be too large to be overcome by the ballast effect.

The implication is that at least an initial MPW assessment should be carried out for all new HSR tunnels during design, whether slab track or ballasted track. However, since assessment of ballasted track tunnels is difficult due to a lack of methods to calculate the beneficial influence of ballast on the propagating pressure wave, the following approach is proposed:

- All slab track tunnels should be assessed.
- As a very rough guide, ballasted track tunnels that are longer than 1 mile (1,600 m) and have a train entry speed less than 150 mph (240 km/h) can be excluded.
- Ballasted track tunnels up to 1 mile long may be assessed using the same methods as for slab track tunnels. The assessment will be somewhat conservative because the wave steepening effect will be overestimated, but with short tunnels the influence is small.
- Ballasted track tunnels longer than 1 mile with train entry speed 150 mph or over require further research.

8.6.1.2 Priorities for Assessment and Mitigation

As has been described in the preceding sections, there are several sources of pressure waves that can each lead to emission of MPWs.

In general, the nose-entry MPWs should be considered first and will result in the greatest amplitude MPWs in the absence of mitigation. If the nose-entry MPWs are

deemed acceptable without requiring mitigation, then the secondary MPWs can be ignored.

In the event that mitigation *is* required for the nose-entry MPWs, attention should then turn to the secondary MPWs which may become the critical case after the nose-entry MPWs have been addressed. For example, after providing a tunnel entrance hood to mitigate nose-entry MPWs, then the critical case for adverse impacts could become MPWs caused by the train exiting from the tunnel or passing an air shaft inside the tunnel.

8.6.1.3 Assessment and Mitigation Summary

The procedures above are summarized in [Figure 8-13](#), together with an outline of the assessment process described in Section [8.6.2.2](#).

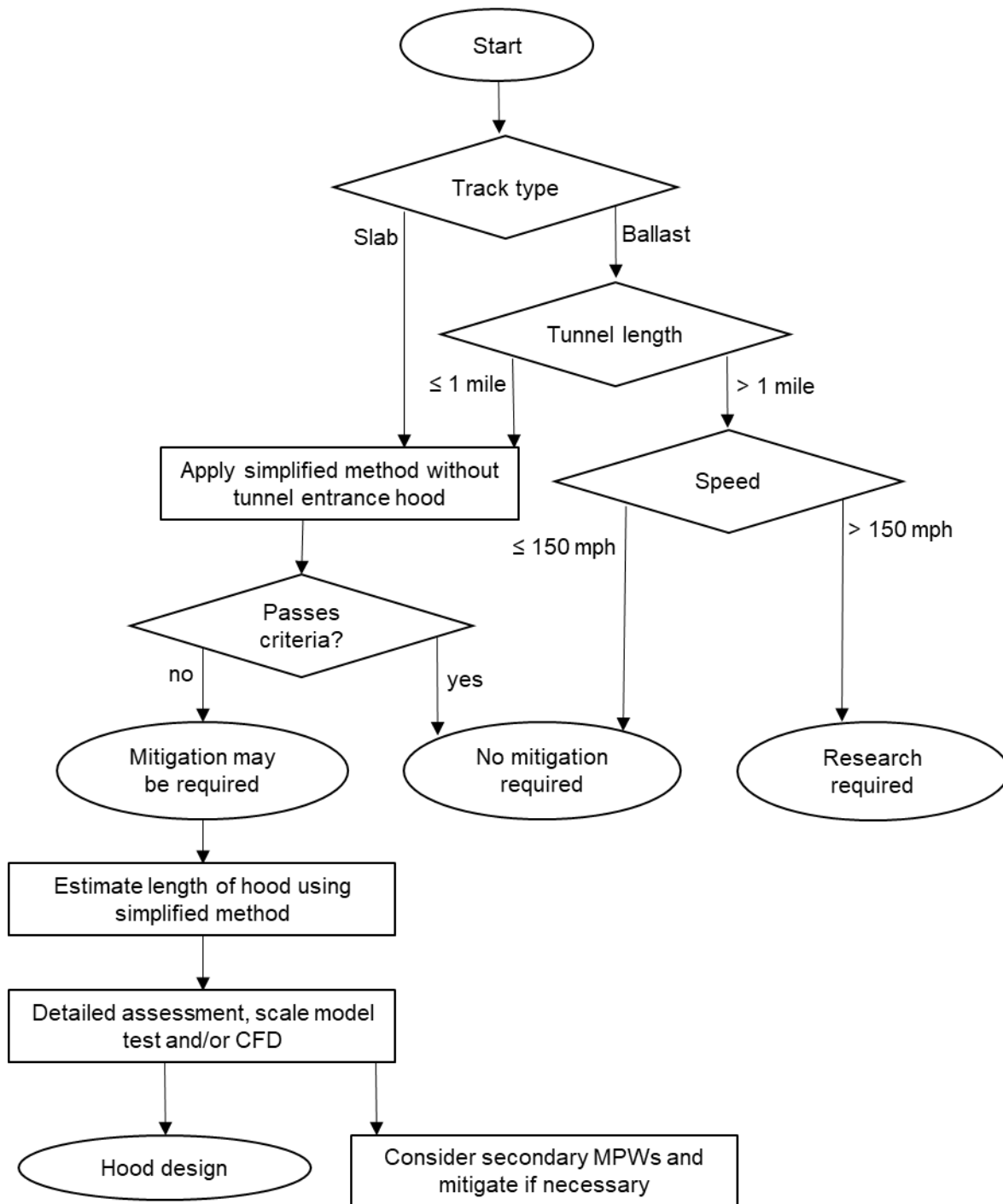


Figure 8-13. MPW assessment and mitigation summary

8.6.2 Assessment Methods

8.6.2.1 Assessment and Calculation Methodologies Summary

The four phases of MPW generation and transmission are evaluated in a sequence chain, with the output from one phase becoming the input for the next. As a baseline for initial assessments, all four phases can be treated by the simplified method based on

formulae described in Section 8.6.2.2 with conservative choices for the input parameters. If this indicates that mitigation for MPW is not required, no further action is necessary. On the other hand, if mitigation is shown to be necessary, the treatment of one or more of the phases may be replaced by more accurate methods, as shown in Table 8-1 below.

Table 8-1. Assessment methods for MPW

Methodology	Wave generation	Wave propagation	MPW emission	MPW transmission
Initial Assessment	Simplified	Simplified	Simplified	Simplified
Detailed Assessment (example given in [68])	Scale model or CFD or 1-D analysis ¹	1-D analysis	Improved formulae or CFD	Improved formulae or CFD
Notes:				
1. 1-D analysis is suitable for tunnels with long perforated hoods only.				

It is usually possible to make conservative assessments of the MPW amplitude that will be emitted from a given tunnel using the simplified method. Because of the conservatism of the method, there will be a tendency to over-design mitigation, potentially leading to unnecessary expense. The main obstacles to more accurate (i.e., less conservative) assessments are:

- The tunnel entry phase requires investment in 3D analysis methods. This is especially important where no hood (or only a short hood) is to be provided, and for very short tunnels (shorter than about ten times the tunnel diameter).
- In long tunnels, the wave propagation phase is subject to beneficial damping and dissipation effects that are difficult to predict.
- Topography around the tunnel exit has an unpredictable influence on MPW transmission to receivers.

8.6.2.2 Simplified Method

The recommended method for assessing MPWs described below is from Vardy [150] and can be carried out using a calculator or spreadsheet. The method applies to plain tunnels without air shafts, cross-passages, or other complex features.

The method includes conservative simplifications and assumptions in order to avoid the need for complex analysis. These tend to stack up through the steps of the calculation, making the overall result very conservative in some cases. If used for design, the method could lead to the over-provision of mitigation and therefore unnecessary expense. Therefore, it is appropriate only as an initial screening assessment to determine whether more detailed consideration is necessary and as an aid to understanding the MPW phenomenon.

The assessment covers the four phases, namely pressure wave generation, wave steepening, MPW emission, and transmission, using theoretically derived equations

with some empirical constants. Note that this simplified method estimates only the amplitude of the MPW; other properties such as the frequency content may influence the audibility and impact of the MPW but are not included in this assessment method.

The calculation steps and the associated assumptions and limitations are explained in Sections 8.6.2.2.1 through 8.6.2.2.4, with a summary of the equations given in Section 8.6.2.2.5. A more comprehensive guide may be found in [150].

All of the equations given in this section require consistent units (see Section 2.7), with SI units being strongly recommended.

8.6.2.2.1 Simplified Method, Phase 1: Wave Generation

For this step, the aim is to estimate the maximum gradient of the pressure wave near the tunnel entrance.

The relevant properties of the nose-entry wave are idealized as shown in Figure 8-14. It should be recognized that wave formation during train nose entry is a 3D process affected by parameters such as the shape of the tunnel and train nose. These complex behaviors cannot be assessed accurately using such simple methods – therefore, the formulae represent a rough guide only.

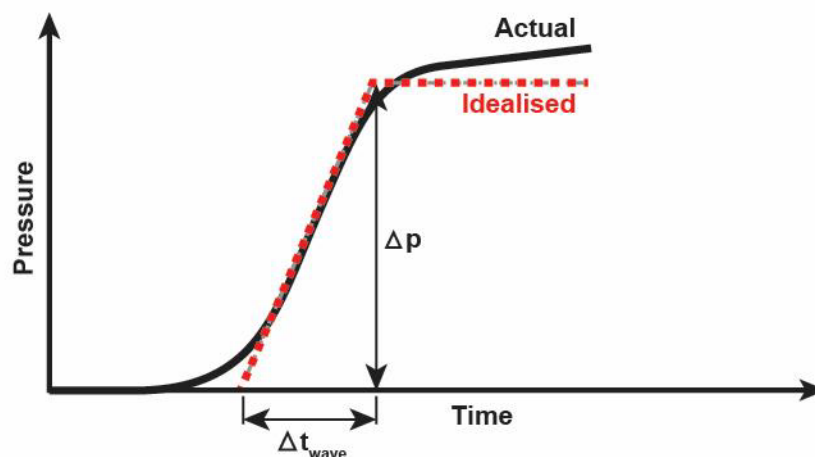


Figure 8-14. Nose-entry wave, actual and idealized

Step 1: Calculate the expected pressure rise caused by the nose entering the tunnel.

Calculate the pressure wave amplitude, Δp , as follows:

$$\alpha = \frac{1 + k_N}{(1 - \beta)^2} - 1 \quad \text{Equation 8-1}$$

$$\Delta p = \rho c \left\{ V_T + \frac{c}{\alpha} \left[1 - \sqrt{1 + \frac{2\alpha V_T}{c}} \right] \right\} \quad \text{Equation 8-2}$$

Where:

k_N = Dimensionless “nose loss factor” of the train, typically 0 to 0.1 for HSTs;

β = Blockage ratio (see Section 7.3.1);

ρ = Density of air, in kg/m³, standard value 1.225 kg/m³;

c = Speed of sound in air, in m/s, standard value 340 m/s;

V_T = Speed of the train in m/s; and,

Δp = Pressure wave amplitude, in Pa.

Step 2: Calculate the “effective entry length” L_E .

The entry length may be thought of as the physical distance through which the train travels at the entrance to the tunnel, over which the idealized pressure wave develops.

As an initial estimate, the following formula may be used for a plain tunnel *without an entrance hood*:

$$D_T = \sqrt{4A_T/\pi} \quad \text{Equation 8-3}$$

$$L_E = \phi D_T \quad \text{Equation 8-4}$$

Where:

A_T = Cross-sectional area of tunnel, in m²;

D_T = Effective diameter of tunnel, in m;

ϕ = Tunnel/train shape coefficient (see below);

ρ = Density of air, in kg/m³, standard value 1.225 kg/m³;

L_E = Effective entry length, in m.

The coefficient ϕ is likely to lie in the range 0.75 to 1.5 for a flat-fronted train, and between 1.0 and 2.0 for the elongated noses that are typical of HSTs. For a more accurate assessment, values can be determined from scale model testing or from three-dimensional analysis methods such as CFD.

For tunnels *with an entrance hood*, the effective train entry length becomes:

$$L_E = \eta_H L_H \quad \text{Equation 8-5}$$

Where:

L_H = Length of hood, in m;

η_H = Efficiency of hood, typically 0.5 to 0.8 for a well-designed hood; and,

L_E = Effective entry length, in m.

Step 3: Calculate the effective rise-time of the pressure wave and its gradient near the tunnel entrance.

$$\Delta t_{wave} = L_E \left(\frac{1}{V_T} - \frac{1}{c} \right) \quad \text{Equation 8-6}$$

Where:

L_E = Effective entry length from [Equation 8-4](#) or [Equation 8-5](#)

c = Speed of sound in air, in m/s;

V_T = Speed of the train in m/s;

Δt_{wave} = Rise time of pressure wave near tunnel entrance, in seconds.

The maximum pressure gradient near the tunnel entrance is given by:

$$\frac{dp_{entry}}{dt} = \frac{\Delta p}{\Delta t_{wave}} \quad \text{Equation 8-7}$$

Where:

Δp = Pressure wave amplitude, in Pa, from [Equation 8-2](#);

Δt_{wave} = Rise time of pressure wave, in seconds, from [Equation 8-6](#);

$\frac{dp_{entry}}{dt}$ = Maximum pressure gradient at tunnel entrance, in Pa/s.

8.6.2.2.2 Simplified Method Phase 2: Wave Propagation (Steepening/Shortening)

It is helpful to think of the steepening of the pressure wave as a reduction of its spatial length while its pressure amplitude remains unchanged. In other words, the wave shortens as it moves down the tunnel. This occurs primarily because the front of the wave is traveling through stationary air, while the rear of the wave is traveling within air moving down the tunnel with velocity $\Delta p/\rho c$. In addition, the speed of sound in the compressed air at the rear of the wave is greater. Therefore, the rear of the wave catches up with the front. This process of shortening of the wave is known as “inertial steepening” and may be estimated using the following equations:

$$\Delta t_{wave,exit} = \Delta t_{wave} - \frac{1.2\Delta p L_T}{\rho c^3} \quad \text{Equation 8-8}$$

Where:

Δt_{wave} = Rise time of pressure wave near tunnel entrance, from Equation 8-6;

Δp = Pressure wave amplitude, in Pa, from Equation 8-2;

L_T = Length of tunnel, in m;

ρ = Density of air in kg/m³, standard value 1.225 kg/m³;

c = Speed of sound in air in m/s, standard value 340 m/s;

$\Delta t_{wave,exit}$ = Rise time of pressure wave near tunnel exit, in seconds.

Note that the equation above considers inertial steepening only. It excludes the beneficial effects of friction and damping which counteract the steepening of the pressure wave, but these effects are difficult to quantify in a formula-based method, and the level of damping cannot be estimated without full-scale measurements. As a conservative first assumption, these effects may be ignored. The longer the tunnel, the more conservative this assumption becomes.

The equation also excludes any beneficial effect of ballast and would be extremely conservative if applied to long ballasted track tunnels. As a rough guide, do not apply this method to ballasted track tunnels longer than 1 mile.

If Equation 8-8 indicates shortening by more than the initial length of the wave, i.e., $\Delta t_{wave,exit} \leq 0$, then a shock is predicted within the tunnel and the MPW is very likely to be unacceptable and assessment can stop at this point. If not, then continue to calculate the pressure gradient at the tunnel exit:

$$\frac{dp_{exit}}{dt} = \frac{\Delta p}{\Delta t_{wave,exit}} \quad \text{Equation 8-9}$$

Where:

Δp = Pressure wave amplitude, in Pa, from Equation 8-2;

$\Delta t_{wave,exit}$ = Rise time of pressure wave near tunnel exit, from Equation 8-8

$\frac{dp_{exit}}{dt}$ = Maximum pressure gradient at tunnel exit, in Pa/s.

The above equations can be combined as follows:

$$\frac{dp_{exit}}{dt} = \frac{1}{\frac{1}{\frac{dp_{entry}}{dt}} - \frac{1.2L_T}{\rho c^3}} \quad \text{Equation 8-10}$$

Where the terms are as defined in Equation 8-7 through Equation 8-9.

If Equation 8-10 gives a negative pressure gradient, a shock is predicted (unacceptable result) and the assessment can stop at this point.

A more accurate assessment of the steepening of the pressure wave during propagation can be obtained from one-dimensional analysis using specialized software. The inclusion of tunnel wall friction in the analysis is beneficial because, as the wave propagates, its amplitude (Δp in the above equations) reduces, thereby reducing the tendency for the wave to steepen. The longer the tunnel, the more beneficial this effect becomes, and the more conservative the above equations become since they omit the friction effect.

8.6.2.2.3 Simplified Method Phases 3 and 4: MPW Emission and Transmission

The amplitude of the MPW at the standard assessment point 165 ft (50 m) from the tunnel exit, and at the critical receiver (such as the nearest residential building), are given by:

$$p_{MPW,sap} = \left(2A_T / \Omega c r_{sap} \right) \frac{dp_{exit}}{dt} \quad \text{Equation 8-11}$$

$$p_{MPW,cr} = \left(r_{sap} / r_{cr} \right) p_{MPW,sap} \quad \text{Equation 8-12}$$

Where:

A_T = Cross-sectional area of tunnel, in m²;

Ω = Solid angle for emission of MPW, in steradians, see below;

c = Speed of sound in air in m/s, standard value 340 m/s;

r_{sap} = Distance to standard assessment point, in m, standard value 50 m;

r_{cr} = Distance to critical receiver, in m;

$\frac{dp_{exit}}{dt}$ = Maximum pressure gradient at tunnel exit, in Pa/s.

$p_{MPW,sap}$ = MPW amplitude at standard assessment point, in Pa;

$p_{MPW,cr}$ = MPW amplitude at critical receiver, in Pa;

The equations are valid only for values of r_{sap} and r_{cr} greater than twice the tunnel diameter.

The equation above assumes that the MPW spreads out uniformly in all directions within the solid angle Ω . Theoretical values of Ω for simple geometries range from π (the solid angle of a quarter-sphere) for emission into the air between a flat ground plane and large vertical cliff face, to 2π (a hemisphere) for emission into the air above a featureless flat ground plane; see [Figure 8-15](#). However, in practice the MPW amplitude varies with the angle between the path to the receiver and the track and is strongly influenced by topography. The directionality of MPWs is not fully understood in practice, and this should be accepted as a limitation of the assessment process. The solid angle Ω may be regarded as an empirical factor describing how the local topography concentrates the MPW in certain preferential directions. Experimental measurements of MPWs show that the values of Ω vary widely according to

measurement position, even at the same tunnel portal [70]. In the absence of better information, values of around π to 1.75π steradians may be used where the line from tunnel exit to receiver is at least 45 degrees from the track direction. Smaller values are more conservative and result in larger predicted MPW amplitudes. Values at the lower end of the range should be used for receivers less than 45 degrees from the track direction.

In the case of tracks emerging from a tunnel into a semi-confined space such as a cut, the solid angle may be as low as 1 to 2 steradians for MPW reaching any critical receivers within the confined space.

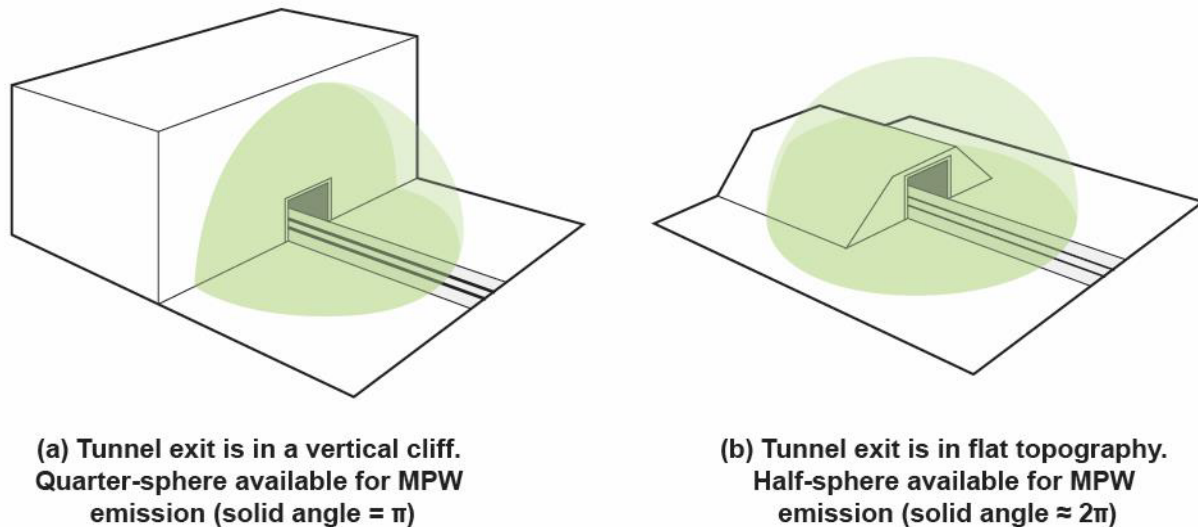


Figure 8-15. Spherical influence of solid angle for vertical cliff face and flat topography

As well as the uncertainty surrounding Ω , the above equation has limitations related to the accuracy of the relationship with distance, and to the range of frequencies for which it applies. More accurate formulae are available in the literature [70][98][150] but, given the other uncertainties, there is little benefit in refining this part of the assessment.

If a hood is provided at the tunnel exit, its effect on MPW emission cannot be assessed by simple methods. Its influence on MPW amplitude is likely to be either neutral or beneficial, with the MPW emission being spread between the holes in the hood and the hood exit portal. However, the addition of the hood could bring the MPW emission point closer to a critical receiver. As a conservative simplification, the following procedure is recommended:

- The pressure gradient and tunnel area in Equation 8-11 should be calculated as if no hood were provided at the tunnel exit.
- The distance to the critical receiver should be measured either to the hood exit portal, or to the nearest hole in the hood, whichever is closer.

- The calculations related to the standard assessment point are the same as if no hood were provided.

If a more accurate assessment is needed, CFD analysis could be undertaken.

8.6.2.2.4 Simplified Method: Assessment Result

The MPW amplitudes at the standard assessment point 165 ft (50 m) from the tunnel exit, and at the critical receiver, should be compared against the criteria set by the operator. For example, if using the criteria proposed in Section 8.6.3.1, then:

$$\begin{aligned} p_{MPW,sap} &\leq 20 \text{ Pa} \\ p_{MPW,cr} &\leq 10 \text{ Pa} \end{aligned} \qquad \text{Equation 8-13}$$

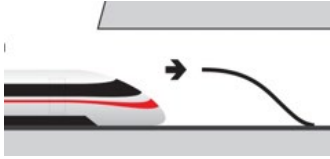
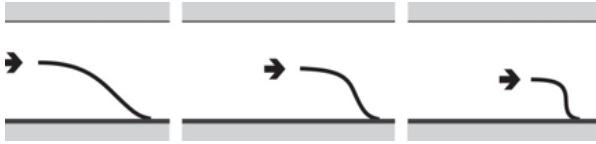
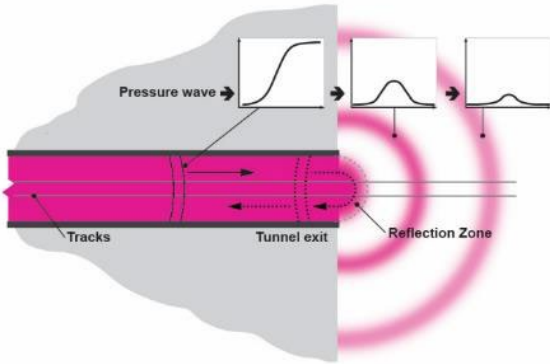
Note the limitations of these criteria, described in Section 8.6.3.1.

If either of the criteria is not met, then mitigation may be required. The approximate length of hood can be estimated by repeating the calculations using hoods of different lengths (L_H in Equation 8-5). The hood length derived by this method is likely to be conservative. The hood design can be refined later using scale model testing and/or CFD. A typical sequence of assessment processes is shown in Figure 8-13.

8.6.2.2.5 Simplified Method: Summary

The key equations are summarized in Table 8-2. For details of the symbols used, see Equation 8-1 through Equation 8-12 in Sections 8.6.2.2.1 through 8.6.2.2.4.

Table 8-2. Summary of simplified assessment method; see Sections 8.6.2.2.1 through 8.6.2.2.4 for details

Phase	Equations
Pressure wave generation 	$\alpha = \frac{1 + k_N}{(1 - \beta)^2} - 1$ $\Delta p = \rho c \left\{ V_T + \frac{c}{\alpha} \left[1 - \sqrt{1 + \frac{2\alpha V_T}{c}} \right] \right\}$ $\Delta t_{wave} = L_E \left(\frac{1}{V_T} - \frac{1}{c} \right)$
Wave propagation 	$\frac{dp_{exit}}{dt} = \frac{1}{\frac{1}{\frac{dp_{entry}}{dt}} - \frac{1.2L_T}{\rho c^3}}$
MPW emission and transmission 	$p_{MPW} = \left(2A_T / \Omega_{cr} \right) \frac{dp_{exit}}{dt}$ $p_{MPW} \leq 20 \text{ Pa for } r = 50 \text{ m}$ $p_{MPW} \leq 10 \text{ Pa for } r = r_{cr}$

8.6.2.2.6 Simplified Assessment Method Outcomes

The simplified method of assessing MPWs tends to produce a conservative result. It may suggest that a hood is required when in reality no impacts would occur without a hood; or, it may exaggerate the required length of hood. This happens for a number of reasons:

- Realistic values of several of the input parameters are unknown for the tunnel being assessed, so it is appropriate to make conservative choices.
- The wave propagation formulae ignore the beneficial effect of friction and damping (the longer the tunnel, the more significant this becomes).
- The acceptability criteria may be conservative in some cases.
- Because the assessment is performed in a chain of steps, the conservative assumptions stack up.

To illustrate the sensitivity of results to the assumptions and calculation methods, two example tunnels are assessed below. In each case, real-life HSR tunnels exist that are similar to the example, and no unacceptable MPW impacts occur. The calculations have been performed using the simplified method with the two sets of input parameters shown in [Table 8-3](#), labelled A and B, with A being more conservative than B. One of the examples has been calculated by a third method, labelled C, which is the same as B except that the wave-steepening step has been analyzed by one-dimensional software including the effects of friction and damping (the input values used for these parameters are broadly representative of European slab-track tunnels).

Table 8-3. Parameters and wave-steepening calculation methods used in assessments of example tunnels

	Assessment basis		
	A	B	C
Train nose loss factor Used in Equation 8-1 .	0.05	0.025	0.025
Tunnel entry shape coefficient ϕ Used in Equation 8-4 when no hood is provided.	1.25	1.6	1.6
Hood efficiency factor η Used in Equation 8-5 when a hood is provided.	0.5	0.7	0.7
Wave steepening calculation method	Simplified method; see Section 8.6.2.2.2 .	Simplified method; see Section 8.6.2.2.2 .	One-dimensional analysis with friction and damping
Solid angle for MPW emission	1.25π	1.5π	1.5π

Example 1: Short, double-track tunnel

The first example is a short double-track tunnel (in this case, 0.25 miles long) with a line speed of 185 mph (300 km/h). There are many tunnels like this in Europe. These short tunnels are not provided with hoods.

Results of the assessments are shown in [Table 8-4](#). Assessment A produces a predicted MPW amplitude 70 percent greater than assessment B. The large difference is indicative of the stack-up effect of the assumptions. Assessment A concludes that a 145 ft long hood is needed. Since the real-life tunnels do not have hoods and no MPW impacts have been noticed, assessment A is conservative. With input parameter set B, the tunnel only just passes the assessment without a hood, suggesting that if the train speed were slightly faster, then the assessment would conclude that a hood is required. The assessment criterion may be conservative for this type of tunnel.

In such a short tunnel, there is negligible wave steepening, so assessment method C (which differs from B only with respect to the wave steepening calculation) was not performed.

For details of how the calculations are carried out, see the examples in Section 8.6.4.

Table 8-4. Example of MPW assessment results: short, double-track tunnel

	Short, double-track tunnel	
Tunnel length	0.25 miles (0.4 km)	
Tunnel area	990 ft ² (92 m ²)	
Train type	European HST	
Train speed	185 mph (300 km/h)	
Real-life hood length	None	
Assessment	A	B
Calculated MPW amplitude at standard assessment point with no hood	0.0049 psi (34 Pa)	0.003 psi (20 Pa)
Assessment result with no hood	Fail	Pass
Calculated hood length to pass the assessment	145 ft (44 m)	Not required

Example 2: Long, single-track tunnel

This example is similar to a German tunnel which has 165 ft (50 m) long hoods. The real-life tunnel also has air shafts which are ignored in the assessment here, but nevertheless the assessment results demonstrate the sensitivity to input assumptions.

Results of the assessments are shown in Table 8-5. With input parameter set A, the assessment predicts a shock in the tunnel which would likely manifest outside the tunnel as a loud bang. Since the real-life tunnel produces no such effect, assessment A is conservative. Assessment B leads to a somewhat conservative conclusion, i.e., that the hood needs to be 180 ft long whereas the real-life tunnel has a 165 ft long hood. The inclusion of friction and damping in the wave-steepening calculation in assessment C leads to an MPW amplitude about half of that from assessment B. The longer the tunnel, the more conservative it becomes to neglect these effects. Assessment C correctly predicts that the real-life hood length is adequate, although the degree to which the numerical result is conservative or non-conservative is unknown.

Table 8-5. Example of MPW assessment results: long, single-track tunnel

	Long, single-track tunnel		
Tunnel length	5.8 miles (9.4 km)		
Tunnel area	646 ft ² (60 m ²)		
Train type	European HST		
Train speed	155 mph (250 km/h)		
Real-life hood length	165 ft (50 m)		
Assessment	A	B	C
Calculated MPW amplitude at standard assessment point with real-life hood length	Shock wave in tunnel – loud bang	0.0045 psi (31 Pa)	0.0022 psi (15 Pa)
Assessment result with real-life hood length	Fail	Fail	Pass
Calculated hood length to pass the assessment	300 ft (91 m)	180 ft (55 m)	-

Given the high sensitivity of assessment results to the input parameter values and calculation methods and the generally conservative results, the simplified method as presented above should be used only as an aid to understanding MPWs and as an initial screening tool; if the tunnel passes the initial assessment, then it can be ruled out from further consideration for MPW impacts.

If assessments are to be used to determine the required length of hood for design purposes, greater accuracy is needed. The parameters related to train entry (nose loss factor, tunnel entry shape coefficient, and hood efficiency factor) may be calibrated against CFD or scale model testing; wave-steepening may be analyzed with one-dimensional analysis, as in assessment C above. The solid angle for MPW emission is subject to high variability in practice and is difficult to predict; therefore, the assessment should consider a range of values.

8.6.2.3 Use of Simplified MPW Assessment Method with Noise-based Criteria

The simplified method can estimate only the amplitude and duration of the air pressure pulse associated with the MPW. Noise is caused by higher-frequency oscillations of air pressure superposed on the basic wave shape. These oscillations are not predictable using simple formulae.

8.6.2.4 Assessment Using Reduced-Scale Model Tests

Reduced-scale moving model tests can be used to assess train entry pressure waves, where the objective is to predict the gradient of the pressure wave near the tunnel entrance. These tests may be used either in their own right to predict the performance

of full-scale tunnels and hoods, or as test cases against which 1D or 3D numerical models can be calibrated.

A detailed scale model of the proposed tunnel entrance (including any hood) is constructed, as shown in [Figure 8-16](#).

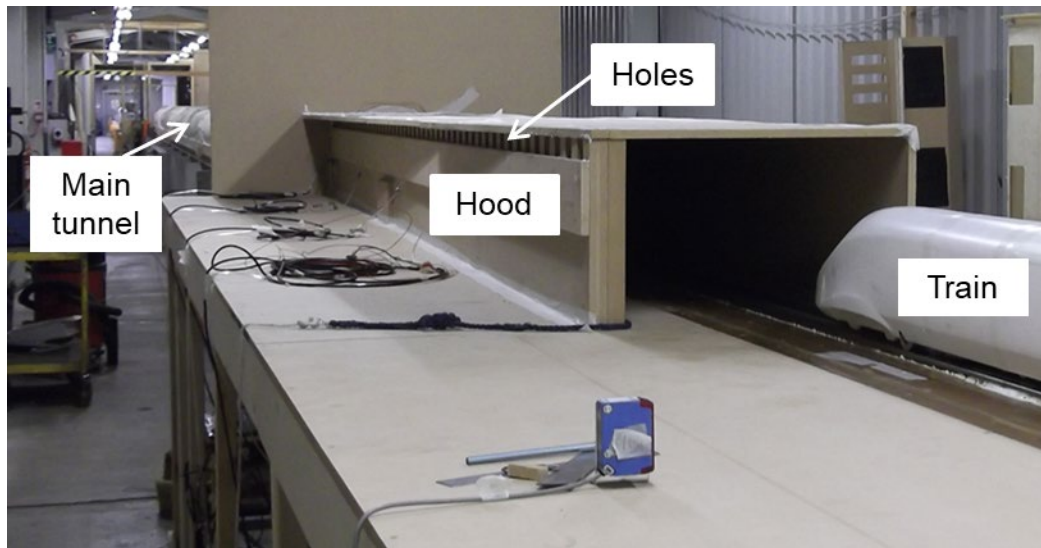


Figure 8-16. Scale model test with tunnel hood [132]

Notes on reduced-scale model testing for tunnel-related applications and how results are converted to full-scale are given in Section [2.4.2](#). Further points to note are as follows:

- The objective of the test is to measure the nose-entry wave pressure gradient at a point inside the tunnel close to the entrance (corresponding to dp_{entry}/dt in [Equation 8-7](#)).
- Only the part of the graph related to train nose-entry pressure wave should be considered, and not, for example, pressure changes occurring when the train passes the pressure gauge. The relevant pressure gradient is the slope of the steepest part of the region of the pressure-time graph relating to nose-entry.
- Filtering of the pressure time-histories may be necessary to remove noise. The filter should only reduce or remove features with timescales shorter than D_T/c where D_T is the effective tunnel diameter (see [Equation 8-3](#)) and c is the speed of sound. A suitable choice is a rolling average with time window length D_T/c .
- To convert between model-scale pressure gradient and full-scale pressure gradient, divide by the geometric scale (e.g., for 1/25 scale, divide the model pressure gradient by 25 – the full-scale pressure gradient is lower than the model-scale pressure gradient). The result is the expected pressure gradient in the full-scale tunnel (corresponding to dp_{entry}/dt in [Equation 8-7](#)) when the train enters the tunnel at the same speed as the scale model train.

- To predict the nose-entry wave pressure gradient for other train speeds, scale the gradient in proportion to train speed cubed.

Scale model testing is not applicable to wave propagation, for the following reasons:

- Scale models cannot accurately reproduce the resistance to wave steepening arising from friction and damping, because these depend on small geometrical details.
- They cannot reproduce ballast effect accurately.
- Most scale model test facilities cannot accommodate a long enough tunnel for significant wave steepening to occur.

Scale model testing may be used for investigating MPW emission and transmission, but the laboratory should be large enough to prevent results being corrupted by pressure waves reflecting off the walls and ceiling.

8.6.2.5 Assessment Using Computational Fluid Dynamics (CFD)

CFD analysis may be used to predict the nose-entry pressure wave for tunnels with or without hoods and is a useful tool for the design of hoods. It can be applied also to pressure waves arising from the train passing geometrical discontinuities inside the tunnel, such as air shafts. CFD is especially relevant to studying the generation of pressure waves for MPW applications because the gradient of the pressure wave must be predicted, and this in turn is influenced by 3D effects that cannot be captured by simpler analysis methods. Further information on the use of CFD is given in Section 2.4.5. Guidance is provided in [112], which also provides a reference case for testing and calibration of CFD methods applied to tunnel-entry for MPW assessments. A reference tunnel-entry case suitable for calibration of CFD models given in [112]; see Section 8.6.3.3.

An example model used for hood design is shown in Figure 8-17. For further details of the analysis method, see [68].

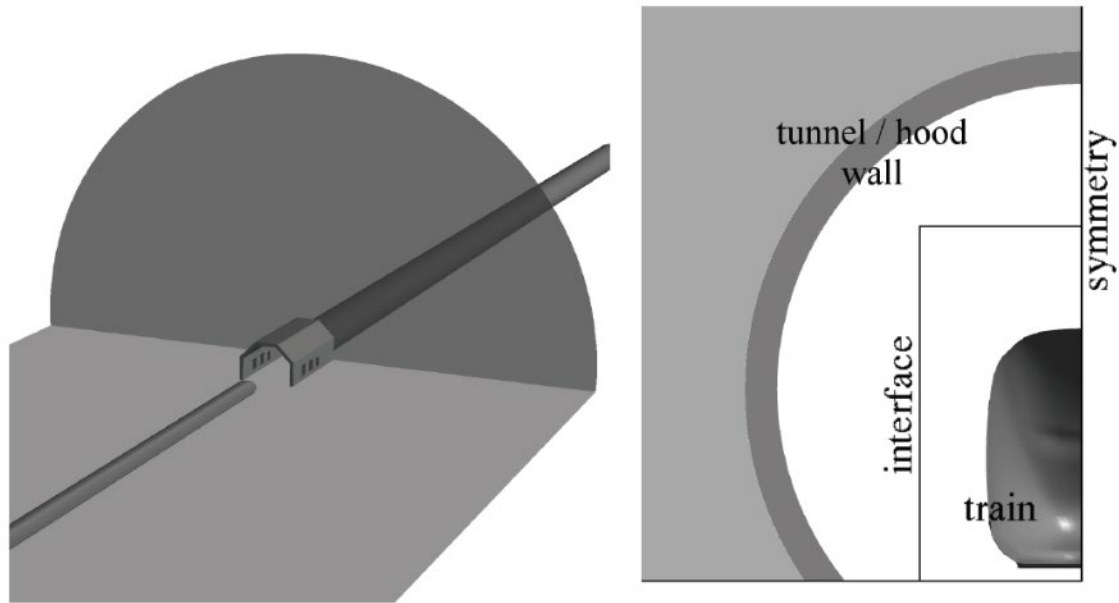


Figure 8-17. CFD model for predicting pressure gradient in a tunnel with a hood, used with permission from [68]

CFD may also be used to predict MPW emission and propagation to receivers, including the influence of different topographies around the tunnel exit.

8.6.2.6 Assessment Using Specialized Software (One-dimensional Pressure Wave Simulation)

One-dimensional pressure wave simulation software (see Section 7.6.5) is applicable to the assessment of MPW as follows:

- Simulation of pressure wave *generation* for long perforated hoods where there is no sharp discontinuity of area at the connection with the main tunnel. Here, “long” means at least three to four times the cross-sectional dimensions of the tunnel. In other cases (short or no hood, or where there is an abrupt step-change of area), pressure wave generation is strongly 3D, and the pressure gradient cannot be predicted by one-dimensional simulation.
- Simulation of pressure wave *propagation* along the tunnel to predict wave steepening. The software can include the beneficial reduction of wave steepening caused by friction (meaning the resistance to a steady flow of air along the tunnel). If the friction value can be estimated, this assessment method leads to more accurate (less conservative) MPW predictions than the simplified method.
- Pressure wave propagation can be analyzed even more accurately when damping (sometimes called unsteady friction) can be modelled by the software. Damping is the resistance to changes of the flow rate of air along the tunnel. It is influenced by the roughness of the tunnel caused by features such as refuge niches, details of the track formation, and equipment in the tunnel. The input parameters for damping need to be calibrated against full-scale measurements in

a tunnel with the same construction type and design details as the tunnel being analyzed.

8.6.2.7 Assessment to Find the Optimal Hood Design

Hood designs are assessed by reduced-scale model testing or by CFD, or in some cases by one-dimensional simulation (see first bullet point in Section 8.6.2.6 above). The objective of the hood is to reduce the maximum gradient of the pressure wave near the tunnel entrance. Different hood designs produce different pressure gradients for a given train entry scenario. The optimal hood design is one that produces a sufficiently low-pressure gradient while minimizing construction cost, land take, etc. In order to know whether the pressure gradient is low enough, consideration should be given to wave-steepening during propagation along the tunnel, MPW emission, transmission to the receiver, and the acceptability criterion (e.g., maximum MPW amplitude) at the receiver – for example, using the assessment methods given in Sections 8.6.2.2.2 through 8.6.2.2.4. The differing conditions of each tunnel (length, distance of receivers from the tunnel exit, etc.) mean that the required hood length and design details may be different for each tunnel.

Examples of results for optimal and non-optimal designs are shown schematically in Figure 8-18. Of the non-optimal designs shown in the figure, “Non-optimal (1)” has the holes too large, while “Non-optimal (2)” has the holes too small. Similar results are described in [132].

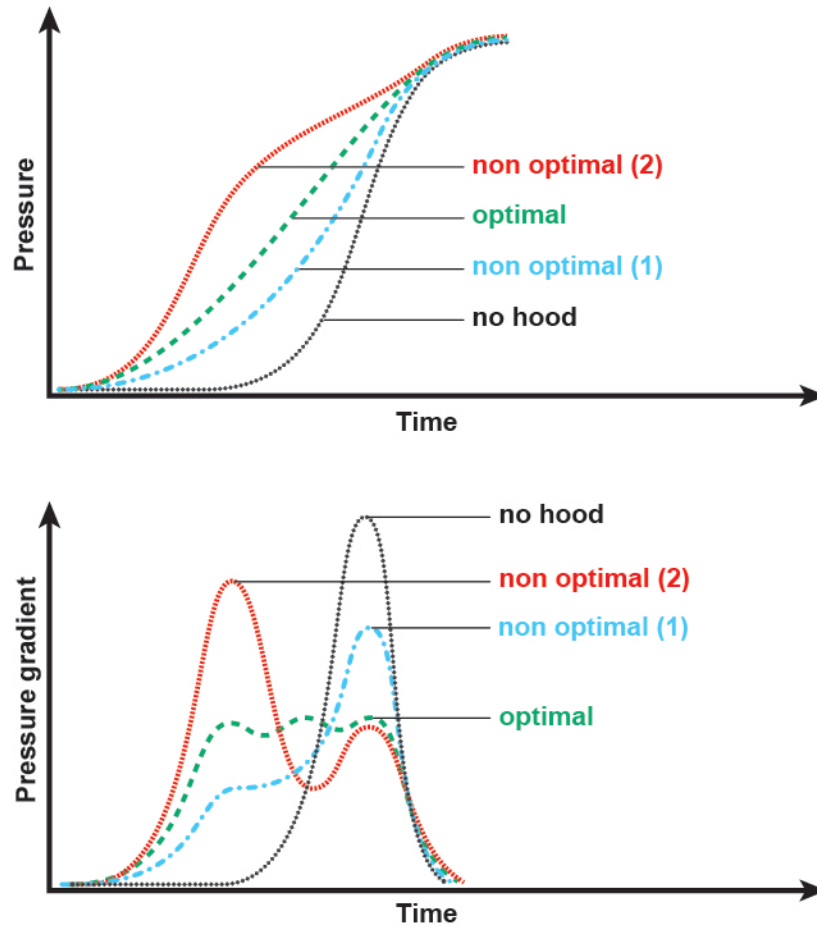


Figure 8-18. Pressure and pressure gradient waveforms with optimal and non-optimal hoods – general form of graphs – after Rety and Gregoire [120]

8.6.2.8 Assessment of Other Mitigation Measures: Acoustic Absorbers and Ballast

There are no well-established methods for assessment of acoustic absorbers or ballast. The influence of these on wave propagation would need to be measured by full-scale tests or assessed by experience with existing tunnels.

8.6.2.9 Assessment of Double-Track Tunnels

Double-track tunnels are assessed in the same way as single-track. There is no need to consider additional effects caused by multiple trains in the tunnel simultaneously. This is different from the assessment of pressure wave impacts in general (described in Section 7), because for MPW it is only the steep part at the beginning of the pressure wave that is of interest and this lasts for only a fraction of a second; it is extremely unlikely that the steep parts of two pressure waves will coincide. However, such coincidences are not impossible; a full-scale experiment has been performed [97] in which two trains running in the same direction entered a double-track tunnel simultaneously and generated an audible MPW, while the MPW from a single train entry

was inaudible. However, this type of event occurs so rarely in practice that the benefits of providing additional mitigation may outweigh the costs.

8.6.2.10 Assessment of Secondary MPWs

Secondary MPWs arise from sources such as trains passing air shafts, as described in Section 8.2.4. If mitigation has already been provided for the nose-entry MPWs, then these secondary MPWs may be the largest remaining ones. Secondary MPWs are not on record as having caused any adverse impacts at existing operating speeds of up to around 185 to 200 mph (300 to 320 km/h), but the possibility that they could become problematic at higher operating speeds should be considered.

Some limited information on air shaft effects is given in [123], including formulae for the amplitude (but not the gradient) of pressure waves caused by trains passing air shafts. Assessment would likely require scale model testing or CFD to quantify the gradient of the pressure wave. One-dimensional analysis could then be used for the wave steepening, and the simplified method for MPW emission and transmission to receivers.

8.6.3 Assessment Criteria

The criteria used to assess MPWs internationally seek to satisfy two goals, which may be summarized as:

- No loud noises that might be dangerous or frightening for people in open air near the tunnel exit. This is assessed at a **standard assessment point** at a fixed distance from the tunnel exit.
- A stricter criterion to prevent significant disturbance at nearby residential buildings, or other places where people may be exposed to the impacts repeatedly. The closest such place to the tunnel exit is termed the **critical receiver** in this report.

In both cases, the criteria are either amplitude-based or noise-based.

Amplitude-based criteria originate from Japanese experience showing that the impacts on people (including audible noise) would be acceptable if the MPW amplitude was kept below a certain level. Because of the lack of a causal link between MPW amplitude and the actual impacts (e.g., audible frequencies superposed on the basic MPW pulse), this criterion may not apply for conditions beyond those tested in Japan, namely, speeds up to around 190 mph, blockage ratios up to around 0.2, and tunnel cross-sectional areas of around 680 ft² (63 m²). However, this type of criterion has the advantage of being easier to apply in assessments of new tunnels during design.

Noise-based criteria (such as those used in Germany) have a more direct relation to the impact on people. The noise contained in MPW emissions from a proposed tunnel design is difficult to calculate or predict in advance, but once the tunnel is built, relatively easy to measure. Therefore, these criteria are useful for testing the performance of existing tunnels but less useful in design.

It would be reasonable for operators or regulatory authorities to decide their own assessment criteria for MPWs based on judgment of the severity of the impacts,

compared with other impacts of HSR such as noise from trains. If no criteria are provided, the following may be used.

8.6.3.1 MPW Amplitude-based Criteria for Use in Preliminary Design

These criteria are proposed for use in preliminary design calculations. Both criteria should be met.

- (a) *MPW amplitude should be ≤ 0.003 psi (20 Pa) at a standard assessment point 165 ft (50 m) from the tunnel exit, at an angle of 45 degrees to the track.*
- (b) *MPW amplitude should be ≤ 0.0015 psi (10 Pa) at the critical receiver (nearest residential building or similar).*

Criterion (a) can be expressed in different combinations of MPW amplitude and distance, as long as the product of amplitude times distance stays the same. In the literature, this same criterion may be described as “50 Pa at 20 m” instead of “20 Pa at 50 m.” The two descriptions are equivalent because an MPW that has an amplitude of 50 Pa at 20 m decays to 20 Pa by the time it reaches a receiver 50 m from the tunnel. If using field measurements to assess tunnels against the criteria, it may be impractical to take measurements at the stipulated standard assessment point, in which case it would be acceptable to measure MPW amplitude at a different distance within the range 65 to 330 ft (20 to 100 m) and adjust the acceptable pressure in inverse proportion to the distance – for example, 0.0076 psi at 65 ft or 0.002 psi at 250 ft.

Criterion (a) is intended to prevent loud noises near the tunnel exit and is equivalent to that applied in Japan, Korea, and China. Empirical evidence in Japan suggests that meeting the 0.003 psi criterion tends to ensure that the MPW does not cause adverse impacts [94]. As well as protecting people from dangerous or frightening loud noises, this criterion would also likely prevent disturbance to livestock or protected species areas. Criterion (a) can be over-conservative because it takes no account of whether the MPW is audible (and therefore capable of producing loud or frightening noises), as explained in Section 8.6.3.1.1 below.

Criterion (b) is intended to provide a greater level of protection for nearby residents who may find frequent disturbances annoying, even if the magnitude of each instance is small. It is stricter by a factor of two than the equivalent one used in Japan, based on the assumption that the American public may be less tolerant of environmental noise and vibration than the Japanese public. There is no experimental evidence supporting the necessity of the proposed 0.0015 psi criterion for American homes, but equally, there is no evidence that meeting this target will guarantee the absence of impacts such as the rattling of windows. Audibility of the MPW is less relevant to criterion (b), because some of the potential impacts (such as rattling windows) can occur irrespective of whether the MPW is audible, and even inaudible infrasound can have impacts on people if they are exposed to it repeatedly.

8.6.3.1.1 Applicability of the Criteria to Tunnels with Large Cross-Sectional Area

The criteria above are proposed for use with all tunnels, even though their applicability is unknown for conditions outside the range of the Japanese tests. Therefore, the criteria may be conservative or non-conservative in some cases. One possible source

of conservatism relates to tunnels with much larger cross-sectional areas than the 645–700 ft² (60–65 m²) Japanese tunnels from which criterion (a) was developed. If the pressure wave in the tunnel has not steepened sufficiently for audible frequency components to be present, then the emitted MPW cannot create a loud noise. However, if the tunnel has a large cross-sectional area, then the MPW amplitude at the assessment point may still exceed 0.003 psi (20 Pa) even if the pressure gradient is too low to contain audible content. This would correspond to high-amplitude infrasound, not dangerous or frightening noises, and therefore criterion (a) may be over-conservative in deeming this to be unacceptable.

Replacing criterion (a) with one related to pressure gradient in the tunnel would be less conservative in these circumstances. However, there is no international precedent for a criterion of this type, nor is there a consensus on what pressure gradient should be deemed acceptable. Furthermore, as with the MPW amplitude-based criteria, there is no evidence that the same limit would be suitable for a wide range of tunnel types. Therefore, the points below are offered for information only:

- According to German experience, if the pressure gradient in the tunnel near the exit exceeds about 5.8 psi/s (40 kPa/s) it is highly likely that the MPW will be strongly audible [68]. Therefore, pressure gradients of this level should be considered unacceptable.
- The results of the Japanese experiments together with Equation 8-11 suggest that loud noises will not be heard near the tunnel exit if the pressure gradient is below about 1.5-2.2 psi/s (10-15 kPa/s).

8.6.3.2 Noise-Based MPW Acceptability Criteria (for reference only)

Noise measurements offer a rational basis for deciding the acceptability of MPWs based on their likely impact on people. Germany uses this method. Full-scale measurements to test compliance with the German criteria are easily achieved using a sound meter. However, the criteria are much more difficult to apply during predictive assessments. Both the amplitude and the frequency content of MPW would have to be predicted. This is difficult even for short tunnels (where wave propagation has a less significant effect), and even with a 3D analysis, high accuracy cannot be expected. For long tunnels, the uncertainties around wave propagation make accurate prediction even more difficult. Because noise-based criteria are difficult to use while designing tunnels, they are provided here for reference only and do not form part of the recommended assessment method.

It might be assumed that the same criteria described in the FRA report, [High-Speed Ground Transport Noise and Vibration Impact Assessment](#) [44] could also be applied to MPW. These criteria employ A-weighting, which reflects the typical human perception of the loudness of sounds of different frequencies, with lower frequencies being attenuated accordingly. Internationally, this is not considered adequate for assessment of MPW. It is thought that A-weighted noise measures would likely underestimate the impact of MPW due to their low frequency content which could be annoying despite being hard to hear. In Germany, as well as the A-weighted noise criteria that are applied to phenomena such as traffic noise, additional C-weighted noise criteria have

been developed that are specific to MPW. C-weighting is more often used to assess impulsive and low-frequency sounds and applies less attenuation to low frequencies than A-weighting. The frequency responses of A and C weighting functions are defined in [74] and shown graphically in Figure 8-19.

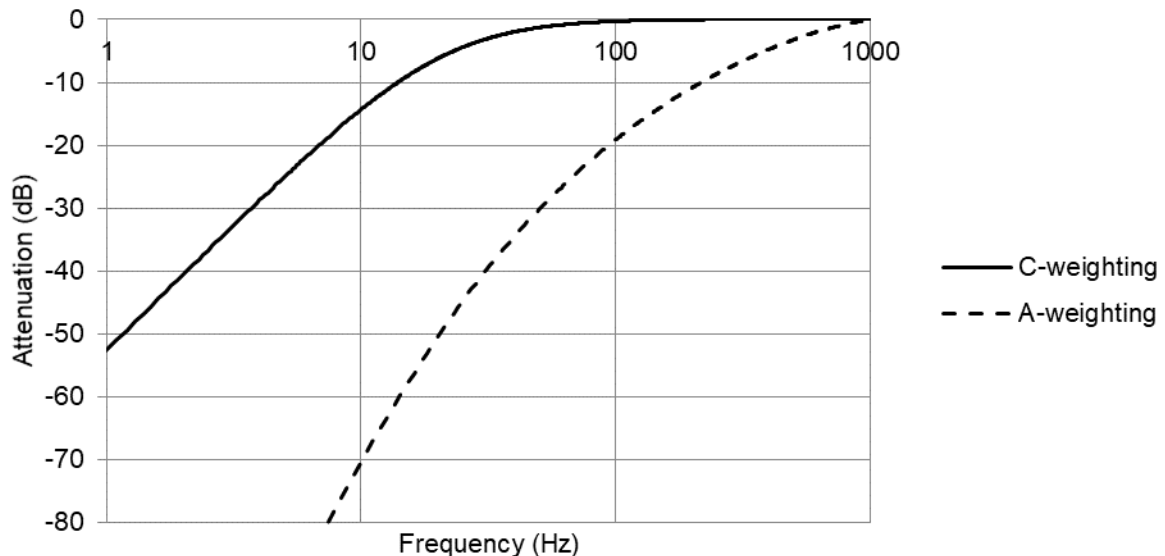


Figure 8-19. C-weighting function (as used in German MPW criteria) compared with the A-weighting function more commonly used in noise assessments

For reference, the German criteria [69][60] are:

- At the nearest dwelling (or other sensitive building such as a school or hospital), the C-weighted Sound Exposure Level (SEL, defined in [80]) should not exceed 70 dB(C). Higher limits apply to garden plots (85 dB(C)) and industrial areas (95 dB(C)). For comparison, experience has shown that MPWs with SEL below 73 dB(C) are hardly audible.
- At 82 ft (25 m) from the tunnel portal, the C-weighted Sound Pressure Level (SPL, defined in [80]) should not exceed 115 dB(C). This limit is intended to protect people near the portal from dangerous sound levels.
- Additionally, the A-weighted SEL should be in accordance with German traffic noise regulations. In the U.S., this requirement should be replaced with the impact assessment described in Section 3 of the FRA report, [High-Speed Ground Transport Noise and Vibration Impact Assessment](#) [44].

These limits form a rational basis for assessing the direct impact of MPWs on human hearing. It is not known whether these limits can always be expected to eliminate the potential impacts of rattling doors and windows.

Note that people living near the tunnel portal will hear noise from the train when it passes by. In the event of wishing to apply noise-based criteria to MPW for nearby residential buildings, operators may prefer to set limits relative to the train noise expected at the same location, rather than an absolute limit. It may seem counter-

intuitive to apply a more stringent criterion to one noise phenomenon (MPWs) than to another (train pass-by). But some allowance should be made for the fact that MPWs can take observers by surprise, being emitted suddenly from the tunnel some time before the train itself can be heard.

8.6.3.3 Rolling Stock Acceptance Criteria

The upcoming version of the European standard on tunnel aerodynamics [112] has added an acceptance criterion for rolling stock, intended to ensure that new HSTs are no more prone to generate problematic MPWs than other typical HSTs. The requirement is met if the new train design generates a pressure wave gradient no steeper than a reference train when entering a reference tunnel at 250 km/h. The shapes and dimensions of the reference train and reference tunnel are defined in [112]; their cross-sectional areas are 11 and 63 m² (118 and 678 ft²), respectively. The requirement can be demonstrated by reduced-scale model testing or CFD. In the case of CFD, in order to show that the numerical methods are accurate, there is an additional requirement that the predicted pressure gradient for the reference train is between 8.8 and 9.5 kPa/s (1.28 and 1.38 psi/s).

This reference case provides a useful benchmark for some of the input parameters in the simplified MPW assessment method. If the equations in Section 8.6.2.2.1 are used to calculate the pressure gradient for the reference train entering the reference tunnel, and taking the train's nose loss coefficient as 0.05, then the tunnel/train shape coefficient must be given a value in the range 1.5 to 1.6 in order that the calculated pressure gradient is in the required range 8.8 to 9.5 kPa/s (1.28 to 1.38 psi/s). Note, however, that the same values might not necessarily be realistic for all blockage ratios, tunnel shapes, and train shapes.

8.6.4 Example Calculations

8.6.4.1 Assessment of MPW for a Tunnel with No Hood

Question	
<p>A new tunnel 2 miles long is being designed for a high-speed railroad. A single-track, twin-tube, slab track design is proposed, with each tube having a free cross-sectional area of 646 ft² (60 m²). The closest residential properties to the ends of the tunnel are 300 ft from the southern end and 500 ft from the northern end. Trains conforming to U.S./Euro Baseline will operate through the tunnel at 175 mph. Assess whether mitigation for micro-pressure waves (MPW) is likely to be required.</p>	
Methodology	
<p>All input data will be converted to SI units.</p> <p>The calculations will proceed through the steps in Sections 8.6.2.2.1 through 8.6.2.2.4.</p> <p>Step 1: Calculate the pressure gradient at the tunnel entrance, assuming initially that no mitigation (hood) is provided.</p> <p>Step 2: Because the tunnel is slab track, the full effect of inertial pressure wave steepening should be assumed (if the tunnel were ballasted track, this assumption would be grossly conservative). Calculate the pressure gradient at the end of the tunnel. If a shock wave is predicted, mitigation is very likely to be required. If not, proceed to Step 3.</p> <p>Step 3: If Step 2 did not predict a shock, calculate the amplitude of the emitted MPW and compare against the criteria. More information about Step 3 is given in the second example; see Section 8.6.4.2.</p>	
Step 1	Methodology
	See Section 8.6.2.2.1 .
	Inputs
	<p>Tunnel cross-sectional area = 646 ft² = 60 m²</p> <p>Train cross-sectional area = 11 m² (U.S./Euro Baseline)</p> <p>Train nose loss factor k_N = 0.05 (assumption, at the middle of the range stated below Equation 8-2).</p> <p>Air density, ρ = 1.225 kg/m³ (standard value)</p> <p>Speed of sound in air, c = 340 m/s (standard value)</p> <p>Train speed, V_T = 175 mph = 78.2 m/s</p> <p>Train/tunnel shape coefficient, ϕ = 1.25 (assumption, toward the conservative end of the range stated below Equation 8-4)</p>

Calculations

Calculate blockage ratio (see Section 8.3.5):

$$\beta = \frac{A_{Train}}{A_{Tun}} = 11/60 = 0.1833$$

Calculate α (Equation 8-1):

$$\alpha = \frac{1 + k_N}{(1 - \beta)^2} - 1 = \frac{1 + 0.05}{(1 - 0.1833)^2} - 1 = 0.574$$

Calculate pressure wave amplitude Δp (Equation 8-2):

$$\begin{aligned}\Delta p &= \rho c \left\{ V_T + \frac{c}{\alpha} \left[1 - \sqrt{1 + \frac{2\alpha V_T}{c}} \right] \right\} \\ &= 1.225 \times 340 \times \left\{ 78.2 + \frac{340}{0.574} \left[1 - \sqrt{1 + \frac{2 \times 0.574 \times 78.2}{340}} \right] \right\} \\ &= 1.225 \times 340 \times \left\{ 78.2 + \frac{340}{0.574} [-0.124] \right\} \\ &= 1.225 \times 340 \times 4.57 = 1907 \text{ Pa}\end{aligned}$$

Calculate effective entry length L_E (Equation 8-3 and Equation 8-4):

$$D_T = \sqrt{4A_T/\pi} = \sqrt{4 \times 60/3.14159} = 8.74 \text{ m}$$

$$L_E = \phi D_T = 1.25 \times 8.74 = 10.92 \text{ m}$$

Calculate rise-time of the pressure wave, Δt_{wave} , (Equation 8-6):

$$\Delta t_{wave} = L_E \left(\frac{1}{V_T} - \frac{1}{c} \right) = 10.92 \times \left(\frac{1}{78.2} - \frac{1}{340} \right) = 0.108 \text{ s}$$

Calculate pressure gradient near tunnel entrance (Equation 8-7):

$$\frac{dp_{entry}}{dt} = \frac{\Delta p}{\Delta t_{wave}} = \frac{1907}{0.108} = 17,700 \text{ Pa/s}$$

Result

Pressure gradient at entrance of tunnel = 17,700 Pa/s

Step 2	Methodology
	Apply Equation 8-10 ; see Section 8.6.2.2.2 .
	Inputs
	Tunnel length = 2 miles = 3,219 m Pressure gradient at tunnel entrance = 17,700 Pa/s from Step 1
	Calculations
	<p>Calculate pressure gradient near tunnel exit (Equation 8-10):</p> $\frac{dp_{exit}}{dt} = \frac{1}{\frac{1}{\frac{dp_{entry}}{dt}} - \frac{1.2L_T}{\rho c^3}} = \frac{1}{\frac{1}{17700} - \frac{1.2 \times 3219}{1.225 \times 340^3}}$ $= \frac{1}{0.0000565 - 0.0000802} = -42,200 \text{ Pa/s}$ <p>A negative value indicates that a shock wave has formed.</p>
	Result
	The MPW emissions will very likely be unacceptable and could take the form of a loud bang. Mitigation is required. There is no need to calculate Step 3. For an example of calculation of Step 3, see Section 8.6.4.2 .

8.6.4.2 Calculation of MPW for a Tunnel with Hood

Question

The same tunnel as in the previous example (see Section 8.6.4.1) is to be provided with a hood 200 ft (61 m) long at both ends to mitigate MPW emissions. All other input is the same as for the previous example. Assess whether the proposed hood length is sufficient.

Methodology

All input data will be converted to SI units.

The calculations will proceed through the steps in Sections 8.6.2.2.1 through 8.6.2.2.4.

Step 1: *Calculate the pressure gradient at the tunnel entrance. The calculation of pressure wave amplitude is the same as in the previous example, but the pressure wave rise-time is longer because of the hood.*

Step 2: *Calculate the effect of pressure wave-steepening using the same method as the previous example.*

Step 3: *Calculate the amplitude of the emitted MPW using the method described in Section 8.6.2.2.3 and compare against the acceptability criteria proposed in Section 8.6.3.1.*

This calculation needs to be performed for both directions of travel through the tunnel. In this case, the input data for Step 1 and Step 2 are the same for southbound and northbound trains, so one calculation will apply to both directions. In Step 3 the receiver distances are different at the north end versus the south end, with the south end being more critical (as per the previous example, the closest residential properties to the ends of the tunnel are 300 ft from the southern end of the tunnel and 500 ft from the northern end).

Step 1	Methodology
	See Section 8.6.2.2.1 .
	Inputs
	Hood length, $L_H = 61\text{ m}$ Hood efficiency $\eta_H = 0.6$ (assumption, toward the conservative end of the range stated below Equation 8-5) Other inputs are the same as in the example in Section 8.6.4.1 .
	Calculations
	<p>The pressure wave amplitude Δp is the same as in the previous example (see Section 8.6.4.1):</p> $\Delta p = 1907\text{ Pa}$ <p>Calculate effective entry length L_E (Equation 8-5):</p> $L_E = \eta_H L_H = 0.6 \times 61 = 36.6\text{ m}$ <p>Calculate rise-time of the pressure wave, Δt_{wave}, (Equation 8-6):</p> $\Delta t_{\text{wave}} = L_E \left(\frac{1}{V_T} - \frac{1}{c} \right) = 36.6 \times \left(\frac{1}{78.2} - \frac{1}{340} \right) = 0.360\text{ s}$ <p>Calculate pressure gradient near tunnel entrance (Equation 8-7):</p> $\frac{dp_{\text{entry}}}{dt} = \frac{\Delta p}{\Delta t_{\text{wave}}} = \frac{1907}{0.360} = 5,290\text{ Pa/s}$
	Result
	Pressure gradient at entrance of tunnel = 5,290 Pa/s

Step 2	Methodology See Section 8.6.2.2.2 .
	Inputs Tunnel length = 2 miles = 3219 m Pressure gradient at tunnel entrance = 5290 Pa/s from Step 1
	Calculations Calculate pressure gradient near tunnel exit (Equation 8-10): $\frac{dp_{exit}}{dt} = \frac{1}{\frac{1}{\frac{dp_{entry}}{dt}} - \frac{1.2L_T}{\rho c^3}} = \frac{1}{\frac{1}{5290} - \frac{1.2 \times 3219}{1.225 \times 340^3}} = \frac{1}{0.000189 - 0.0000802}$ $= 9,190 \text{ Pa/s}$
	Result The pressure gradient near the tunnel exit is 9,190 Pa/s.
Step 3	Methodology See Sections 8.6.2.2.3 and 8.6.2.2.4 .
	Inputs Area of tunnel, $A_T = 60 \text{ m}^2$ Distance to standard assessment point, $r_{sap} = 50 \text{ m}$ (see Section 8.6.3.1) Distance to critical receiver, $r_{cr} = 300 \text{ ft} = 91 \text{ m}$ Solid angle for MPW emission, $\Omega = 1.25\pi$ (assumption, toward the conservative end of the range stated below in Equation 8-12) Speed of sound in air, $c = 340 \text{ m/s}$ (standard value) Pressure gradient near tunnel exit, $\frac{dp_{exit}}{dt} = 9,190 \text{ Pa/s}$ from Step 2
	Calculations MPW amplitude at the standard assessment point (Equation 8-11): $p_{MPW,sap} = \left(\frac{2A_T}{\Omega c r_{sap}} \right) \frac{dp_{exit}}{dt} = \left(\frac{2 \times 60}{1.25\pi \times 340 \times 50} \right) \times 9,190 = 16.5 \text{ Pa}$ <p>$p_{MPW,sap}$ is less than the 20 Pa limit proposed in Section 8.6.3.1</p> MPW amplitude at the critical receiver (Equation 8-12): $p_{MPW,cr} = \left(\frac{r_{sap}}{r_{cr}} \right) p_{MPW,sap} = \left(\frac{50}{91} \right) \times 16.5 = 9.1 \text{ Pa}$ <p>$p_{MPW,cr}$ is less than the 10 Pa limit proposed in Section 8.6.3.1</p>

Result

The calculated MPW amplitude complies with both parts of the acceptability criterion, so the proposed 200 ft hood length is adequate.

The governing consideration is the MPW amplitude at the critical receiver 300 ft from the south end of the tunnel. The calculation result is close to the limit for the critical receiver (9.1 Pa compared to 10 Pa), indicating that the proposed hood length is close to the minimum that will satisfy this criterion. However, the receivers at the north end are further from the tunnel than at the south end, suggesting that one of the two hoods could be shortened. In general, if the hood lengths are different at each end of the tunnel, Steps 1, 2, and 3 need to be calculated separately for the two hood lengths. In this case, the governing criterion for receivers at the north end of the tunnel is Criterion (a), 0.003 psi at 165 ft (20 Pa at 50 m) and a suitable hood length to meet this criterion is 180 ft (55 m). Note that the hood length at the north end of the tunnel controls MPW emissions from the south end of the tunnel, and vice-versa (see [Figure 8-1](#)). Therefore, since the critical receivers are closer at the south end of the tunnel, the hood needs to be longer at the north end (200 ft) and can be shorter at the south end (180 ft).

Note that these assessments are appropriate for initial concept design only. The actual hood design should be undertaken with appropriate software and scale model experiments or using experience of closely similar hoods that are already in operation.

9 Aerodynamic Drag Effect

9.1 Introduction

Aerodynamic drag is the principal source of resistance to motion for trains operating at high speed and is responsible for 60 to 80 percent of the energy costs for a typical high-speed operation. The aerodynamic drag force is approximately proportional to the square of the train speed, and the power required to overcome that force is approximately proportional to the cube of the train speed. For example, almost twice the power is required to overcome aerodynamic drag at 250 mph compared to the same train at 200 mph. The impacts of aerodynamic drag on energy cost and power requirement can be primary considerations when deciding the operating speeds on new routes.

This section includes:

- Aerodynamic principles and phenomena
- Impacts on operations and planning
- Impacts on infrastructure design
- Mitigation methods
- A summary of the methods for making the assessments
- Examples and calculations

9.2 Aerodynamic Principles and Phenomena

Aerodynamic drag is the force opposing the train motion that arises from the interaction between the train and air. This is distinct from **mechanical drag** which arises from sources within the train and from wheel-rail interactions. Mechanical drag is not covered in this report, nor are the forces associated with curving, grades or acceleration.

Aerodynamic drag arises from energy loss in the airflow, and is commonly thought of as having two physical causes:

- **Pressure drag** (also known as **form drag**) is the force caused by higher pressure acting on forward-facing surfaces (e.g., the nose of the train) compared to the pressure acting on rearward-facing surfaces (e.g., the tail of the train). As the train pushes air out of its way, the air in front of the nose is compressed, while there is a region of suction behind the tail as air moves back into the space left by the train. The difference between these pressures acts on the cross-sectional area of the train to generate a net force opposing the train's motion.
- **Friction drag** (also known as **skin drag**, **skin friction**, or **viscous drag**) is the sum of the shear forces associated with air sliding over the train's surfaces. The forces arise from the viscosity of the air and the roughness of the train surfaces, and also to some extent the roughness of the trackbed (since the train has to provide the energy to make the air flow over the trackbed under the train).

In practice, pressure drag and friction drag are inter-related. For example, a contributing factor in pressure drag is the low pressure in the turbulent wake behind the train, which in turn is caused by friction along the sides of the train.

The drag forces that act on the train to resist its motion have equal and opposite reactions on the air, causing it to accelerate in the direction of the train's motion and leading to the slipstream effects described in Section 3.

It is sometimes convenient to group the aerodynamic forces by the part of the train on which they occur, instead of by the physical causes, so that the influence of train length on drag may be accounted for. In this report the following terms are used:

- **Nose/Tail drag**, consisting mainly of the pressure drag effect explained above acting on the nose and tail. This drag force is independent of train length.
- **Railcar surface drag**, defined in this manual as the sum of all aerodynamic forces acting on the sides, roof, and underside of the train, including forces arising from friction on surfaces parallel to the train motion as well as pressure on forward-facing surfaces such as those associated with car-to-car connections, pantographs, trucks, and the underbody equipment, but excluding forces on the nose and tail. The railcar surface drag force may be considered as being proportional to train length. In open air, railcar surface drag typically forms 80–90 percent of the aerodynamic drag on HSTs with the remainder being nose/tail drag.

Estimates of the proportions of the aerodynamic drag caused by the different features of the train may be found in the literature; for example, see [64][126][95]. Note that some references use the above terms differently – for instance, “friction drag” is sometimes used in the same sense as the definition of railcar surface drag given above. This can lead to confusion regarding the proportions of drag associated with different sources quoted in some references.

9.2.1 The Davis Equation

The **Davis Equation** (Equation 9-1) is one of the fundamental elements in the study of drag [22]. It was developed in the 1920s and is still used today to estimate the total mechanical and aerodynamic drag force that a train will experience when it travels at a given speed.

$$R = A + BV_T + CV_T^2 \quad \text{Equation 9-1}$$

Where:

R = Total drag force resisting the motion of the train;

A, B = Coefficients related to mechanical drag;

C = Coefficient related to aerodynamic drag; and,

V_T = Speed of the train.

The equation includes mechanical and aerodynamic drag only. Forces due to curving, grades, or acceleration need to be added separately.

Notes on units are given in Section 9.6.2.3.

The constants A , B , and C in [Equation 9-1](#) are called **Davis Equation coefficients**. These have fixed values for a given train. The higher the values of the coefficients, the greater the drag. Of particular interest in this report is the C coefficient, which expresses the level of aerodynamic drag inherent in the train design. Further information about the interpretation and use of the Davis Equation in assessments is given in [Section 9.6.2.3](#).

The user should understand that the Davis Equation will likely not produce precise values of absolute train resistance. In practice, when considering an entire train, there is significant variability in the coefficients that are applied in the equation and what happens in a “real world” condition. Consequently, the Davis Equation should be used only for comparative estimates between scenarios of interest.

9.2.2 Drag Coefficient

A term commonly encountered in the literature is **drag coefficient**, which expresses the level of aerodynamic drag inherent in a given vehicle design. Whereas the Davis Equation relates to a whole full-scale train, drag coefficients usually apply to individual vehicles. The drag coefficient is assumed to have the same value at full-scale and reduced-scale – it expresses the degree to which a given vehicle *shape* causes drag, and can be thought of as a measure of the efficiency of the design regarding drag. Drag coefficient is defined in [Equation 9-2](#).

$$c_D = \frac{R_a/A}{\frac{1}{2}\rho U^2} \quad \text{Equation 9-2}$$

Where:

c_D = Drag coefficient;

R_a = Aerodynamic drag force;

A = Frontal area of the vehicle;

ρ = Air density; and,

U = Speed of the air relative to the train.

This equation requires consistent units, see [Section 2.7](#).

The drag coefficient is found numerically (by CFD) or experimentally (by wind-tunnel testing or full-scale testing of individual vehicles).

The C coefficient of the Davis Equation for a whole train relates to the drag coefficients of the individual vehicles in the manner shown in [Equation 9-3](#).

$$C = \frac{1}{2} \rho (c_{D1}A_1 + c_{D2}A_2 + c_{D3}A_3 \dots) \quad \text{Equation 9-3}$$

Where:

C = Davis Equation C coefficient;

$c_{D1}, c_{D2}, c_{D3} \dots$ = Drag coefficients of all the vehicles in the train;

$A_1, A_2, A_3 \dots$ = Frontal areas of all the vehicles in the train; and,

ρ = Air density.

This equation requires consistent units, see Section 2.7.

9.3 Influencing Factors

9.3.1 Speed

Aerodynamic drag force is approximately proportional to the square of train speed, while mechanical drag is often idealized as being linearly dependent on speed. This is indicated in the Davis Equation (Section 9.2.1) in which the term CV_T^2 represents aerodynamic drag. High-speed rail operations are particularly affected because the aerodynamic contribution to total drag increases significantly with speed.

Energy consumption associated with overcoming aerodynamic drag is equal to drag force times distance, and therefore the energy consumption is proportional to the square of train speed for a given journey.

The instantaneous power required to overcome the aerodynamic drag is given by drag force times speed and is therefore proportional to the cube of the train speed. Table 9-1 shows the power required to overcome aerodynamic drag force, normalized against the power required at 125 mph. Operating a train at 250 mph requires about eight times as much power to overcome aerodynamic drag as operating the same train at 125 mph.

Table 9-1. Approximate influence of speed on aerodynamic drag force and instantaneous power required to overcome aerodynamic drag

Speed (mph)	125	150	175	200	225	250
Normalized Aerodynamic Drag Force	1.0	1.4	2.0	2.6	3.2	4.0
Normalized Instantaneous Power	1.0	1.7	2.7	4.1	5.8	8.0

9.3.2 Aerodynamic Properties of Rolling Stock

Manufacturers pay considerable attention to reducing drag during the design of railcars, using measures such as those described in Section 9.5.2 that increase the smoothness of the airflow over the train. Procurement of trains with lower drag can impact significantly on energy costs.

9.3.3 Headwind

Because aerodynamic drag is dependent on the speed of the train relative to the air, (not the speed relative to the ground), drag increases if there is a headwind. For example, if the train speed relative to the ground is V_T and the speed of the headwind is $0.15V_T$, then the speed of the train relative to the air is $1.15V_T$ and aerodynamic drag increases by a factor of 1.15^2 , i.e., 1.32.

9.3.4 Crosswind

Drag increases in a crosswind, even if the wind is blowing perpendicular to the track (i.e., even if it does not include any headwind component). According to formulae in the literature [126][110], aerodynamic drag force has a linear relationship with yaw angle (defined in Section 6.2.5) and the increase of drag force can be as much as 15–20 percent in the case of wind blowing perpendicular to the track and the wind speed equal to 0.15 times the train speed.

9.3.5 Tunnels

Aerodynamic drag is increased in tunnels for three inter-related reasons:

- The piston effect pressurizes air ahead of the nose of the train more than in open air. Similarly, the pressure drop behind the tail of the train becomes greater in tunnels. These effects increase the nose/tail drag. See [Figure 9-1](#)
- Air flows backward through the gap between the train and tunnel walls, due to the pressure difference between the high-pressure zone ahead of the train and the low-pressure zone behind it (this point is explained further in Section 7.2.1 and [Figure 7-3](#)). Thus, the speed of the train relative to the air is increased, leading to greater railcar surface drag. Furthermore, the railcar surface drag on the train increases the pressure in the air ahead of the train relative to the pressure in the air behind the train, thereby increasing the nose/tail drag.
- The pressure ahead of the train is increased by friction on the tunnel walls resisting the airflow along the tunnel between the nose of the train and the tunnel exit. Likewise, the pressure behind the train is reduced because of friction resisting the airflow between the tunnel entrance and the tail of the train. The difference between these two pressures contributes to nose/tail drag. This effect is greater in longer tunnels.

A more detailed explanation of these points may be found in [\[149\]](#).

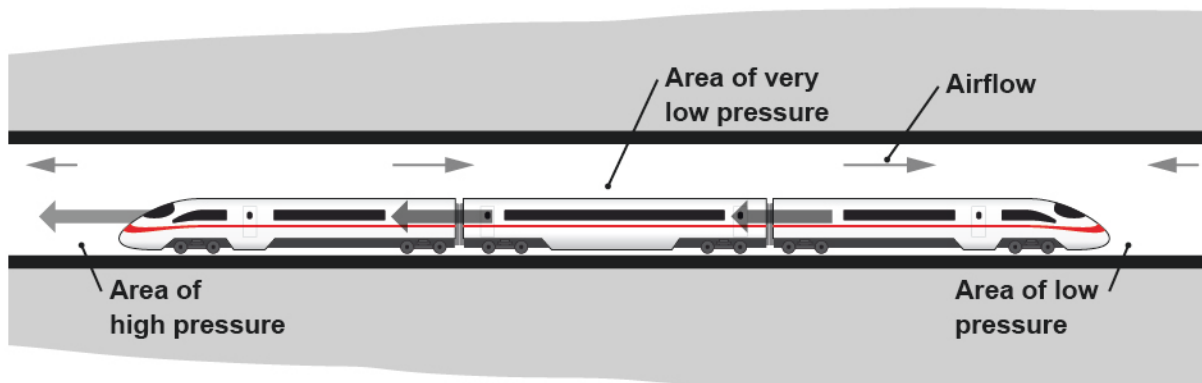


Figure 9-1. Tunnel drag effects (train moving from right to left)

Typically, the total drag force is roughly 1.5 to 2 times greater in tunnels than the same train at the same speed in open air. However, the exact amount of increase depends on many factors such as the blockage ratio, the length of the tunnel and the train, the presence of airshafts, and the presence of other trains within the tunnel. Furthermore, the drag force is affected by pressure waves because these result in sudden changes of airflow speed along the tunnel. Each pressure wave causes a step-change in the drag force when it passes over the train (these can be seen in [Figure 9-5](#)). Information on assessing drag in tunnels is given in [Section 9.6.2.5](#).

9.4 Impacts

9.4.1 Impacts on Operation and Planning

The energy consumption to overcome the effects of aerodynamic drag creates impacts on the costs of operation. Aerodynamic drag is responsible for about 60–80 percent of the energy consumption of an HST running at constant speed on flat ground, according to sources such as [\[114\]\[126\]\[140\]](#). The faster the trains, the greater the percentage of energy consumed due to aerodynamic drag. In addition to aerodynamic and mechanical drag, energy is used to accelerate the train, to overcome curving resistance, and to ascend grades. Some energy may be recovered by regenerative braking. Nevertheless, aerodynamic drag accounts for over half of total energy consumption in typical HSR operations and therefore has a major impact on cost. Formulae are available for estimating operating costs, including the cost of electrical energy, as functions of average train speed; see [\[57\]](#).

Aerodynamic drag is a key limiting factor on the speed achievable by a given train. When all the installed power of the train is being used to overcome drag, no power is available for acceleration.

As well as economic impact, there are environmental impacts of energy consumption, such as carbon dioxide emissions. Because aerodynamic drag increases with train speed, so do the environmental impacts associated with energy consumption.

9.4.2 Impacts on Infrastructure Design

Because aerodynamic drag is a principal source of energy consumption for HSR, it impacts the energy supply system. The greater the operating speed, the more power is required. The railroad's electrical supply system should be designed to accommodate the power consumption of the trains in terms of the locations, frequency, and specification of substations. The ability of local electric utility producers to supply the substations should be considered.

Tunnel design can be affected by aerodynamic drag considerations, but this is usually the case for long tunnels only. For short tunnels, the train may be in the tunnel for too little time for the increase of drag to have any significant impact on the speed of the train. For long tunnels, larger tunnel cross-sectional area and/or air shafts may need to be provided in order to reduce aerodynamic drag, thus impacting construction cost.

9.5 Mitigation Methods

9.5.1 Reducing Train Speeds

Reducing operating speed is an obvious way to reduce drag and therefore energy usage and operating costs. The business case for a new HSR operation may involve tradeoffs between energy costs (lower speed equals lower costs) versus journey time (faster journey times could yield more income from passengers).

9.5.2 Procurement of Trains with Low Drag

Aerodynamic drag as measured by the coefficients described in Section 9.6 may be among the criteria used by operators to select new HSTs.

During the design of rolling stock, manufacturers try to minimize roughness along the length of the train, thus reducing railcar surface drag. Effective measures include covering inter-car gaps (see Figure 9-2), underbody fairings, and pantograph fairings.

Streamlined design of the nose and tail typically have only a secondary impact on drag (because the nose/tail drag is typically only 10–20 percent of total drag), although rolling stock manufacturers still put considerable effort into this area and such design does significantly mitigate other aerodynamic effects, such as the nose pressure pulse.



Figure 9-2. Car-to-car gap covering [138]

9.5.3 Tunnels

Aerodynamic drag within tunnels can be reduced by increasing the cross-sectional area of tunnels and/or by providing air shafts.

9.6 Assessment

9.6.1 Assessment Objectives

For *rolling stock manufacturers*, assessments aim to measure or predict the aerodynamic drag associated with a particular design as part of a process to optimize the design to reduce drag. Drag characteristics of the train are an *output* of the assessment. They can take the form of drag coefficients or Davis Equation coefficients.

For *operators*, aerodynamic drag is one of the *inputs* into assessments of whole journeys or operations. The objectives may include:

- Calculations of energy expended per journey
- Calculations of power requirements along the route
- Calculations of achievable speed profile and journey time
- Optimizations of journey time versus energy cost by adjusting the speed profile and,
- Environmental impacts that may be considered by some operators.

9.6.2 Assessment Methods

The methods for measuring or predicting the aerodynamic drag associated with a particular train design include:

- Full-scale testing; see Section [9.6.2.1](#) below.

- Wind tunnel testing (see Section 2.4.4), generally used to measure drag coefficients of individual vehicles or components such as pantographs. It is difficult to measure drag on a whole train by wind tunnel testing.
- Numerical analysis (CFD); see Section 2.4.5. As with wind tunnel testing, CFD is useful for predicting the drag coefficients of individual vehicles and components. Predicting the drag on a whole train by CFD could be very resource-intensive.

Wind tunnel testing and CFD are useful during design development for finding vehicle shapes that reduce drag but may not always be capable of predicting drag for the full-scale vehicle accurately. Reasons include the difficulty of reproducing the small geometrical details that influence drag.

Reduced-scale moving model testing is not applicable to assessing drag, for the reasons stated in Section 9.6.2.2.

Assessments of journeys or operations (referred to here as **journey modelling**) typically calculate drag using the Davis Equation, described in Section 9.6.2.3. This requires input of the Davis Equation coefficients, which can either be representative of a particular train (e.g., provided by the manufacturer and resulting from assessment by testing or CFD); or, they can be generic and representing typical HSTs (like those given in Section 9.6.2.4).

One-dimensional analysis is applicable to calculations of aerodynamic drag in tunnels, as described in Section 9.6.2.5. As with the Davis Equation, the input coefficients relating to drag should be established first.

9.6.2.1 Full-Scale Testing

All full-scale testing methods suffer from high cost, difficulty of separating mechanical drag from aerodynamic drag, and the lack of control over experimental conditions like grade and crosswinds. The same methods can be applied in open air and in tunnels.

Full-scale testing may involve **coasting**, also known as **run down**. The train is run up to a certain speed and then, immediately before entering the test section of track, all tractive effort and sources of magnetic resistance are stopped, and the train is allowed to coast. The test section should be a level, tangent track in order to isolate aerodynamic drag from curving and grade forces. Train speed is measured as a function of time, and the deceleration is measured directly with accelerometers.

Different methods of calculating Davis Equation coefficients from the test results are available. For example, the measured data can be expressed as a series of points on a graph of resistance force versus train speed, and the values of the Davis coefficients that provide the best fit to the measured data can then be found by regression analysis. Alternatively, the coefficient values that provide the best prediction of the train's velocity time-history in a dynamic simulation of the coasting test can be found by an iterative process.

European Standard EN14067 Part 4 [33] contains some requirements and guidance for performing coasting tests and describes methods of calculating the Davis Equation coefficients from the test results.

As an alternative to coasting tests, a **dynamometer car** with an instrumented coupler can be incorporated into the train [126]. The measured force is the drag on the part of the train ahead of (or behind, dependent on the specific setup) the dynamometer car. Therefore, the drag on a whole train cannot be measured with this type of test.

It is also possible to estimate the total resistance of the train by carefully monitoring the power consumption of the traction motors.

9.6.2.2 Reduced-Scale Moving Model Testing

It is difficult to obtain reliable measures of drag (or drag coefficient) from reduced-scale moving models, for reasons including the following:

- The scale-model trucks and wheels often have to be suited to the test facility's track and propulsion system and it may not be possible to reflect the actual design of these components which contribute significantly to drag.
- The length of some scale model facilities may be too short for coast-down experiments (i.e., the reduction of velocity within the length of the test track may be too small to measure reliably).
- As with full-scale coast-down tests, it can be difficult to separate aerodynamic drag from mechanical drag;
- Drag can depend on small details of the design that are difficult to reproduce at reduced-scale.
- Friction effects can vary with geometric scale, even if the geometry is reproduced exactly to scale in the reduced-scale model and the airflow speed is the same as at full-scale (in fluid mechanics terms, this is known as Reynolds Number dependence).

The last two of the above are also relevant to wind tunnel testing.

9.6.2.3 Assessment Using the Davis Equation

Once the drag characteristics of a particular train are known, the drag force at any train speed can be estimated by the **Davis Equation**. This was introduced in Section 9.2.1 as Equation 9-1 in its basic form and is repeated here for convenience, with additional details relevant to using it in assessments. The equation should not be relied on to predict train resistance precisely. It is useful mainly as a comparative tool, for example to estimate the energy usage in one scenario relative to another.

$$R = A + BV_T + CV_{Ta}^2$$

From Equation 9-1

Where:

R = total drag force resisting the motion of the train;

A, B = coefficients related to mechanical drag;

C = coefficient related to aerodynamic drag;

V_T = speed of the train relative to the ground; and,

V_{Ta} = speed of the train relative to the air (see notes in the text below).

The equation includes mechanical and aerodynamic drag only. Forces due to curving, grades, or acceleration need to be added separately.

See notes below concerning units.

The linear term of the Davis Equation BV_T is sometimes broken into separate terms $B_1V_T + B_2V_{Ta}$ where the B_2 term accounts for the forces to accelerate the mass of air ingested by the train for combustion, cooling, and air conditioning [126]. However, at the speeds covered by this manual these effects are much less significant than aerodynamic drag. Therefore, this manual uses the simpler version of Davis Equation.

It is important to know the units in which the **Davis Equation coefficients** (A , B , and C in Equation 9-1) are specified, and to use them appropriately. For example, the coefficients could be given in SI units (where V_T must be provided in m/s and R is the force in N, as per the examples in this report) or in km/h, kN units (where V_T must be provided in km/h and R is the force in kN) or in English units such as mph, lbf. In each case the values of A , B , and C will differ according to the unit system. There is a high potential for critical errors in calculations if this point is not attended to.

Note also that the Davis Equation coefficients are specific not only to a particular train type, but also to a particular train length, so it is important to establish to what train length the provided Davis coefficients apply. Higher values are expected for longer trains.

The term V_{Ta} in Equation 9-1 (train speed relative to the air) becomes different from V_T (train speed relative to the ground) when assessing drag in the presence of wind. For example, in a 10-mph headwind, V_{Ta} would be 10 mph greater than V_T . The effect of natural wind is often ignored in drag calculations because the wind is different every day and is not known in advance, whereas the aim of the assessments is to calculate energy costs for an operation generally rather than under particular wind conditions. Therefore, in Equation 9-1, both V_T and V_{Ta} would normally be set equal to the train speed. However, it may be useful to include natural wind for the following reasons:

- Although the wind blows from different directions and with different speeds on different days, the net effect of wind on energy consumption over a long period of time does not cancel out. Headwind increases drag by more than a tailwind of the same speed reduces it, and crosswind increases drag even when blowing perpendicular to the track. Therefore, on average, wind increases drag and

hence increases energy costs. For example, aerodynamic drag has been estimated to increase by 10 percent due to wind, even on a relatively calm day [59]. It may be desirable to add a notional wind speed to the train speed (or alternatively to increase the C coefficient) in order to include the average effect of wind on drag in assessments.

- As a sensitivity study to understand the influence of wind on drag, or to estimate the wind conditions under which the train will have insufficient power to maintain the planned speed. In that case, the maximum credible headwind speed can be added to the train speed to provide an upper limit on V_{Ta} and hence an upper limit on aerodynamic drag force.

Note that the true influence of wind on drag is complex. If the effect of wind blowing from different angles were to be included rigorously in assessments, it would make the Davis Equation impractical to use (for example, the C coefficient would no longer have a constant value). The addition of a simple headwind term to represent the overall effect of different wind conditions, or else an increased “wind-average” C coefficient, is useful as a rough approximation instead.

Just as the aerodynamic drag is influenced by wind, the mechanical resistance (represented in the Davis Equation by the A and B terms) is subject to significant variability in different real-world conditions.

Equations for energy usage and power are given below. These equations are not particular to aerodynamics but are provided here because they are used in the examples at the end of this section of the report.

The energy usage to overcome drag is given by Equation 9-4:

$$E = RD \quad \text{Equation 9-4}$$

Where:

E = energy usage for a segment of the journey during which the resistance force stays the same;

R = force resisting the motion of the train; and,

D = length of the segment.

Total energy usage is obtained by summing E across all the segments of the journey.

Consistent units are required for this equation, see Section 2.7. SI units are recommended: E in Joules, R in Newtons, and D in meters.

The power required to overcome drag is given by Equation 9-5:

$$P = RV_T \quad \text{Equation 9-5}$$

Where:

P = power required to overcome resistance at an instant in time;

R = force resisting the motion of the train at that instant in time; and,

V_T = speed of the train relative to the ground.

Consistent units are required for this equation, see Section 2.7. SI units are recommended: P in Watts, R in Newtons, and V_T in meters per second.

9.6.2.4 Values for the Davis Equation Coefficients for Baseline Trains

Davis Equation Coefficients A , B , and C are specific to each particular train design. Values should be sought from train manufacturers where possible, although the data are often considered by the manufacturers as confidential and may be hard to obtain. In the absence of train-specific data, the approximations given in Equation 9-6 through Equation 9-8 may be used instead. The equations have been derived from formulae and data for TGV trains given in [122] together with the dimensions of the Baseline Trains given in Table 2-2 and an assumed train mass of 2 tonnes per meter length (1,344 lbs per ft). The values given by these equations are likely to be conservative compared with the actual values for many currently-available HSTs.

$$A = k_A L \quad \text{Equation 9-6}$$

$$B = k_B L \quad \text{Equation 9-7}$$

$$C = k_{C1} + k_{C2} L \quad \text{Equation 9-8}$$

Where:

A, B, C = Davis Equation coefficients with train speed in m/s (*note, not mph or km/h*) and force in Newtons;

k_A = 18 N/m (U.S./Euro Baseline Trains) or 20 N/m (U.S./Asian);

k_B = 0.8 Ns/m² (U.S./Euro Baseline Trains) or 0.9 Ns/m² (U.S./Asian);

k_{C1} = 1.3 Ns²/m² (U.S./Euro Baseline Trains) or 1.4 Ns²/m² (U.S./Asian);

k_{C2} = 0.031 Ns²/m³ (U.S./Euro Baseline Trains) or 0.034 Ns²/m³ (U.S./Asian); and,

L = Train length, in meters.

The dependence of drag force on train speed calculated from the above data and converted back to English units is shown in Figure 9-3. The dependence on train speed of the power required to overcome drag is shown in Figure 9-4.

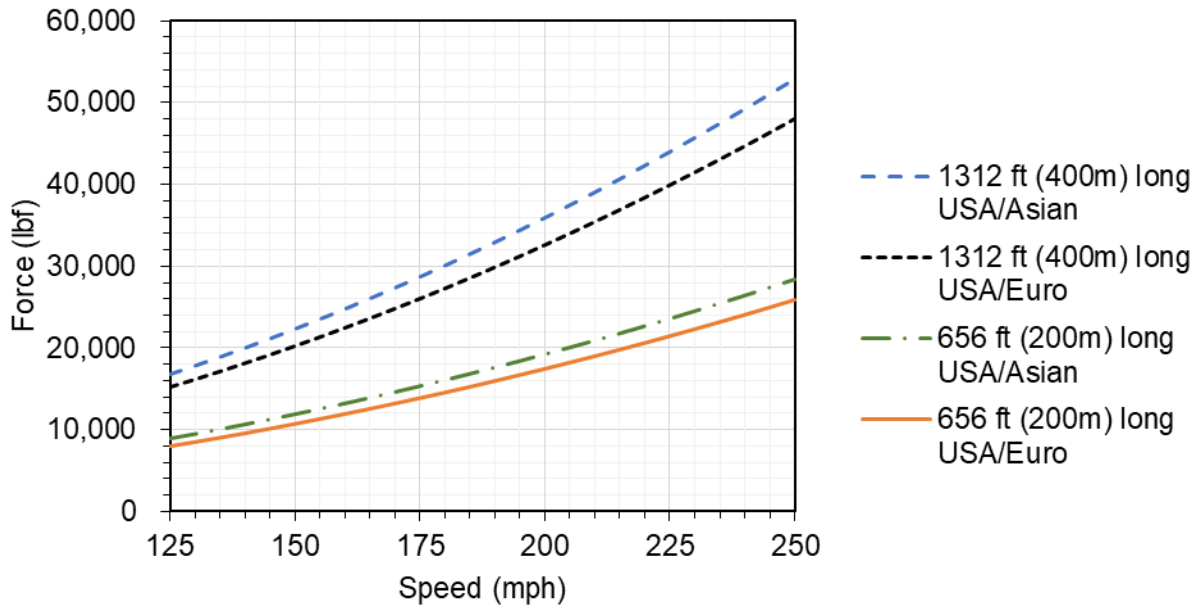


Figure 9-3. Drag force in open air, Baseline Trains with Davis Equation coefficients from Equation 9-6 through Equation 9-8

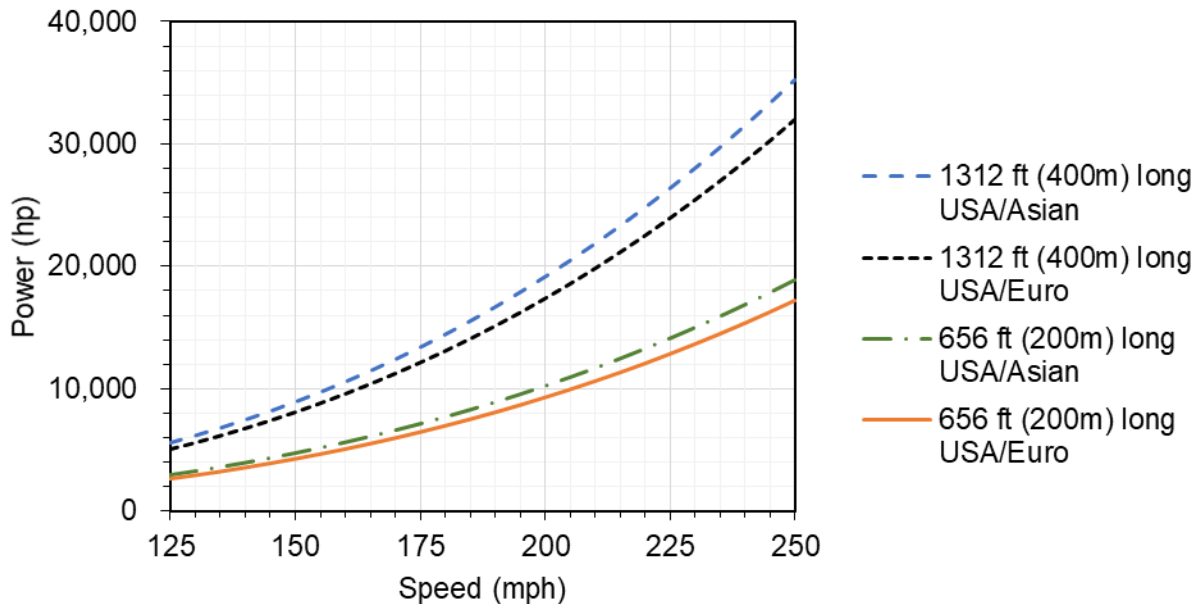


Figure 9-4. Power required to overcome drag in open air, Baseline Trains with Davis Equation coefficients from Equation 9-6 through Equation 9-8

9.6.2.5 Drag in Tunnels

Two approaches are available for estimating drag in tunnels: the Davis Equation, and One-Dimensional Analysis. Both require tunnel-specific input information from train manufacturers or from full-scale tests in tunnels before drag can be calculated.

9.6.2.5.1 Assessing Drag in Tunnels Using the Davis Equation

The Davis Equation is adapted for the tunnel environment using a Tunnel Factor as shown in Equation 9-9. Sometimes the Tunnel Factor is presented for simplicity as a single number, but in practice it depends not only on train type, but also on tunnel length and blockage ratio, and its value is therefore specific to each train/tunnel combination. Some train manufacturers may be able to supply tables or equations from which the Tunnel Factor for a specific train/tunnel combination can be calculated. The drag force also varies with time as the train passes through the tunnel, although it is not usually necessary to include that effect in assessments of drag impacts along a whole route.

$$R = A + BV_T + T_f CV_T^2 \quad \text{Equation 9-9}$$

Where:

T_f = Tunnel Factor.

and the other terms are the same as in Equation 9-6, Equation 9-7, and Equation 9-8.

Note that the aerodynamic drag term uses V_T (the speed of the train relative to the ground, not relative to the air). Although the speed and direction of airflow has a large influence on drag in tunnels, this effect is included in the Tunnel Factor.

9.6.2.5.2 Assessing Drag in Tunnels Using One-Dimensional Analysis

Many of the software packages that perform the specialized one-dimensional analysis described in Section 7.6.5 can output the aerodynamic drag force on the train. The inputs that influence the drag (such as friction coefficient and nose and tail loss coefficients, see Table 7-8) should first be calibrated against full-scale test data, consisting of measurements of pressure and/or air velocity in a tunnel when the train in question passes through the tunnel [149]. Data from the tunnel-entry pressure wave test described in Section 7.6.17 is suitable for this purpose. After calibration, the software may be used to analyze the same train passing through tunnels of different lengths and blockage ratios, resulting in a prediction of aerodynamic drag force for those tunnels. This process relies on the assumption that the calibrated values of the input coefficients remain valid for tunnel lengths and blockage ratios different from the ones in the full-scale test. In practice, some of the input may have a dependence on blockage ratio. Some software packages can correct for this, but others do not, so drag results from the software may become less accurate as the blockage ratio becomes more different from the tested condition.

If full-scale test data are not available, but the trains are expected to pass the tunnel-entry pressure wave test described in Section 7.6.17, the software may be calibrated so as to generate a pressure wave matching the limits shown below Figure 7-31. This provides a conservative estimate: if the drag characteristics in tunnels were any worse than this, the train would not pass the tunnel entry test. This is how the data in Figure 9-5 have been generated.

Two example time-histories of aerodynamic drag force in tunnels calculated by one-dimensional analysis software are shown in [Figure 9-5](#). These analyses simulate a 1,312 ft (400 m) long U.S./Euro Baseline Train running at 175 mph (280 km/h) through single-track tunnels of the Nominal Tunnel Size which is 646 ft² (60 m²). The two examples differ with respect to the length of the tunnel. Note that the software only calculates drag for the parts of the train that are inside the tunnel, and not for the parts that are in open air. This is why the graphs fall to zero at each end before and after the tunnel. In reality the drag in open air would not be zero.

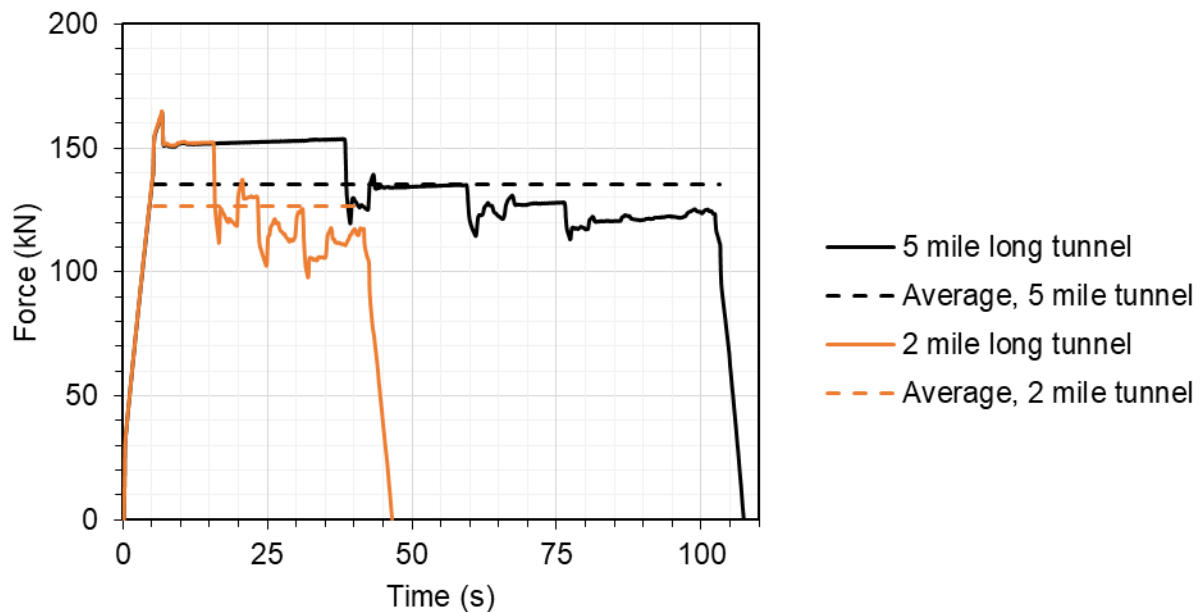


Figure 9-5. Example aerodynamic drag force time-histories from one-dimensional analysis software

As can be seen in the Figure, the drag force is not constant, but varies in a series of steps which occur when pressure waves pass over the train. The average aerodynamic drag force predicted by the software is 136 kN (30,300 lbf) in the 5-mile-long tunnel and 126 kN (28,100 lbf) in the 2-mile-long tunnel, corresponding to power consumption of 10.6 MW (14,200 hp) and 9.9 MW (13,300 hp) respectively required to overcome aerodynamic drag.

The software calculates only the aerodynamic drag force. To obtain total drag force, mechanical drag should be added. [Equation 9-9](#) may be used, replacing $T_f C V_T^2$ with the average aerodynamic drag force calculated by the software. Note that the total tractive effort would also include the effects of any curves or grades in the tunnel. These are not included in [Equation 9-9](#) and should be added separately when applying the equation in assessments.

The aerodynamic drag in the tunnel predicted by the software may be used to provide a Tunnel Factor for use in journey modelling based on the Davis Equation, see [Equation 9-10](#). Note that the Davis Equation coefficients used to predict drag in open air are not directly linked to the input data for the tunnel analysis. These may even come from

different sources and may be conservative or non-conservative to different extents. The Tunnel Factor derived in this way should not be assumed to be applicable in general, it is specific both to the particular train/tunnel combination and also to the Davis Equation C -coefficient assumed for open air drag, see [Equation 9-10](#).

$$T_f = R_a / CV_T^2 \quad \text{Equation 9-10}$$

Where:

T_f = Tunnel Factor for use in Davis Equation;

R_a = Average aerodynamic drag force predicted by the analysis, in N;

C = Davis Equation C coefficient used to predict drag in open air, in Ns^2/m^2 ; and,

V_T = Train speed in the analysis, in m/s.

9.6.3 Acceptability Criteria

In general, aerodynamic drag is not assessed against acceptability criteria. Operators form their own judgments as to the acceptability of the impacts on energy costs together with considerations around power supply, environmental impacts, potential revenue, and other operator-specific issues

China has acceptability criteria for rolling stock based on drag characteristics [\[21\]\[101\]](#). The objective of the criteria is to limit power consumption by HSR nationally.

The Chinese criteria are expressed as maximum allowable drag coefficients (defined in [Section 9.2.2](#)) for different vehicle types such as leading vehicle, intermediate vehicle and trailing vehicle. The limit values are speed-dependent, with trains capable of higher speeds being subject to lower limits. Approximately, after adding together the drag contributions from the separate vehicles, the Chinese criteria correspond to Davis Equation C -coefficient values for a whole train around 5 to 15 percent less than those given in [Equation 9-8](#) for U.S./Asian Baseline Trains.

For the U.S. HSR market, operators will make their own choices with regard to rolling stock, therefore specific recommendations regarding acceptability criteria for drag are not provided in this manual. If drag-related performance criteria for rail vehicles are required, it may be preferable to express these in terms of the desired outcomes (such as energy consumption per mile at a given speed, or maximum attainable speed for given power consumption), rather than drag coefficients of each vehicle.

9.6.4 Examples

9.6.4.1 Using the Davis Equation

Question

Assuming 1,312 ft (400 m) long U.S./Euro Baseline Trains with the drag characteristics given in Section 9.6.2.4, calculate the drag force, power requirement and energy usage for a journey segment during which the train covers 50 miles at 175 mph. There are no tunnels.

Methodology

Convert input data to SI units.

Calculate Davis Equation coefficients from Equation 9-6 through Equation 9-8.

Apply Davis Equation (Equation 9-1), ignoring headwind.

Calculate energy usage from Equation 9-4 and power from Equation 9-5.

Calculations

Davis Equation coefficients in N, m/s units from Equation 9-6 through Equation 9-8:

$$A = k_A L = 18 \times 400 = 7,200 \text{ N}$$

$$B = k_B L = 0.8 \times 400 = 320 \text{ N s/m}$$

$$C = k_{C1} + k_{C2} L = 1.3 + 0.031 \times 400 = 13.7 \text{ N s}^2/\text{m}^2$$

Convert train speeds to m/s and segment lengths to m:

$$50 \text{ miles} = 80,467 \text{ m}; 175 \text{ mph} = 78.2 \text{ m/s}$$

Apply Davis Equation to calculate drag force:

$$R = A + BV_T + CV_{Ta}^2 = 7,200 + 320 \times 78.2 + 13.7 \times 78.2^2 = 116,000 \text{ N} = 116 \text{ kN}$$

Calculate energy usage from Equation 9-4:

$$E = RD = 116,000 \times 80,467 = 9.33 \times 10^9 \text{ J} \approx 9.3 \text{ GJ}$$

Calculate power from Equation 9-5:

$$P = RV_T = 116,000 \times 78.2 = 9.07 \times 10^6 \text{ W} \approx 9.1 \text{ MW}$$

Result

The total drag is 116 kN (25,900 lbf), the energy usage is 9.3 GJ (2590 kW-h) and the required power is 9.1 MW (12,200 hp). These figures exclude the effects of grades, curves and acceleration. For comparison, the energy required to accelerate the train to 175 mph is 2.4 GJ (670 kW-h) (assuming 800 tonnes train mass), and the energy required to ascend a grade through 300 vertical feet (91 m) is 0.8 GJ (220 kW-h).

9.6.4.2 Calculating and Using the Tunnel Factor

Question

Based on the example one-dimensional analysis result in Section 9.6.2.5.2 for a 5-mile-long tunnel and a 1,312 ft (400 m) long U.S./Euro Baseline Train at 175 mph, calculate the Tunnel Factor for use in the Davis Equation for this particular train/tunnel combination.

If the train has 21,500 hp (16 MW) of installed power, would it be able to sustain a speed of 200 mph in this tunnel, ignoring grades?

Methodology

Convert train speeds to m/s. The Davis Equation coefficients for this train in open air have already been calculated in the previous example ($A=7,200$ N, $B=320$ Ns/m, $C=13.7$ Ns²/m²).

Use the average aerodynamic drag force from the analysis (136 kN, see Section 9.6.2.5.2) in Equation 9-10 to calculate the Tunnel Factor.

Use the Tunnel Factor in Equation 9-9 to calculate drag force at 200 mph, calculate power from Equation 9-5. If the required power is less than or equal to the installed power (16 MW), then the train can sustain this speed in the tunnel.

Calculations

Convert train speeds to m/s: 175 mph = 78.2 m/s; 200 mph = 89.3 m/s.

Calculate the Tunnel Factor from Equation 9-10:

$$T_f = R_a / CV_T^2 = 136,000 / 13.7 \times 78.2^2 = 1.62$$

Use Equation 9-9 to calculate drag force at 200 mph (89.3 m/s):

$$R = A + BV_T + T_f CV_T^2 = 7,200 + 320 \times 89.3 + 1.62 \times 13.7 \times 89.3^2 = 213,000 \text{ N}$$

Calculate power from Equation 9-5:

$$P = RV_T = 213,000 \times 89.3 = 19.0 \times 10^6 \text{ W} = 19 \text{ MW}$$

Result

The Tunnel Factor is 1.62.

The power required to overcome drag at 200 mph in the same tunnel is 19 MW (25,500 hp) which exceeds the installed power of the train. Therefore, this speed cannot be sustained by the train. Repeating the calculation with different train speeds shows that the maximum sustainable speed is 188 mph, ignoring grades. Note, however, that if the train entered the tunnel at 200 mph applying full power, the initial deceleration rate due to the excess drag is only 0.042 m/s² (equivalent in this example to less than 2 mph loss of speed per mile of tunnel).

10 Ballast Flight

10.1 Introduction

The risk of ballast flight should be considered when selecting track types for new operations, when designing ballasted track and developing ballast installation and maintenance procedures on high-speed lines, and when speed increases on existing ballasted track lines are proposed.

In this report, the term **ballast flight** refers to the movement of ballast particles under the influence of aerodynamic effects from passing trains, and not to particles displaced by objects and ice or snow dropping from trains. Flying ballast can damage trains, rails, wayside structures, and may even pose a risk to maintenance personnel near the track.

Ballast flight is known to be highly speed-dependent, with risks and potential damage increasing dramatically at higher train speeds. Ballast flight could present a limiting factor on the operating speeds achievable on ballasted track, even when best practices are followed. The phenomenon is not completely understood, and it is not possible to make a calculation of whether ballast flight will occur. Current guidelines for mitigating ballast flight are derived from experience and are based around ballast selection, placement, and maintenance. Aerodynamic design of the underside of the train is another relevant factor.

For a more complete treatment of the subject, see FRA report, [Identification of High-Speed Rail Ballast Flight Risk Factors and Risk Mitigation Strategies \[45\]](#), which contains information on recent research efforts and a Risk Screening Tool.

This section includes:

- Aerodynamic principles related to ballast flight
- Influencing factors
- Impacts on trains, structures, and people
- Mitigation methods
- Assessment methods

10.2 Ballast Flight Principles and Phenomenon

Aerodynamic-induced ballast flight constitutes a complex vehicle/track/aerodynamics system issue. Ballast particle motion is initiated by aerodynamic effects: when the airflow under a train picks up a ballast particle, e.g., from on top of a tie. Initiation of motion of particles may also be influenced by vibration of ties and/or track bed causing an upward acceleration of ballast particles, thereby making it easier for the airflow to move them.

A ballast particle is unlikely to travel far under aerodynamic loading only. However, when a flying particle is hit by the moving train, it can be projected at high speed with potential for a range of damaging impacts.

Flying ballast can cause a **chain reaction** where ballast is sequentially displaced by the interaction with other displaced ballast; impact with the underside of the moving train throws some of the particles violently against the ballast surface, ejecting further particles and continuing the chain reaction, as shown in [Figure 10-1](#).

In [Figure 10-1](#), a ballast particle (whose path is represented by the blue arrows) impacts the train at point 1, and rebounds at high speed into the trackbed at point 2, where two new particles are ejected (red and orange arrows). These impact the train at points labelled 3, and rebound to hit the trackbed at 4, where a further particle (green arrow) is ejected. Since each impact with the trackbed can lead to ejection of multiple ballast particles, the consequence is a continuous shower of particles being flung at high speeds at the underside of the train. Some particles may also be ejected laterally.

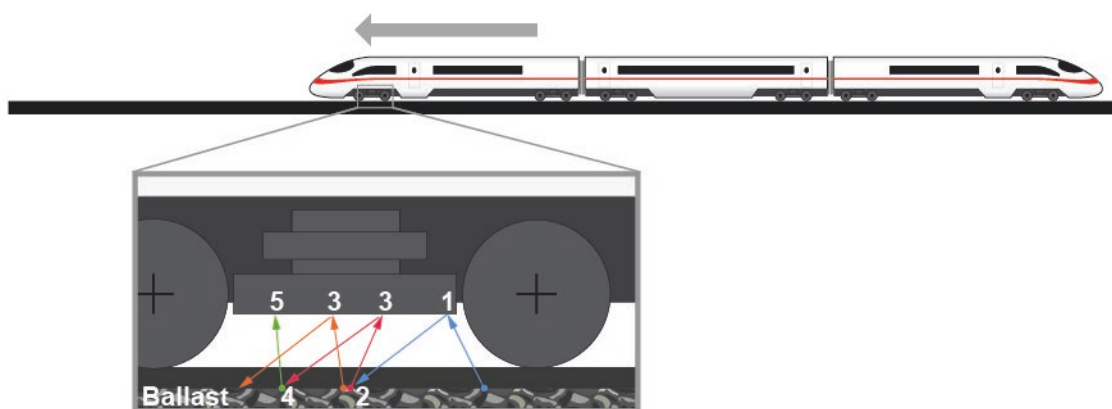


Figure 10-1. Ballast flight chain reaction⁸

Ballast flight arises from a sequence of events that each have a certain probability – e.g., a particle light enough to be picked up lies in an exposed position on top of the ballast or tie; and, a vibration occurs that bounces the particle upwards; and, at the same time, there is a gust of air from a passing train fast enough to carry the particle away; and, the particle hits a part of the moving train – and so on. It is not surprising, therefore, that there is not a fixed train speed at which ballast flight does or does not occur. Instead, the probability of ballast flight increases with train speed. This may be expressed as the number of particles flying per unit time or per unit distance along the track. In general, ballast flight becomes a problem when the number of particles projected is great enough for significant damage to occur.

Ballast flight may also be caused by objects, ice, or snow, falling from trains onto the track (**winter conditions ballast flight**), and this sometimes causes a chain reaction similar to that described above. Aerodynamic forces can contribute to the initial detachment of ice or snow from the train, but apart from that the initiation mechanism is essentially non-aerodynamic. It can occur at much lower speeds than aerodynamic-induced ballast flight and is not specific to HSR. Winter conditions ballast flight is not

⁸ Sequential impacts of ballast particles labelled 1 through 5 are described in [Section 10.2](#). Arrows are color-coded to represent the paths of different particles.

covered in this report. This section relates to aerodynamic-induced ballast flight only. What distinguishes aerodynamic-induced ballast flight chain reactions from the occasional flight of particles under normal conditions is the potential for large numbers of particles to be involved, greatly increasing the impacts such as damage to the underside of the train.

10.2.1 Recorded Incidents of Ballast Flight

If there were any clear pattern regarding, for example, the train speed above which aerodynamic-induced ballast flight always occurred, it might be revealed by studying previous ballast flight incidents. Various HSR ballast flight incidents through the early part of this century are summarized below in [Table 10-1 \[45\]](#). The causes of each incident are not clear, although those occurring in winter conditions may have been due to falling ice or snow rather than aerodynamic effects. Since winter conditions ballast flight incidents cannot provide any information regarding the conditions for aerodynamic-induced ballast flight, these are grouped separately in [Table 10-1](#). The table also includes for comparison notable HSR operations where ballast flight does not (or did not) occur.

Table 10-1. Reported ballast flight incidents (2001–2007) (adapted from [45])

Date	Train Type	Location	Speed (mph) ¹	Speed (km/h)	Track Type	Remarks
Ballast Flight Occurred – Possibly Due to Winter Conditions						
2001	ICE3	Fulda – Gottingen, Germany	145	230	Mono-block ties, lowered ballast	
2003	ICE3	Lille-Calais, France	200	320	Bi-block ties	
2004	ICE3	Mannheim – Stuttgart, Germany	155	250	Mono-block ties, lowered ballast	Foreign parts in the track have been found.
2006	ICE-T	Hamburg – Berlin, Germany	145	230	Mono-block ties, lowered ballast	
Ballast Flight Occurred – Not Due to Winter Conditions, Likely to Be Aerodynamic-Induced						
2003	KTX	South Korea	185	300	Mono-block ties	
2003	ICE3	Belgium	185	300	Mono-block ties, ballast not lowered	Speeds up to 170 mph (275 km/h) did not cause problems.
2004	ICE3	France	200	320	Bi-block ties	During homologation test runs
2004	ETR500	Rome – Naples, Italy	170	270	Mono-block ties, ballast above ties	Ballast flight ceased when ballast profile was lowered below ties.
Ballast Flight Did Not Occur						
2007+	TGV	Daily operations throughout France	185 to 200	300 to 320		
2007	TGV	Paris – Strasbourg, test run, France	320	515		
2013	ACE	Madrid – Barcelona, Spain	195	310		
Note: 1. Speeds rounded to nearest 5 mph.						

The table above shows that there is no consistent pattern in terms of train operating speed, track type, and train type for which these incidents resulted. This is indicative of the phenomenon of ballast flight. It is complex and not fully understood and caused by a number of often interacting factors.

10.3 Influencing Factors

Substantial recent research programs summarised in [45] have provided understanding of the influencing factors but have also revealed the complexity of the phenomenon and the high degree of variability from case to case. This section summarizes the influencing factors on risk of ballast flight.

10.3.1 Train Speed

The risk of aerodynamic-induced ballast flight increases sharply as train speed approaches a critical speed [89][125]. The critical speed is unique to the combination of train and track and can be established only by full-scale testing. As described in Section 10.2.1, problematic ballast flight chain reaction has been observed in one set of tests at speeds as low as 170 mph, but not in another test at 350 mph, nor during regular operations of HSTs at 200 mph. As a result, it is impossible to determine a threshold or critical speed applicable to all ballasted track at which ballast flight becomes prevalent.

Based on the information above, the approximate risks associated with different operating speeds are shown in Table 10-2.

Table 10-2. Ballast flight risk profiles

Speed	Risk
0–125 mph	Low risk of ballast flight chain reactions
125–200 mph	Low to medium risk is achievable with best international HSR practice on ballast.
>200 mph	Higher risk

10.3.2 Aerodynamic Design of the Train

Different train designs have different potential to cause ballast flight. Smooth airflow under the train is desirable, as is the minimization of air velocity at the level of the ties. This can be achieved by aerodynamic design of the underside of the train.

10.3.3 Considerations for Ballast

Important considerations for the ballast:

- The surface height relative to ties – if the ballast is recessed relative to the ties, the ties may shield the ballast from the highest air speeds (Figure 10-2). Lowering the ballast profile by 0.8 to 1.6 in (20 to 40 mm) has been successfully implemented as a mitigation strategy in Europe and China. However, lowering the ballast profile may lead to decreased lateral track resistance. The track designer should confirm that the lateral resistance of the track structure is appropriate for the anticipated lateral loads.



Figure 10-2. Left: Typical track ballast conditions. Right: lowered profile ballast less susceptible to aerodynamic effects from trains (Figure 3.3 from [45])

- Ballast particle size – small particles are more prone to be set in motion and travel further under aerodynamic loading [81], so the absence of small particles makes initiation of ballast flight less likely at a given train speed.
- Compaction of the ballast reduces the tendency of particles to become detached and fly away.
- Track maintenance procedures have an important role to play. Risk of ballast flight is reduced when the tops of the ties are kept clear of ballast particles, and the ballast is well-compacted with minimal irregularity of support conditions for the ties.

10.3.4 Dynamics of Track

Dynamic vertical movement of the track has the potential to cause bouncing ballast particles, which may then be more easily picked up by the airflow under the train [113]. This can be linked to a lack of vertical stiffness of the track, subgrade, or supporting structures such as viaducts, localized soft spots or poorly supported ties, or a particular train type that exerts a high dynamic load on the track.

10.3.5 Environmental Factors

Environmental conditions that disturb the ballast could lead to smaller particles reaching the ballast surface, moving onto the tops of the ties, or becoming less tightly packed and therefore more readily detached.

10.3.6 Secondary Factors

Trains operating inside a tunnel where the airflow is bounded to some extent has an impact on the potential for ballast flight compared to a train operating in open air. Ballast flight may occur at lower speeds compared to trains operating in open air [45].

Trains passing or meeting on adjacent tracks can cause higher air velocities above the ballast and therefore increase the risk that particles may fly.

10.4 Impacts

For each of the types of impacts described below, the severity depends not only on the speed and size of the flying particles but also on the number of particles involved. The flight of occasional one-off particles may be tolerated and is probably unavoidable, even in situations where the risk of ballast flight is considered low. Ballast flight chain reactions, on the other hand, would never be tolerated due to the extremely high level of damage to trains and, potentially, risk to people near the track.

10.4.1 Damage to Trains and Rails

Carbodies can receive scratches and dents. Pipes, brakes, traction system, drive train components, and other systems can be damaged. In the case of ballast flight chain reactions, the damage occurring during a single train passage can be substantial and can require the train to be taken out of service for repairs.

Particles landing on the rails may cause pitting or other damage to the wheels and rail head. This can become a maintenance issue over time, even when particles are picked up only occasionally and ballast flight chain reactions do not occur.

10.4.2 Damage to Trackside Signs and Equipment

In the most severe cases, ballast can fly away from the train and damage existing structures, signage, or equipment.

10.4.3 Impacts on People

Flying ballast might also have potential to strike maintenance personnel on the trackside. This could occur either when a flying ballast particle is hit by the train and is ejected away from the track, or else when a particle lands on a rail and is later ejected by the wheels of another train. However, the risk to people from aerodynamic-induced ballast flight chain reactions appears to be limited, for two reasons:

- If large numbers of particles are being projected, that condition would likely be identified during testing and would not be permitted to continue during regular operation. Thus, the risk from ballast flight chain reactions may exist for personnel present during testing but is unlikely to affect track workers during normal operation.
- For passengers on platforms, the speeds mandated for trains running alongside platforms is generally too low for ballast flight to be a possibility. On high platforms, passengers would be shielded by the vertical face of the platform.

Occasional ejection of a ballast particle (as opposed to a chain reaction) is possible at any train speed. Track workers could potentially be struck.

10.4.4 Impacts on Operations and Selection of Track Type

Ballast flight is one of the limiting factors on the speeds achievable on ballasted track. For speeds above about 200 mph (the highest speed of existing HSR operations on ballasted track), there is a risk that ballast flight chain reactions cannot be prevented, even if the ballast design, installation and maintenance follow international best practice

for HSR. Ballasted track may, in any case, be a less favorable choice for very high-speed operation due to the sharp increase of maintenance costs with increasing operating speed.

10.5 Mitigation Methods

10.5.1 Reduction of Speed

Reduction of operating speeds below the critical threshold that causes ballast flight may be required across the route. Alternatively, speed restrictions may be appropriate on affected or the most susceptible sections of track. The critical speed will vary based on the influencing factors described in Section [10.3](#).

10.5.2 Rolling Stock Design

Rolling stock design is an important factor in mitigating ballast flight. Aerodynamic rolling stock design that ensures smooth airflow under the cars and low airflow speeds at the level of the ties and ballast will serve to reduce the probability of ballast particles being picked up. This might be achieved by including fairings on trucks, installing underbody equipment in smoothly enclosed housings in the center of the car, and ensuring that the underbody of the car is as smooth and streamlined as possible.

10.5.3 Track Type

The difficulty of predicting and preventing ballast flight is an important consideration when choosing ballasted or non-ballasted track types, especially for speeds above about 200 mph. The risk of ballast flight can be eliminated by selecting slab track instead of ballasted track.

10.5.4 Ballast Design and Maintenance

In the event that ballasted track is selected, the risk of ballast flight can be reduced by designing and maintaining the track to ensure:

- The top surface of the ballast is around 1.6 inches (40 mm) below the top of the ties, thus protecting the ballast to some extent from the airflow induced by trains. This is now considered best practice internationally for mitigating ballast flight [\[63\]\[139\]](#). The lateral stability of the ties with this reduced embedment depth should be checked, increasing the depth of the ties if necessary.
- An absence of small particles
- Adequate compaction of ballast, high vertical stiffness and absence of soft spots and track defects (these points are required for HSR operations irrespective of ballast flight). Chinese practice [\[139\]](#) sets a minimum ballast density of 1,750 kg/m³ (109 lb/cu ft).
- No ballast particles are left on top of the ties after maintenance.

10.5.5 Additional Measures

Other potential mitigation measures described in research papers include:

- Design the track to reduce air velocity at the ballast surface and/or provide less flat surface for ballast particles to land on. For example, specially designed ties (see [Figure 10-3](#)) have been reported to reduce aerodynamic forces experienced at the trackbed by over 20 percent [\[10\]](#). Furthermore, if ballast particles land on these ties, they are more likely to roll off, and this may contribute to a reduced tendency for ballast flight.



Figure 10-3. Example special aerodynamic tie [\[1\]](#) (Aerotraviesa sleeper, a SENER project (©ADIF), used with permission)

- The use of bonding material to increase ballast interlocking, or steel or plastic screens set atop the ballast, or enclosing ballast in bags (see [Figure 10-4](#)). While these may be effective mitigation measures for ballast flight, they increase capital costs, present problems for maintenance, and increase maintenance costs. For example, the ballast bags in [Figure 10-4](#) have to be removed for maintenance.



Figure 10-4. Japanese ballast bags (Figure 3.4 from [45])

10.6 Assessment

There are currently no calculation methods for predicting the speed at which ballast flight will occur. Full-scale testing is the only method currently available. Conclusions of such testing would be limited to the particular train type and the section of track that was tested. During testing, inspections for evidence of damage from ballast particles to the underside of the train should be performed.

Risk factors for ballast flight may be assessed using the Risk Screening Tool described in [45].

Testing methods for assessing the propensity of particular train designs to cause airflow likely to result in ballast flight are being developed; see, for example, the test specification given in Annex A of EN 14067-4 [33], but acceptability criteria are not provided. In the future, this type of testing could form the basis of a criterion for selecting or specifying rolling stock.

Since research in this area is ongoing at the time of writing, the designer should search the online research databases for up-to-date information on the subject.

11 Conclusion

This report provides the basic concepts, mitigation methods, criteria, standards, assessment methods, design guidance, and example calculations for the identified aerodynamic phenomena of high-speed trains in open-air and tunnel environments, including slipstreams, pressures on wayside structures, train-to-train aerodynamic effects, crosswinds, pressure waves inside tunnels, micro-pressure waves emitted from tunnels, aerodynamic drag effects, and ballast flight.

The main aerodynamic risks and the means of mitigating them are summarized below in checklist format.

Aerodynamic considerations for new HSR operations:

- Mitigate aerodynamic interactions between trains by setting the center-to-center track separation no less than indicated in Section 5.5.1. The separation distances are speed-dependent.
- When dedicated high-speed tracks run adjacent to conventional tracks in shared corridors, the separation between the two types of tracks must be at least 25 ft (and could be greater due to ROW protection for derailment events); this will very likely be sufficient to ensure that aerodynamic impacts between HSTs and conventional trains either do not occur at all or are no worse than aerodynamic impacts between conventional trains on conventional tracks. In shared ROWs (where the spacing can be less than 25 ft), Tier III equipment will be limited to no more than 125 mph. Therefore, no special consideration is necessary for these situations with respect to aerodynamics.
- If there is any possibility of track workers being present while HSTs are operating, risks from train slipstreams such as people being blown over, being struck by tools, etc., should be considered. Safety distances from the track should be no less than the distances given in Section 3.5.2.
- Risks of trains overturning or derailling in strong winds are mitigated by installing wind barriers in high-risk locations and/or imposing operational restrictions at times of high wind. Methods for assessing the risk and developing mitigation is provided in Section 6.
- The impacts of aerodynamic drag on energy costs and power supply design should be considered when planning operations, as described in Section 9.
- On ballasted track, ballast flight presents risks of extensive damage to trains. For speeds up to 200 mph (320 km/h), the risk is mitigated by suitable ballast placement and maintenance practices. For higher speeds, the efficacy of such measures is unknown and the potential for ballast flight could present a limitation on operating speed for ballasted track.

Aerodynamic considerations for structures near the track:

- Structures near the track such as noise barriers can suffer fatigue failure due to aerodynamic loading from passing trains. Structures should be designed to

resist loading from train pressure pulses, considering the potential for resonant effects and fatigue, as described in Section 4.

Aerodynamic considerations related to stations:

- Risk of passengers standing on platforms being blown over by train slipstreams can be mitigated by imposing a platform track speed limit for HSTs of 125 mph and providing safety markings at 5 ft from the edge of the platform. Lower speed limits may be needed for non-HST traffic passing platforms, especially freight. See Section 3.5.1 for further information.
- Regarding passengers on platforms, there are particular risks to wheelchair users and children in strollers and buggies which may be set rolling by train slipstreams and colliding with the train or falling onto the track. This risk is increased in confined spaces, e.g., where there is a wall behind the platform.
- Any surfaces and structures near the track, e.g., wall coverings, canopies, signs, advertising boards, should be designed to resist loading from pressure pulses (Section 4).
- Considerations related to aerodynamic effects in underground stations are given in Sections 7.4.7 and 7.6.14.

Potential aerodynamic impacts on residents with homes near the track, members of the public, and wildlife near the tracks:

- Check that the public will not be able to approach closely enough to open track that risks from slipstream effects become problematic, for example by providing fences or other barriers separating the public from ROWs.
- Micro-pressure wave emissions from tunnels can cause annoying or frightening noises and can rattle doors and windows of nearby houses. Primary mitigation is by adding entrance hoods to the tunnels. Methods for assessing micro-pressure waves and estimating the required size of hood for a particular tunnel are given in Section 8.

Aerodynamic considerations in the design of tunnels:

- Mitigation of pressure wave effects often governs the size of HSR tunnels and requires significant attention during design. The issues to be considered include the aural comfort and safety of passengers and crew, fatigue loading of trains, and fatigue loading of structures, doors, and equipment in the tunnel.
- Mitigation measures include selection of larger tunnel sizes for higher train speeds, either by reference to Table 7-1 and Table 7-2 or via case-by-case analysis with specialized software as described in Section 7.6.5.
- It is important to specify and/or design railcars and structures and equipment inside the tunnels to withstand the expected pressure loading, including fatigue effects from repeated applications of pressure loading.
- Environmental impacts from micro-pressure waves emitted from tunnels should be considered, as described above.

Items to consider when setting specifications for new rolling stock:

- Cross-section dimensions and cross-sectional area should be compatible with the design of the infrastructure. Sizes based on European and Asian HSTs are given in [Table 2-2](#).
- Aerodynamic performance in standard tests for slipstream air velocity and open-air pressure pulse. See figures given for Baseline Trains in Section [2.3.2](#).
- Stability in crosswinds which is described by Characteristic Wind Curves; see Section [6.2.8](#). Operators may wish to consider specifying the CWCs given in Section [6.6.3.2](#) as a minimum standard.
- Tunnel entry pressure wave characteristics of the train compared to the requirements described in Section [7.6.17](#).
- Tunnel entry pressure wave gradient (with respect to micro-pressure wave emissions); see Section [8.6.3.3](#).
- Dynamic sealing time-constant for aural comfort in tunnels, as described in Section [7.3.7](#). See the sample values in [Table 2-2](#) and the aural comfort performance obtainable with those values described in Section [7.6.4.2](#). Note also the need to control operation of the sealing and ventilation systems to avoid sudden changes of pressure inside the railcars.
- Tolerance of the railcar body structure, windows, etc., to repeated pressure loading in tunnels and to pressure pulse loading when trains pass each other on neighboring tracks.
- Aerodynamic drag: consider specifying a maximum allowable value for Davis Equation C coefficient for each relevant train length – see Section [9.6.2.3](#) – or else performance-related criteria such as energy consumption per mile at a given speed.
- Criteria relating to the propensity of the train design to cause ballast flight. At the time of writing, such criteria are not available but may be developed in future.

The user is also reminded to consider the environmental issues associated with noise and vibration described in the FRA report, [High-Speed Ground Transportation Noise and Vibration Impact Assessment](#).

12 References

- [1] Adif. AeroTraviesa New design of sleeper for High Speed lines. Retrieved from http://www.adif.es/en_US/compromisos/doc/PT_13-Aerotraviesa_Eng.pdf.
- [2] Alam, F., & Watkins, S. (2007). Effects of Crosswinds on Double Stacked Container Wagons. Proceedings of the 16th Australasian Fluid Mechanics Conference (AFMC), 758-761.
- [3] American Railway Engineering and Maintenance of Way Association. (2017). AREMA Manual for Railway Engineering.
- [4] American Society of Civil Engineers. (2017). Minimum design loads and associated criteria for buildings and other structures. ASCE/SEI 7-16. 2, 800.
- [5] Baker, C. (2010). The flow around high-speed trains. Journal of Wind Engineering & Industrial Aerodynamics, 123, 130-142.
- [6] Baker, C. Quinn, A., Sima, M., Hoefener, L., & Licciardello, R. (2013). Full scale measurement and analysis of train slipstreams and wakes: Part 1 Ensemble averages. Proceedings of the Institute of Mechanical Engineers, Part F: Journal of Rail and Rapid Transit.
- [7] Baker, C., Dalley, S., Johnson, T., Quinn, A., & Wright, N. (2001). The slipstream and wake of a high-speed train. Proceedings of the Institution of Mechanical Engineers, Part F: Journal of Rail and Rapid Transit, 215, 83-99.
- [8] Baker, C., Gilbert, T., & Jordan, S. (2013). The validation of the use of moving model experiments for the measurement of train aerodynamic parameters in the open air. 10th World Congress on Railway Research.
- [9] Banko, F. P., & Xue, J. H. (2013). Pioneering the Application of High Speed Rail Express Trainsets in the U.S. Parsons Brinckerhoff Group Incorporated.
- [10] Barrow, K. (2012). Innovative high-speed sleeper keeps ballast in its place. International Railway Journal.
- [11] Baycrest. (2016). Platform 7-8, Futian Railway Station. Retrieved from https://commons.wikimedia.org/wiki/File:Futian_Railway_Station_Platform_7-8.jpg.
- [12] Berlitz, T. (2003). Pressure comfort - meeting future demands of high speed trains. in Proceedings of the World Congress of Railway Research.
- [13] Bigbug21. (2006). Platform barriers at the station of Paulinenaue. Retrieved from https://commons.wikimedia.org/wiki/File:Hamburg_berlin_track_platform_barriers.jpg.
- [14] Busslinger, A., Hagenah, B., Rienke, P., & Rudin, C. (2009). Aerodynamics in Loetschberg Base Tunnel - simulations and measurements in the second longest

- European high-speed rail tunnel. Proceedings of the 13th International Symposium on Aerodynamics and Ventilation of Tunnels, 767-783.
- [15] California High-Speed Train rail Authority. (2014). California High-Speed Train Project: Design Criteria, Rev. 1.
 - [16] Chakraborty, A. (2019, January 3). Train accident on Great Belt Bridge in Denmark kills six people. Retrieved from <https://www.railway-technology.com/news/train-accident-on-great-belt-bridge-in-denmark-kills-eight-people/>.
 - [17] Cheng, J.-J., et al. (2017). Unloading Characteristics of Sand-drift in Wind-shallow Areas along Railway and the Effect of Sand Removal by Force of Wind. Sci. Rep. 7, 41462.
 - [18] China Railway Urumqi Group Co. Ltd.. (2014). Measures for Safe Operation of Trains in Windy Weather by Urumqi Railway Bureau. WLG/CW106-2014. [In Chinese].
 - [19] China Railway. (2006). GB/T 16904.2-2006 Limiting gauge inspection of standard gauge railway rolling stock - Part 2: Limiting gauges, 645. [In Chinese].
 - [20] China Railway. (2014). Railway Technical Management Regulations. TG/01-2014. [In Chinese].
 - [21] China Railway. (2014). The tentative technical requirements for China standard EMUs of 350 km/h. TJ/CL 342-2014. [In Chinese].
 - [22] Davis, W.J. (1926). The Tractive Resistance of Electric Locomotives and Cars. General Electric Review, vol. 29 (10).
 - [23] Deeg, P., Franck, G., Matschke, G., & Schulte-Werning, B. (2000). Prediction of the aerodynamic environment in subterranean railway stations. In Proceedings of the 10th International Symposium on Aerodynamics and Ventilation of Tunnels, 719-735.
 - [24] Degen, K., Gerbig, C., & Omnich, H. (2007). Acoustic Assessment of Micro-pressure Waves Radiating from Tunnel Exits of DB High-Speed Lines. Proceedings of the 9th International Workshop on Railway Noise, Munich, Germany.
 - [25] Deutsche Bahn. (2013). Lärmschutzanlagen an Eisenbahnstrecken. Ril 804.5501. [In German].
 - [26] Deutsche Bahn. (2002). Eisenbahntunnel planen, bauen und instandhalten. DB Netz AG. [In German].
 - [27] Diedrichs, B., Krajnovic, S., & Berg, M. (2008). On the Aerodynamic of Car Body Vibration of High Speed Trains Cruising Inside Tunnels. Engineering Applications of Computational Fluid Mechanics, 2(1), 51-75.

- [28] Dundee Tunnel Research. ThermoTun home page, available at www.thermotun.com.
- [29] E3uematsu (2014). Platform screen doors Tohoku Shinkansen. Retrieved from https://commons.wikimedia.org/wiki/File:Platform_screen_doors_tohokushinkansen.JPG.
- [30] EN 14067-1:2003. Railway Applications - Aerodynamics - Part 1: Symbols and units, ed: CEN/TC 256. (2013).
- [31] EN 14067-2:2003. Railway applications - Aerodynamics - Part 2: Aerodynamics on open track, ed: CEN/TC 256. (2003).
- [32] EN 14067-3:2003. Railway applications - Aerodynamics - Part 3: Aerodynamics in tunnels, ed: CEN/TC 256. (2003).
- [33] EN 14067-4:2013+A1:2018. Railway applications - Aerodynamics - Part 4: Requirements and test procedures for aerodynamics on open track, ed: CEN/TC 256. (2013).
- [34] EN 14067-5:2006+A1:2010. Railway applications - Aerodynamics - Part 5: Requirements and test procedures for aerodynamics in tunnels, ed: CEN/TC 256. (2006).
- [35] EN 14067-6:2018. Railway applications - Aerodynamics - Part 6: Requirements and test procedures for cross wind assessment, ed: CEN/TC 256. (2018).
- [36] EN 15273-2:2013+A1:2016. Railway applications – Gauges. Part 2: Rolling stock gauge, ed: CEN/TC 256. (2016).
- [37] EN 1991-2:2003. Eurocode 1. Actions on structures. Traffic loads on bridges. (2003).
- [38] European Commission. (2014). Commission Regulation (EU) No 1299/2014 of 18 November 2014 on the technical specifications for interoperability relating to the 'infrastructure' sub-system of the rail system in the European Union.
- [39] European Commission. (2014). Commission Regulation (EU) No 1302/2014 of 18 November 2014 concerning a technical specification for interoperability relating to the 'rolling stock' sub-system of the trans-European high-speed rail system.
- [40] European Commission. (2014). Commission Regulation (EU) No 1303/2014 of 18 November 2014 concerning the technical specification of interoperability relating to safety of railway tunnels of the rail system of the European Union.
- [41] European Rail Research Institute. (1998). Aerodynamic aspects of train operation in tunnels - Specification of a medical health criterion for pressure changes. ERRI report C218/RP5.
- [42] Federal Emergency Management Agency. (2007). Tornado risks and hazards in the Midwest U.S. HSFEHQ-07-J-0020. Retrieved from

https://www.fema.gov/media-library-data/20130726-1619-20490-0806/ra1_tornado_risks_in_midwest_us_final_9_14_07.pdf.

- [43] Federal Railroad Administration. (2013). Federal Railroad Administration Office of Safety Analysis: Train Accidents. Retrieved from <http://safetydata.fra.dot.gov/OfficeofSafety/publicsite/Query/inctally1.aspx>.
- [44] Federal Railroad Administration. (2012). High-speed ground transportation noise and vibration impact assessment manual. Washington, D.C.: DOT/FRA/ORD-15/32.
- [45] Federal Railroad Administration. (2015). Identification of High-Speed Rail Ballast Flight Risk Factors and Risk Mitigation Strategies – Final Report. Washington, D.C.: DOT/FRA/ORD-15/32.
- [46] Federal Railroad Administration. (2019). Hazards Associated with HSR Operations Adjacent to Conventional Tracks – Enhanced Literature Review Part I: Summary Report. DOT/FRA/ORD-19/27.
- [47] Federal Railroad Administration. (2019). Hazards Associated with HSR Operations Adjacent to Conventional Tracks – Enhanced Literature Review Part II: Draft Guidance Document. DOT/FRA/ORD-19/28.
- [48] Federal Railroad Administration. (2019). Hazards Associated with HSR Operations Adjacent to Conventional Tracks – Enhanced Literature Review Part III: Literature Review. DOT/FRA/ORD-19/29.
- [49] Federal Railroad Administration. (2015). High-speed rail aerodynamic assessment and mitigation report. Washington, D.C.: DOT/FRA/ORD-15/40.
- [50] Federal Railroad Administration. (n.d.). High Speed Intercity Passenger Rail (HSIPR) Program. Retrieved from <https://www.fra.dot.gov/Page/P0134>.
- [51] Federal Railroad Administration. (2016). Passenger Equipment Safety Standards; Standards for Alternative Compliance and High-Speed Trainsets. Washington, D.C.: Federal Register, FRA-2013-0060.
- [52] Federal Railroad Administration. (2009). Vision for high-speed rail in America. Washington D.C.: U.S. Department of Transportation.
- [53] Figura-Hardy, G. (2000). Pressure relief - trends and benefits of incorporating airshafts into railway tunnels. In the Proceedings of the 10th International Symposium on Aerodynamics and Ventilation of Tunnels.
- [54] Fujii, T., Maeda, T., Ishida, H., Imai, T., Tanemoto, K., & Suzuki, M. (1999). Wind-induced accidents of train/vehicles and their measures in Japan. Quarterly Report of RTRI, 40(1), 50-55.
- [55] Fukuda, T., Miyachi, T., & Iida, M. (2006). Propagation of compression wave in a long slab-tracked tunnel and ballast-tracked tunnel. in Proceedings of the 12th International Symposium on Aerodynamic and Ventilation of Tunnels, 213-233.

- [56] Fukuda, T., Miyachi, T., Takami, H., Iida, M., & Saito, S. (2011). Interior explosive sound caused when a train encounters a compression wave inside a long slab-tracked tunnel. In Proceedings of the 14th International Symposium on Aerodynamic and Ventilation of Tunnels, 213-226.
- [57] Garcia, A. (2010). Relationship between rail service operating direct costs and speed. Study and Research Group for Economics and Transport Operation. International Union of Railways & Fundaci3n de los Ferrocarriles Espa1oles.
- [58] Gautier, P., Sacre, C., Delaunay, C., Parrot, M., Dersigny, C., & Bodere, S. (2001). TGV Mediterranee high speed line safety against cross-winds : a slow down system based on anemometric and spatial short-term meteorological prediction. Presented at the WCRR-2001.
- [59] Gawthorpe, R. (1983). Train drag reduction from simple design changes. In Impact of aerodynamic on vehicle design, M. Dorgham, Ed., ed London: Inderscience, 308-341.
- [60] Gerbig, C. & Hieke, M. (2013). Micro-pressure wave emissions from German high-speed railway tunnels. An approved method for prediction and acoustic assessment. In Proceedings of the 11th international Workshop on Railway Noise.
- [61] Gilbert, T. (2013). Aerodynamic eddies of high speed trains in confined spaces, PD Thesis. University of Birmingham.
- [62] Gilmartin, B. & Griffin, D. (2012). Guidance on protecting people from the aerodynamic effects of passing trains. Rail Safety and Standards Board–T479 Report.
- [63] Goossens, H. (2010). Maintenance of high speed lines (report by E-Rail consult for international Union of Railway).
- [64] Guihew, C. (1983). Resistance to forward movement of TGV-PSE trainsets: evaluation of studies and results of measurements. French Railway, 1.
- [65] Hagenah, B., Reinke, P., & Vardy, A. (2006). Effectiveness of pressure relief shafts-full scale assessment. Proceedings 12th International Symposium on Aerodynamics and Ventilation of Vehicle Tunnels.
- [66] Hibino, Y., Misui, Y., Kurihara, T., Moriyama, A., Shimamura, M. (2011). Study of new methods for train operation control in strong winds, JR EAST Technical Review, 19.
- [67] Hemida, H. Baker, C., & Gao, G. (2012). The calculation of train slipstream using large-eddy simulation. In Proceedings of the Institution of Mechanical Engineers, Part F: Journal of Rail and Rapid Transit, 228(1), 25-36.
- [68] Hieke, M. Kaltenbach, H., & Tielkes, T. (2009). Prediction of micro-pressure wave emissions from high-speed railway tunnels. in Proceedings of the 13th International Symposium on Aerodynamics and Ventilation of Tunnels 2009, 487-503.

- [69] Hieke, M., Gerbig, C., & Tielkes, T. (2013). Mastering micro-pressure wave effects at the Katzenbergtunnel - Design of measures, prediction of efficiency and full-scale test verification. Proceedings of 11th International Workshop on Railway Noise.
- [70] Hieke, M., Gerbig, C., Degen, K., & Tielkes, T. (2011). Assessment of micro-pressure wave emissions from high-speed railway tunnels. presented at the 9th World Congress on Railway Research.
- [71] Hoffmeister, B. (2007). Development and Design of noise barriers for high speed railway. IABSE Symposium Report, Weimar.
- [72] Holmes, S. & Schroeder, M. (2002). Aerodynamic effects of high-speed passenger trains on other trains. US Department of Transportation FTA-AL-26-7001.3.
- [73] Houxiong, W., & Zhu, Y. Y. G. (1993). The Effects of Roof Shape of Railroad Cars on Aerodynamic Lateral Stability and Other Characteristics of Cars. *Acta Aerodynamica Sinica*, (1), 13.
- [74] IEC 61672-1:2013. (2013). Electroacoustics – Sound level meters – Part 1: Specifications. ed: International Electrotechnical Commission.
- [75] Iida, M., Tanaka, Y., Kikuchi, K., & Fukuda, T. (2001). Pressure waves radiated directly from tunnel portals at train entry or exit. Quarterly Report of RTRI, 24, 83-88.
- [76] Imai, T., Fujii, T., Tanemoto, K., Shimamura, T., Maeda, T., Ishida, H., & Hibino, Y. (2002). New Train Regulation Method Based on Wind Direction and Velocity of Natural Wind against Strong Winds. *Journal of Wind Engineering and Industrial Aerodynamics*, 90, 1601-1610.
- [77] International Union of Railways. (2015). 2nd edition: Effect of Slipstream of passing trains on structures adjacent to the track. in UIC leaflet 779-1.
- [78] International Union of Railways. (2002). 2nd Edition: Measures to ensure the technical compatibility of high speed trains. in UIC leaflet 660.
- [79] International Union of Railways. (2005). 2nd edition: Determination of railway tunnel cross-sectional areas on the basis of aerodynamic considerations. in UIC leaflet 779-11.
- [80] ISO 3095:2001. Railway applications - Acoustics - Measurement of noise emitted by railbound vehicles. (2001).
- [81] Jing, G. Q. et al. (2014). Aerodynamic characteristics of Individual ballast particles by wind tunnel tests. *Journal of Engineering Science and Technology Review*, 7(2). 137-142.
- [82] Johnson, T. & Holding, J. (2003). Better understanding of high speed train slipstream velocities. presented at the World Congress on Railway Research.

- [83] Johnson, T. (2009). Aerodynamics in the Open Air European Project. GB Perspectives.
- [84] Jucember. (2012). CRH380AL EMU at Shanghai Hongqiao Station. Retrieved from: <https://commons.wikimedia.org/wiki/File:CRH380A-6068L.jpg>.
- [85] Kimura, N., Shinohara, Y., Fukuda, T., Nakamura, S., Saito, S., & Miyachi, T. (2016). Field-test for micro-pressure waves reduction method focused on the propagation of compression waves through the slab track tunnel. Proceedings of 11th World Conference on Railway Research.
- [86] Klaver, E. & Kassies, E. (2000). Dimensioning of tunnels for passenger's comfort in the Netherlands. In the Proceedings of the 10th International Symposium on Aerodynamics and Ventilation of Tunnels, 737-756.
- [87] Kobayashi, N. & Shimamura, M. (2003). Study of a strong wind warning system, JR EAST Technical Review, 2.
- [88] Kobayashi, M., Suzuki, Y., Akutsu, K., Iida, M., & Maeda, T. (1991). New Ventilating System of Shinkansen Cars for Alleviating Aural Discomfort of Passengers. in Proceedings of the 7th International Symposium on the Aerodynamics and Ventilation of Vehicle Tunnels, 155-172.
- [89] Lazaro, B., Gonzalez, M., Rodriguez, S., Osma, S., & Iglesias, J. (2011). Characterization and modeling of flying ballast phenomena in high speed lines. Proceedings 9th World Congress on Railway Research.
- [90] Lee, H. (1999). Assessment of potential aerodynamic effects on personnel and equipment in proximity to high-speed train operations. US Department of Transportation.
- [91] Lee, H. S.-H. (2009). The Aerodynamic Effects of Passing Trains to Surrounding Objects and People. Washington D.C.: Office of Research and Development.
- [92] Liao, S., Mosier, P., Kennedy, W., & Andrus, D. (1999). Aerodynamic effects of high-speed trains on people and property at stations in the Northeast Corridor. US Department of Transportation DOT/FRA/ORD-99/12.
- [93] Licciardello, R., Grappein, E., & Rueter, A. (2015). On the accuracy of the assessment of open-air pressure loads due to passing trains: Part 2P Assessment by simulation. Proceedings of the Institution of Mechanical Engineers, Part F: Journal of Rail and Rapid Transit, 229(6), 657-667.
- [94] Maeda, T. Iida, M., Fukuda, T., Sakuma, Y., & Takasaki, T. (2004). A micro pressure wave radiating from a tunnel portal. In Proceedings of 18th International Congress on Acoustics.
- [95] Maeda, T., Kinoshita, M., Kajiyama, H., & Tanemoto, K. (1989). Aerodynamic drag of Shinkansen electric car; series 0, series 200, series 100. Quarterly Report of RTRI, 30.

- [96] Mancini, G. & Malfatti, A. (2002). Full scale measurements on high speed train ETR 500 passing in open air and in tunnels of Italian high-speed line. TRANSAERO: A European Initiative on Transient Aerodynamics for Railway System Optimisation, 101.
- [97] Matschke, G., & Heine, C. (2002). Full Scale Tests on Pressure Wave Effects in Tunnels. Notes on Numerical Fluid Mechanics and Multidisciplinary Design (NNFM) TRANSAERO — A European Initiative on Transient Aerodynamics for Railway System Optimisation, 187–195. doi: 10.1007/978-3-540-45854-8_15.
- [98] Matsuo, K., Aoki, T., Kashimura, H., Yasunobu, T., & Mashino, S. (1994). Generation Mechanism of Impulsive Wave Emitted from High-Speed Railway Tunnel Exit. In Proceedings of 8th International Symposium on the Aerodynamic and Ventilation of Vehicle Tunnels, 199-209.
- [99] National Ministry of Railways of the People's Republic of China. (2014). Code for design of high-speed railway (Trial). TB10621-2014. [In Chinese].
- [100] National Ministry of Railways of the People's Republic of China, Tie-Ji-Cheng. (2010). Document No. 166. The guidance on adjustment, commissioning, and operation of high-speed railway [In Chinese].
- [101] Ministry of Railways of the People's Republic of China. Ke-Jiao-Zhuang-Han. (2008). Document no. 08(2008), Preliminary Requirements for High-Speed Train Aerodynamic Performance Calculation and Conformation Test [In Chinese].
- [102] Montenegro-Palmero, N. & Vardy, A. (2013). Tunnel gradients and aural health criterion for train passengers. Journal of Rail and Rapid Transit, IMechE, 228 (7), 821-832.
- [103] Morden, J, Hemida, H., & Baker, C. J. (2015). Comparison of RANS and detached eddy simulation results to wind-tunnel data for the surface pressures upon a class 43 high-speed train. Journal of Fluids Engineering, 137(4), 041108.
- [104] Nakao, S., Aoki, T., Tanino, T., Miyaguni, T., & Matsuo, K. (2011). A new passive control method of the pressure wave propagating through in a high-speed railway tunnel. in Proceedings of the 14th International Symposium on Aerodynamics and Ventilation of Tunnels, 227-236.
- [105] National Fire Protection Association. (2014). NFPA 130: Standard for fixed guideway transit and passenger rail systems.
- [106] National Railroad Passenger Corporation. (2005). AMTRAK Electrical Operating Instructions (AMT-2).
- [107] Ozawa, S., Maeda, T., Matsumura, T., Uchida, K., Kajiyama, H., & Tanemoto, K. (1991). Countermeasures to reduce micropressure waves radiating from exits of Shinkansen tunnels. In Proceedings of the 7th International Symposium on Aerodynamic and Ventilation of Tunnels, 253-266.

- [108] Ozawa, S., Murata, K., & Maeda, T. Effect of ballasted track on distortion of pressure wave in tunnel and emission of micro pressure wave. In Proceedings of the International Symposium on Aerodynamic and Ventilation of Tunnels, 935-947.
- [109] Paradot, N. Gregoire, R., Stiepel, M., Blanco, A., Sima, M., Deeg, P., Schroeder-Bodenstein, K., Johnson, T., & Zanetti, G. (2015). Crosswind sensitivity assessment of a representative Europe-wide range of conventional vehicles. *Journal of Rail and Rapid Transit*, 229(6), 594-624.
- [110] Peters, J. (1990). Bestimmung der aerodynamischen Widerstandes des ICE/V im Tunnel und auf freier Strecke durch Auslaufversuche. *Eisenbahntechnische Rundschau*, 39, 559-564.
- [111] Pope, C. (2007). Effective management of risk from slipstream effects at trackside and platforms. Rail Safety and Standards Board–T425 Report.
- [112] prEN 14067-5:2018. Railway applications - Aerodynamics - Part 5: Requirements and test procedures for aerodynamics in tunnels, ed: CEN/TC 256. (2018).
- [113] Quinn, A., Hayward, M., Baker, C., Schmid, F., Priest, J., & Powrie, W. (2010). A full-scale experimental and modelling study of ballast flight under high-speed trains. Institution of Mechanical Engineers, Part F: *Journal of Rail and Rapid Transit*, 224, 61-74.
- [114] Raghunathan, R., Kim, H., & Setoguchi, T. (2002). Aerodynamics of high-speed railway train. *Progress in Aerospace sciences*, 38, 469-514.
- [115] RAIB Rail Accident Report – Occupied wheelchair contacting a passing train at Twyford station, 7th April 2016.
- [116] Rail Safety and Standards Board Railway Safety. (2007). Effective management of risk from slipstream effects at trackside and platforms Project T425.
- [117] Rail Safety and Standards Board Railway Safety. (2001). Railway Industry Standard GC/RC5521: Calculation of enhanced permissible speeds for tilting trains (superceded).
- [118] Rail Safety and Standards Board Railway Safety. (2018). Railway Industry Standard RIS-7704-INS: Calculation of enhanced permissible speeds for tilting trains.
- [119] Railway Bureau Ministry of Land, Infrastructure, Transport and Tourism. (2012). Technical Regulatory Standards on Japanese Railways. Retrieved from https://www.mlit.go.jp/english/2006/h_railway_bureau/Laws_concerning/14.pdf.
- [120] Rety, J. & Gregoire, R. (2002). Numerical investigation of tunnel extensions attenuating the pressure gradient generated by a train entering a tunnel. In *TRANSAERO - a European Initiative on Transient Aerodynamics for Railway System Optimisation*, ed: Springer.

- [121] Roadway Worker Protection, 49 C.F.R. § 214 C (2011).
- [122] Rochard, B., & Schmid, F. (2000). A review of methods to measure and calculate train resistances. in Proceedings of the Institution of Mechanical Engineers, Part F: Journal of Rail and Rapid Transit, 185-199.
- [123] Saito, S., Miyachi, T., Fukuda, T., Takami, H., Lida, M., & Kajiyama, H. (2006). Pressure changes generated inside and outside a tunnel with a shaft in high speed railway. in Proceedings of the 12th International Symposium on Aerodynamics and Ventilation of Tunnels, 213-232.
- [124] Sakurai, K., Saeki, K., Takakuwa, Y., & Watanabe, A. Development of new tunnel entrance hoods. JR EAST Technical Review, 12.
- [125] Saussine, G., Allain, E., Paradot, N., & Gaillot, V. (2011). Ballast Flying Risk Assessment Method on High Speed Line. Presented at the 9th World Congress on Railway Research.
- [126] Schetz, J.A. (2001). Aerodynamics of high-speed trains. Annual Review of Fluid Mechanics, 33, 371-414.
- [127] Schwanitz, S., Wittkowski, M., Rolny, V., & Basner, M. (2012). Pressure variations on a train - Where is the threshold to railway passenger discomfort? Applied Ergonomics, 44, 200-209.
- [128] Shepherd, D., Welch, D., Hill, E., McBride, D., & Dirks, K. (2011). Evaluating the impact of wind turbine noise on health-related quality of life. Noise and Health, 13(54), 333.
- [129] Sima, M., Grappein, E., Weise, M., Paradot, N., Hieke, M., & Baker, C. (2011). Presentation of the EU FP7 AeroTRAIN project and first results. presented at the 9th World Congress on Railway Research.
- [130] Smith, N. (2013). Mansfield sound Acela warning. The Sun Chronicle. Retrieved from https://www.thesunchronicle.com/news/local_news/mansfield-sounds-acela-warning/article_63f2f7ac-7b9a-5890-a4b5-b09d76e75b5b.html.
- [131] Soper, D., Gillmeier, S., Baker, C., Morgan, T., & Vojnovic, L. (2019). Aerodynamic forces on railway acoustic barriers. Journal of Wind Engineering and Industrial Aerodynamics, 191, 266-278.
- [132] Sturt, R., Baker, C. J. B., Soper, D., Vardy, A., Howard, M., & Rawlings, C. (2015). The design of HS2 tunnel entrance hoods to prevent sonic booms. In M. Forde (Ed.), Proceedings of the 13th International Conference & Exhibition on Railway Engineering E.C.S. Publications.
- [133] Sugimoto, N. (1993). Shock-free tunnel for future high-speed trains. In Proceedings of International Conference on Speedup Technology for Railway and Maglev Vehicles, 284-292.

- [134] Takami, H., Kikuchi, K., Lida, M., Maekawa, T., Kurita, T., & Wakabayashi, Y. (2006). Low-frequency noise radiated from a high-speed train running in an open section. In Proceedings of 13th International Congress on Sound and Vibration, 73, 2275-2282.
- [135] Takei, Y., Izumi, Y., Yamada, S., Lida, M., & Kikuchi, K. (2008). Evaluation Method for Air Pressure Variation and Station Facility Member Deterioration Caused by High-Speed Train Passage in Stations. Quarterly Report of RTRI, 49, 89-95.
- [136] Tanemoto, K. & Kajiyama, H. (2003). Train draft and pressure variation on a platform. RTRI Report, 17, 53-56.
- [137] Temple, J. (2006). West coast main line upgrade: railway tunnel pressure relief in practice. In Proceeding of the 12th International Symposium on Aerodynamics and Ventilation of Tunnels.
- [138] Tennen-gas. (2009). Outer bellows of N700 series Shinkansen train. Retrieved from: https://commons.wikimedia.org/wiki/File:JR_Central_N700_052.JPG.
- [139] The Third Railway Survey and Design Institution Group Co., Ltd. (2010). Code for design of high-speed railway (Trial). Beijing: Ministry of Railways of the People's Republic of China.
- [140] Tian, H. (2009). Formation mechanism of aerodynamic drag of high-speed train and some reduction measures. Journal of Central South University of Technology, 16, 166-171.
- [141] Tian, H., Xu, P., Liang, X., & Lui, T. (2006). Correlation between pressure wave of train passing and running speed. Chine Railway Science, 27, 64-67.
- [142] Tielkes, T. (2006). Aerodynamics aspects of Maglev systems. in the 19th International conference on magnetically levitated systems and linear drives, 1-29.
- [143] Tielkes, T., Heine, C., Moller, M., & Driller, J (2008). A probabilistic approach to safeguard cross wind safety of passenger railway operation in Germany: the new DB guideline Ril 80704, In proceedings of the 8th World Congress on Railway Research, 2008
- [144] Toddler killed after passing train sucks buggy onto tracks. (2015, April 30). Retrieved from <http://www.telegraph.co.uk/news/worldnews/europe/austria/11575021/Toddler-killed-after-passing-train-sucks-buggy-onto-tracks.html>.
- [145] Train Operations at Track Classes 6 and Higher, 49 C.F.R. § 213 G (2013).
- [146] Transit Development Corp., Washington, D.C.; Urban Mass Transportation Administration, Washington, D.C. (1976). Subway environmental design handbook. Volume 1. Principles and Applications. Second Edition. U.S. Department of Commerce. Retrieved from: <https://ntrl.ntis.gov/NTRL/dashboard/searchResults/titleDetail/PB254788.xhtml>.

- [147] Transportation for Individuals with Disabilities --Detectable Warnings, Standees on Lifts, Equivalent Facilitation, Priority Seating, Rail Car Acquisition. (2015, August 31). Retrieved from <https://www.transit.dot.gov/regulations-and-guidance/civil-rights-ada/transportation-individuals-disabilities-detectable>.
- [148] Vardy, A. & Haerter, A. (1991). Pressure fluctuations and comfort criteria on new railways. Proceedings of the 7th International Symposium on Aerodynamics and Ventilation of Tunnels, 189-204.
- [149] Vardy, A. & Reinke, P. (1999). Estimation of train resistance coefficients in tunnels from measurements during routine operations. Proceedings of the Institution of Mechanical Engineers, Part F: Journal of Rail and Rapid Transit, 213, 71-87.
- [150] Vardy, A. (2008). Generation and alleviation of sonic booms from rail tunnels. Proceedings of The ICE - Engineering and Computational Mechanics, 161, 107-119.
- [151] Vardy, A., (1976). The use of airshafts for the alleviation of pressure transients in railway tunnels. Proceedings 2nd International Symposium on the Aerodynamics and Ventilation of Vehicle Tunnels, British Hydromechanics Research Association.
- [152] Vardy, A., Rhodes, N., & Wang, A. (2009). Train induced pressures and flows in large underground stations. Proceedings of the 13th International Symposium on Aerodynamics and Ventilation of Tunnels, 445-546.
- [153] Yanase, N. (2011). High Speed System in Japan. Presented at the Workshop on High Speed Railway.
- [154] Yumada, M. (1998). Study of aging of finish materials for enclosed shelters of railroad stations in Summaries of technical papers of annual meeting of the Architectural Institute of Japan.

Abbreviations and Acronyms

Abbreviation or Acronym	Name
AREMA	American Rail Engineering and Maintenance-of-Way Association
ASCE	American Society of Civil Engineers
ADA	Americans with Disabilities Act
ACI	Aural Comfort Index
CFR	Code of Federal Regulations
CFD	Computational Fluid Dynamics
CWC	Characteristic Wind Curve
DES	Detached Eddy Simulation
DB	Deutsche Bahn (German Railroads)
DLR	Deutsches Zentrum für Luft- und Raumfahrt (German Aerospace Center)
EN	European Norm
FRA	Federal Railroad Administration
HSR	High-Speed Rail
HST	High-Speed Train
ICE3	Intercity-Express 3
LES	Large Eddy Simulation
SI	International System of Units
KTX	Korea Train Express
MRI	Mean Recurrence Interval
MPW	Micro-pressure Wave
MBS	Multi-Body Simulation
NFPA	National Fire Protection Association
NOAA	National Oceanic and Atmospheric Administration
NEC	Northeast Corridor
RTRI	Railway Technical Research Institute
RANS	Reynolds-Averaged Navier-Stokes
ROW	Right-of-Way

Abbreviation or Acronym	Name
STBR	Single Track Ballasted Rail Simulation
SEL	Sound Exposure Level
SPL	Sound Pressure Level
SEI	Structural Engineering Institute
TSI	Technical Specifications for Interoperability
TOR	Top of Rail
TGV	Train à Grande Vitesse (High-Speed Train)
TRAIN	Transient Railway Aerodynamics Investigation
ULA	Unbalanced Lateral Acceleration
UIC	Union Internationale des Chemins de Fer (International Union of Railways)